
Energy Modelling for Machine Tool Axis and Toolpaths

A thesis submitted to

The University of Manchester

for the degree of

Doctor of Philosophy (PhD)

in the Faculty of Science and Engineering

2016

Isuamfon Friday Edem

**School of Mechanical, Aerospace and Civil
Engineering**

(This page is intentionally left blank)

TABLE OF CONTENTS

TABLE OF CONTENTS.....	3
LIST OF FIGURES	9
LIST OF TABLES.....	14
ABBREVIATIONS	16
NOMENCLATURE	19
LIST OF PUBLICATIONS	22
ABSTRACT.....	23
DECLARATION.....	24
COPYRIGHT STATEMENT.....	25
ACKNOWLEDGEMENTS	26
DEDICATION	27
CHAPTER 1 INTRODUCTION.....	28
1.1 Overview of global energy demand	28
1.2 Sustainable manufacturing and machine tools.....	30
1.3 Environmental impact of machining	31
1.4 Energy demand strategies in machining operation.....	32
1.5 Research aim and objectives.....	33
1.6 Outline of thesis	34
CHAPTER 2 LITERATURE REVIEW	37
2.1 Sustainability	37
2.2 Environmental sustainability	39
2.2.1 Carbon dioxide emission in the United Kingdom.....	39
2.2.2 The manufacturing sector and its energy consumption impacts	42

2.3	Machining operations.....	42
2.3.1	Basics of the cutting process	43
2.3.2	The milling process and cutting power	44
2.4	Environmental aspects of machining.....	47
2.5	Energy efficiency of machine tools.....	47
2.5.1	Electrical energy consumption monitoring of machine tools.....	48
2.6	Energy consumption in machining processes at machine tool level	51
2.6.1	Energy consumption models	55
2.6.1.1	<i>Specific energy based models</i>	<i>55</i>
2.6.1.2	<i>Machine tool component based models</i>	<i>58</i>
2.6.1.3	<i>CNC codes based models.....</i>	<i>60</i>
2.6.1.4	<i>Energy consumption modelling based on simulation techniques.....</i>	<i>62</i>
2.7	Knowledge gaps identified	64
 CHAPTER 3 DEVELOPMENT OF THE EXPERIMENTAL APPROACH AND ITS IMPLEMENTATION		
66		
3.1	Introduction	66
3.2	Experimental setup and procedures for the research	66
3.2.1	Experimental procedures for measuring current and voltage in machining.....	67
3.3	Machine tool.....	70
3.4	Fluke 434 three-phase power quality analyser	73
3.4.1	Connection of Fluke 434 power analyser to machine tools	74
3.4.2	Data acquisition.....	76
3.5	Workpiece material details.....	78

3.6	Cutting tool details	79
3.7	Vickers hardness testing machine.....	80
3.8	Surface roughness checker	81
3.9	Grinding and polishing machines	83
3.9.1	OmegaPol grinding machine.....	83
3.9.2	LaboPol-35 polishing machine	83
3.10	Equipment for microscopy	84
3.10.1	Leica DM2500 microscope.....	84
3.10.2	Keyence VHX-500F digital microscope.....	85
3.11	Conclusion.....	85
CHAPTER 4 IMPACT OF FEED AXIS ON ELECTRICAL ENERGY DEMAND IN MECHANICAL MACHINING PROCESSES.....		86
ABSTRACT		86
4.1	Introduction	87
4.1.1	Research aim and objective.....	90
4.2	Experimental details.....	90
4.2.1	Research methodology.....	90
4.2.2	Experimental setup and procedure.....	91
4.3	Results and discussions	94
4.3.1	Determining the dominant factors for energy demand of machine tool axis	94
4.3.2	Modelling of the power demand of the feed axes	95
4.3.3	Implementation and validation of the power demand model of the feed axes during a milling process	103

4.4	Conclusions	111
CHAPTER 5 ENERGY DEMAND REDUCTION IN MILLING BASED ON COMPONENT AND TOOLPATH ORIENTATIONS..... 113		
	ABSTRACT	113
5.1	Introduction	114
5.1.1	Electrical energy demand of machine tools	114
5.1.2	Energy efficiency of machining toolpaths	116
5.1.3	Research aim and objectives	117
5.2	Experimental details.....	117
5.2.1	Research methods	117
5.2.2	Experimental setup and procedures	118
5.3	Results and discussions	119
5.3.1	Impact of machine tool vice and toolpath orientations on electrical energy demand of a milling process	119
5.3.2	Surface roughness for different machine tool vice and toolpath angles.....	121
5.3.3	Influence of toolpath strategies on the electrical energy demand	122
5.3.4	Influence of toolpath strategies on surface quality of machined material.....	124
5.4	Conclusions	125
CHAPTER 6 MODELLING OF ENERGY DEMAND FROM COMPUTER NUMERICAL CONTROL (CNC) TOOLPATHS 127		
	ABSTRACT	127
6.1	Introduction	128
6.1.1	Energy demand modelling in mechanical machining processes	128
6.1.2	NC-codes energy modelling in mechanical machining.....	130
6.1.3	Research aim and motivation	133

6.2	Modified electrical energy modelling through the analytical methods	133
6.2.1	Feed energy demand	134
6.2.1.1	<i>G00 - Rapid feed energy demand.....</i>	<i>135</i>
6.2.1.2	<i>G01 - Feed axes energy demand for linear interpolation.....</i>	<i>135</i>
6.2.1.3	<i>G02/G03 - Feed axes energy demand for circular interpolation.....</i>	<i>138</i>
6.2.2	Time required to run an NC block	141
6.3	NC code based energy demand prediction software	143
6.3.1	Design and development of the NC-code based energy demand prediction software.....	143
6.3.2	Implementation of the NC-code based energy demand prediction software and graphical user interface (GUI)	147
6.4	Case study	148
6.4.1	Experimental setup.....	148
6.5	Results and discussions	151
6.5.1	Analytical estimation of total electrical energy demand based on NC codes	151
6.5.2	Validation of the analytical estimation and NC-code based energy demand prediction software.....	157
6.6	Conclusions	158
CHAPTER 7 SENSITIVITY ANALYSIS OF THE EFFECT OF THE WORKPIECE ON THE VARIABILITY OF ENERGY IN MACHINING.....		160
ABSTRACT		160
7.1	Introduction	161
7.1.1	Brief description of the production sequence of hot rolled flat bars of AISI 1018 steel	161
7.1.2	Machinability of AISI 1018 steels	163

7.1.3	Surface roughness	164
7.2	Research aim and objectives.....	165
7.3	Experimental details.....	165
7.4	Results and discussions	169
7.4.1	Hardness analysis.....	169
7.4.2	Electrical energy demand for face milling of AISI 1018 steel.....	170
7.4.3	Surface integrity characterisation.....	171
7.4.3.1	<i>Surface roughness</i>	171
7.4.3.2	<i>Microstructure</i>	172
7.4.4	Tool wear	176
7.5	Conclusions	178
CHAPTER 8 CONCLUSIONS AND FUTURE RESEARCH		179
8.1	Overall conclusions.....	179
8.2	Contribution to knowledge	180
8.3	Recommendations for future research	181
REFERENCES.....		182
APPENDIX.....		197

LIST OF FIGURES

Figure 1.1	World energy consumption projection, 1990-2040 [2]	29
Figure 1.2	World energy consumption from fuels by sectors for 2011 [3]	29
Figure 1.3	UK CO ₂ emission by sectors for 2011 (in million tonnes of CO ₂ equivalent) [6]	30
Figure 1.4	Thesis contents and chapters	36
Figure 2.1	Three sustainability rings [30]	37
Figure 2.2	Sustainability in the context of CNC machining and machine tools as adapted from Fang et al. [34]	38
Figure 2.3	UK energy consumption by sectors in 2011 [6]	40
Figure 2.4	Sources of electricity generation in the UK for 2011 [38]	40
Figure 2.5	Orthogonal cutting model	44
Figure 2.6 a,b:	Up milling process	45
Figure 2.7 a,b:	Down milling process	45
Figure 2.8	Cutting geometry in milling	46
Figure 2.9	Power consumption breakdown of a Cincinnati Milacron automated milling machine adapted from Dahmus and Gutowski [9]	52
Figure 2.10	Power breakdown for Takisawa Mac-V3 milling machine [66]	54
Figure 2.11	Power breakdown of the Takisawa milling machine showing the various machining states as adapted from Balogun and Mativenga [66].....	54
Figure 3.1	Experimental setup for energy measurement and surface roughness check of the machined part.....	67
Figure 3.2	Research methodology outline and energy states according to ISO 14955-1:2014 [15]	69
Figure 3.3	Takisawa Mac-V3 milling machine.....	70
Figure 3.4	Machine tool axes configuration showing the x-axis and y-axis.....	72
Figure 3.5	Fluke 434 power quality analyser.....	73
Figure 3.6	Fluke 434 power quality analyser clamped on three live wires at the back of the Takisawa Mac-V3 milling machine.....	75
Figure 3.7	Delta three phase power configuration	75
Figure 3.8a	Current demand profile for each phase	76
Figure 3.8b	Voltage demand profile for each phase.....	77

Figure 3.8c	Power demand profile for the three phases.....	77
Figure 3.9	Picture of 8 mm diameter short carbide end mill cutter	79
Figure 3.10	Vickers hardness tester	80
Figure 3.11	Surtronic 25 portable surface roughness checker	81
Figure 3.12	Electro-formed surface roughness comparison standard.....	82
Figure 3.13	OmegaPol grinding machine with rotating disc	83
Figure 3.14	LaboPol-35 polishing machine	84
Figure 3.15	Leica DM2500 microscope.....	84
Figure 3.16	Keyence VHX-500F digital microscope	85
Figure 4.1	Schematic diagram showing Fluke 434 power quality analyser setup and data acquisition.....	93
Figure 4.2	Factors affecting the power demand of feed axes	94
Figure 4.3	Power required for x- and y- axis of Takisawa Mac-V3 milling machine when not cutting traversing with no workpiece and with the spindle off	96
Figure 4.4	Power demand for the z-axis when the spindle was going up and down for Takisawa Mac-V3 milling machine	97
Figure 4.5	Variation of power with feedrates when specified weights are placed on the table of Takisawa Mac-V3 milling machine along the x-axis.....	97
Figure 4.6	Variation of power with feedrates when specified weights are placed on the the table of Takisawa Mac-V3 milling machine along the y-axis.....	98
Figure 4.7	Variation of x-axis power with weights at feedrate of 0.083 m/s (5000 mm/min) for zero cutting operation	99
Figure 4.8	Variation of y-axis power with weights at feedrate of 0.0083 m/s (500 mm/min) for zero cutting operation	99
Figure 4.9	Variation of specific power per weight with feedrates for Takisawa Mac-V3 milling machine while not cutting along the x-axis.....	101
Figure 4.10	Variation of specific power per weight with feedrates for Takisawa Mac-V3 milling machine while not cutting along the y-axis.....	101
Figure 4.11	Toolpaths at different angles	104
Figure 4.12a	Power profile for Takisawa Mac-V3 milling machine during air cutting of a slot at zero degrees with feedrate of 500 mm/min	106
Figure 4.12b	Power profile for Takisawa Mac-V3 milling machine during air cutting of a slot at 30 degrees with feedrate of 500 mm/min.....	107
Figure 4.12c	Power profile for Takisawa Mac-V3 milling machine during air cutting	

	of a slot at 90 degrees with feedrate of 500 mm/min.....	107
Figure 4.13a	Power profile for Takisawa Mac-V3 milling machine during air cutting of slot at 0 degrees with feedrate of 3000 mm/min.....	108
Figure 4.13b	Power profile for Takisawa Mac-V3 milling machine during air cutting of slot at 30 degrees with feedrate of 3000 mm/min.....	109
Figure 4.13c	Power profile for Takisawa Mac-V3 milling machine during air cutting of slot at 90 degrees with feedrate of 3000 mm/min.....	109
Figure 5.1	Power consumption profile for peripheral milling of AISI 1018 steel on the Takisawa Mac-V3 milling machine	115
Figure 5.2 (a)	Machine tool vice and component oriented at 0 degrees showing direction of direction of of feed drive and toolpath (feed drive moves in the x-axis direction)	119
Figure 5.2 (b)	Machine tool vice and component oriented at 45 degrees showing feed drive and toolpath directions (feed drive moves in the x- and y-axes direction).....	119
Figure 5.3 a,b	Energy demand when executing air cutting and cutting with machine tool	120
Figure 5.4	Surface roughness measured perpendicular to the cutting direction when rotating the machine tool vice at varying orientations and varying feedrates	121
Figure 5.5	CAM toolpath showing different toolpath strategies	123
Figure 5.6	Feed axes energy demand for different toolpath strategies during pocket milling of AISI 1018 steel along the x- and y- axes of Takisawa Mac-V3 milling machine	124
Figure 5.7	Surface roughness of toolpaths along the x- and y- axes of Takisawa Mac-V3 milling machine	125
Figure 6.1	Linear interpolation	136
Figure 6.2a:	Absolute coordinate programming mode (G90 Mode).....	136
Figure 6.2b	Incremental coordinate programming mode (G91 Mode).....	136
Figure 6.3	Circular interpolation with G02 and G03 codes	138
Figure 6.4	Circular interpolation with centre at the origin of CNC coordinates [120].	139
Figure 6.5	Circular path with centre not at origin of the CNC coordinates [137]	140
Figure 6.6a,b	Acceleration and deceleration phase of the feed drive as it undergoes trapezoidal and triangular axes movements respectively.....	142

Figure 6.7	Flow chart for development of NC-code based energy demand software...	146
Figure 6.8	Graphical user interface (GUI) for uploading NC program and energy demand	147
Figure 6.9	Diagram of the workpiece with machined toolpath.....	148
Figure 6.10	Spindle power demand for Takisawa Mac-V3 milling machine at zero load.....	151
Figure 6.11	Experimental power demand of NC codes	152
Figure 6.12	Predicted (theoretical) electrical energy demand distribution for slot milling from NC program.....	156
Figure 6.13	Measured power consumption profile for half bottle slot milling of AISI 1018 steel on the Takisawa Mac-V3 milling machine	157
Figure 7.1	Production sequence of hot rolled flat bars of AISI 1018 steel as adapted from Kalpakjian and Schmid [44].....	161
Figure 7.2a	Schematic diagram of the hot-rolling process showing the deformation and recrystallization of the metal being rolled [142]	162
Figure 7.2b	Schematic diagram of the cold-rolling process showing the deformed and elongated grains in the direction of working [142].....	163
Figure 7.3	AISI 1018 steel workpiece	166
Figure 7.4	Image of an 8 mm 4 flute carbide end mill cutter	167
Figure 7.5	Workpiece showing the sides considered for hardness test.....	167
Figure 7.6	Workpiece with zag toolpath strategy in the x-axis direction of the x-y plane.....	168
Figure 7.7	Hardness test for the as-received AISI 1018 steel	170
Figure 7.8	Energy demand for face milling of AISI 1018 steel when workpiece is oriented at 0 (x-axis) and 90 degrees (y-axis)	171
Figure 7.9	Variation of surface roughness measured perpendicular to the feed direction and workpiece orientations	172
Figure 7.10	Microstructure of as-received AISI 1018 steel, etched in 2% Nital solution for 15 s.....	173
Figure 7.11a, b	Microstructure of the top machined surface for AISI 1018 steel when orienting workpiece at 0 and 90 degrees respectively	173
Figure 7.12a	Sub-surface microstructure of the as-received surface (viewed from the side).....	174
Figure 7.12b	Sub-surface microstructure of the machined surface for AISI 1018	

	steel when orienting at 0 degrees.....	175
Figure 7.12c	Sub-surface microstructure of the machined surface for AISI 1018 steel when orienting at 90 degrees.....	175
Figure 7.13a	Cutting tool showing four cutting edges when machining in 0 degrees	177
Figure 7.13b	Cutting edge 1.....	177
Figure 7.13c	Cutting edge 2.....	177
Figure 7.13d	Cutting edge 3.....	177
Figure 7.13e	Cutting edge 4.....	177
Figure 7.14a	Cutting tool showing four cutting edges when machining in 90 degrees ..	177
Figure 7.14b	Cutting edge 1.....	177
Figure 7.14c	Cutting edge 2.....	177
Figure 7.14d	Cutting edge 3.....	177
Figure 7.14e	Cutting edge 4.....	177

LIST OF TABLES

Table 2.1	Breakdown of 2011 UK greenhouse gas emission by sector (MtCO _{2e}) [39]..41	
Table 3.1	ISO 14955-1:2014 - Machine tools - Environmental evaluation of machine tools - Part 1: Design methodology for energy efficient machine tools [15]...68	
Table 3.2	Takisawa Mac-V3 milling machine parameters71	
Table 3.3	Technical specification for Fluke 434 power quality analyser74	
Table 3.4	Details of AISI 1018 steel.....78	
Table 3.5	Technical specifications of 8 mm short carbide end mill cutter79	
Table 3.6	Technical specification for Vickers pyramid hardness testing machine.....81	
Table 3.7	Technical specifications for Surtronic 25 surface roughness checker82	
Table 4.1	Machine tool parameters for machining strategy.....91	
Table 4.2	Experimental plan for determining the effect of known weights on the electrical energy demand of feed axes92	
Table 4.3	Experimental design and responses for Taguchi L4 orthogonal array.....94	
Table 4.4	Response table for signal to noise ratios.....95	
Table 4.5	Gradients from the linear variation of axis power with feedrates for the Takisawa Mac-V3 milling machine along the x-axis.....100	
Table 4.6	Gradients from the linear variation of axis power with feedrate for the Takisawa Mac-V3 milling machine along the y-axis.....100	
Table 4.7	Predicted and measured energy demand of the feed axes.....110	
Table 6.1	Summary of energy consumption models for toolpaths based on CNC codes.....130	
Table 6.2	Energy demand models and their relationships to NC codes133	
Table 6.3	NC codes for absolute and incremental programming137	
Table 6.4	Additional inputs to be provided for the graphical user interface (GUI).....144	
Table 6.5	Workpiece parameters.....149	
Table 6.6	Cutting parameters149	
Table 6.7	NC code sequences for half bottle toolpath generated with hyper mill software.....150	
Table 6.8	Power demand values of NC codes determined experimentally.....152	
Table 6.9	Theoretical electrical energy demand and processing time for slot milling	

	of AISI 1018 steel	154
Table 6.10	Comparison between total predicted energy demand and time from model and software, and total measured electrical energy and time required for running an NC program	158
Table 7.1	AISI 1018 steel workpiece	166

ABBREVIATIONS

AC	Alternating current
AISI 1018 steel	American Iron and Steel Institute grade 1018
AISI H13 steel	American Iron and Steel Institute Chromium hot-work tool steels grade H steels
AJM	Abrasive jet machining
Al ₂ O ₃	Aluminium oxide
APT	Automatically programmed tools
ASCII	American Standard Code for Information Interchange
AWJM	Abrasive water-jet machining
BAP	Best available practice
Btu	British thermal units
CAM	Computer aided manufacturing
CCD	Charge-coupled device
CECIMO	The European Association of Machine Tool Industries
CEP	Complex event processing
CES	Carbon emission signature
CH ₄	Methane
CM	Chemical machining
CNC	Computer numerical control
CO ₂	Carbon dioxide
CO2PE!	The cooperative effort on process emissions in manufacturing
CRT	Cathode ray tube
CVD	Chemical vapour deposition
DC	Direct current
DECC	Department of Energy and Climate Change
DESA	Department of Economic and Social Affairs
DIN	German Institute for Standardisation
DUKES	Digest of United Kingdom Energy Statistics
ECG	Electrochemical grinding
ECM	Electrochemical machining

EDM	Electrical-discharge machining
EIA	Energy Information Agency
F-codes	Program feedrate
F-gases	Fluorinated gases
FEM	Finite element method
G-codes	Preparatory functions
GHG	Greenhouse gases
GUI	Graphical user interface
HMI	Human machine interface
HP	Horse power
IEA	International Energy Agency
IEO	International Energy Outlook
IPCC	Intergovernmental panel on climate change
ISO	International Organisation for Standardisation
KERS	Kinetic energy recovery system
kWh	Kilowatt hour
LBM	Laser beam machining
LCA	Life cycle analysis
LSD	Least significant digit
LULUCF	Land use, Land-use change and forestry
M codes	Miscellaneous functions
MATLAB	Matrix laboratory
MQL	Minimum quantity lubrication
Mt	Million tonnes
MtCO ₂ e	Million tonnes of carbon dioxide equivalent
MT Connect	Manufacturing technology connect
Mtoe	Million tonnes of oil equivalent
N ₂ O	Nitrous oxide
NC	Numerical control
OC4 USB	Optical cable for USB
OECD	Organisation for Economic Cooperation and Development
OEEM	Online energy efficiency monitoring
PVD	Physical vapour deposition

Abbreviations

RSM	Response surface method
S-code	Program spindle speed
SEC	Specific energy consumption
SRI	Self-Regulatory Initiative
STEP AP224	Standard for Exchange of Product Model specifically in Application Protocol 224
TiAlN	Titanium aluminium nitride
TiC	Titanium carbide
TiN	Titanium nitride
TiCN	Titanium carbonitride
TWh	Terawatt hour
USB	Universal serial bus
USM	Ultrasonic machining
WC	Tungsten carbide
WJM	Water jet machining
XML	Extensible mark-up language

NOMENCLATURE

$A_1, A_2, A_3, B, C, D, a, b$	Constants
α	Rake angle
a_p	Axial depth of cut
a_e	Radial width of cut
a_i	Motion (distance) travelled by the tool or axis in specified axis direction
A_{rms}	Amps root mean square
β	clearance angle
C_{0f}	Gradient of the power model of the feed drive
C_{1f}	Constant
$\cos\varphi$	Power factor
E	Energy demand of a machining process
E_{fi}	Feed axes energy demand in the specified axis direction
E_{spec}	Specific cutting energy
F	Cutting force
F_f	Feed force
F_t	Tangential force
g	Acceleration due to gravity
h	Instantaneous or varying undeformed chip thickness
h_{max}	Maximum undeformed chip thickness
I	Current
INT	Integer
k	Specific cutting resistance of the material
K	Specific cutting resistance
kHz	kilo hertz
kS/s	Kilo-samples per second
kV	kilo volt
kW	kilowatt
kVA	kilo volt-ampere
L	Distance travelled by tool or feed axis

MRR	Material removal rate
M_x, M_y	Mass of the x- and y axes
μ_x, μ_y	Friction coefficient for the x- and y- axes
$M\Omega$	Mega ohm
n	Number of tools used
$\eta_{spindle}$	Efficiency of the spindle
η_{drives}	Efficiency of the drives
P	Power drawn by machine tool
P_b, P_r	Basic and ready-state power required by the machine tool
$P_{tc}, P_{air}, P_{cool}$	Power demand for tool change, air cutting, and coolant
P_c	Cutting power
$P_{c,Weil}$	Mechanical power according to Weilenmann
P_e	Endpoint on the arc
P_f	Power requirement of the feed motor
P_{f_i}	Power of the feed axes in the specified axes direction
P_{f_x}, P_{f_y}	Power demand of the feed axes along the x- and y- axes
P_{idling}	Machine tool idling power
P_n	Previous point on the arc
P_{n+1}	Current point on the arc
P_0	Idle power demand of a machine tool
P_s	Start point on the arc
$P_{feed_axes}^f$	Power demand for feed axes
$P_{approach}^r$	Power demand for tool approach
$P_{retract}^r$	Power demand for tool retract
Q	Material removal rate
rms	Root mean square
R	Radius of the arc
s	Distance
SEC	Specific energy consumption
t	Processing time
t_{cut}	Cutting time
t_{cy}	Cycle time

t_b, t_r, t_{air}	Setup time, ready time, air cutting time
t_{tool} or t_{tc}	Time required for tool change,
T_L or T	Tool life
φ	Shear plane angle
φ_s	Swept angle
W	Weight of axis, weight of vice, weight of workpiece
W_i	Weight of the specified axis
V	Voltage
V_c	Cutting velocity or Cutting speed
V_{rms}	Voltage root mean square
v_f	Table transverse velocity
v_{fa}	Tool approach or tool retract at specified feedrate or rapid feedrate in z-axis direction
v_{fi}	Rapid feedrate or table feedrate in the specified axis direction
v_{fx}, v_{fy}	Feedrate along the x- and y- axes
$V_{material}$	Volume of material removed
x	Constant
x_e, y_e	x and y coordinates of the endpoint on the arc
x_n, y_n	x and y coordinates of previous point on the arc
x_t, y_t	Motions along the x- and y-axes
X	Ratio of the feed force to the cutting force in milling
Δu	Chord segment
$\Delta\theta$	Angular segment
θ_s	

Words count: 48,304 words

LIST OF PUBLICATIONS

- I. **Edem, I. F., and Mativenga, P. T.,** Impact of feed axis on electrical energy demand in mechanical machining processes, *Journal of Cleaner Production* (2016) 137: 230 - 240.

- II. **Edem, I. F., and Mativenga, P. T.,** Energy demand reduction in milling based on component and toolpath orientations, in *Procedia Manufacturing* 7 (2016) 253-261, International Conference on Sustainable Materials Processing and Manufacturing, SMPM 2017, 23-25 January 2017, Kruger National Park.

- III. **Edem, I. F., and Mativenga, P. T.,** Modelling of energy demand from computer numerical control (CNC) toolpaths sent to *Journal of Cleaner Production*, (Submitted on xx/xx/2016).

ABSTRACT

The University of Manchester

Isuamfon Friday Edem

PhD Mechanical Engineering

Energy Modelling for Machine Tool Axis and Toolpaths (2016)

The manufacturing sector is one of the significant consumers of electricity, with about 42.3% (8249 TWh) of the global electricity consumption attributable to this sector. This electricity is generated from fossil fuels at the power stations, resulting in increased CO₂ emission and subsequently global warming. Thus, energy efficiency could play a vital role in reducing electrical energy demand and environmental impacts in the manufacturing sector.

Mechanical machining is one of the widely used techniques in manufacturing. Machine tools consist of auxiliary units, spindle, feed axes including the x-axis, y-axis, z-axis, and the tool change system which are the main electrical energy consumers. The feed axes control the relative motion between the workpiece and cutter, and also determine the workpiece geometry. In literature, a number of studies focused on the machining process as a whole, while the energy demand for axis and toolpaths was relatively unexplored.

This PhD research was aimed at assessing the electrical energy demand in mechanical machining, focusing on feed motions and toolpaths in order to identify energy saving strategies of the machine tool. To achieve this, a current measurement device was used to acquire the current and voltage, from which the power and electrical energy requirements were evaluated. This study included (i) energy consumption analyses of the machine tool in different feed axes directions, (ii) cutting of components in different axes orientations (iii) and electrical energy demand studies of different toolpath strategies.

From the study, a new method and model for predicting the electrical energy demand of feed axes was developed. This model encompasses the weights of feed axes, machine tool vice, and workpiece placed on the machine table. Moreover, the newly developed feed axes energy demand model was integrated into other energy consumption models to predict the energy demand for toolpaths. CNC toolpaths are generated manually or by computer aided manufacturing (CAM). Enabling an energy rating of CNC toolpaths is vital to be able to quantify energy demand, compare toolpaths, and develop energy demand reduction strategies.

The results show that machining along the x-axis which carries minimal weights significantly reduced the energy demand of the feed drive, which in turn reduces the non-cutting energy demand of the machine tool.

Thus, this Thesis contributes to the improvement of energy efficiency in machining through the development of a new and novel model and method for predicting the feed axes energy demand; determining the most efficient axes and component orientation; as well as the most efficient toolpath strategy for minimal energy demand in machining. This PhD Thesis has laid the foundation model and information source for a post processor to estimate energy demand from CNC toolpaths. Such a capability was not available in CAM software or on CNC machines.

DECLARATION

I hereby declare that no portion of the work referred to in the thesis has been submitted in support of an application for another degree or qualification of this or any other university or other institute of learning.

COPYRIGHT STATEMENT

- I. The author of this thesis (including any appendices and/or schedules to this thesis) owns certain copyright or related rights in it (the “Copyright”) and he has given The University of Manchester certain rights to use such Copyright, including for administrative purposes.

- II. Copies of this thesis, either in full or in extracts and whether in hard or electronic copy, may be made **only** in accordance with the Copyright, Designs and Patents Act 1988 (as amended) and regulations issued under it or, where appropriate, in accordance with licensing agreements which the University has from time to time. This page must form part of any such copies made.

- III. The ownership of certain Copyright, patents, designs, trademarks and other intellectual property (the “Intellectual Property”) and any reproductions of copyright works in the thesis, for example graphs and tables (“Reproductions”), which may be described in this thesis, may not be owned by the author and may be owned by third parties. Such Intellectual Property and Reproductions cannot and must not be made available for use without written permission of the owner(s) of the relevant Intellectual Property and/or Reproductions.

- IV. Further information on the conditions under which disclosure, publication and commercialisation of this thesis, the Copyright and any Intellectual Property and/or Reproductions described in it may take place is available in the University IP Policy (see <http://www.campus.manchester.ac.uk/medialibrary/policies/intellectual-property.pdf>), in any relevant Thesis restriction declarations deposited in the University Library, The University Library’s regulations (see <http://www.manchester.ac.uk/library/aboutus/regulations>) and in The University’s Policy on presentation of Theses.

ACKNOWLEDGEMENTS

I hereby express my profound gratitude to the Almighty God for providing me with the enabling grace to pursue this research

I remain highly indebted to my Supervisor Prof. Paul T. Mativenga for his valuable support and guidance in the timely and successful completion of the report. His constructive criticism and encouragement has been of immense benefit to me.

I also want to thank the Federal Government of Nigeria through the Tertiary Education Trust Fund (TETFund) programme for their financial support to study in the UK. Furthermore, I would like to thank my employers, Akwa Ibom State University for giving me the opportunity to pursue a PhD in The University of Manchester, UK.

I will not fail to also thank the technicians in the Royce Laboratory of The University of Manchester, UK whose support and patience has enabled me perform my research work successfully.

Finally, my special thanks go to my lovely and caring parents and siblings for giving me the necessary mental support throughout my difficult moments in the course of this research.

DEDICATION

This work is dedicated to my dear father who gave me the inspiration and courage to undertake this PhD research, my mother, and my siblings.

CHAPTER 1

INTRODUCTION

1.1 Overview of global energy demand

The United Nations Department of Economic and Social Affairs (DESA) reported that in 2015, the global population reached 7.3 billion, with 60% of the global population living in Asia [1]. The United Nations projected the global population to reach 9.6 billion by 2050. The increase in the world population leads to increase in the demand for natural resources and especially electricity demands. Natural resources such as fossil fuels (natural gas, crude oil, and coal) are used for electricity generation at the power stations. According to the International Energy Outlook, 2013 (IEO2013), the global energy consumption has been predicted to significantly increase by 56% between 2010 and 2040 (i.e. increase from 524 quadrillion Btu in 2010 to 820 quadrillion Btu in 2040) [2].

Figure 1.1 presents the world total energy consumption projection between 1990 and 2040. From Figure 1.1, it is observed that between 2010 and 2020, global energy demand increases from 524 quadrillion Btu to 630 quadrillion Btu in 2020, and further increases to 820 quadrillion Btu in 2040. Most of the global energy increase is expected to come from Non-OECD countries (i.e. Developing or Non-Organisation for Economic Cooperation and Development countries including China, India, The Central African Republic, Chad, Chile, Colombia, Ukraine, Iran, Turkey, and Mexico) due to long term economic growth in these countries. The energy consumption in Non-OECD countries, according to the projection would increase by 90%, while that of the OECD countries (i.e. countries including the United States, the United Kingdom, Belgium and the Netherlands, etc.) would increase at 17% till 2040. Even though the demand for renewable energy sources increases yearly at 2.5%, it was projected that energy supply from fossil fuels would continue to lead in the global energy supply till 2040. The reason behind this is that the continued use of coal and natural gas is expected to increase by 1.7% yearly due to China's dependence on coal for electricity generation [2].

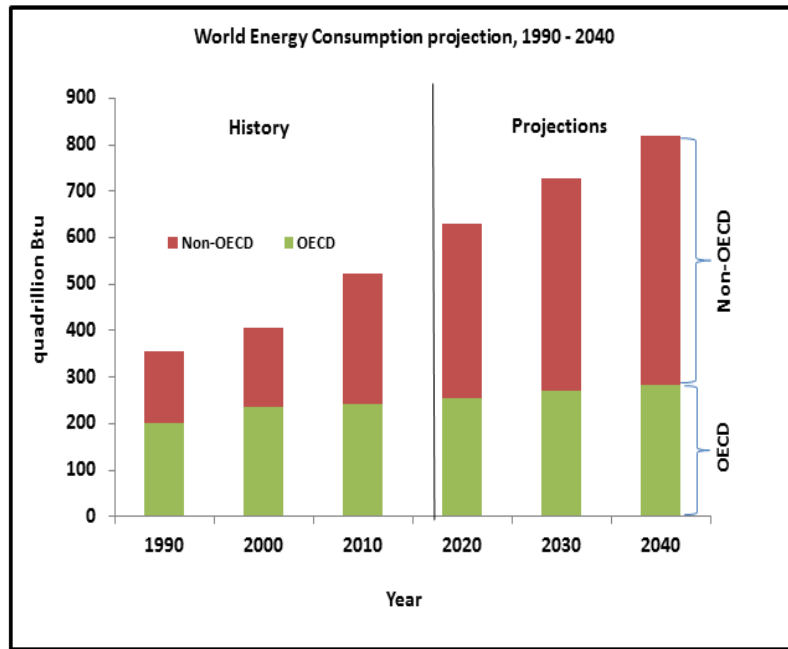


Figure 1.1 World energy consumption projection, 1990-2040 [2]

Moreover, energy related CO₂ emissions produced through the combustion of liquid fuels, natural gas, and coal is projected to increase from 31.2 billion metric tons in 2010 to 45.5 billion metric tons in 2040 [2].

In 2011, the total global energy demand from fuels by sectors was 8917.53 million tonnes of oil equivalent (Mtoe) (103710.87 TWh), of which about 28.67% was attributable to the industrial sector as shown in Figure 1.2 [3].

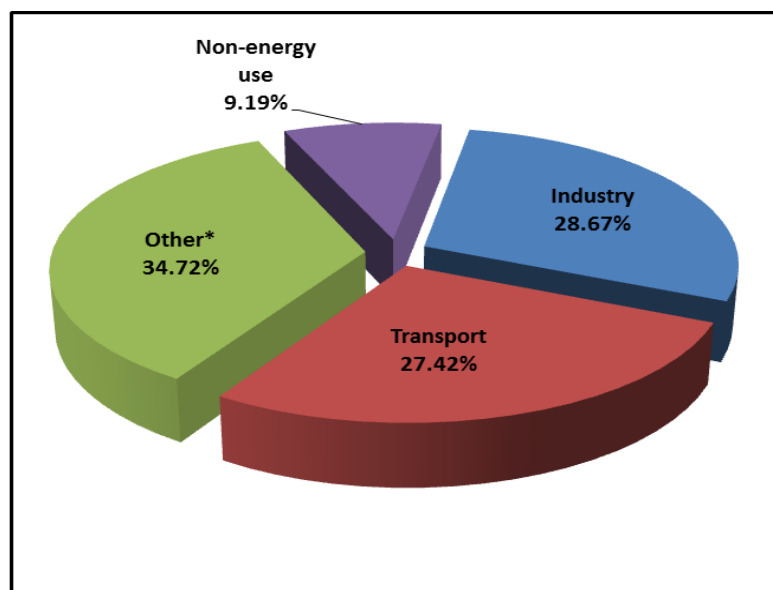


Figure 1.2 World energy consumption from fuels by sectors for 2011 [3]

*Other includes Solar, geothermal, wind, electricity and heat, etc.

It was also reported that 42% of global CO₂ emissions in 2011 was from electricity and heat generation [4]. In 2004, the International Energy Agency (IEA) reported that about 33% of the final global industrial energy use was attributable to the food, tobacco and machinery industries, together with some non-specified industrial uses [5]. In the UK, in 2011, the Department of Energy and Climate Change (DECC) reported that the total energy consumed from fuel by sectors was 203.4 million tonnes of oil equivalent (Mtoe), of which 44.4 million tonnes of oil equivalent (Mtoe) was attributed to the industrial sector, being 22% of the total UK energy consumption [6].

Additionally, the UK net emissions of carbon dioxide were reported to be 457.5 million tonnes (Mt) of CO₂ equivalent, of which 182.3 million tonnes (Mt) (including power stations and other sources of energy supply) and 10.1 million tonnes (Mt) were attributed to the energy supply and industrial process sectors respectively. Figure 1.3 shows UK carbon dioxide emission by sectors.

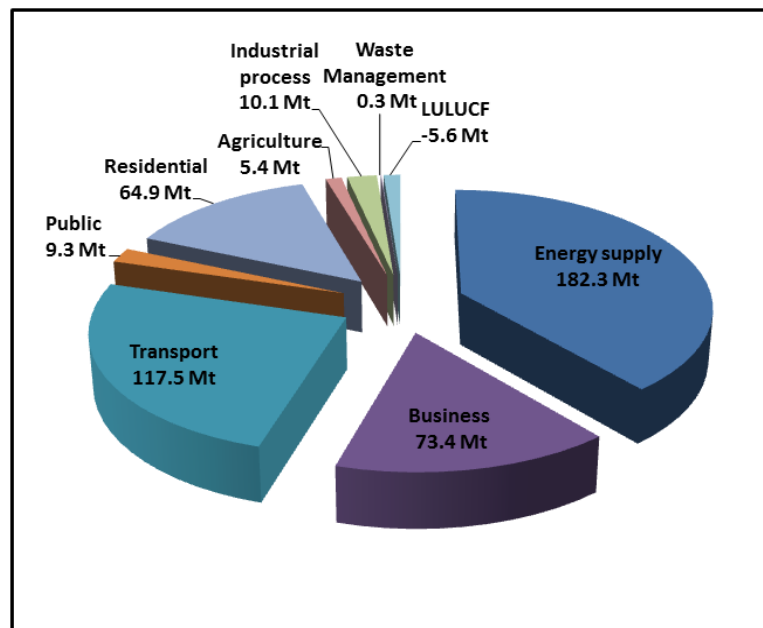


Figure 1.3 UK CO₂ emission by sectors for 2011 (in million tonnes of CO₂ equivalent) [6]

1.2 Sustainable manufacturing and machine tools

The United States Department of Commerce defined sustainable manufacturing as the production of goods with minimal use of energy and natural resources, with less effects on

the environment, and are economically sound and safe for consumers, employees and communities [7].

Mechanical machining is amongst the widely used technologies in the manufacturing sector due to its versatility and accuracy in the fabrication of products.

1.3 Environmental impact of machining

It has been reported that machine tools impact negatively on the environment through energy consumption during their use phase [8]. Dahmus and Gutowski [9] noted that the electricity consumed by machine tools increase the environmental impacts through CO₂ emissions. Furthermore, Zulaika et al. [10] conducted life cycle analysis (LCA) on the use phase of machine tools during a 10 year life span. They reported that 95% of environmental impacts of machine tools mainly from energy consumption occur during their use phase. Diaz et al. [11] conducted life cycle energy consumption analysis of two milling machines in their use phase. Reports show that 60% – 90% of CO₂ equivalent emissions result from the use phase of milling machines in their total life cycle. Santos et al. [12] performed a full life cycle analysis of an all-hydraulic system and found that the machine tool structure contributed about 40% to the global life-cycle environmental impact of machine, while about 46% was attributable to its electricity consumption during its use phase.

The European Union's Eco-design Directive 2009/125/E classified machine tools as one of the energy consuming equipment [13]. Thus, in a bid to improve energy efficiency, the European Association of Machine Tool Industries (CECIMO) Self-Regulatory Initiative (SRI) has intensified efforts towards ecological improvements and energy saving of machine tools by producing machine tools that are energy efficient, as well as cost effective [8]. Additionally, the Cooperative effort on process emissions in manufacturing (CO2PE!) [14], ISO 14955-1 [15] all prioritise energy demand reduction for machine tools. To minimise environmental impacts of machine tools, as well as improve energy efficiency, efforts have been made to achieve this through the modelling of energy consumption and identifying strategies for saving energy in machining processes [16].

1.4 Energy demand strategies in machining operation

Dahmus and Gutowski [9] studied the energy consumption of machine tools in a Toyota automobile company and reported that the auxiliary units of machine tools dominated the total energy demand by 85.2%, while the energy required for the actual material removal process was 14.8%.

Few researchers have made efforts and given suggestions on how to reduce the non-cutting energy demand of machine tools. Li et al. [17] suggested that redesigning of machine tool components can bring about a reduction in power consumption. Mori et al. [18] synchronized the spindle acceleration/deceleration with rapid feed movements in order to reduce energy consumption and therefore increase the energy efficiency of machine tools. Diaz et al. [19] proposed a method of recovering energy from the spindle deceleration by applying a kinetic energy recovery system (KERS). Kroll et al. [20] maintained that reducing the weight of machine components, which produce gravity and inertia forces results in the minimisation of the acceleration time which in turn reduces the processing time, and the overall energy. Duflou et al. [21] suggested a number of energy demand reduction strategies applicable to machine tools including the use of efficient machine tool components such as drives, pumps and spindles; technology leaps; and recovery of waste streams such as heat losses within a machine.

The main input data for computer numerical control (CNC) machining are the toolpath data [22]. Toolpaths are the paths guiding the cutter through the machined region. The choice of the best toolpath strategy is necessary for better utilisation of the milling process [23]. Efficient toolpaths may improve energy efficiency. Few researchers studied the energy efficient toolpath orientations in milling. For example, Rangarajan and Dornfeld [23] investigated the impacts of toolpath orientations with respect to the feed axes. Results show that minimal cycle time was achieved when machining at 36.9° leading to 2 – 4% of energy savings in cycle time. Monreal and Rodriguez [24] performed pocket milling using the zigzag toolpath relative to the x-axis at different angles of orientation including 0° , 30° , 60° , and 90° . Results show that machining at 90 degrees was the most inefficient angle of orientation in terms of cycle time. Kong et al. [22] investigated the movement of machine tool axes along different orientations (between 0° and 90°). From results, it was shown that maximum feedrate in the x-y plane of the machine axes occurs at 45° . Nevertheless, the effects of machine tool vice and toolpath orientations on the electrical energy demand of a

milling process, as well as the surface finish of the machined part were not explicitly documented.

Computer numerical control (CNC) machining is critical to mass manufacturing due to its capability to accept computer commands for motion control, as well as facilitating high accuracy and precision of manufactured products. Wang et al. [25] maintained that computer numerical controlled (CNC) codes can interpret a whole machining process and the performance process of the associated auxiliary equipment, as well as model and predict an entire energy profile. Few researchers modelled the energy demand of machine tools in machining by relating energy consuming components with NC codes [26], and also developed energy demand prediction software by relating the energy consuming components of a machine tool to NC codes [27]. Nonetheless, the proposed electrical energy models utilised for implementing the energy demand software failed to incorporate a feed axes energy model which takes into account the weights of feed axes, workpiece, and the machine tool vice into their energy estimation approaches.

Modelling of power and energy required in machining processes is regarded as the basis for manufacturing processes optimisation and energy demand reduction [28]. In view of this, informed decisions in selecting the most energy efficient option could be made by utilising an accurate energy consumption model to improve the prediction of energy required in machining processes [29]. Therefore, one of the motivations of this research was to assess the electrical energy demand in milling in order to develop an energy consumption model for evaluating the electrical energy demand of machine tool, as well as to identify strategies for reducing electrical energy demand in mechanical machining.

1.5 Research aim and objectives

The aim of this research was to model and analyse the total electrical energy demand in milling operations, and to develop the framework for energy demand reduction strategy in machining toolpaths. This is to support energy centric and sustainable product and process planning. The objectives are as follows:

1. To model energy demand for machine tool feed axes and define strategies for energy demand reduction.

2. To assess the influence of toolpath orientations and strategies on the electrical energy demand and surface finish of a milling process.
3. To develop a scientific base for evaluating the electrical energy consumption for CNC programs

1.6 Outline of thesis

This thesis is structured into eight chapters, and is presented in the alternative format where the core context is in the form suitable for submission to research journal and peer-reviewed conference papers. In this format, research papers are appended to a literature review and conclusions are then developed from all the papers. Further explanations on the chapters are provided in the next paragraphs. The thesis' content and chapters are illustrated in Figure 1.4.

Chapter 1 Introduction

This chapter introduces the background of the study for this research. The content of the research work was presented from the global perspective and structured in such a way to defining the aim and objectives of the investigation.

Chapter 2

This chapter provides a critical review of past, present and on-going research work on electrical energy demand and estimation methodology in machining processes.

Chapter 3

This chapter outlines the research methods and equipment, as well as details of the cutting tests and evaluation.

Chapter 4

This chapter focuses on the development of a new mathematical model and logic for predicting the direct electrical energy requirements of machine tool feed axes. This chapter was published and this is the full reference.

Chapter 5

Chapter 5 assesses the influence of machine tool vice and toolpath orientations on the electrical energy demand and surface roughness of the machined part. In this study, the electrical energy demand when orienting the machine tool vice at different angles in the x-y plane of the machine tool was assessed; surface roughness of the machined pockets were checked; the impacts of toolpath strategies on the electrical energy demand and the corresponding surface finish were investigated.

Chapter 6

This chapter provides new and scientific base methods for analytically modelling the total electrical energy demand of a machining process based on CNC toolpaths and NC-codes, as well as the implementation of the model in developing NC-code based energy demand prediction software for estimating the energy in time series.

Chapter 7

Chapter 7 presents a sensitivity analysis of the effect of the workpiece on the variability of energy in machining. In this study, the as-received workpiece material was analysed with regards to electrical energy demand and surface integrity in a milling process. This was achieved by measuring the hardness of the as-received workpiece material; analysing the microstructure of the as-received workpiece and subsurface of the machined part; assessing the electrical energy demand when orienting the workpiece in the x-axis (0 degrees) and y-axis (90 degrees) directions while cutting was maintained in one direction; and checking the surface finish of each machined surface based on their orientations.

Chapter 8

This chapter summarizes the major findings and conclusions deduced from this research work and suggests areas for future research.

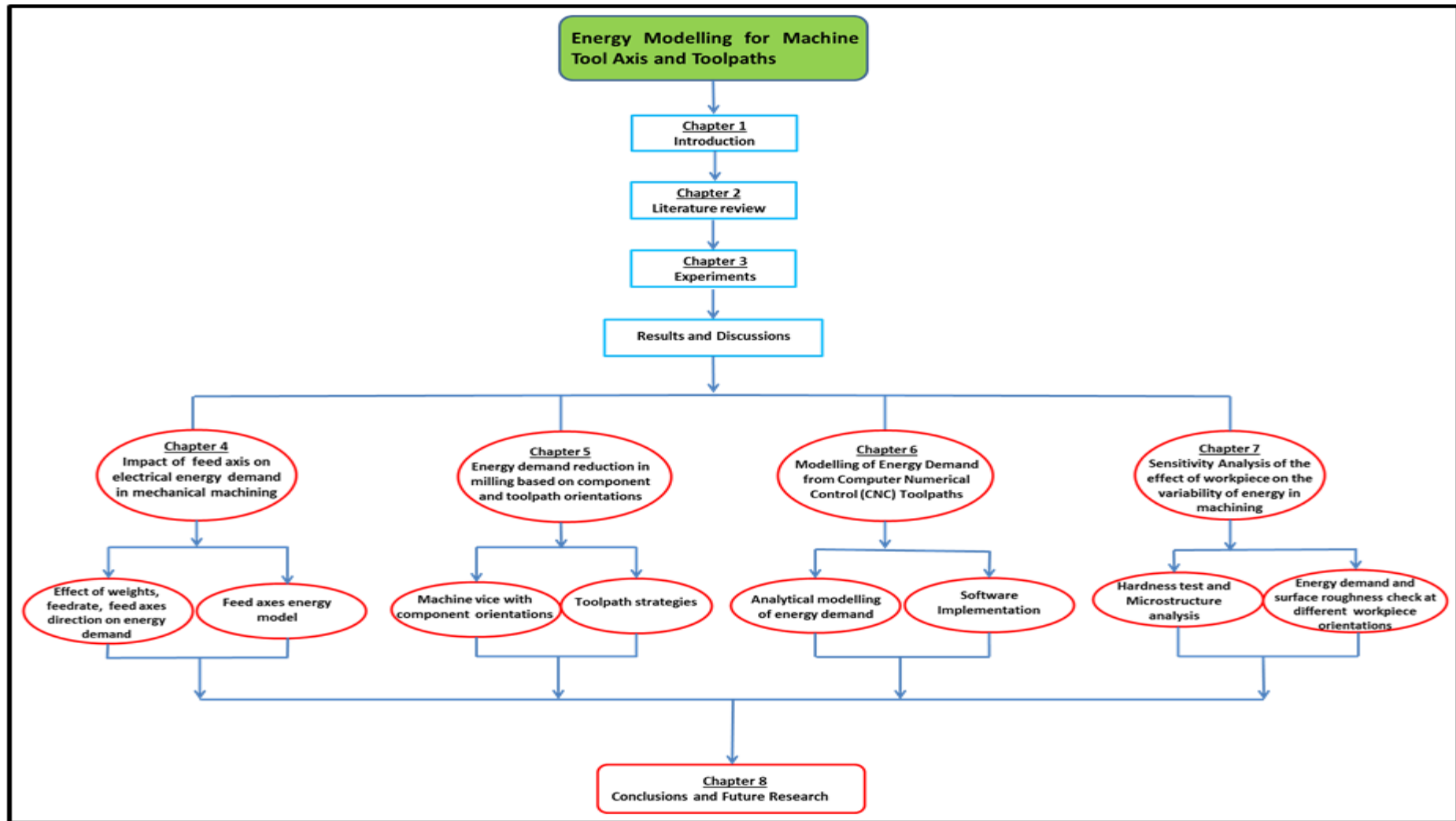


Figure 1.4 Thesis contents and chapters

CHAPTER 2

LITERATURE REVIEW

2.1 Sustainability

The World Commission on Environment and Development defined sustainability as the ability to meet the needs of the present without compromising the ability of the future generations to meet their own needs [30]. This definition further clarifies that sustainability is based on the idea that human beings and their communities are made up of unified social, economic and environmental systems which need to be balanced and maintained for the present generation and posterity [31]. Figure 2.1 shows the three sustainability principles or fundamentals.

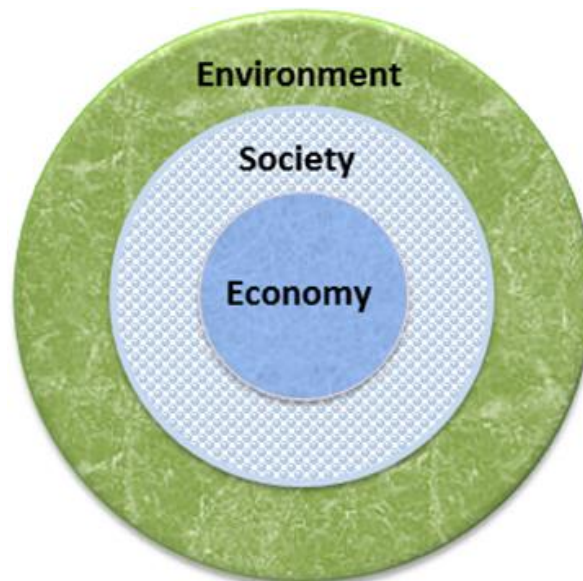


Figure 2.1 Three sustainability rings [30]

The projected scarcity of natural resources for posterity has resulted in the implementation of sustainability in the manufacturing sector due to resources consumption. This also includes strict legislations and increased environmental awareness of the people with the aim of promoting sustainability [31].

Manufacturing may be referred to as a process which involves the conversion of raw materials into products. Sustainable manufacturing is important in the manufacturing sector due to the consumption and limited availability of non-renewable resources (i.e. bauxite/aluminium, iron, natural gas, uranium, crude oil, copper, tin, lead, gold, and silver) which has led to increase in their prices [32]. The United States Department of Commerce defined sustainable manufacturing as the production of goods and services with minimal use of energy and natural resources, with minimal environmental impacts, and are economically viable and safe for consumers, employees and the community [7]. Sustainable production may also be referred to as the management of the whole product life cycle starting from the design, production, distribution, and up to the disposal stage. This involves the reduction in the use of material and energy resources [33].

The global challenges (such as climate change, poverty, ageing population, social exclusion, soil loss, and traffic congestion etc.) being faced today could be addressed using the economical, societal, environmental, and technological aspects of sustainable manufacturing [32]. Challenges are also faced in the manufacturing science and engineering context based on the design and manufacture of products with minimal negative environmental impacts, from which the main driver is technology. Technology (included in Figure 2.2) is critical for processes to convert raw materials into useful products [32].

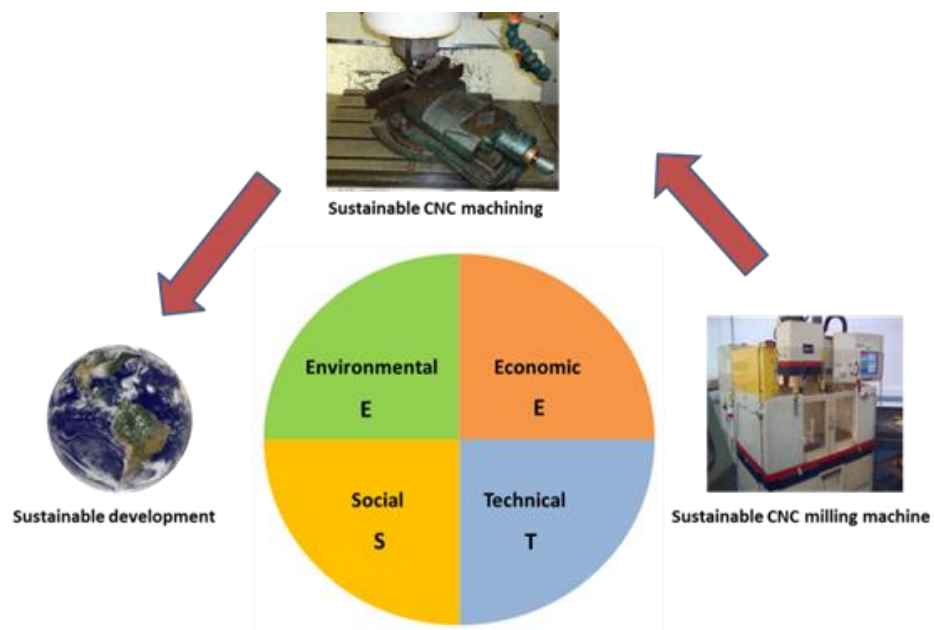


Figure 2.2 Sustainability in the context of CNC machining and machine tools as adapted from Fang et al. [34]

CNC machines are critical for promoting modern advanced manufacturing. Thus, sustainable machine tools manufacturing could be achieved by continuously improving the sustainable design and performance of machine tools (determined during the design stages of the machine tool).

The environmental impacts of CNC machines are mainly based on their energy demand and CO₂ emissions [35]. This therefore means that machine tools would continually consume energy and pollute the environment (lubricant oil) throughout its entire use phase [34]. Sustainable manufacturing in the environmental aspect may be achieved through the limited use of non-renewable resources for electricity generation at power stations and reduction in the use of lubricant oil, as well as utilising dry cutting [32].

The economic impacts of CNC machining may include parameters such as machining time and tool life, as they affect production cost and energy consumption [36]. Thus, the economic impact of machine tools could be improved by reducing the machining time which therefore results in minimal energy demand, lower production cost and improved tool life [37].

The occupation safety and health of machine tool operators are critical for the social aspect of sustainable CNC machining as they focus on the degree of injury, type of injury, and the probability of the injury [34]. For example, considerable noise is generated during the metal cutting process in the quest for improved productivity through increased speeds and feedrates. This high cutting noise could cause hearing loss to machine tool operators, and therefore affect productivity. In view of this, noise levels during the machining process should be controlled [37].

The technical aspects of sustainable CNC machines include their accuracy and process capability, which are of critical importance to customers and markets [34].

2.2 Environmental sustainability

2.2.1 Carbon dioxide emission in the United Kingdom

In the UK, in 2011, the Department of Energy and Climate Change (DECC) reported that a total of 146.87 million tonnes of oil equivalent (Mtoe) of energy was consumed.

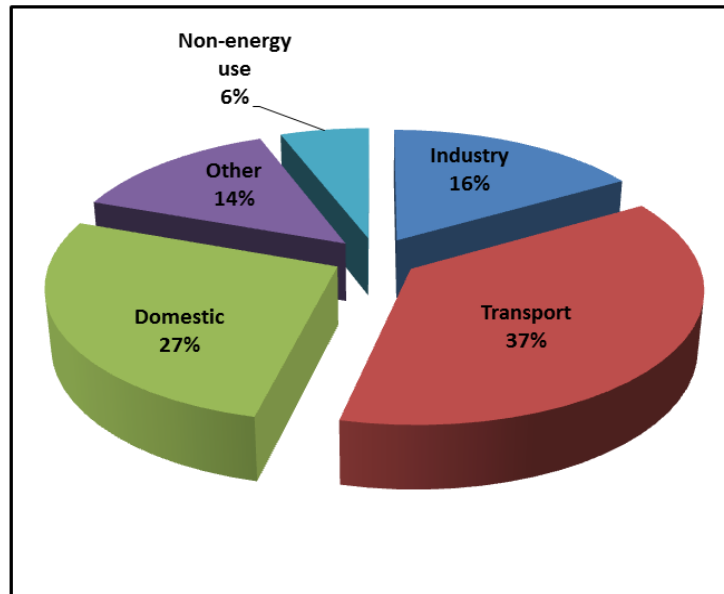


Figure 2.3 UK energy consumption by sectors in 2011 [6]

From Figure 2.3, it is shown that 24.34 million tonnes of oil equivalent (Mtoe) was attributed to the industrial sector, being 16% of the total UK energy consumption [6]. The metal products, machinery and equipment subsection of the industrial sector consumed 12.5% of the total industrial energy consumption [38].

Also in the UK, in 2011, it was reported that 368 TWh of electricity was generated from various energy sources. Gas (40%) overtook coal (30%) to become the main source of electricity generation with 147 TWh of electricity generated [38] as shown in Figure 2.4.

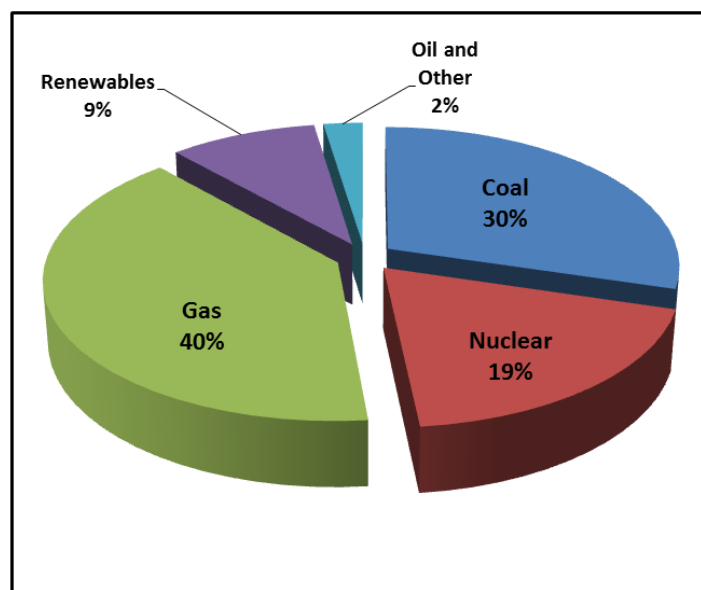


Figure 2.4 Sources of electricity generation in the UK for 2011 [38]

Therefore, high carbon energy sources accounted for the highest electricity generation source for the UK in 2011 resulting in high carbon dioxide emission through electricity generation.

The Department of Energy and Climate Change (DECC) reported that the total greenhouse gas (Carbon dioxide, methane and nitrous oxide) emission for UK in 2011 was 566.2 million tonnes of carbon dioxide equivalent ($MtCO_2e$). The total UK net carbon dioxide emission was reported to be 457.5 million tonnes (Mt). The energy supply sector's carbon dioxide emission was estimated to be 182.3 million tonnes (Mt) [39]. The breakdown of UK greenhouse gas emission by gas and end-sector is depicted in Table 2.1.

Table 2.1 Breakdown of 2011 UK greenhouse gas emission by sector ($MtCO_2e$) [39]

Energy supply	182.3
<i>from power stations</i>	144.1
<i>other Energy supply</i>	38.3
Business	73.4
Transport	117.5
Public	9.3
Residential	64.9
Agriculture	5.4
Industrial process	10.1
Waste Management	0.3
LULUCF	-5.6
Total CO_2	457.5
Other greenhouse gases	108.7
Total greenhouse gases	566.2

* LULUCF is Land use, Land-Use Change and Forestry

It should be noted that in 2011, the Land use, Land-Use Change and Forestry (LULUCF) sector did not contribute to the greenhouse gas emission. This is because plants and trees absorbed most of the CO_2 emissions as well as an efficient soil management through the conversion of land to cropland and forest land. As a result, this sector was referred to as the greenhouse gas sink.

2.2.2 The manufacturing sector and its energy consumption impacts

The global industrial energy demand was projected to increase between 2010 and 2040 from 200 quadrillion Btu (0.06 quadrillion kWh) to 307 quadrillion Btu (0.09 quadrillion kWh), which indicates an average increase of 1.4 % per annum [2]. In 2011, the U.S. Energy Information Agency (EIA) reported that the industrial sector consumed 266 quadrillion Btu (0.08 quadrillion kWh) which is 51% of the total global energy demand [40]. For example, in the UK, in 2011, the Department of Energy and Climate Change (DECC) reported that the industrial energy consumption was 24 million tonnes of oil equivalent (Mtoe), accounting for 16% of the total energy use in the UK [6]. This further affirms the contributions of the manufacturing sector to energy consumption and pollution. These conditions could be exacerbated by high demand of manufactured consumer goods, Therefore, the use of sustainable technologies and best available practices could provide significant energy saving and CO₂ reduction strategies in the manufacturing sector [41].

2.3 Machining operations

Machining is embraced in almost all the sectors of manufacturing [42]. Mechanical machining is defined as a process in which a wedge-shaped tool removes a thin layer of metal in form of chips or swarfs from a workpiece [42]. Conventional machining processes such as turning, milling, drilling, broaching and abrasive machining (grinding) are based on the removal of materials in the form of chips. However, instances may occur which may render the conventional methods of machining ineffective. These may be as a result of complex sizes of parts to be machined, mechanical properties of materials such as brittleness, surface precision requirements, high temperature of the workpiece, machining of micro workpiece that are too fragile to clamp and miniaturisation requirements etc. [43]. These challenges may be overcome by utilising non-conventional machining processes including ultrasonic machining (USM) which uses high frequency and low amplitude vibrations of a tool to remove material from the part surface in the presence of fine abrasive particles; chemical machining (CM) which are used for shallow removal of large flat surfaces; electrochemical machining (ECM) used for machining of complex shapes with deep cavities; electrochemical grinding (ECG) which are used for sharpening hard

materials such as tungsten carbide; electrical-discharge machining (EDM) used for cutting intricate components of hard materials; wire EDM used for contour cutting of curved surfaces; laser-beam machining (LBM) used for machining and drilling of holes on thin materials; water jet machining (WJM) used for machining all types of non-metallic materials to greater thickness; abrasive water-jet machining (AWJM); and abrasive jet machining (AJM) used for cleaning and cutting of metallic and non-metallic materials [44].

Machining is widely used in the manufacturing sector due to the following reasons:

- It is the cheapest method of part production when compared with other manufacturing processes, especially when few numbers of parts are to be produced.
- It offers the best dimensional accuracy of the produced parts when compared with other manufacturing processes.
- It can be adopted for the fabrication of complex part designs which may be difficult to produce with other manufacturing processes [44].

2.3.1 Basics of the cutting process

A two-dimensional orthogonal cutting, as shown in Figure 2.5 is normally used to describe the basic mechanics of a cutting process and chip formation. Orthogonal cutting is referred to as a process in which the cutting tool edge is perpendicular to the cutting direction. The model assumes that the cutter is a single point tool having a positive rake angle α and a clearance angle β . The clearance angle which is normally in the range of 6° - 7° prevents the cutting tool from rubbing on the newly machined surface thereby controlling the tool wear [45].

The un-deformed chip thickness of the material is sheared along the shear plane angle ϕ . A tool with specified cutting speed, V_c moves along the workpiece surface with the depth of cut, t_1 . A chip is formed as a result of the continuous shearing of the workpiece material along the shear plane [44].

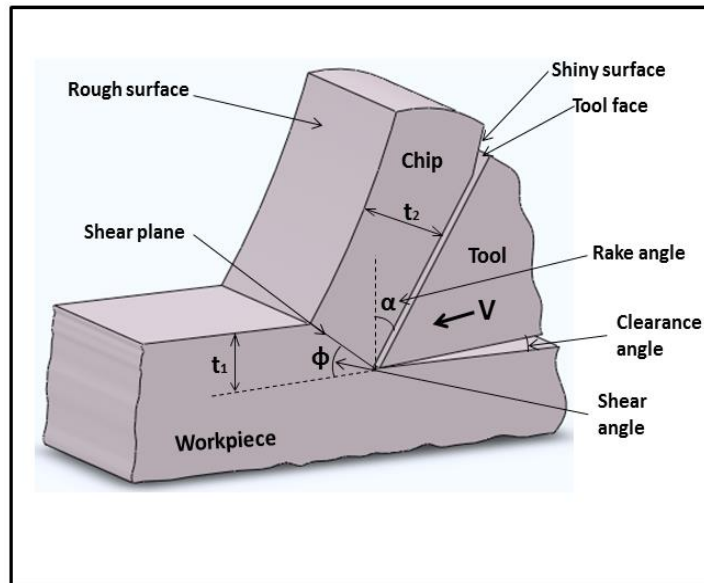


Figure 2.5 Orthogonal cutting model

2.3.2 The milling process and cutting power

Milling is defined as the process in which a rotating, multi-tooth cutter removes material in the form of chips in one revolution while travelling along various axes with respect to the workpiece [46]. This cutting process is intermittent, in that the cutter periodically engages the workpiece.

There are two basic modes of milling which include up milling and climb or down milling. In up milling, the cut thickness at the tool exit (i.e. end of cut) is at the maximum, while the cut thickness is at the minimum at the end of cut in the case of down milling process. The cutting velocity V_c and the table transverse velocity v_f of the workpiece and the cutter have the opposite sense during conventional milling (up milling), and are the same for climb milling as depicted in Figures 2.6 a, b for Up milling and Figures 2.7 a, b for Down milling process respectively.

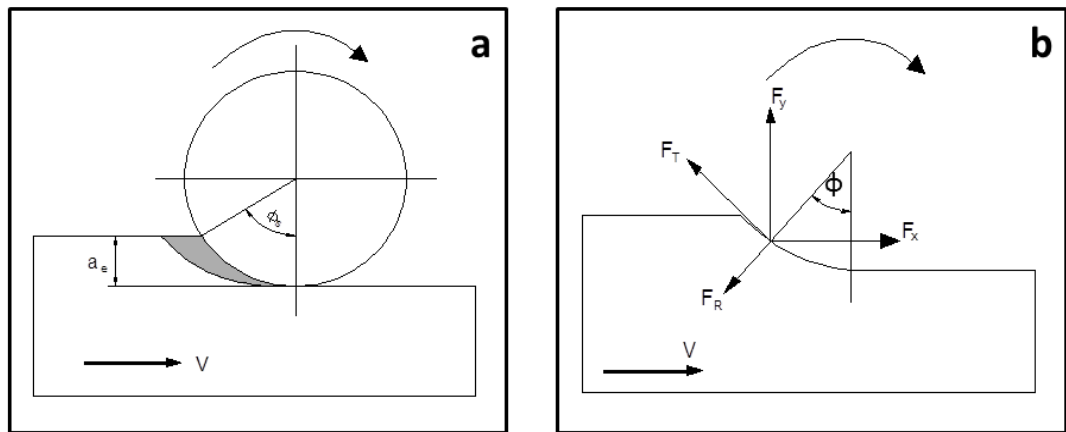


Figure 2.6 a,b: Up milling process

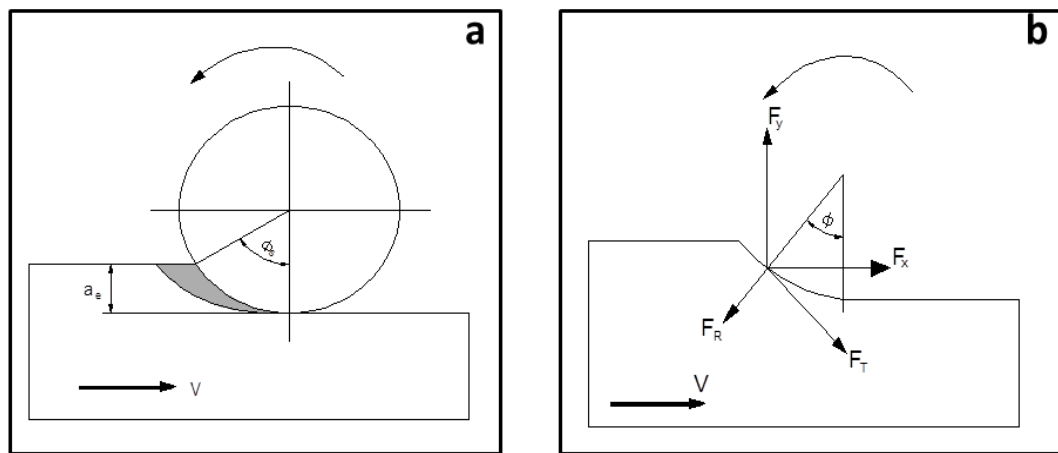


Figure 2.7 a,b: Down milling process

Figure 2.6a shows the swept angle ϕ_s of the cutting tool and the radial width of cut (a_e) during the up milling operation while Figure 2.6b shows the tangential force acting in the direction of the cutter, the cutting angle ϕ and the radial force acting perpendicular to the tangential force during up milling. Moreover, Figure 2.7a shows the swept angle ϕ_s of the cutting tool and the radial width of cut during down milling while Figure 2.7b shows the tangential force acting in the direction of the cutter, the cutting angle ϕ and the radial force acting perpendicular to the tangential force during down milling.

Figure 2.8 shows the cutting geometry in milling with varying cut thickness and the angle of cut.

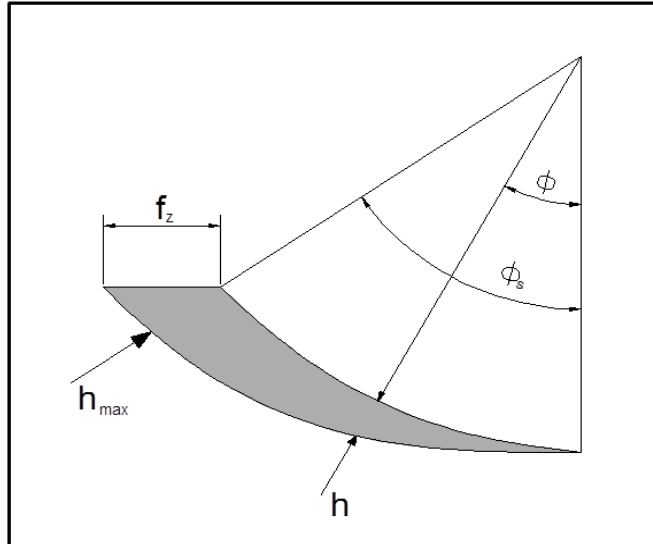


Figure 2.8 Cutting geometry in milling

where h is the varying undeformed chip thickness, h_{max} is the maximum undeformed chip thickness, ϕ is the angle of cut or swept angle in degree, ϕ_s is the swept angle or angle of cut in radian. From Figure 2.8, the undeformed chip thickness may be estimated as shown in Equations (2.1) and (2.2) [47]

$$h = f_z \sin \phi \quad (2.1)$$

$$h_{max} = f_z \sin \phi_s \quad (2.2)$$

Thus, the tangential force F_v (F_t) which acts on the tool at any location on the cutting edge to the chip thickness during milling process and proposed by Koenigsberger and Sabberwal [48] is expressed as shown in Equation 2.3.

$$F_v = k \cdot h \cdot a_p \quad (2.3)$$

where k - specific cutting resistance of the material in N/mm^2 , h - instantaneous chip thickness in mm , a_p - axial depth of cut in mm

The power demand, P_v can be estimated thus

$$P_v = \frac{F_v V_c}{60} \quad (2.4)$$

where F_v is as described above and V_c is the cutting velocity in m/min .

2.4 Environmental aspects of machining

Material removal processes such as turning, milling, drilling etc. are essential machining strategies in the determination of finished products characteristics. Machine tools produce waste resource in terms of scrap and chips. However, increase in the number of machine tools could result to high conversion of large amounts of metals into low grade scraps. This scraps, coupled with the used lubricants and coolants increase the environmental impacts of machining processes [42].

For the total life cycle of a typical milling machine, it was reported that 60% – 90% of CO₂ equivalent emissions [49] was attributable to its electricity consumption during its use phase [12].

The European Union's Eco-design Directive 2009/125/E regarded machine tools as one of the categories for inclusion in their directive due to their increased environmental impacts through energy consumption [13]. Also, the Kyoto protocol set some targets to cut down the emission of greenhouse gases [50]. Thus, more energy demand reduction strategies are necessary for energy efficiency optimisation. In light of this, one of the objectives of this research is to analyse the electrical energy demand of machine tool axes and develop strategies for energy demand reduction.

2.5 Energy efficiency of machine tools

Energy efficiency, according to ISO 14955-1:2014 [15] is defined as the correlation between the results obtained and used resources. Energy efficiency is regarded as a measure of manufacturing with less energy demand and resources to obtain a product of high quality [51]. Generally, energy efficiency may be referred to as the utilisation of limited amounts of energy to acquire similar beneficial output or services [52] as presented in Equation 2.5.

$$\text{Energy efficiency} = \frac{\text{Useful output of a process}}{\text{Energy input into a process}} \quad (2.5)$$

Efficiency is also defined as the use of minimal resources to achieve a given output [21]. Dietmar and Verl [53] suggested that machine efficiency may be referred to as the ratio of

the absolute minimum of energy that is required theoretically for a task and the actual energy turnover of the real machine. Hence, energy efficiency may be defined through the machine efficiency by relating the instantaneous power demand of the process to the real instantaneous power demand/consumption of the machine. This was recently used by Zhou et al. [54] when they presented energy efficiency of the machine tool based on the specific energy consumption (SEC), being the energy required to remove a unit volume of material as shown in Equations 2.6 to 2.8. The following Equations show the use of SEC in evaluating machine tool energy efficiency.

$$SEC = \frac{E}{V_{material}} \quad (2.6)$$

$$SEC = \frac{P_c}{MRR} \quad (2.7)$$

$$SEC = \frac{F}{a_e \cdot h} \quad (2.8)$$

where $V_{material}$ represents the total volume of removed material, t is the processing time, the material removal rate (MRR) refers to quantity of removed material per unit time, F is the cutting force, a_e is the cutting width, h is the thickness of the chip, and P_c is the cutting power.

It is important to note that the Equation in (2.6) indicates the energy efficiency of the whole machining process, while the Equations in (2.7) and (2.8) indicate the energy efficiency of the machine tool during the material removal process.

2.5.1 Electrical energy consumption monitoring of machine tools

Sustainable manufacturing could be achieved by embracing standardised methods of monitoring the energy demand of machine tools which would aid in comparable data analyses and accurate estimation of the energy efficiency of various machine tools [55]. In view of this, few studies and standards have been proposed in order to monitor the energy consumption of machine tools. For example, Behrendt et al. [55] proposed a new and logical method of determining the energy efficiency of machine tools based on

standardised workpieces. In this approach, a number of similar workpieces of different sizes were tested on nine machining centres from which the acquired data were compared with the aim of using the data for energy labelling of machine tools.

Also, several regulatory bodies presented procedures in acquiring standardised data from machine tools. In 2010, the Japanese Standards Association (JSA) published the first methodology for acquiring standardised power data based on standard workpiece for power measurements for three axis milling machines. Further work on standardised methods of acquiring energy data was presented by the International Organisation of Standardisation (ISO) in ISO 14955-1:2014 (Machine tools - Environmental evaluation of machine tools - Part 1: Design methodology for energy efficient machine tools). This standard focuses on the energy efficiency of machine tools (metal working numerically controlled (NC) machine tools) during their use phase [15].

Some researchers studied and monitored the power and electrical energy demand of machine tools. For example, Dahmus and Gutowski [9] analysed the electrical energy consumption, and the environmental impacts of machining at the system level. The authors characterised the electrical energy into energy required at the tool tip and the energy required to bring the machine to the ready for operation state. It was reported that the tool tip energy is small (14.8% of the total energy). Also, Delvodere et al. [56] investigated the energy consumption of two discrete part machines namely the press brake and the multi-axis milling machine in order to identify energy saving potentials and offer recommendations for the design improvement. The authors concluded that 65% of the total energy consumption yearly was attributable to the idle mode while 47% of the total energy requirements for the multi-axis machine tool are as a result of the idle time.

Real time event monitoring of electrical energy demand based on sensor devices or software applications for online measurement have been proposed by few researchers [57, 58]. The challenges faced in using multi-sensor systems in monitoring process and energy consumption such as integration of several sensors into commonly accepted sensor codes and protocol to form a unified monitoring scheme can be solved through standardisation [57]. Standardisation allows communication to take place within a monitoring system in a common language which offers easy access to data on sensors and enables the effective reduction of the sampling rates [59]. Standardisation also shows significant reduction in the time required to set up and develop any sensor system through the provision of a common interface within the monitoring system [60]. These standards are implemented by the use of interoperability solutions such as Manufacturing Technology Connect (MT

Connect). The aim of MT Connect standard is to provide a common means of communication between varying machines and their related devices in terms of sharing and exchanging data. MT Connect is regarded as an open communication standard which allows various machines, equipment, devices and systems to output data in a format which can be understood by another device or system using the same open communication standard [59]. The MT Connect standard is based on an XML (Extensible Markup Language) for exchanging machine readable data.

Few researchers have utilised MT Connect standard to monitor the energy consumption of machine tools. For example, Vijayaraghavan and Dornfeld [58] proposed a software-based method for automated energy reasoning which can support decision making across the multiple temporal levels. The automated energy monitoring software was developed by utilising interoperability standard such as MT Connect for acquiring manufacturing data which can normalise data exchange in the manufacturing system; and a rules engine and complex event processing (CEP) system to handle data reasoning and information processing. Diaz et al. [57] utilised MT Connect to develop a unified monitoring system for the Mori Seiki NV1500DCG milling machine centre through the successful integration of thermal sensors, controller data (including x, y, z position, speed, feed, power status, and NC program information), and a Watt Node power meter. This was necessary in order to monitor and measure power requirements wirelessly. Shin et al. [61] adopted the step-NC and MT Connect standardised interface for data monitoring and process planning data in order to analyse energy sources on the machine tool. Ak and Bhinge [62] adopted the MT Connect agent to collect time-synchronized (i.e., time stamped) raw data, such as process control parameters and power from the target machine in order to evaluate the energy required to fabricate a workpiece on a machine tool. Hu et al. [63] utilised an online energy efficiency monitoring approach to model the energy consumption of a machining process by developing a software architecture for the online energy efficiency monitoring system (OEEM system). Minimum energy cost, reduction in energy consumption and improved energy reliability can further be achieved by utilising smart grid technologies which in turn may be used to study in detail the energy delivery, transmission and generation characteristics which ensures that energy demand data can easily be transmitted to the grid, thereby activating smart grid technologies in manufacturing systems [58].

2.6 Energy consumption in machining processes at machine tool level

The spindle and servo-motor drives constitute the main sources of electrical energy demand of a machine tool. Other sources of energy consumption are: hydraulic unit, coolant pumps, cooling devices, and peripheral units (i.e. controller unit) [64].

The power and energy consumption of machine tools can be characterised based on the machining states. Kordonowy [65] categorised the energy demand of machine tools into constant energy (i.e. constant start up and constant run-time energy) and variable energy. The constant energy is the energy required at machine tool start-up and the auxiliary units (i.e. computer and display, fans, lighting, coolant pumps, hydraulic pumps, and servo motors etc.), while the variable energy is consumed during the actual material removal processes and is dependent on the material removal rate. Dahmus and Gutowski [9] characterised energy demand of machine tools into constant start-up operations, constant run time operations and machining operations. The constant start-up operation is the power required by the auxiliary units including the computer and display, fans, servos, and unloaded motors. This power is constant and is independent of the machining state, and is consumed for the entire time the machine tool is in use. The constant run-time operation power is required for work table and cutting tool positioning, and is consumed by the spindle, feed axes, feed motors, spindle motors, tool change and axes jogging. The machining power or variable power is required for the actual cutting process, and is dependent on the material removal rate or on the load applied to the machine. Figure 2.9 shows the power consumption of a Cincinnati Milacron Automated Milling machine.

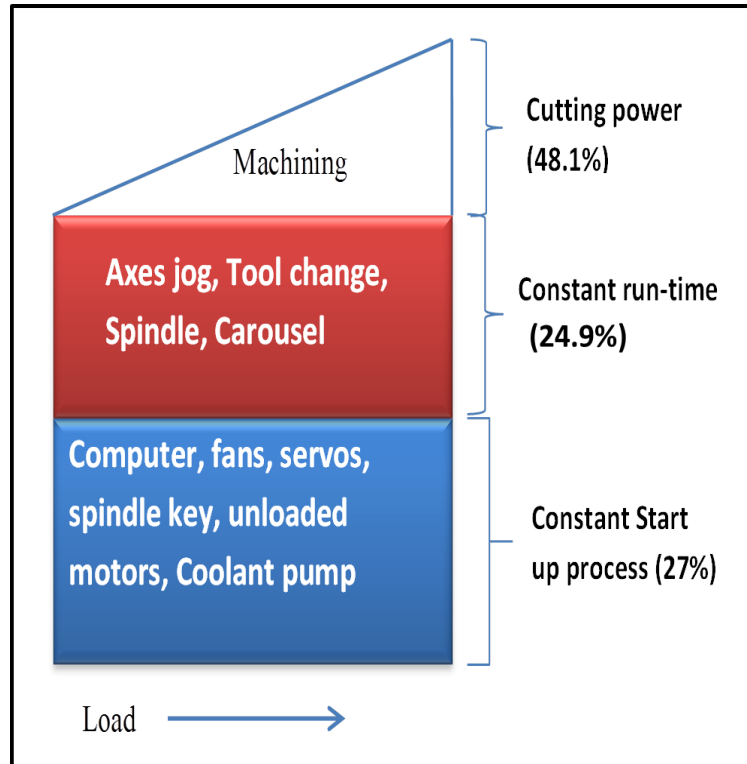


Figure 2.9 Power consumption breakdown of a Cincinnati Milacron automated milling machine adapted from Dahmus and Gutowski [9]

Gutowski et al. [16] classified the energy requirements of a manufacturing process into fixed energy demand, operational energy and tip energy demand. Balogun and Mativenga [66] proposed a new machining state called the 'ready state' in their work. The ready state is the state in which the drives and spindle movement bring the tool and workpiece to the correct, about to cut position. The ready state power consuming operations include tool change, rapid positioning and spindle rotation at defined speeds etc. Recently, in 2016, Lv et al. [67] characterised the energy required by generation motions into energy demand of air cutting motions and energy required for removing a material. These air cutting motions include spindle rotation without cutting, zero load feed axes movements, automatic tool change motion and cutting fluid spraying (i.e. ancillary motions are also part of the generation motions). Jia et al. [68] characterised energy demand into steady state and transient states.

It has been reported in literature [9, 16], that the power required for the actual material removal process is lower when compared to the total power available for the machining process. For example, the energy use breakdown of a large Toyota production machining centre shows that 14.8% of the total energy required in manufacturing was used for the

actual cutting process while 85.2% was consumed during machine idle state. Devolder et al. [56] evaluated the energy consumption of a 5-axis milling machine and the press brake. From their results, the power consumed during the idle mode of the machine tool was 1.7 kW which is substantial and therefore has a potential for energy saving. In the case of the press brake, 65% of the total energy consumed by the machine tool was attributable to the non-productive energy consumption, while 35% was used for productive purposes. Santos et al. [12] assessed the baseline power of three press-brake (bending) machines. It was reported that the baseline power for each of the machine tools were 43%, 27%, and 83% of the total energy demand. Behrendt et al. [55] evaluated the baseline power for nine different CNC machine tools. They observed that the baseline power differs for different machines with power demand ranging between 340 W and 4040 W. Reports also showed that machine tools with high ancillary components including hydraulic systems and cooling systems for increased automation had high baseline power. Li et al. [17] investigated the baseline power requirements of two CNC grinding machines, a CNC lathe with milling capability, a CNC lathe, a vertical milling machining centre and a 5-axis machining centre in order to determine and recommend energy saving strategies. It was reported that power requirements of these machine tools ranged from 1020 W to 5450 W. The results obtained also showed that the amount of baseline power consumed depends on the machine tool type and the number of ancillary components installed.

Balogun and Mativenga [66] reported that the electrical energy consumption in the basic machine state for the MHP CNC Lathe, MAC-V3 Takisawa Milling Machine, and Mikron HSM 400 High Speed Milling machining centre was 53%, 72% and 63% respectively. On the other hand, the ready state energy for each of the machines was 47%, 28% and 37% respectively. Assuming that the tip power is on average 25% of total direct electrical energy demand, the basic state and ready state power demands (constant power) makes up 75% of the total direct electrical energy required by the machine tool [69] as shown in Figure 2.10.

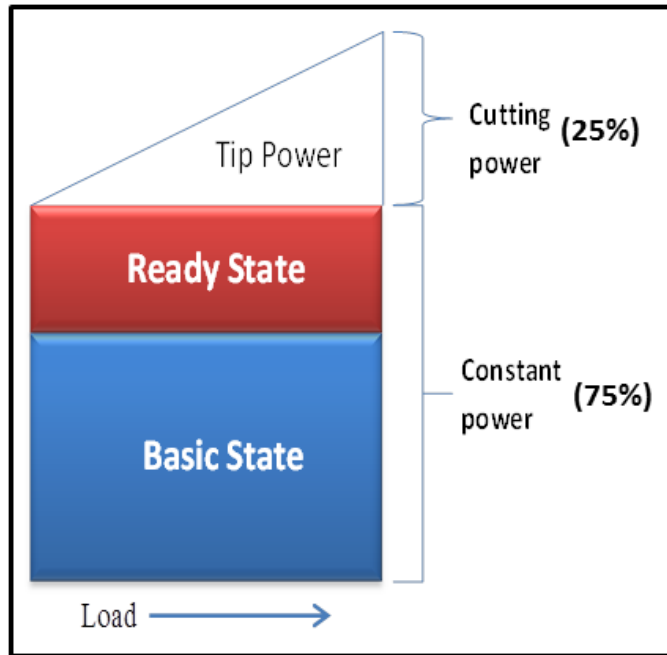


Figure 2.10 Power breakdown for Takisawa Mac-V3 milling machine [66]

Moreover, the ready state power demand varies and may increase due to the loads on the spindle as well as weights of workpieces on the feed drives. As a result, these could add up to the constant power demand of the machine tool as depicted in Figure 2.11.

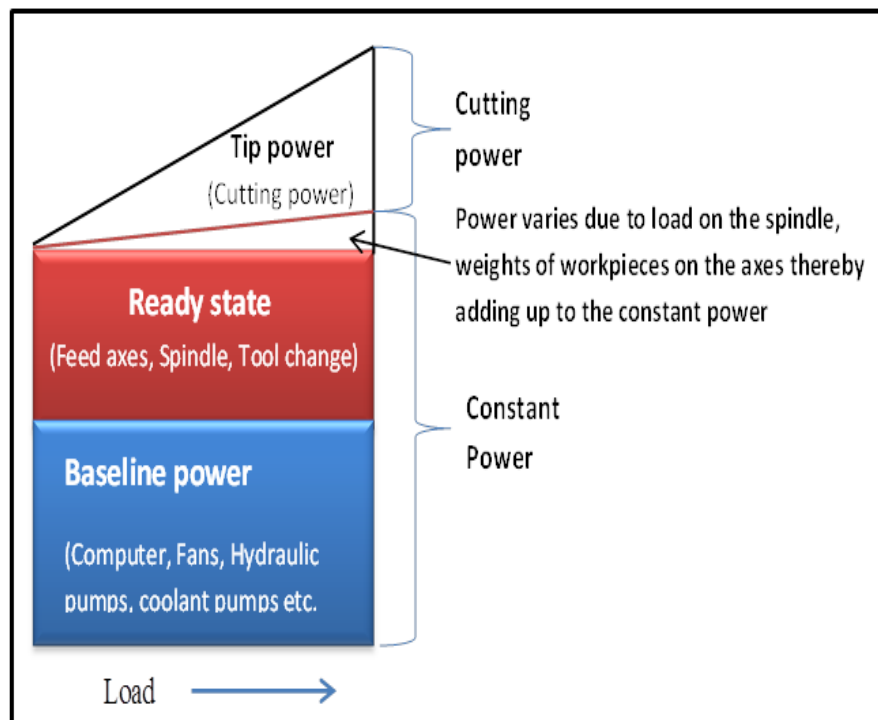


Figure 2.11 Power breakdown of the Takisawa milling machine showing the various machining states as adapted from Balogun and Mativenga [66]

Few researchers have proposed different measures for reducing the constant energy consumption of machine tools. Li and Kara [17] reported that it is possible to consider energy reduction at the design stages of machine tool components. Other energy reduction strategy proposed includes 1) switching off the machine during long idle periods, 2) through constant time breaks and 3) the provision of the Human Machine Interface (HMI) device to trigger manual operations on the machines. Mori et al. [18] developed a new acceleration and deceleration control method for machine tool energy reduction. Duflou et al. [21] proposed the use of more energy efficient machine tool components such as drives, pumps and spindles. Kroll et al. [20] reported that weight reduction of machine components tends to decrease the acceleration time and hence reduces the processing time. This is because lower gravitational and inertia force is created and the overall energy for moving masses is reduced. In light of this, Eberspacher and Verl [70] proposed a graph-based energy optimization approach to cut the energy demand during the intended and unintended idle periods, taking into account the important optimisation limitations.

2.6.1 Energy consumption models

Broadly in literature, energy models in machining can be grouped and classified thus:

- Specific energy based models
- Machine tool component based models
- CNC codes based models
- Simulation techniques based models

2.6.1.1 Specific energy based models

The specific cutting energy values for various materials, otherwise referred to as the minimum energy required to remove a volume of material from a workpiece may be used to determine the tool tip energy or the cutting energy [9, 71]. The specific cutting energy can be evaluated by normalising the total cutting energy in machining (E) by the volume of

material removed (V). This minimum energy can be influenced by the workpiece material, cutting tool material, cutting fluid, and cutting conditions etc. [72].

This principle for estimating the specific energy demand in machining was adopted by few researchers. For example, Gutowski et al. [16] presented a direct electrical energy demand model for estimating the specific energy demand at machine tool level as stated in Equation 2.9.

$$E_{spec} = \frac{P_0}{Q} + k \quad (2.9)$$

where P_0 is the constant power demand of the machine tool, and Q is the material removal rate (MRR) in mm^3/s ; k is the specific cutting energy in J/mm^3 and it is related to the workpiece hardness characteristics and cutting mechanics.

Draganescu et al. [73] developed a statistical model using the response surface method (RSM) to determine the efficiency of machine tool and specific consumed energy in machining. The model presented energy consumption of machine tools as the function of material removal rate (MRR), cutting power and machine tool efficiency. This model focused only on the tool tip energy demand while other high energy consuming units (i.e. auxiliary and peripheral units of the machine tool) were ignored. This means that the proposed model is not generic and is not suitable for determining the total energy demand.

Shao et al. [74] proposed a cutting power model which incorporates the cutting conditions and average tool wear. This model could be deployed when monitoring and measuring tool wear in a face milling process. Kara and Li [72] developed an empirical model for predicting the energy required to remove a unit volume of a material. This model was validated by undertaking cutting tests on a number of turning (Colchester Tornado A50, Mori Seiki NL2000MC/500, Ikegai AX 20, Mori Seiki SL-15, Nakamura TMC-15) and milling (Fadal VMC 4020, Mori Seiki Dura Vertical 5100, DMU 60P) machine tools, with a 90% accuracy prediction of specific energy consumption of the processes. However, this model only considers the energy demand at tool tip and ignored the constant and variable energy demand of the machine tool.

Also, Schlosser et al. [75] proposed a model to evaluate the specific cutting energy of a drilling process. Li et al. [29] presented an energy consumption model from a function of material removal rate and spindle speed in order to evaluate the relationship between

process parameters and energy demand in machining based on empirical modelling and thermal equilibrium. Yan and Li [76] utilised the grey relational analysis and the response surface methodology to determine the optimal cutting parameters (including feedrate, spindle speed, depth of cut, and width of cut) that would enhance the identification of the most efficient cutting parameter to achieve minimal cutting energy demand, improved surface finish, and increased material removal rate in a milling process. It was reported that machining at low spindle speeds results in minimal energy demand. Uluer et al. [77] proposed a theoretical model for estimating the tip energy required for producing a rotational part, as well as the corresponding CO₂ emission with regards to the volume removed for each Standard for Exchange of Product Model specifically in Application Protocol 224 (STEP AP224) feature and the specific cutting energy for the given material. Balogun and Mativenga [78] investigated the specific electrical energy consumption of a machine tool with respect to the thickness of material removed. They reported that machining at feedrates greater than the tool edge radius could result in the reduction of the specific cutting energy consumption of the roughing process. Velchev et al. [79] developed an empirical model based on the relationship between the specific energy consumption and material removal rate when turning steel. This is critical for cutting parameters optimisation for minimum energy demand.

In 2016, Liu et al. [80] investigated the specific energy required for dry milling of AISI H13 at the process level, machine tool level, and the spindle level, as well as taking into consideration the influence of tool wear and process parameters on the specific energy demand at these levels. From their results, it was observed that tool wear is directly proportional to the total specific energy demand at the process level. Jia et al. [81] proposed a procedure for modelling the electrical energy demand of a variable material removal process (MRR). The model takes into consideration the varying power changes and the effects of cutting conditions on the specific cutting energy required for machining a workpiece. Sealy et al. [82] developed a power model for estimating the specific energy demand which includes depth of cut, width of cut, cutting speed and the chip load. Liu et al. [83] utilised the force model to analytically model the cutting power required at the tool tip.

Further models were developed empirically based on the relationship between the total power demand and cutting power at the tool tip in order to determine the effects of specific cutting parameters on power demand. Of all these models based on the specific energy evaluation, none has been able to comprehensively determine the total energy demand

during the machining operation. Hence, the need to further determine this hypothesis further in such a way as to proffer better, robust and generic energy model for machining energy.

2.6.1.2 *Machine tool component based models*

The machine tool components include auxiliary units, peripheral units, coolant pumps, spindle, feed axes, tool change system, axes chiller, chip conveyer etc.; and these were defined to influence the energy requirement in machining.

Mativenga and Rajemi [84] further modified Gutowski et al.'s [16] model by integrating the spindle power demand characteristics. It was reported that the spindle power increased linearly with spindle speed at zero cutting load. Mori et al. [18] proposed a mathematical model for evaluating the power consumption of a machine tool while in normal operation. This model takes into consideration the positioning and acceleration of the spindle immediately before or after the tool change operations, cutting process, and after the machining operation. Nevertheless, the power consumption model focused mainly on the machine tool spindle thereby masking the process variable and the feed axes power consumption.

Avram and Xirouchakis [85] studied the mechanical energy requirements of the spindle and feed axes. The model included the energy required for acceleration and deceleration of the spindle and feed axes, cutter positioning, speed values extracted from the APT file, cutting forces, as well as the energy required at constant speeds of the spindle and feed axes. They reported that low speed machining increases the energy consumption by 32.12%. Balogun and Mativenga [66] proposed a direct electrical energy consumption model for milling machine tools. This model proposed the electrical energy consumption of the machine tool components including the auxiliary and peripheral units. However, the power demand of the feed axes was not explicitly modelled. Calvanese et al. [86] proposed an analytical model to evaluate the total energy consumption in a milling process and accurately model the machine tool energy consuming components. Moreover, the effect of weights on the power demand of machine tool axes was not considered.

Jia et al. [87] proposed a model for estimating the total energy demand of a machining process on the CK6153i lathe. This model relates the different machining states with the

energy requirements of basic motions of the CNC machine tools. Results show that the highest energy consumer was Therblig-SR (Therblig for spindle rotation) which consumes about half of the total energy demand. However, the study ignored the contribution of the weights of feed axes, workpiece, and machine tool vice on the therblig feed axes energy. Building on Jia et al. [87]'s work on Therbligs, Lv et al. [88] proposed an improved methodology for estimating energy demand of machine tools. This model has some limitations in that the therblig feed axes was not explicitly modelled to include the weights of the feed axes, workpiece, and machine tool vice. Li et al. [89] assessed the energy demand of machine tools in order to model their energy consumption in spatial and temporal dimensions for quantifying the energy flow. In this work, the energy demand for producing three different parts (performing three tasks) on two vertical machining centres including HAAS VF5.50 and PL700, a manual lathe CD6140A, one CNC lathe C26136HK and one air compressor in a machine tool workshop was assessed. Nevertheless, the power of the feed axes was not explicitly modelled to incorporate the weight of the axes, weight of the vice, and workpiece. Campatelli et al. [90] reported that energy reduction strategies can be achieved if machining on the milling machine tool is conducted on the x-axis. This is because the y-axis required more power than the x-axis as a result of the attached masses. Yoon et al. [91] disintegrated the energy demand of a milling machine into individual energy consuming elements, and Lv et al. [67] reported that the power required for milling and the non-cutting motions of the machine tool were significantly influenced by the machine tool, while the power consumption of turning is almost independent from the machine tools.

In 2016, Albertelli et al. [92] proposed a new analytical model for predicting the energy required by the machine tool to produce prismatic workpiece components. The model was developed by relating the power demand of each machine tool component including the auxiliary systems, feed axes, axes chiller, tool change system, chip conveyor and the spindle system to the cutting parameters. In addition, optimisation of the energy demand based on feedrate, cutting speed and radial depth of cut was undertaken. They showed that machining at maximum radial depth of cut and minimum feedrate could result in minimal energy demand. Lee et al. [93] proposed a generic model for estimating the energy demand of various machine tools by disintegrating the cutting energy from the energy demand of the machine tool components. They proposed a power profile simulator that evaluates the power profile before and after machining operations. Recently, Altintas et al. [94] proposed an analytical model for predicting the energy demand in milling prismatic

components based on the Standard for the Exchange of Product (STEP) Application Protocol 24 for the material properties of the prismatic part and volumetric information. This study is limited due to the fact that NC codes were not used to estimate the total energy demand in the milling process.

In all these studies, it can be deduced that the presented energy models are generic and cannot be adopted to evaluate the total energy demand of machining operations. This is because the models ignored the contributions of the machine tool feed axes, weights of the feed axes, workpiece and machine vice to the power demand. Also, the NC codes (linear and circular interpolations) were not related to energy consuming components for estimating the total electrical energy demand in machining. Hence the need for a more comprehensive energy model that would incorporate the feed axes and NC code characteristics. These should also include the attributed weights on the machine tool axes.

2.6.1.3 CNC codes based models

A complete energy profile could be evaluated and modelled based on a set of computer numerical controlled (CNC) codes. CNC codes determine the operational modes and positional movement of machine tool axes and can interpret machining process and the dynamic processes of the associated auxiliary equipment. Few researchers evaluated the energy demand of machine tools based on CNC codes. For example, Narita et al. [95] proposed an NC code based software for predicting the environmental impacts of a machining process. The outputs of the software related the environmental impacts, cycle time and the set up time to the total energy requirements. Also, Avram and Xirouchakis [85] evaluated the energy requirements of the feed axes, spindle, and load/unload cycles of the machine tool based on toolpaths generated from NC programs. He et al. [26] proposed a model through an analytical approach of modelling the electrical energy demand of a CNC machine tool by relating the energy consuming components to NC codes. Although the model can be used to estimate the total energy consumption of the machine tool including the feed axes and spindle, it neglected the influence of weights on the power/energy demand of machine tool axes. The model also defined the constant power of the machine tool via the power of the fan motor and servo motor. Therefore, adopting this utility undermine the inclusion of other auxiliary components such as

lighting, coolant pump motor, hydraulic pump motor, computer and display panel etc. in the energy model.

Kong et al. [22] proposed a web-based energy consumption model with regards to toolpaths strategy in order to estimate the energy requirements of a CNC machining operation, and to assess the corresponding environmental impact of the machining process. It can be deduced from their work that different toolpath strategies affect the energy and time required in machining the same component. However, this study did not include the weights of the machine tool feed axes, workpiece and machine tool vice in the feed axes power model. Aramcharoen and Mativenga [96] presented a methodology for predicting the energy consumption of mechanical machining processes by focusing on toolpaths and energy states. In addition, their model also included energy consumption for cutting fluid and the influence of tool wear. Significant energy savings can be achieved by accurately selecting toolpath orientations due to its influence on cycle time. It should be noted that the inclusion of the feed axes and weight on the proposed model could enhance its generic usage.

In 2015, Guo et al. [97] incorporated the simulation of machining processes (i.e. turning and drilling) for energy demand prediction. The model was validated by performing face turning, external turning and grooving operations. Pavanaskar and McMains [27] utilised the geometric characteristics of toolpaths in estimating the energy consumption of CNC machine tools. From the proposed model, web-based software for predicting energy demand based on NC codes was developed. Even though this study provided insight into the development of NC-code based energy consumption software, the weights of the feed axes, machine tool vice and workpiece were not incorporated in explicitly modelling the feed axes power. Recently, Balogun et al. [98] utilised NC codes and CNC toolpaths as the basis for developing an e-smart software which was implemented using their previously proposed energy consumption model. The machine tool block was disintegrated into energy consuming units followed by the NC code analysis for the total electrical energy demand computation. Yingjie [64] maintained that energy saving opportunities in machine tools can be obtained by utilising optimal machining strategies (toolpath strategies or optimum axes orientations) and optimal cutting parameters. In view of this, Rangarajan and Dornfeld [23] proposed a method of feedrate losses reduction due to abrupt toolpath changes and to determine the best feedrate for machining a segment. They reported that energy savings of 2 – 4% in cycle time may be achieved.

From the reviewed work above, CNC code based energy estimation is another important basis for energy evaluation; however it is also important to incorporate weights of the feed axes, machine tool vice, and workpiece in the feed axes energy consumption model. This is important in order to relate the machine tool energy consuming components to their corresponding NC codes. With this in mind, it could be possible to compare machining energy based on the theoretical, experimental and simulation results.

2.6.1.4 Energy consumption modelling based on simulation techniques

Simulation could be a suitable option for modelling the power required by machine tools to perform a machining task due to the complexity of some production systems which might be difficult to estimate the direct electrical energy demand through measurements. However, this could be solved by utilising the simulation models and approaches for determining energy efficiency of the machine tool [99]. In view of this, few researchers developed simulation models for predicting the electrical energy demand in a machining process. Dietmar and Verl [53] proposed a lean, scalable modelling procedure which enhances the prediction of machine tool energy efficiency with regards to the operation and design of the machine tool. This model was based on discrete states and transitions of the machine tool. They presented an improved modelling technique for assessing the energy efficiency of machine tools based on operating states. A usage profile (which takes note of the points of time when the machine changes its operational state) was established offline using numerical control program simulation. They found that power consumption of the machine tool varies with the operating states. Nevertheless, the model did not take into account the dynamic behaviour of the machine tool.

Shao et al. [100] proposed a virtual numerical control (NC) machining model for evaluating the environmental impact of machine tools (analysing the sustainability impacts of machining and determine various ways to improve the sustainability performance of machining processes in a virtual environment) based on Life Cycle Assessment (LCA). Rahimifard et al. [101] proposed a detailed simulation model for the estimation of the total energy demand of manufacturing a product, with 20-50% reduction in energy requirements due to enhanced production and product design. Additionally, Seow and Rahimifard [102] proposed a new strategy for the energy demand model that is based on data obtained at

plant and process level for manufacture of a product. Malagi and Rajesh [103] developed a software to estimate the cutting forces. The model incorporates the depth of cut and feedrate. Thiede et al. [104] developed a method for monitoring energy efficiency at the factory level. It was reported that energy savings of about 6% was realised from the simulation model. Eberspächer et al. [105] presented a detailed power simulation model for monitoring energy demand through controlled signal and information systems. Also, Herrmann et al. [106] proposed an energy-based simulation model for the design of manufacturing systems. Two instances were considered for the model validation. Firstly, the electricity consumption of a highly automated aluminium die casting process chain and secondly, the direct electricity demand, the compressed air and steam of weaving mill with over 40 weaving machines were investigated. The validation results for both instances depicted a value of model consistency greater than 95%.

Furthermore, few number of researchers have also analysed energy efficiency at the manufacturing systems or factory level based on discrete event simulation. For example, Fysikopoulos et al. [107] proposed a simulation model to investigate the energy consumption of an automotive assembly line with respect to various scenarios and demand profile. Nils et al. [108] presented an energy block methodology for energy demand forecast. In their model, each of the operating state of the production equipment is characterised as part of the specific energy demand for the respective operating states. In addition, Larek et al. [109] presented a discrete event simulation method for modelling machining operations, as well as generating power demand profiles and energy footprints.

The work in Larek et al. [109] was further expanded by Rentsch and Heinzl [110]. In their work, a model which estimates the resources demand and process operations based on the NC codes, as well as estimating the processing cycle time was developed based on discrete events of process parameters for a milling process. In addition, the energy requirement, tool wear, coolant, volume of material removed and the operating time were considered for the consumption optimisation of the machine tool. Abele et al. [111] proposed a simulation approach to develop a generic model for estimating the energy demand of machine tools. This involved the disintegration of machine tool into a number of components. This approach was further utilised by connecting the hardware of the machine control system to utilise the NC- code information for predicting the energy required to perform a specific production task. Braun and Heisel [112] proposed a model for estimating and predicting the electrical energy demand in turning process by using virtual CNC-Module that generates toolpath data from given (simple DIN) G-Code sets.

Frigerio et al. [113] utilised discrete event simulations approach to model the energy demand of complex machine tools based on the activation (ON) and deactivation (OFF) of functional components at different operation states of the machine tool. The energy demand of these functional components is modelled using automata theory with regards to the operation states and discrete events.

In another development, Pervaiz et al. [114] proposed a methodology for estimating the energy demand and environmental impact of the machining process. This is achieved by utilising the finite element methods (FEM). The FEM simulation adopted was the DEFORM-3D software package. It was reported that geographical location of the machine tool during its use phase significantly influences its CO₂ emission. This is because the carbon emission signature CES varies at different geographical locations.

From the reviewed literature, it can be deduced that although simulation based models can be one of the methods through which energy consumption in machining can be estimated, the methods reviewed ignored the linear and circular interpolations (NC codes) and the impact of weights of the feed axes were not included in the energy consumption software. Hence, the need for new and compressive energy estimation model to be investigated.

2.7 Knowledge gaps identified

The reviewed literature included sustainability concepts, energy demand in machining. From the reviewed literature, the following knowledge gaps were identified:

1. Modelling of the electrical energy required in machining processes is regarded as the basis for manufacturing processes optimisation and energy demand reduction. The proposed models found in literature has not focused on feed axes power and (including the weights of feed axes, vice, workpiece, and the feed force) the electrical energy demand. It is therefore critical to further investigate and address this knowledge gap in order to be able to evaluate the total energy demand in toolpaths and to develop strategies for energy demand reduction.

2. Few researchers have studied the effects of toolpath strategies on energy demand. However, the impact of toolpath orientation and strategies on the electrical energy demand and surface finish of the machined part was not explicitly studied.

3. The influence of interpolation modes (i.e. rapid move, linear and circular interpolation) on the electrical energy demand of CNC toolpaths was relatively unexplored. Thus, this knowledge will enable comparison of alternative machining strategies in order to reduce energy consumption.

CHAPTER 3

DEVELOPMENT OF THE EXPERIMENTAL APPROACH AND ITS IMPLEMENTATION

3.1 Introduction

Mechanical machining consumes electrical energy, and modelling energy demand requires a strategy for sustainable optimisation of processes and parameters. This is necessary for developing recommendations for energy demand management. To achieve this, milling tests were performed and the measured current and voltage were used to derive power demand and energy consumption. This information formed the basis of the energy modelling and process study. Thus, this chapter presents details of the experimental setup and procedures.

3.2 Experimental setup and procedures for the research

Machine tools require electrical energy to perform various complex tasks. Thus, the electrical energy required by the machine tool is influenced by the power consumed and the cycle time duration based on the actual machining states. The challenge in modelling energy demand is that the machine tool executes different activities during the cutting process. In view of this, controlled experimental conditions were adopted in the course of this research.

Figure 3.1 presents the experimental setup for current and voltage measurement, as well as for the surface roughness of the machined component. This work was performed by designing the experimental plan, varying the cutting parameters (i.e. feedrates, spindle speeds), as well as selecting the appropriate workpiece material (AISI 1018 steel). Based on the event streaming and current monitoring technique, the current and voltage drawn by the CNC machine were directly measured over a period of time using the 3-phase FLUKE

434 Power Quality Analyser which enabled the calculation of power requirements during the operation of the machine, and hence the energy demand. Also, the surface roughness of the machined components was checked using the Surtronic 25 surface roughness checker in the direction perpendicular to the lay.

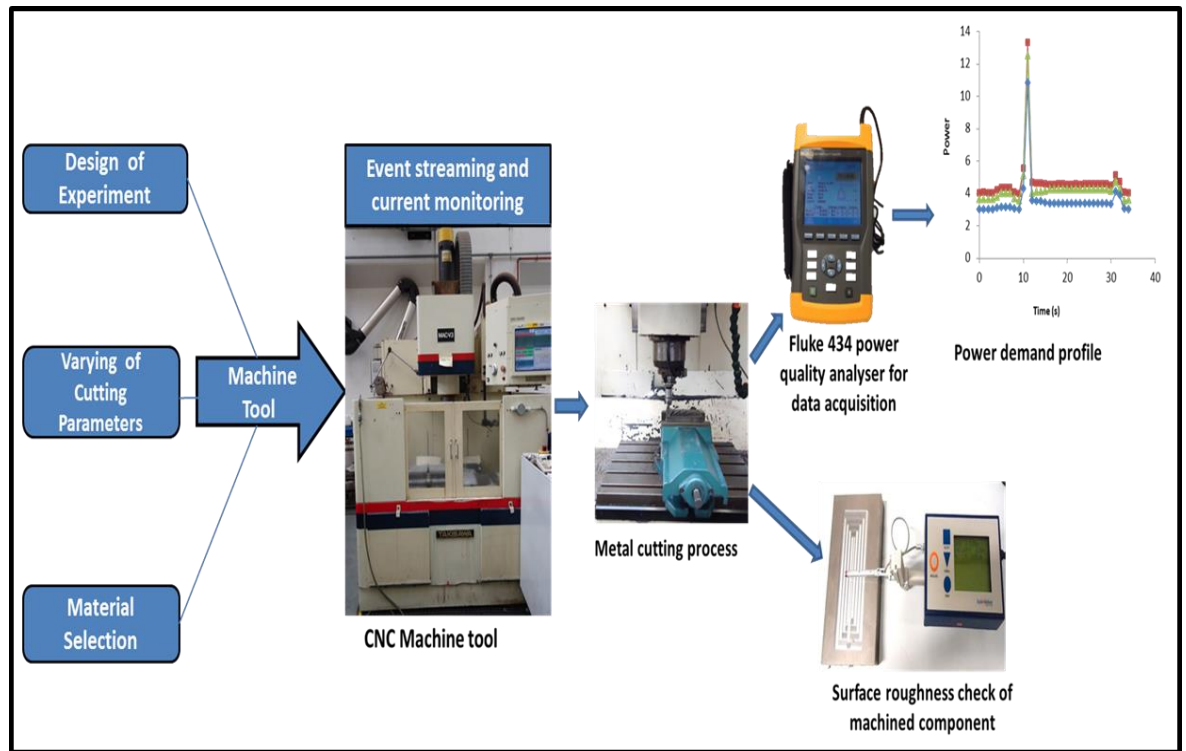


Figure 3.1 Experimental setup for energy measurement and surface roughness check of the machined part

Detailed Experimental procedures for measuring current consumption during the cutting tests, checking the surface roughness of machined surfaces, and microstructure analyses of the as-received workpiece surface and subsurface are further explained below.

3.2.1 Experimental procedures for measuring current and voltage in machining

For all set of machining trials conducted, standardized research methods as shown in Figure 3.2 were carefully considered as follows:

- The current measurement point was identified at the back of the machine tool

- The baseline power requirement was measured based on ISO 14955-1:2014 [15] definition of machine tools operating states as shown in Table 3.1. At this state (ready for operation), the mains power is on, the machine control is on, peripheral units are on, the machining processing unit is on-hold, machine motion unit is off, machine axes are not moving, and spindle is not rotating.
- The current drawn by moving each axis at varying feedrates (when no workpiece was placed on the table and the spindle not rotating) was measured. All measurements were recorded based on ISO 14955-1 operating state definition for machine tools (i.e. processing state but no machining, spindle off) in which the mains power is on, machine control is on, peripheral units are on, spindle is off, machine axes are moving.
- The current drawn by the machine table when different weights were placed on the table was measured.
- Finally, the electrical current consumption during the material removal process was measured. At this state, the mains power is switched on, machine control is on, peripheral units are on, machine processing unit is on, machine motion unit is on and the machine axes are moving to perform the material removal process.

Table 3.1 ISO 14955-1:2014 - Machine tools - Environmental evaluation of machine tools - Part 1: Design methodology for energy efficient machine tools [15]

Operating States	Mains	Machine control	Peripheral units	Machine processing unit	Machine motion unit	Machine axes
OFF	OFF	OFF	OFF	OFF	OFF	NOT MOVING
Stand by with peripheral units off	ON	ON	OFF	OFF	OFF	NOT MOVING
Stand by with peripheral units on	ON	ON	ON 1)	OFF	OFF	NOT MOVING
Ready for operation	ON	ON	ON 1)	HOLD	HOLD	NOT MOVING
Warm up	ON	ON	ON 1)	ON NO MACHINING	ON	MOVING
Processing	ON	ON	ON 1)	ON MACHINING	ON	MOVING

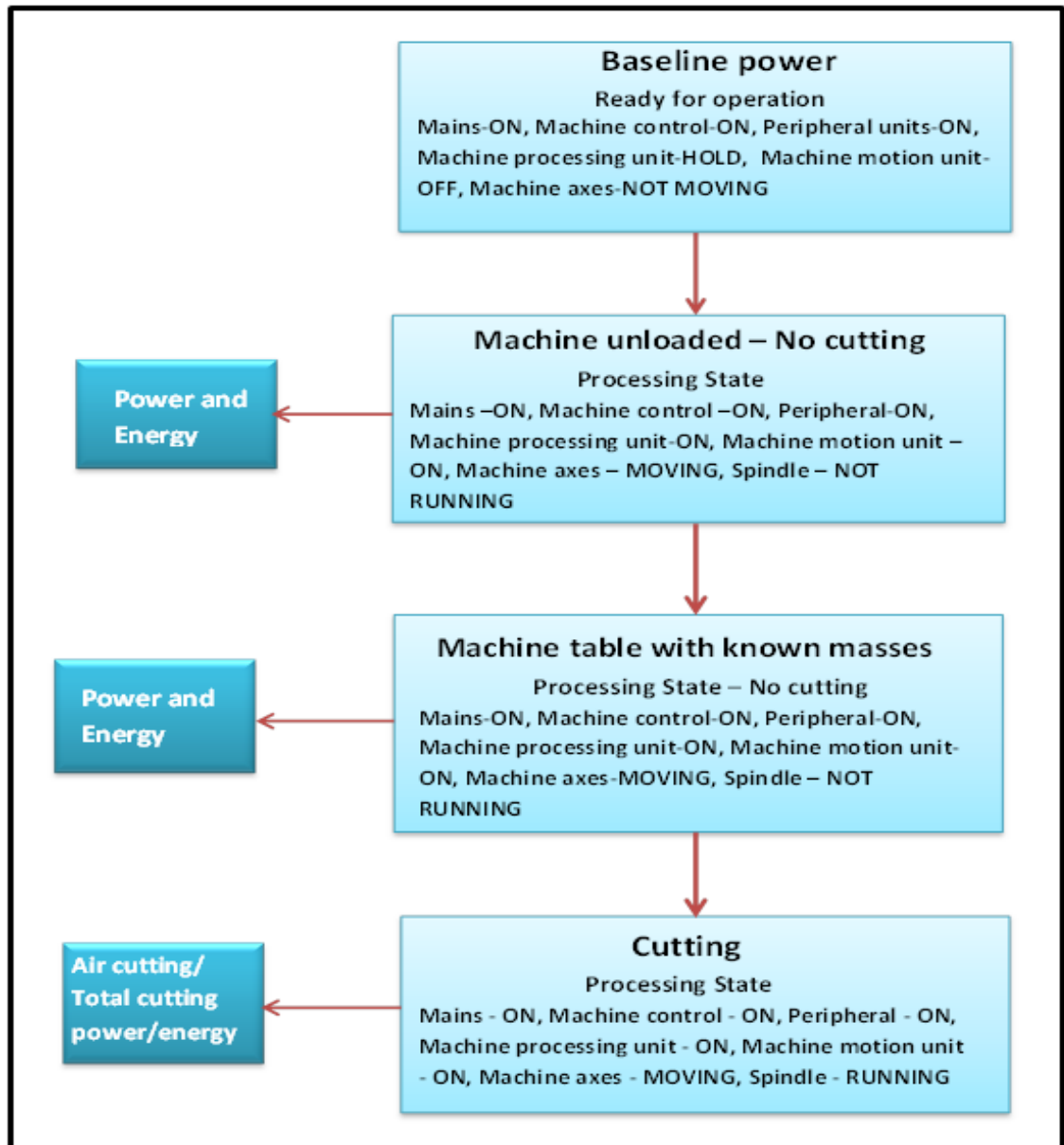


Figure 3.2 Research methodology outline and energy states according to ISO 14955-1:2014 [15]

Details of the cutting conditions, the results obtained from analyses based on this study are presented in the relevant chapter within the thesis. Also, other experimental procedures (i.e. hardness testing of the as-received workpiece, microstructure analyses of the as-received workpiece surface and subsurface, and tool wear) reported in the relevant chapters of this thesis.

The technical details of the equipment used in this research are highlighted in subsequent sections of this Thesis chapter.

3.3 Machine tool

The milling tests were conducted on the Takisawa Mac-V3 milling machine. This machine was adopted in order to analyse its electrical energy demand during machining. The Takisawa Mac-V3 milling machine is a CNC vertical machining centre with FANUC control system. This milling machine's spindle designated A060-0652-B can hold up to 80 mm cutter diameters with spindle speeds up to 10,000 rev/min controlled by a DC servo motor model 20M. The spindle motor has a rated power of 7.5 kW. The machine tool has feedrates up to 12000 mm/min on the X- and Y- axis, and up to 10,000 mm/min on the Z-axis. The machine is actuated by a 3-phase 415V \pm 10 AC 20 k VA power which is supplied from the electricity grid. The worktable dimension and work envelope is 600 \times 400 mm with a permissible load of 200 kg. Figure 3.3 shows a picture of the Takisawa Mac-V3 milling machine, while Table 3.2 provides its technical specification.

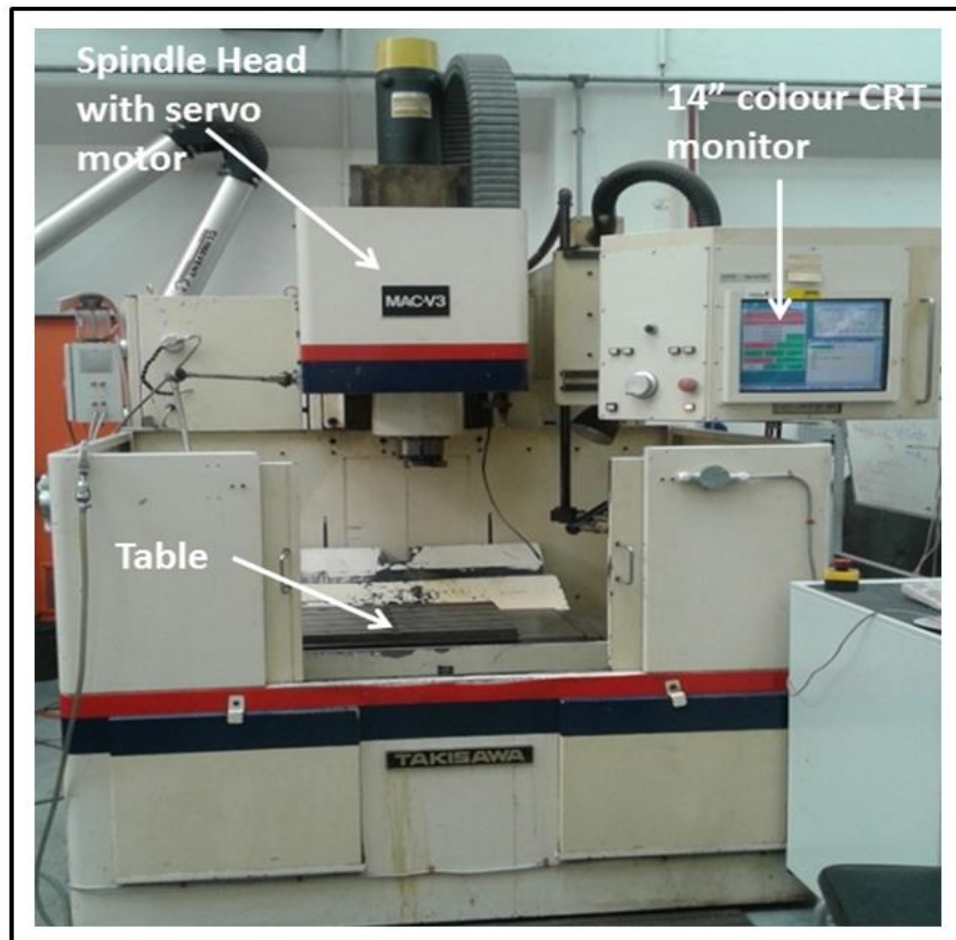


Figure 3.3 Takisawa Mac-V3 milling machine

Table 3.2 Takisawa Mac-V3 milling machine parameters

Type of machine tool	TAKISAWA milling machine (with DC servo motor model 20M, spindle A06B-0652-B)
Feed drive: Maximum feedrate/ rapid rate on the: X axis Y axis Z axis Milling Feed	12000 mm/min 12000 mm/min 10000 mm/min 1 – 5000 mm/min
Feed Mechanism: Diameter of feed screw, mm Pitch, mm Nut preload of the ball screw for X/Y-axis Z-axis Ball screw type Backlash compensation	32 10 100 kg 150 kg Precision grade ball screws directly coupled with feed servo motors by coupling 0 – 0.255 mm
Acceleration on the: X axis Y axis Z axis	10 m/s ² 10 m/s ² 10 m/s ²
Working range: Longitudinal X, mm Cross Y, mm Vertical Z, mm	400 mm 240 mm 350 mm
Work table	Table dimension - 600× 400 mm Permissible Load on Table: 200 kg
Spindle speed/Output – Torque characteristics: Spindle speed, rev/min Mac-V3 Spindle motor T_{max}	60 – 6000 7.5 kW or 10.2 HP 716 kgcm – 4.90 kW
Motors: Main motor Hydraulic pump motor Lubricant pump motor Feed motor: X Y Z	AC 5.5 kW/30 min rating 0.75 kW 0.01 kW 0.85 kW 0.85 kW 1.2 kW
Number of axis	3 (X, Y, Z)
Power supply Total capacity of power supply Compressor T_{max}	AC 3- phase 415V \pm 10 20 kVA 22 kW (3kVA)(200 min ⁻¹) 215 kgcm – 1.50 kW

The feed axes of the Takisawa Mac-V3 milling machine considered in this study consist of the x-axis, y-axis, and the z-axis (spindle). The electrical energy demand of these axes was investigated in order to develop an energy consumption model, as well as identify energy saving measures so as to reduce the non-cutting energy demand of machine tools. As shown in Figure 3.4, the machine tool axes configuration has the machine table and x axis mounted directly on the y axis. Thus, the weights moved by the y axis are more than the x axis. The z-axis moves up and down in the vertical direction. The axes drives are powered by the AC servo motors connected directly to the ball screw drive. The masses for the x and y axes were modelled on Solid works software and was roughly 315 kg and 750 kg respectively. Some technical specifications of the feed axes were previously presented in Table 3.2.

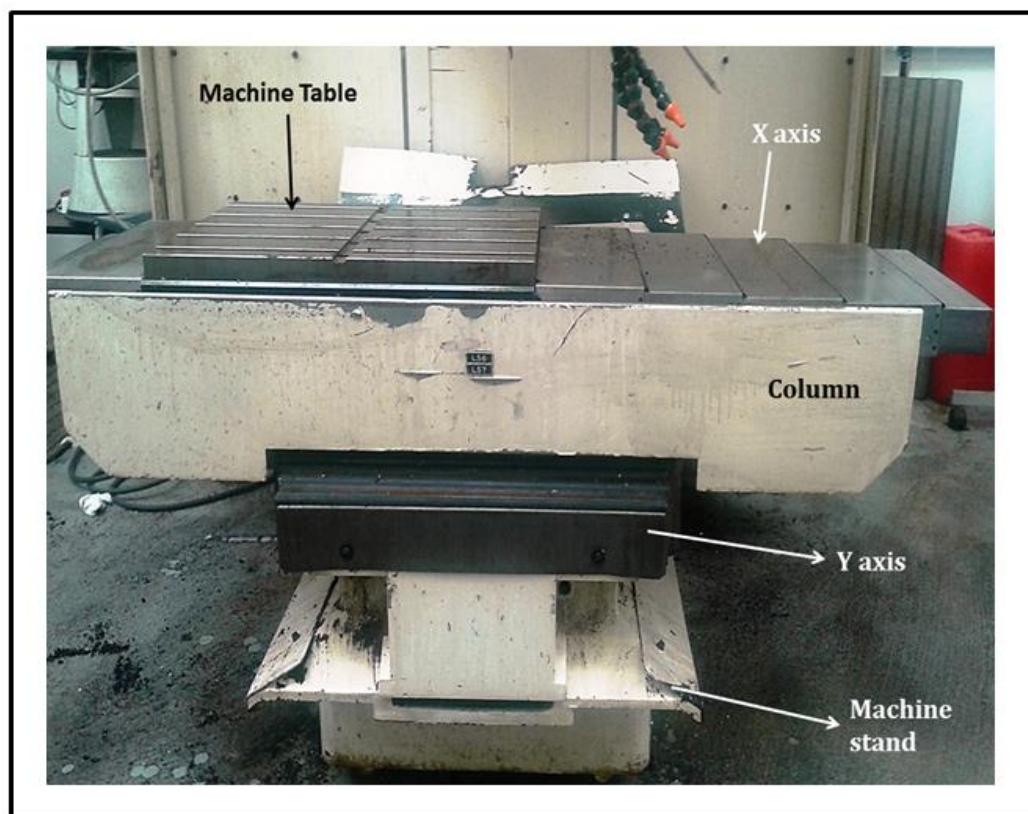


Figure 3.4 Machine tool axes configuration showing the x-axis and y-axis

3.4 Fluke 434 three-phase power quality analyser

The Fluke 434 power quality analyser is single hand-held equipment with inbuilt functions for measuring 3-phase root mean square (rms) and peak currents, 3-phase rms and peak voltages plus their respective neutrals, power, energy, frequency, mains signalling as well as data logging. The power analyser has measurement ranges of 1 – 1000 Vrms and 0 – 40/400 Arms for both the voltage and current respectively. The wye and delta connection configurations may be used depending on the type of machine tool load. The Fluke 434 power quality analyser works on the Hall effect principle which enables the measurement of current and voltage without breaking or interrupting the circuit. Figure 3.5 shows Fluke 434 power quality analyser, while Table 3.3 provides its technical specifications.



Figure 3.5 Fluke 434 power quality analyser

Table 3.3 Technical specification for Fluke 434 power quality analyser

Voltage inputs	
Number of inputs	4 (3 phases + neutral) dc-coupled
Maximum input voltage	1000 Vrms
Nominal voltage range	50 V to 500 V, Selectable from 1V to 1000 V
Maximum peak measurement voltage	6 kV
Input impedance	4 M Ω //5 pF
Bandwidth	> 10 kHz, up to 100 kHz for transient display
Scaling	1:1, 10:1, 100:1, 1000:1 and variable
Current inputs	
Number of inputs	4 (3 phases + neutral) dc-coupled
Type	Clamp on current transformer with mV output
Range	1 Arms to 400 Arms with included clamps (i400s/Fluke 434) 30 A to 3000 Arms with included clamps (i430-flex/Fluke 435) 1 Arms to 3000 Arms with optional clamps
Input impedance	50 k Ω
Bandwidth	> 10 kHz
Scaling	0.1, 1, 10, 100, 1000 mV/A, variable, i5s and i430-flex
Nominal frequency	40 Hz to 70 Hz
Sampling system	
Resolution	16 bit analog to digital converter on 8 channels
Maximum sampling speed	200 kS/s on each channel simultaneously
RMS sampling	5000 samples on 10/122 cycles according IEC 61000-4-30
PLL synchronisation	4096 samples on 10/122 cycles according IEC 61000-4-7

The Fluke 434 power quality analyser has a sampling rate of 200 kS/s for recording the current and voltage. Three i400s clamps and alligator clips for both the current and voltage inputs are connected to the three live wires supplying current to the machine tool.

3.4.1 Connection of Fluke 434 power analyser to machine tools

The FLUKE 434 power quality analyser was clamped by an electrical technician to the three live wires supplying current to the machine tool from the power grid as shown in Figure 3.6.

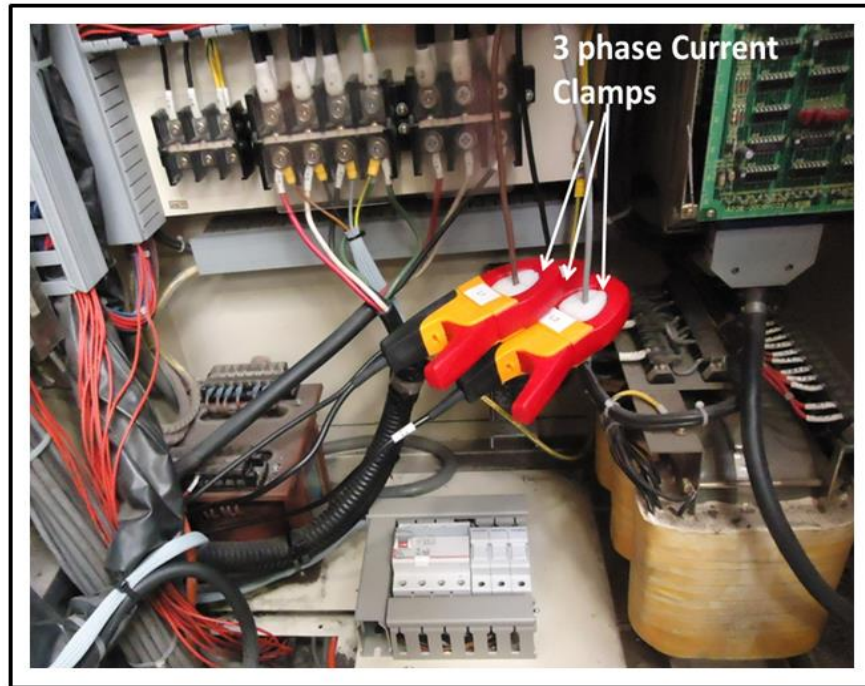


Figure 3.6 Fluke 434 power quality analyser clamped on three live wires at the back of the Takisawa Mac-V3 milling machine

The Takisawa Mac-V3 milling machine uses three phase motor with the delta configuration type of connection. A typical power connection diagram (Delta configuration) is shown in Figure 3.7.

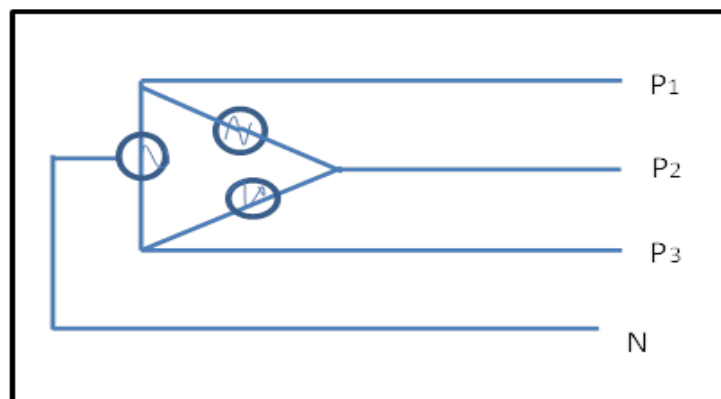


Figure 3.7 Delta three phase power configuration

where P_1, P_2, P_3 represents each of the single phase power, and N is neutral

This connection is made up of three single phase sources of power connected in series with the load [115], and the voltage phases are connected in parallel with the load. Hence, in

order to measure the power per phase, the setup consisted of three wires [116]. This configuration type was selected because the machine tool does not support the neutral phase connection that is usually common with single phase electric motors.

3.4.2 Data acquisition

Data from the Takisawa Mac-V3 milling machine was acquired with the Fluke 434 power quality analyser. In order to acquire data from the power meter, the optical interface cable model OC4USB was connected to the computer via the USB port. The measured current and voltage data from the machine tool were then downloaded from the power clamp meter with the power log software. The power log software is the visual and analyses software that enables the data acquired from the equipment to be visualised with the aid of a computer system. The data were analysed and evaluated in Microsoft excel to give the average power drawn by the machine tools in the machining processes.

In this study, current and voltage measurements were performed with the FLUKE 434 power quality analyser. This power meter measures three phase currents and voltages. Due to varying current and voltage values in the three phases, peripheral milling tests of AISI 1018 steel were conducted. Figures 3.8 a, b, c show three phase current and voltage for peripheral cutting test runs of a material at 500 mm/min feed rate.

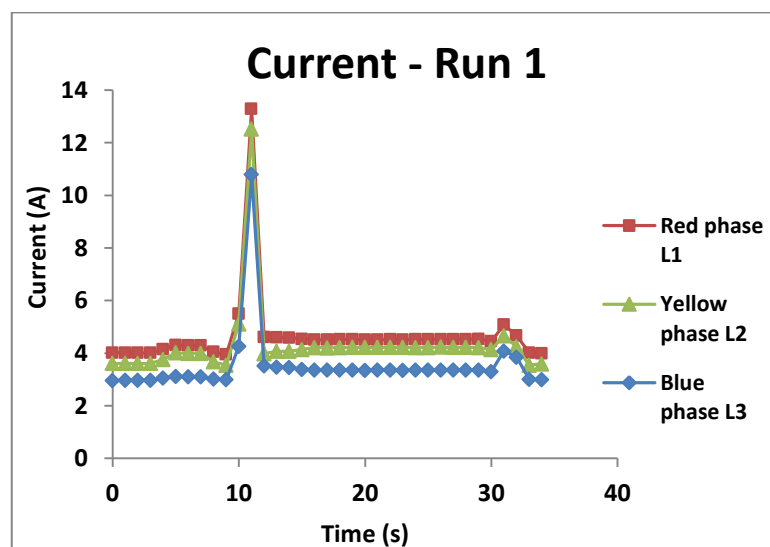


Figure 3.8a Current demand profile for each phase

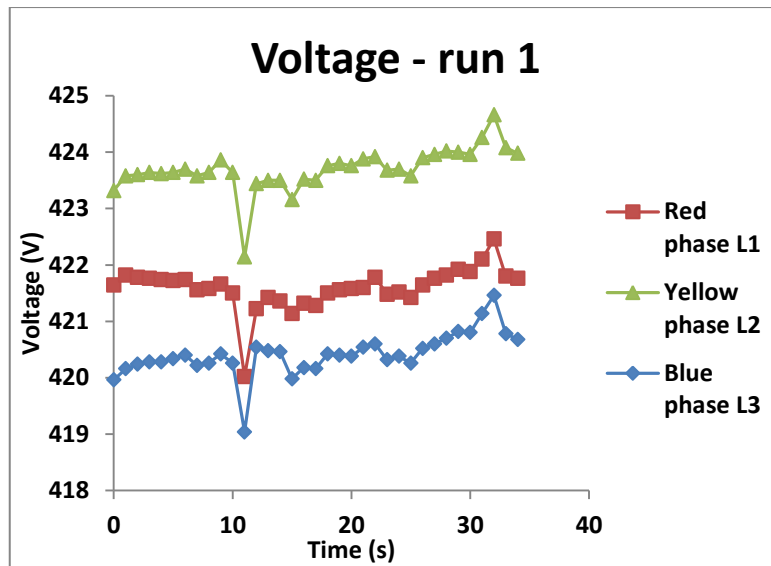


Figure 3.8b Voltage demand profile for each phase

Figure 3.8a shows that L1 current (red phase) for test run 1 is 35% higher than L3 (blue phase) which has the lowest current requirement. In Figure 3.8b, the voltage L2 (yellow phase) is 1% more than L3 which has the lowest voltage requirement. Each voltage phase differ from each other by 0.4%. As shown in Figure 3.8c, the power consumption for each phase was evaluated by multiplying the line currents (L1, L2, L3) with their corresponding line voltages (L1, L2, L3). It is observed that L1 (red phase power) is 22% higher than L3 (blue phase power). Similar trend was obtained for the other two runs.

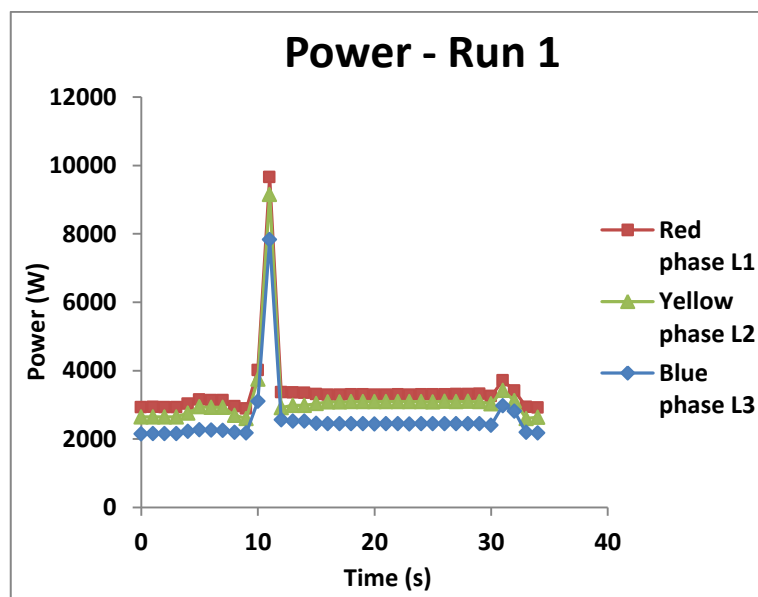


Figure 3.8c Power demand profile for the three phases

Subsequently, the power consumption for this experiment was evaluated using the L1 current and voltage. Hence, the electricity consumed by the machine tool provides power which may be distinguished into voltage and current. Therefore, the power drawn by the machine tool may be estimated using the formula in Equation (3.1) as presented in [117].

$$P = I \times V \times \sqrt{3} \times \text{Cos}\phi \quad (3.1)$$

where V represents the voltage in V, I is the current in A, $\sqrt{3}$ is a constant that indicates the phase to phase voltage, $\text{Cos}\phi$ is the power factor.

3.5 Workpiece material details

AISI 1018 steel was selected as the workpiece material for the cutting tests throughout this work. This workpiece material was considered due to the fact that it is suitable for numerous applications, and used for the manufacture of industrial products such as bolts, axles, shafts, machinery parts, gears, worms, pins, ratchets, parts requiring bending, swaging, cold forming, or crimping, sheet, plate, tubes, as well as for manufacturing machine parts that require low strength. The as-received material was cast into ingot on an electric arc furnace in order to produce billets for manufacturing hot rolled bars of mild steel. Cutting tests were conducted in order to determine the influence of toolpath strategies on the electrical energy demand, effects of machine tool axes configurations on the electrical energy demand, impacts of toolpath orientations etc. The AISI 1018 workpiece material was cut to the required sizes for each of the specified milling operations. Table 3.4 shows the details of AISI 1018 steel.

Table 3.4 Details of AISI 1018 steel

Mechanical properties of the workpiece:	
- Yield strength, MPa	340 – 600
- Tensile strength, MPa	430 - 750
Chemical composition of the workpiece	0.17 wt% C, 0.27 wt% Si, 0.80 wt% Mn, 0.050 wt% S max, 0.050 wt% P max
Working process	Cast and hot rolled

3.6 Cutting tool details

The 8 mm diameter short carbide end mill cutter from Swiss Tech was used for all the machining tests in this research. This end mill cutter was considered in this research due to its general use in milling processes, and its coating characteristics which enables the cutting tool to dissipate and resist heat, reduce surface friction at the chip-tool cutting interphase. Figure 3.9 is a pictorial view of the 8 mm diameter short carbide end mill, while Table 3.5 presents the technical specifications.



Figure 3.9 Picture of 8 mm diameter short carbide end mill cutter

Table 3.5 Technical specifications of 8 mm short carbide end mill cutter

Criteria	Description
Manufacturer	Swiss Tech
Cutter diameter (mm)	8
Length of cutter (mm)	60
Length of flute (mm)	20
Shank diameter (mm)	8
Number of flutes	4
Helix angle	30°
Weight of cutter (g)	39
Material	Solid carbide
Milling Application	Finishing Profiling Semi-finishing Slotting

3.7 Vickers hardness testing machine

Vickers hardness testing machine is normally used to measure the hardness of workpiece materials. The diamond tool creates an impression of depth that is proportional to the hardness of the surface to be measured. The indentation is then sized with the calibrated square optical mirror. The readings obtained can be translated via a table.

For this research, the Vickers pyramid hardness testing machine from UK Calibrations Limited with an attached load of 200 N was used in order to determine the variations in hardness properties of the as-received AISI 1018 steel workpiece. The two diagonals of the indentation from the diamond indenter left on the surface of the as-received workpiece material after the removal of the load were measured using a microscope and the average calculated. The Vickers hardness value was obtained from the hardness conversion chart. Image of the Vickers pyramid hardness testing machine is presented in Figure 3.10 while Table 3.6 presents the technical specifications for the Vickers pyramid hardness testing machine.

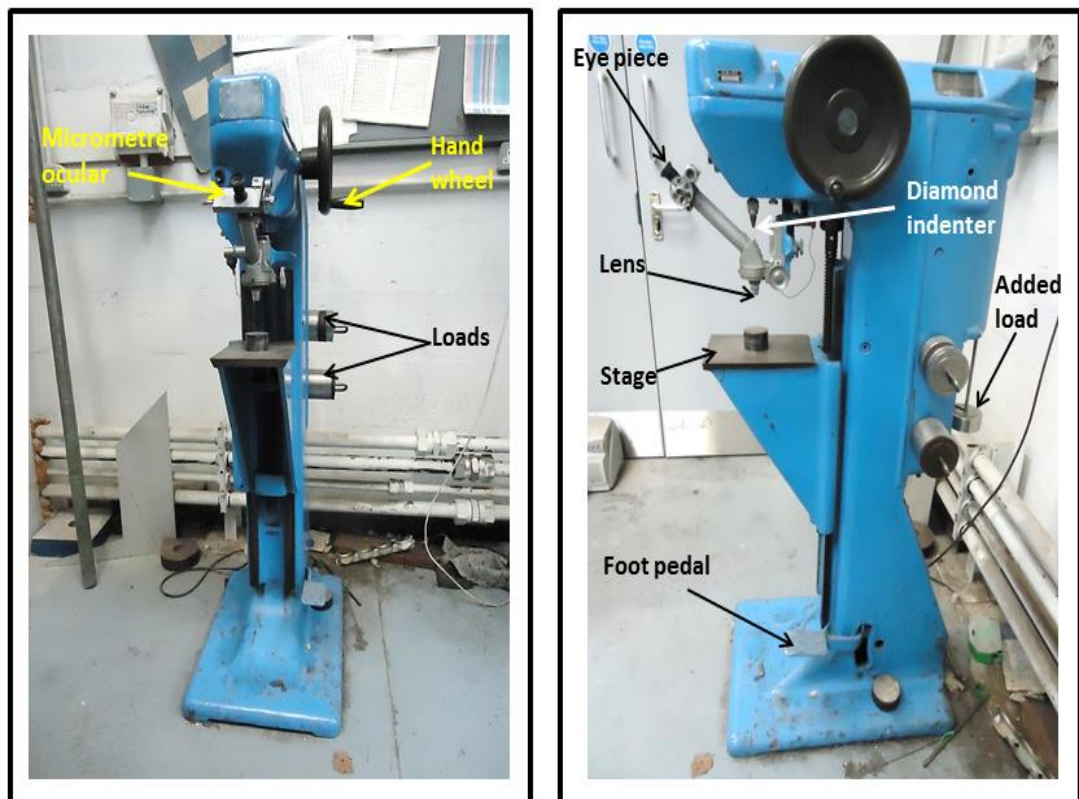


Figure 3.10 Vickers hardness tester

Table 3.6 Technical specification for Vickers pyramid hardness testing machine

Capacity and Dimensions	
• Accommodation for work	Up to 330 mm
• Maximum load	1200 N
• Minimum load	10 N
• Eye-piece to floor	1104 mm
• Diamond to floor	1003 mm
• Overall height	1263 mm
• Floor space	609 mm × 711 mm

3.8 Surface roughness checker

The Surtronic 25 portable surface roughness checker is a portable stylus type instrument with the stylus travelling over the machined surface as shown in Figure 3.11. Surface roughness was measured with the stylus running perpendicular to the lay of the machined surface. The surface roughness checker was calibrated using an Electro-formed surface roughness comparison standard as shown in Figure 3.12 before the commencement of each surface roughness check. Three different points on the machined surface were measured to determine the average surface roughness. The cut-off lengths are 0.25 mm, 0.8 mm, and 2.5 mm. Table 3.7 presents technical specifications for the surface roughness checker.

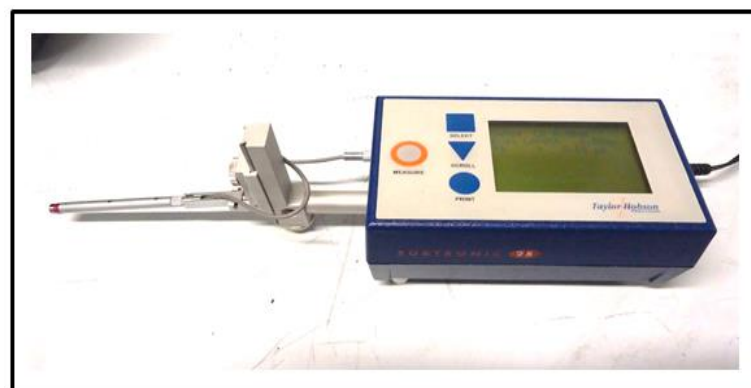


Figure 3.11 Surtronic 25 portable surface roughness checker

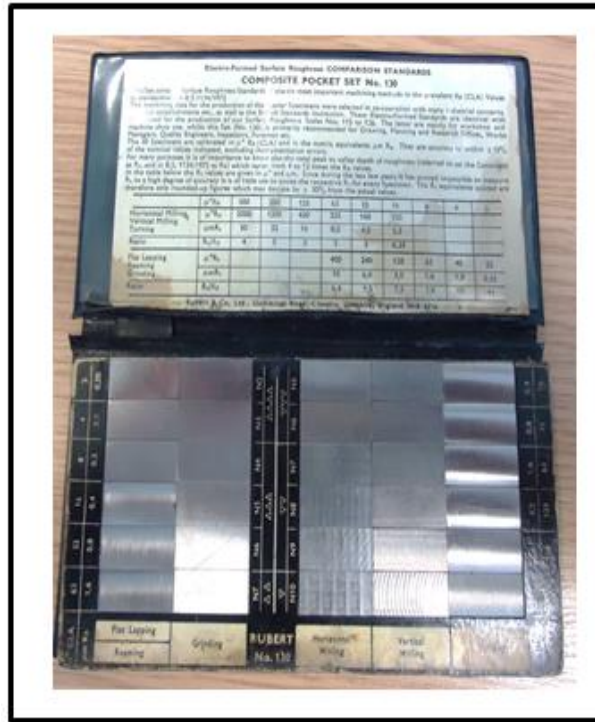


Figure 3.12 Electro-formed surface roughness comparison standard

Table 3.7 Technical specifications for Surtronic 25 surface roughness checker

Criteria	Description
Gauge range	300 μm (0.012 in)
Accuracy	2% of reading + least significant digit (LSD) μm
Traverse length	0.25 - 25 mm
Roughness parameters	$R_a, R_z, R_t, R_{z1\ max}, R_p$

where R_a is the arithmetic mean deviation

R_z is average peak to valley height

R_t is the total height of profile

$R_{z1\ max}$ is the maximum peak to valley

R_p is the maximum profile peak height

3.9 Grinding and polishing machines

3.9.1 OmegaPol grinding machine

The OmegaPol grinding machine is ideal for manual metallurgical grinding and polishing for analysing the microstructure of materials. The microstructure of the as-received AISI 1018 steel was analysed by grinding the top surface of the material with electro-coated Silicon carbide waterproof abrasive paper while water was simultaneously applied. The grit sizes of the abrasive paper ranged from 80, 120, 320, 600, 800, and 1200. Figure 3.13 is an image of the OmegaPol grinding machine. Technical specifications of the OmegaPol grinding machine are presented in the appendix section of this thesis.

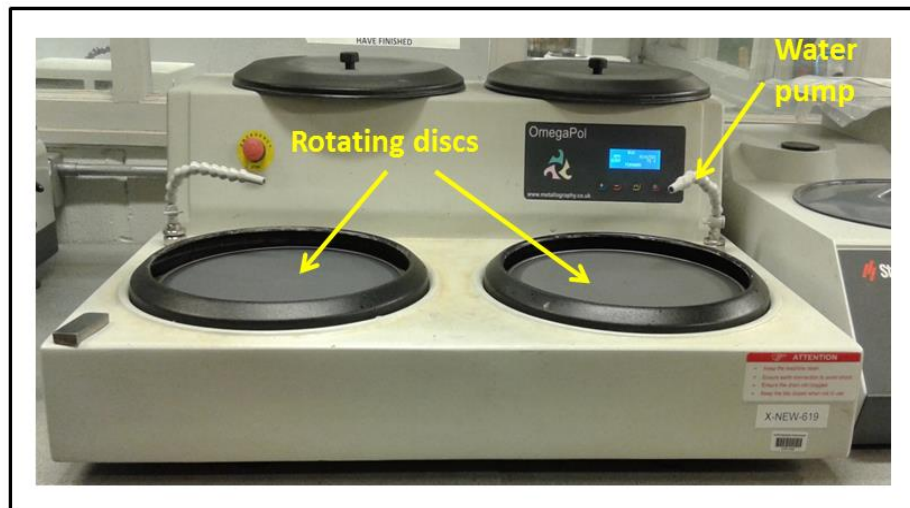


Figure 3.13 OmegaPol grinding machine with rotating disc

3.9.2 LaboPol-35 polishing machine

After the grinding process was completed, the LaboPol-35 polishing machine from Struers UK was used to polish the ground surface of the as-received material. This was achieved by using three 200 mm diameter 62105 MAIA polishing cloths on a magnetic bag which were placed on the rotating disc of the polishing machine. Gemini Diamond monocrystalline slurry with 6 micron, 3 micron, and 1 micron were sprayed on the polishing cloth in order to moisten it and allow for easier polishing operations. Figure 3.14 shows the LaboPol-35 polishing machine. Technical details of the LaboPol polishing machine are presented in the appendix section of this thesis.



Figure 3.14 LaboPol-35 polishing machine

3.10 Equipment for microscopy

3.10.1 Leica DM2500 microscope

The Leica DM2500M microscope shown in Figure 3.15 was used for material examinations. It has magnifications of 1X, 1.5X and 2X respectively depending on the magnification desired to give a clearer image of the specimen. This microscope is suitable for the analysis of materials' microstructure. After the etching process was completed, the optical microscope (LEICA DM2500) was used to acquire images of the etched sample. Details of the microscope are presented in the appendix section of this thesis.

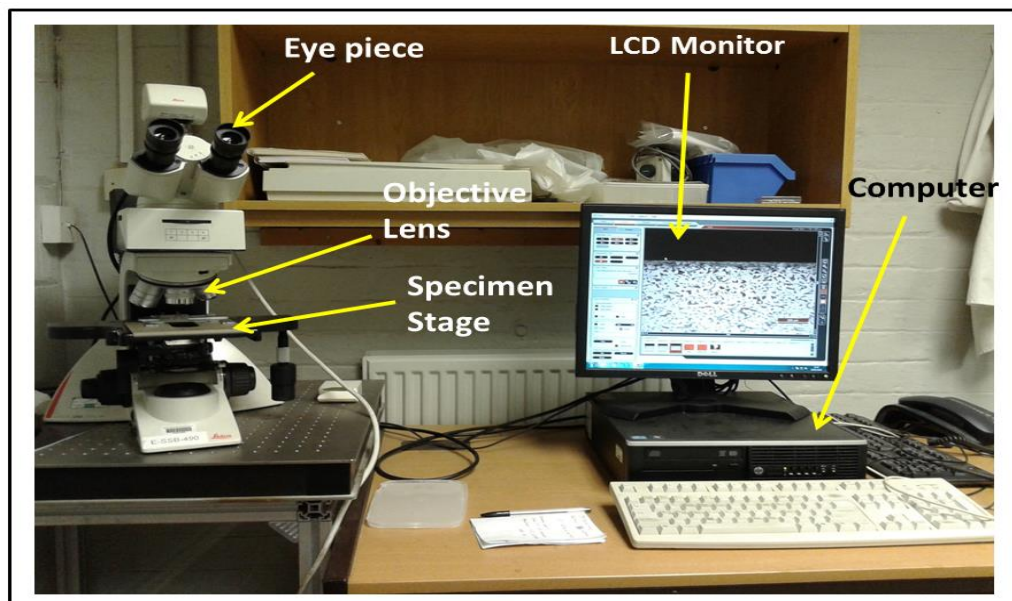


Figure 3.15 Leica DM2500 microscope

3.10.2 Keyence VHX-500F digital microscope

The Keyence VHX-500F digital microscope is a high resolution charged couple device (CCD) camera based system with a high intensity halogen lamp and image processing capabilities that integrates observation, recording, and measurement functions. This microscope is equipped with a liquid crystal display (LCD) monitor for observing acquired images.

In this study, the Keyence VHX-500F digital microscope was considered in order to observe tool wear conditions for each tool used in the cutting process. An image of the digital microscope is presented in Figure 3.16. Technical details of the Keyence VHX-500F digital microscope are presented in the appendix section of this thesis.

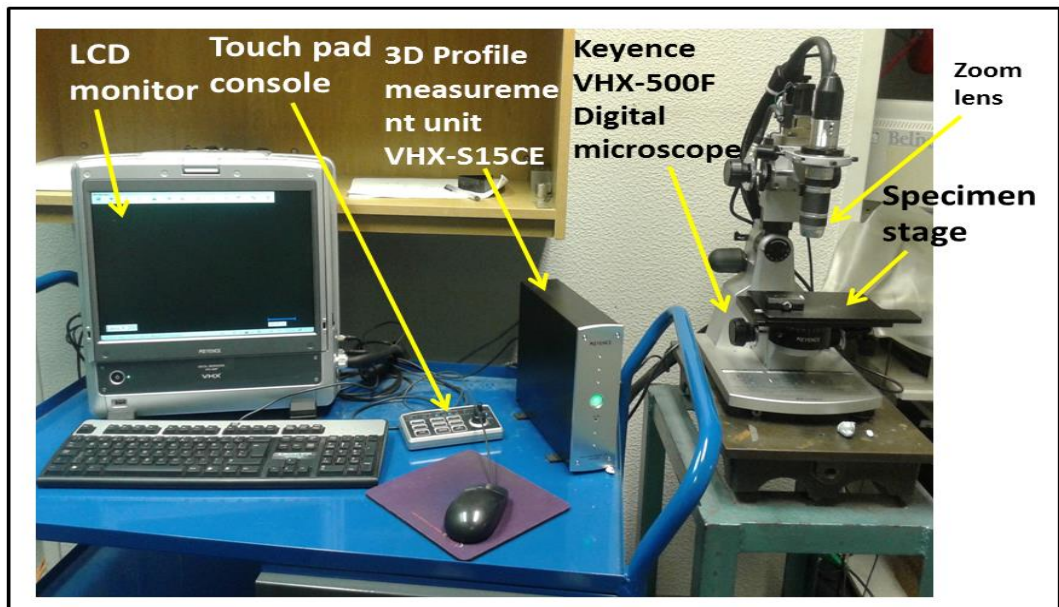


Figure 3.16 Keyence VHX-500F digital microscope

3.11 Conclusion

This chapter provided detailed report on the machine tool used in monitoring and measuring the power demand during the cutting tests. This was in addition to details on the power measuring device, experimental setups and procedures undertaken in this research. The next chapters of this thesis present the studies conducted and their corresponding explanations.

CHAPTER 4

IMPACT OF FEED AXIS ON ELECTRICAL ENERGY DEMAND IN MECHANICAL MACHINING PROCESSES

Reformatted version of the following paper:

Paper title: **Impact of feed axis on electrical energy demand in mechanical machining processes**

Authors: **Isuamfon F. Edem, Paul T. Mativenga**

Published in: **Journal of Cleaner Production 137 (2016) 230-240**

ABSTRACT

To reduce energy demand in manufacturing, it is important to make products using the most energy efficient process plan and resources. In machining, understanding the factors that influence the electrical energy demand for CNC toolpaths is vital in order to determine the optimum machining conditions to minimise energy demand. In this study, a new model for estimating the electrical energy demand of machine tool feed axes which incorporates the weights of feed axes and weights of the materials placed on the machine table is presented. This was achieved by studying the electrical energy demand for machine tools when air cutting in defined axis directions, carrying a range of masses, and in actual cutting, while the electrical current was measured. The newly proposed model was validated on milling CNC toolpaths. The information enabled the development of suggestions for reducing energy demand. The energy reduction hypothesis developed was explored and validated by machining components in defined orientations on the machine table. The results are important for manufacturers in industry when process planning. The information is also valuable for the range of machine tool design and manufacturing companies in the development of energy efficient machine tools.

Keywords: Energy efficiency, electrical energy demand, feed axes, machining, modelling, CNC toolpaths

4.1 Introduction

Electrical energy demand modelling and reduction in manufacturing is important because of energy costs and the carbon footprint associated with energy generation. The electrical energy consumed by machine tools throughout their use phase results in increased environmental impact. For example, Diaz et al. [11] conducted life cycle analysis of two milling machines and reported that 60% to 90% of CO₂ equivalent emissions result from the use phase of milling machines. Santos et al. [12], performed a life cycle analysis and reported that 46% of the environmental impact of the machine tool was attributable to its electricity consumption during its use phase. While the above life cycle analysis did not focus on the embodied energy of materials production it is clear from literature that when machine manufacture and machine use are considered, the environmental impact during the use phase is a significant factor that needs to be considered and managed.

Developments in Europe, such as the European Association of Machine Tool Industries (CECIMO)'s Self-Regulatory Initiative (SRI), aim for ecological improvements and energy saving of machine tools [8]. In 2012, Duflou et al. [21] outlined a number of energy demand reduction strategies applicable to machine tools. These included: more efficient machine tool components such as drives, pumps and spindles; technology leaps; recovery of waste streams such as heat losses within a machine tool; and integrated or central delivery of consumables. Prior work by these authors has demonstrated that cutting conditions can be selected to minimise energy footprint [84] and the selection of tool path strategies can lead to energy savings in machining processes [96]. Kara and Lee [72] advocated that a reduction of energy consumption and improvement of environmental performance can be applied proactively during product design and process planning stage.

To model and reduce the energy demand in CNC toolpaths, there is need to understand the effect of interpolation modes and table feed on energy demand in machining. While a number of studies have looked at the machining process as a whole, the energy demand for interpolation modes is relatively unexplored.

Machine tool feed drives control the relative motion between the workpiece and cutter, as well as determining the workpiece geometry [118]. Thus, the performance of machine tool feed drives significantly influences the productivity and quality of machine tools [119]. The feed mechanism consists of the electrical units (i.e. feed motors) and the mechanical units (i.e. ball/lead screws). Control signals are sent from the machine tool control unit to activate the feed drive motors. This ensures the rotation of the ball/lead

screws to position the machine tool spindle and the work table. Angular motion to the workpiece or cutting tool is provided by the spindle drives which rotate over a wide range of speeds. The feed drive mechanism converts the angular motion of the motors to linear motion of the guide ways and work table [120].

Feed drives are either powered by linear motors directly, or by rotary motors via ball screw and nut assembly [120]. Few researchers have modelled the feed drives. For example, Avram and Xirouchakis [85] modelled the power of the feed axes based on the torque supplied by the servomotor of each axis. Unfortunately, weights of the axes, workpiece, and machine vice were not considered in the model. He et al. [26] considered the importance of feedrates in their feed axes power demand model while the weights of the axes, workpiece, and machine vice were not considered. Calvanese et al. [86] modelled the feed axes by considering the mechanical power and the dissipated power. However, their model did not consider the feed axes, workpiece, and machine vice weights. Xie et al. [119] utilised an object-oriented simulation approach to model the feed drives. However, energy demand of the feed drives was not considered. Lv et al. [88] modelled the power requirements of the feed motor P_f using Equation 4.1.

$$P_f = A_1 v_f + B v_f^2 \quad (4.1)$$

where v_f is the feedrate in mm/min, A_1 and B are constants related to loading and friction respectively. The feed drive of the considered CNC lathes in their work was powered by an AC servo motor connected to the ball screw. Other researchers, Li et al. [29], assumed that the operational power for feed motor follows an approximate linear relationship with the feedrate and modelled it as shown in Equation 4.2.

$$P_f = A_2 v_f + C \quad (4.2)$$

where v_f retains its usual meaning, A_2 and C are constants. The feed drive of the CNC machine tool considered in their work was driven by rotary motors via ball screw and nut assembly. Campatelli et al. [90] presented an analytical model of the energy demand for feed axis, taking into account the effect of masses and friction. The analytical approach is interesting in that it proposes a basis for the key parameter constants within the energy demand model. This is shown in Equation 4.3.

$$P = \int_0^S ((M_x a_x + \mu_x M_x g) + (M_y a_y + \mu_y M_y g)) ds \quad (4.3)$$

where M_x and M_y are the equivalent masses of the axes in kg , a_x and a_y the instantaneous accelerations in m/s^2 , μ_x and μ_y are the equivalent friction coefficients for the x and y axes for the length of the toolpath. The parameter g is the acceleration due to gravity in m/s^2 and s is the distance along the toolpath length in mm . In their work, the feed drive of the considered 5-axis CNC machining centre was powered by rotary motors for the x- and y-axes, and by direct drives motor for the B and C axes.

From Equation 4.3, it was assumed by Campatelli et al. [90] that the energy demanded by the table motions was independent of feedrate. In 2015, Guo et al. [97] used air cutting experiments to develop a power demand model for the feed drives. This is shown in Equation 4.4.

$$P_{axes} = A_3 v_f^2 + D v_f \quad (4.4)$$

where P_{axes} is the power demand for the specified axis in W , A_3 and D are constants while v_f retains its usual meaning.

Recently, Lee et al. [93] proposed a model for estimating the power demand of feed axes. This is shown in Equation 4.5.

$$P_{feed} = C_{0f} \cdot v_f + C_{1f} \quad (4.5)$$

where P_{feed} is the feed drive power consumption in W , C_{0f} is the gradient of the power model of the feed drive, v_f is the specified feedrate in mm/min , C_{1f} is a constant.

Equations 4.1, 4.2, 4.4, and 4.5 by Lv et al. [88], Li et al. [29], Guo et al. [97], and Lee et al. [93] respectively model the importance of feedrate, but do not capture the impact of weights on the energy demanded by the machine table feed axis.

From the literature, it is clear that there is no general agreement on the dominant factors that control energy demand for machine tool table feed axis. In light of this, the importance of moved weights by the feed drive (i.e. weights of feed axes, workpiece, and machine tool

vice), feedrate, and direction of axis travel on power demand are considered in this study in order to improve the prediction capability of feed axes power demand models. Therefore, developing this knowledge is important for evaluating the energy demand in toolpaths and in developing strategies for energy demand reduction.

The motivation of this study was to contribute towards and better the understanding of the power required and hence energy demanded by machine tool axes. The ultimate motive is to enable the generation of guidelines for industry in support of energy smart machining, thus reducing the energy and carbon intensity of machined products, as well as energy costs.

4.1.1 Research aim and objective

This work is aimed at assessing the electrical energy demand of machine tool feed axes in order to develop recommendations for modelling and energy consumption management. This study will contribute towards the development of a robust model for estimating the electrical energy demand of feed axes, taking into consideration the weights of the feed axes and materials placed on the machine table, as well as the feed force acting on the machine table. Thus, the knowledge acquired in this study shall aid in contributing towards better understanding of factors influencing the energy demand of feed axes, as well as providing suggestions for minimum energy consumption.

4.2 Experimental details

4.2.1 Research methodology

The research methodology was based on energy evaluation in milling, focussing on the net power and energy demanded by table feed axes. The evaluations were done when (i) executing table feed without any workpiece on the table and with no spindle rotation, (ii) when the machine is carrying different weights (surrogate for workpiece weight) and with no spindle rotation, and (iii) when machining components. To elucidate the impact of individual axis, the motions of the feed table were made in the x, y and z axes directions.

The current and voltage drawn by the CNC machine were directly measured using the 3-phase FLUKE 434 Power Quality Analyser which enabled the calculation of power requirements during the operation of the machine. The energy demand was modelled by relating the activity and state of the machine to the net 3-phase current and voltage measurement, and hence evaluating the power and ultimately the energy based on the cycle time. Further validating of the trends observed was done by machining test workpieces. The energy reduction hypothesis developed was explored and validated by machining components in defined orientations on the machine table.

4.2.2 Experimental setup and procedure

The milling tests were conducted on a 3-axis CNC Takisawa Mac-V3 milling machine (conventional milling machine). This machine has a DC servo motor model 20M with spindle model A06B-0652-B, and a FANUC controller. Other machine parameters are as stated in Table 4.1. The x, y and z axes accelerate at 10 ms^{-2} with rated power requirements of 0.85 kW for the x- and y- axes, and 1.2 kW for the z- axis. The spindle motor had a rated power of 7.5 kW. The axes drives were powered by the AC servo motors connected directly to the ball screw drive. Zero load motion tests were first conducted on the CNC milling machine. The experimental plan for this study is as shown in Table 4.1.

Table 4.1 Machine tool parameters for machining strategy

Type of machine tool	TAKISAWA Mac-V3 milling machine with DC servo motor model 20M
Spindle model	A06B-0652-B
Machine tool controller	FANUC
Feedrate, mm/min (m/s)	
X- axis ; Y- axis	500 – 5000 (0.0083-0.083)
Feedrate, mm/min (m/s)	
Z - axis	50 – 500 (0.0008-0.0083)
Tool travel along the X-,Y-, and Z-axes in (mm)	150
Workspace (mm)	600 x 400
Allowable weight of material on machine tool table (N)	2000

The zero load motion test was performed at six different feedrate values i.e. 500, 1000, 2000, 3000, 4000, 5000 mm/min for x- and y-axes and 50, 100, 200, 300, 400, 500 mm/min for the z-axis. The feedrates were varied on the positive feed direction along the x- and y- axes as well as in positive and negative feed directions for the z axis. The table traverse distance was 150 mm. The electrical current consumed along the x– and y- axes and z (+) and z (-) axes toolpath were recorded simultaneously. The test runs were repeated three times for data consistency and repeatability.

Further studies to determine the influence of known weights on the electrical energy demand of machine tool axes when executing movements in the x-axis and y-axis directions were conducted by placing known weights of materials on the worktable of the CNC machine tool. Table 4.2 presents the experimental plan for this study.

Table 4.2 Experimental plan for determining the effect of known weights on the electrical energy demand of feed axes

Type of machine tool	TAKISAWA Mac-V3 milling machine with DC servo motor model 20M
Spindle model	A06B-0652-B
Machine tool controller	FANUC
Feedrate, mm/min (m/s)	
X- axis ; Y– axis	500 – 5000 (0.0083-0.083)
Tool travel along the X- and Y- axes in (mm)	150
Known weights (N)	250; 350; 450; 550; 650; 750
Weight of machine tool vice (N)	570

The known weights of the workpiece material were varied for each test as shown in Table 4.2. The feedrates were also varied for each of the zero load motion tests in the x-axis and y-axis directions. The travel distance of the table was kept at 150 mm as before. The electrical current consumed when the feed axis executes movement in the x– and y- axes directions, with the specified weight of workpiece material placed on the machine tool table was recorded simultaneously. An illustration of the experimental setup for current/voltage measurement and data acquisition on the Takisawa Mac-V3 milling machine is presented in Figure 4.1.

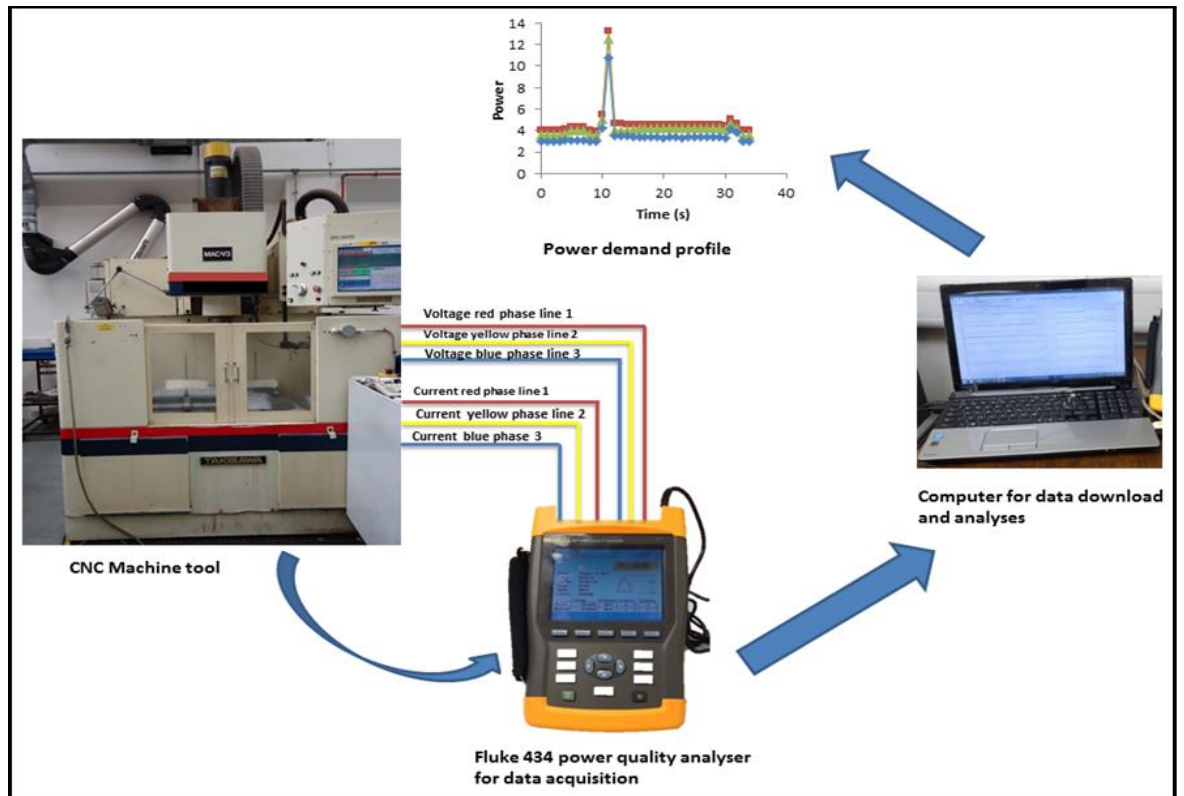


Figure 4.1 Schematic diagram showing Fluke 434 power quality analyser setup and data acquisition

As shown in Figure 4.1, the current measurement point was first located at the back of the machine tool. The 3-phase current and voltage cables were clamped on the live wires supplying current to the machine tool from the power grid. Then, the input current and voltage cables were connected to the Fluke 434 power quality analyser for acquiring the current and voltage data during the machining process. The measured current and voltage data from the machine tool were then downloaded from the power clamp meter to a computer for analysis using the Power log software. The test runs were repeated three times for data consistency and repeatability. The newly proposed model was validated by conducting milling tests on a square workpiece of AISI 1018 steel material.

The next section presents the use of Taguchi design of experiments to determine the dominant parameter influencing the electrical energy demand of feed axes considering feedrates, weights and feed axes direction. It also includes results on the modelling of the feed axes power demand, as well as validation of the model.

4.3 Results and discussions

4.3.1 Determining the dominant factors for energy demand of machine tool axis

In order to understand the dominant factors that influences power demand of feed axes, three factors were selected namely feedrate, weights of materials added to the table, and direction of axis feed. An L4 Taguchi orthogonal array Design of Experiments was used. The Minitab 16 software was used to analyse the results. The response of the tests is as shown in Table 4.3. The tests responses as analysed with Minitab 16 software is as shown in Figure 4.2.

Table 4.3 Experimental design and responses for Taguchi L4 orthogonal array

Feedrate (mm/min)	Weights (N)	X- and Y- axes direction of feed	Repeat 0, Power (W)	Repeat 1, Power (W)	Repeat 2, Power (W)	Average Power (W)
1000	250	X	142	140	150	144
1000	750	Y	192	182	192	189
3000	250	Y	169	158	158	162
3000	750	X	212	194	216	207

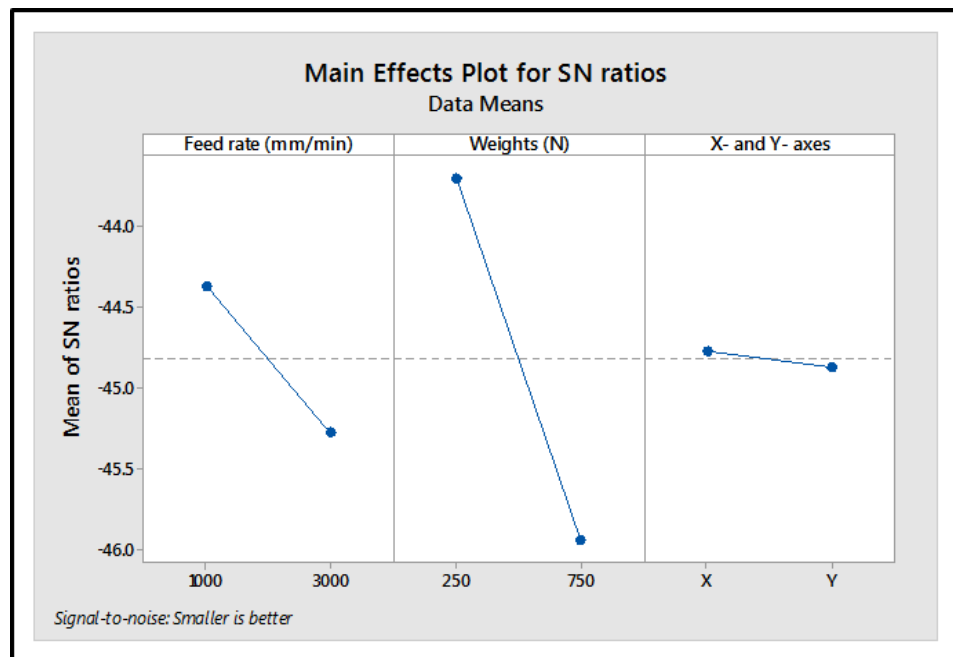


Figure 4.2 Factors affecting the power demand of feed axes

Considering Figure 4.2, the objective is to reduce power requirements. This is realised when the signal to noise ratio is at its highest point for each factor. Thus operating the machine at the lower feedrate, with the least weights would reduce power requirements. This has to be balanced against using higher feedrates to reduce cycle time and energy demand.

Table 4.4 Response table for signal to noise ratios

Level	Feedrate (mm/min)	Weights (N)	X- and Y- axes
1	-44.37	-43.71	-44.77
2	-45.28	-45.95	-44.87
Delta	0.91	2.25	0.10
Rank	2	1	3

From Figure 4.2 and Table 4.4, it is shown that compared to feedrate and direction of travel, weights placed on the machine table are the most dominant factors that influence the power demand of the feed axes. From the Figure 4.2, the high gradient of the signal to noise ratio also shows that feedrate and weight are significant factors for power demand. The axis of interpolation is not as dominant as the feedrate or weights. Therefore it is important to model power demand of machine feed axis as a function of feedrate and weight of component placed on the Table.

4.3.2 Modelling of the power demand of the feed axes

In order to model the electrical energy demand of the feed axes and to estimate the influence of known weights of workpiece material on machine tool axes, machine axis power was studied by placing known weights of materials on the worktable of the Takisawa Mac-V3 milling machine. The machine table and axis movement were then executed without cutting and with no spindle rotation. The added weights were 250, 350, 450, 550, 650 and 750 N. The table travel distance was 150 mm. The weights for each axis were 3150 N for the x-axis (including the weight of the table), 7500 N for the y-axis, and 6900 N for the z-axis. This experiment was performed with a transverse along the x-and y-axes when the predetermined weights were placed on the worktable.

The plot in Figure 4.3 shows the variation of x and y feed axes net power for different feedrates when traversing with zero load on the table and with no spindle rotation. In Figure 4.3, while the norm in machining is to express table feedrate in mm/min, in this paper, for utility reasons, a unit of m/s has been used since the focus is on evaluating energy which is in Watt seconds (*Ws*). From Figure 4.3, a strong positive correlation exists between power required by the table axes and the feedrate the machine is executing when not cutting. An increasing trend of power demand of the feed axes is obtained as the feedrate increases, which is in line with the research reported in Guo et al. [97].

Additionally, the net y-axis feed power requirement is on average 2% more than that of the x-axis. The reason for this is because the x-axis on this particular machine is mounted on the y-axis and hence the y-axis carries more weights than the x-axis. This difference in power can be greater for larger machines with bigger table weights.

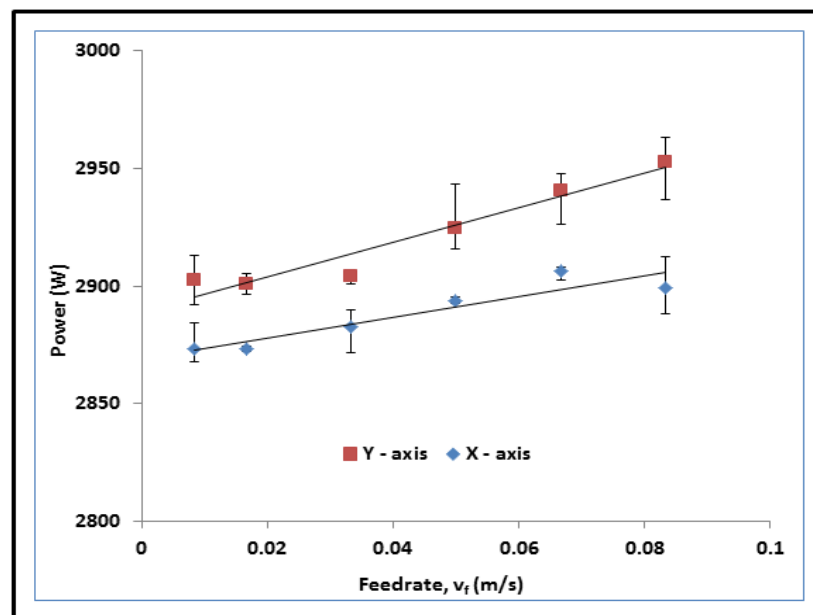


Figure 4.3 Power required for x- and y- axis of Takisawa Mac-V3 milling machine when not cutting traversing with no workpiece and with the spindle off

Similarly the power demand of the z-axis was evaluated when the axis was descending and ascending for 150 mm. The results are shown in Figure 4.4. In this case the spindle was OFF so as not to measure the power requirement of the spindle. Again the power requirement increases with feedrate. The axis power demand when the spindle is going up was 2% higher compared to the spindle going down. This is expected due to the weight of the spindle column and hence, the effect of moving weights is evident from the power requirement for the vertical spindle axis.

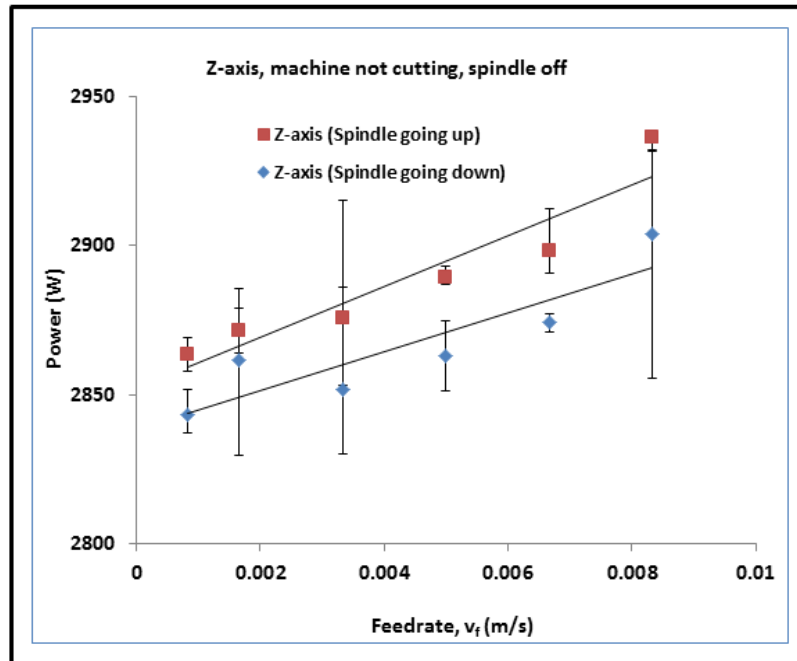


Figure 4.4 Power demand for the z-axis when the spindle was going up and down for Takisawa Mac-V3 milling machine

The second part of the study investigated the effect of known weights of materials on the power required by the machine axis when traversing over 150 mm linear length along the x- and y- axes. The results are shown in Figures 4.5 and 4.6. All tests were repeated three times for each of the weights.

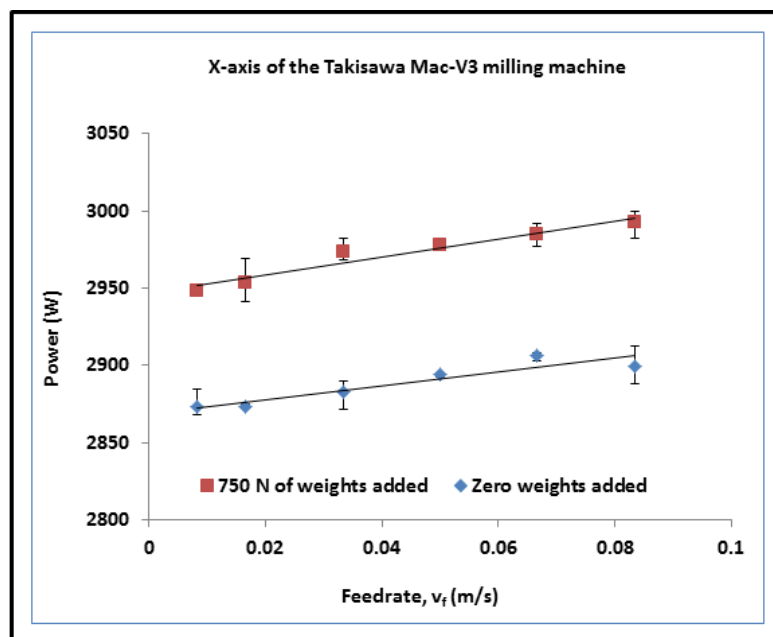


Figure 4.5 Variation of power with feedrates when specified weights are placed on the table of Takisawa Mac-V3 milling machine along the x-axis

Placing 750 N of weight on the net x-axis increases the power requirement by 3% compared to the machine axis with zero load. In addition, placing 750 N of weight on the net y-axis increases power requirement by 4% compared to the machine axis with zero load. It is also clear comparing Figure 4.5 to Figure 4.3 and Figure 4.6 to Figure 4.3 that the workpiece weight can have a larger impact on power requirements compared to the variation in feedrates. This further supports the analysis of the variance in results reported in Figure 4.2. The dominance of weights suggests that machining from a net shape or reducing the weight of machine tables has a significant impact on decreasing the power requirements and hence energy demanded by machine tool axis.

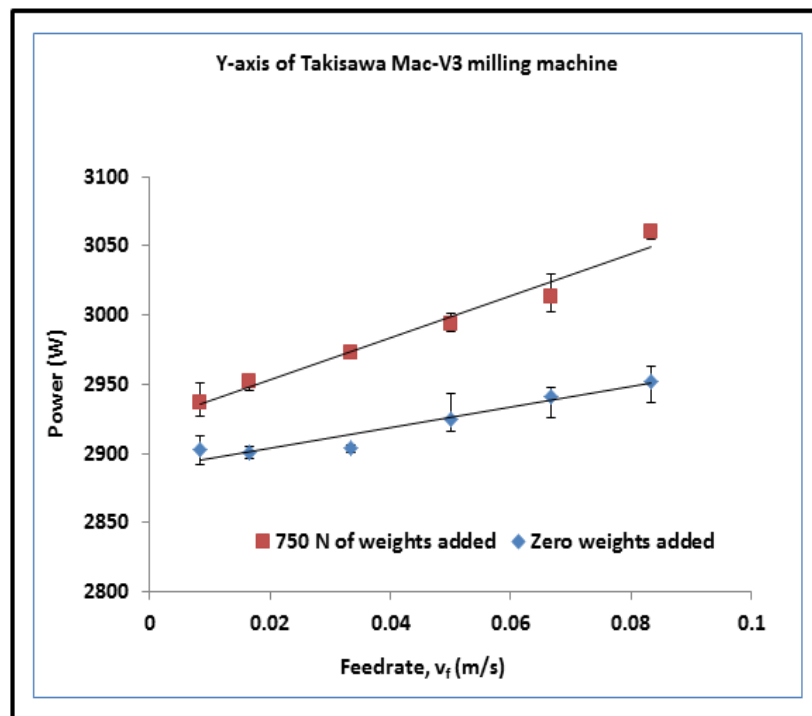


Figure 4.6 Variation of power with feedrates when specified weights are placed on the table of Takisawa Mac-V3 milling machine along the y-axis

Further tests were done along the x- and y- axes of the Takisawa Mac-V3 milling machine at different feedrates while varying the weights added on the table. Examples of such data are plotted in Figures 4.7 and 4.8.

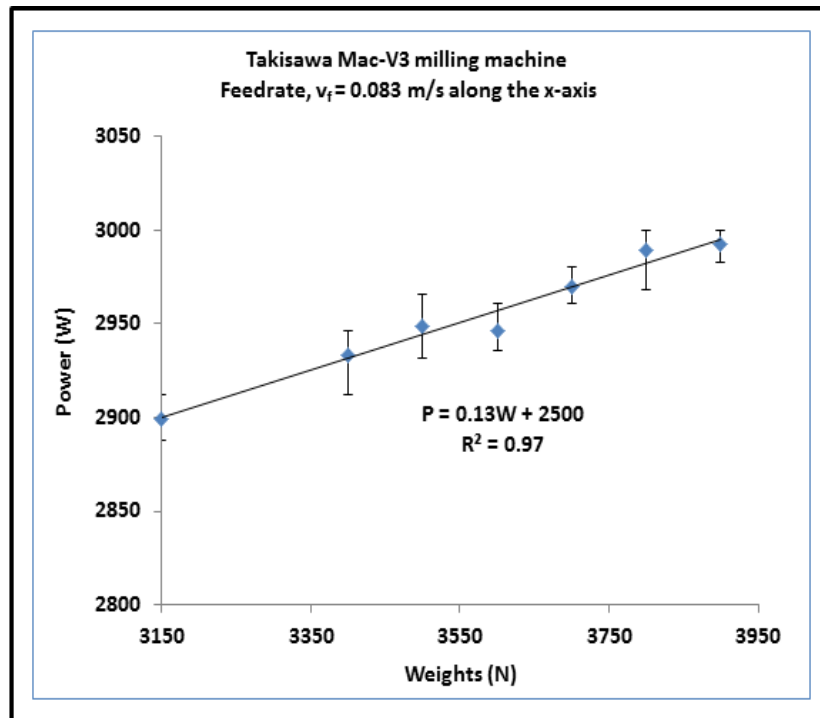


Figure 4.7 Variation of x-axis power with weights at feedrate of 0.083 m/s (5000 mm/min) for zero cutting operation

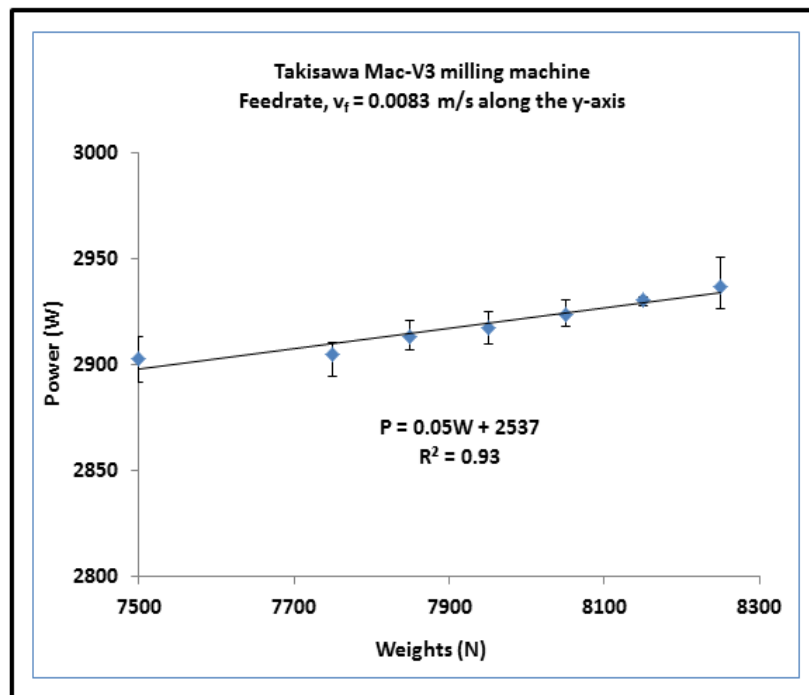


Figure 4.8 Variation of y-axis power with weights at feedrate of 0.0083 m/s (500 mm/min) for zero cutting operation

Considering Figures 4.7 and 4.8, it is seen that for selected table feedrates the power required by the machine when air cutting increases fairly linearly with the weights on the table. The study was done for feedrates of 500, 1000, 2000, 3000, 4000 and 5000 mm/min and the gradients of the resulting trends are shown in Tables 4.5 and 4.6 along the x- and y- axes respectively.

Table 4.5 Gradients from the linear variation of axis power with feedrates for the Takisawa Mac-V3 milling machine along the x-axis

Feedrate (m/s) / (mm/min)	Slope (W/N)	R ²
0.008 / 500	0.105	0.83
0.017 / 1000	0.106	0.92
0.033 / 2000	0.107	0.93
0.050 / 3000	0.113	0.89
0.067 / 4000	0.116	0.85
0.083 / 5000	0.127	0.97

Table 4.6 Gradients from the linear variation of axis power with feedrate for the Takisawa Mac-V3 milling machine along the y-axis

Feed rate (m/s) / (mm/min)	Slope (W/N)	R ²
0.008 / 500	0.050	0.93
0.017 / 1000	0.070	0.83
0.033 / 2000	0.090	0.91
0.050 / 3000	0.100	0.83
0.067 / 4000	0.100	0.80
0.083 / 5000	0.130	0.85

The data obtained from the effects of feedrates and weights were analysed to normalise the power demand per unit weight placed on the table for different table feedrates. The gradients in Tables 4.5 and 4.6, i.e. Watt per Newton (W/N) of workpiece weight, were used to derive a relation between power, weight and feedrate as shown in Figures 4.9 and 4.10 along the x- and y- axes of the CNC machine. Interestingly a linear relationship is obtained in both graphs.

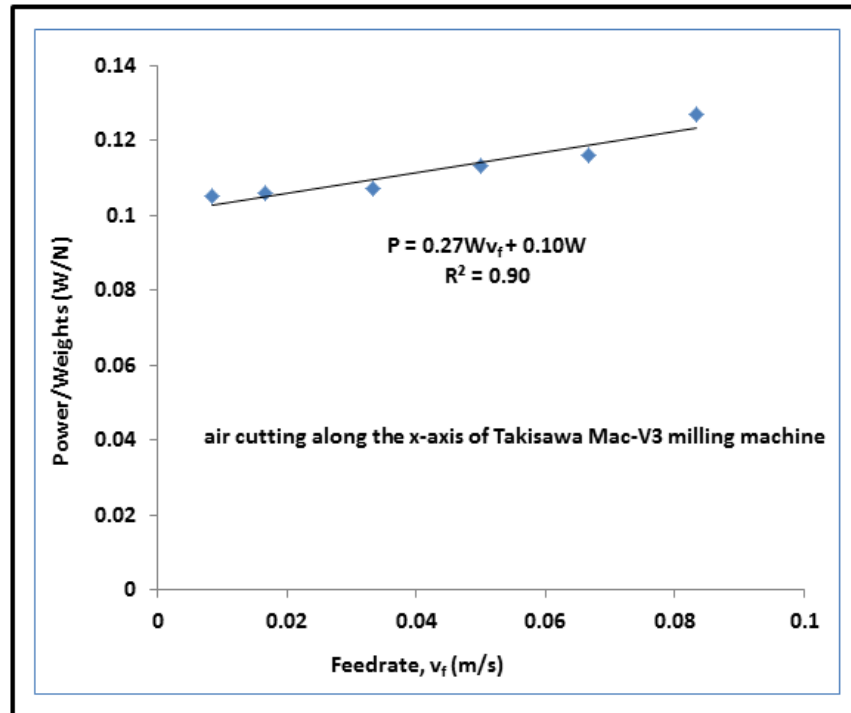


Figure 4.9 Variation of specific power per weight with feedrates for Takisawa Mac-V3 milling machine while not cutting along the x-axis

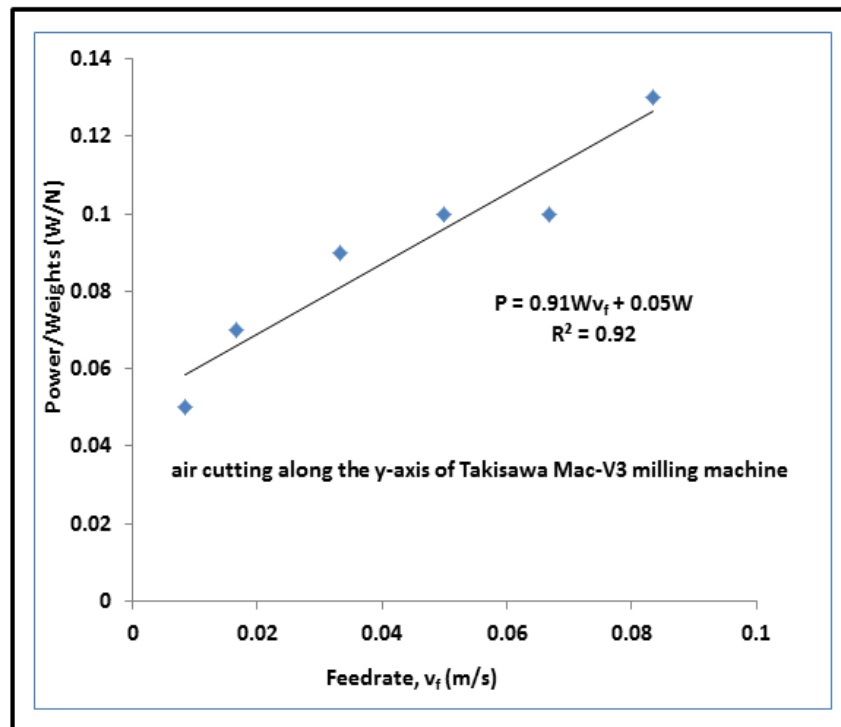


Figure 4.10 Variation of specific power per weight with feedrates for Takisawa Mac-V3 milling machine while not cutting along the y-axis

The trends in Figures 4.9 and 4.10 are linear graphs with $R^2 = 0.90$ and 0.92 respectively. These graphs can be used to derive a mathematical relationship between power, weight and feedrate. On this basis a relationship between power requirement and weight (Weights of workpiece, machine vice and feed axis), and table feedrate is obtained for the x-axis and the y-axis as shown in Equations 4.6 and 4.7. The baseline power (P_0) is incorporated into the equation since it is the power required at idle mode or ready state.

$$P_{f_x} = P_0 + (0.27Wv_f + 0.10W) \quad (4.6)$$

$$P_{f_y} = P_0 + (0.91Wv_f + 0.05W) \quad (4.7)$$

It should be noted that the parameter $W =$ (weight of axis + weight of vice + weight of workpiece).

where P_{f_x}, P_{f_y} are the power demand of the feed axes along the x- and y- direction, v_f retains its usual meaning, P_0 is the baseline power, W is the weight of the axis, workpiece, and machine vice. Equations 4.6 and 4.7 can be generalised into Equation 4.8.

$$P_f = P_0 + (aWv_f + bW) \quad (4.8)$$

where a and b are constants and v_f and W , retain their usual meanings of table feedrate and workpiece, machine vice plus axis weight respectively.

The power demanded at the tip when cutting is well modelled in the past. The feed power can be calculated from the feed force and table linear feed velocity. Therefore, in dry cutting the power demand by the axis can be modelled as shown in Equation 4.9.

$$P_f = P_0 + (aWv_f + bW) + F_f v_f \quad (4.9)$$

If the energy demand for machining is required then the power variation in Equation 4.9 and the cycle time can be considered to evaluate the energy. This can be modelled with Equation 4.10. To implement Equation 4.10, the effective feedrate of the machine table either from the CAM software at the planning stage or from the CNC toolpath needs to be determined.

$$E_f = P_0 t_{cy} + (aWv_f + bW)t_{cy} + F_f v_c t_c \quad (4.10)$$

where E_f is the energy demand for a table feed axis in dry cutting and t_{cy} and t_c is the total cycle time and the actual cutting time in seconds respectively.

In this paper cycle time is preferred, instead of distance travelled as in Campatelli et al. [90] because this enables analysis in relation to tool life and hence economics. In a milling process the feed force depends on the number of cutting edges engaged, the chip thickness and depth of cut as well as the specific cutting resistance. The feed force can be modelled as shown in Equation 4.11.

$$F_f = XKa_p f_z^x \sin\varphi^x \quad (4.11)$$

where X is the ratio of the feed force to the cutting force in milling, K is the specific cutting resistance in N/mm^2 , a_p is the depth of cut, f_z is the feed per tooth, φ is the swept angle in machining and x is a constant. Thus Equation 4.11 enables fusion of cutting conditions into energy analysis for an individual machine table axis, presenting a good link to optimisation at the process planning stage. It should be noted that the proposed equation is axis dependent and does not account for the power demanded by the spindle and coolant. This can be modelled separately and is adequately addressed in literature.

The limitations of the model are that, the dynamic characteristics of the feed drive were not considered in the model equation. In the machining considered, the relatively high acceleration meant that the machine was only accelerating for far less than 1 mm of travel and less than 1% of the toolpath. In this case these dynamic aspects can be safely ignored in estimating energy demand. However, the model may not be valid for micro or nano machining processes where the length of cut is less than 1 mm.

4.3.3 Implementation and validation of the power demand model of the feed axes during a milling process

In order to validate the newly proposed power model in Equation 4.9, air cutting runs were performed on the Takisawa Mac-V3 milling machine. A blank of billet stock of AISI 1018 steel was cut into size with dimensions of 100 mm long, 100 mm wide, and 20 mm in

height. These involved air cutting of linear tool paths along the x- and y- axes (i.e. at 0° and 90°), as well as at an angle of 30° to each axis. The sample workpiece is shown in Figure 4.11.

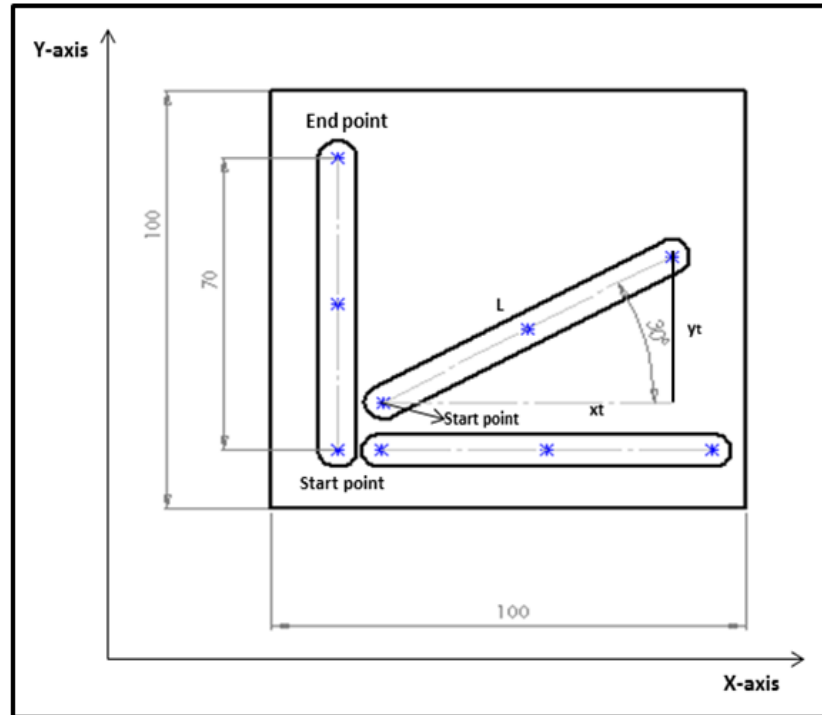


Figure 4.11 Toolpaths at different angles

The length of the toolpath was 70 mm. The spindle speed was kept constant at 4000 rev/min. The depth of cut was maintained at 0.5 mm, while feedrates of 500 mm/min and 3000 mm/min were considered for the validation. An 8 mm diameter uncoated carbide short end mill with 4 flutes was used in this study.

The power demands during air cutting of the slots were measured using the Fluke 434 power quality analyzer. In order to obtain the experimental power of the feed axes required for slot milling during air cutting, the tool executed specified linear tool paths at the feedrate of 500 mm/min and 3000 mm/min while the power consumed was simultaneously measured. Also, the spindle power characteristics at 4000 rev/min was measured to be 3113 W. Hence, subtracting the power required for spindle run from the air cutting power is equivalent to the power demand of the feed axis for executing a linear toolpath. The next step explains the manual estimation of the power demand of the feed axis based on a simple Numerical Control (NC) program.

In order to estimate the power demand for milling a linear toolpath at an angle of 30°, an NC code was generated for moving the tool from the start position to the end position at an angle of 30° (Figure 4.11). An example of the NC code is given below:

```
G00 X23.69 Y25.50 (Start point)
G01 X84.31 Y60.50 F500 (End point)
```

In the above NC code, the tool moves rapidly to the start point, and then performs a linear interpolation to the end point at the specified angle.

The actual travel motion along each axis can be estimated by comparing the values of the NC codes at the start and end points of the program. Hence, the actual feed rate along each axis can be estimated as in Smid [121]. This is shown in Equation 4.12.

Thus,

$$v_{f_i} = \frac{a_i}{L} \cdot v_f \quad (4.12)$$

where v_{f_i} is the actual feedrate moved by the specified axis, a_i is the motion (distance) travelled by the tool or axis in specified axis direction, L is the compound motion (distance) travelled by the toolpath in mm , while v_f is the given feedrate.

In the case of tool movement from point to point either at 0° or 90° (i.e. machining a toolpath either along the x- or y- axis direction), the total distance travelled, L is equivalent to the distance travelled. The feedrate remains constant.

Power demand models for each feed axis have been developed in this study (refer to Equation 4.9). Hence, these equations shall be adapted to estimate the predicted power demand for air milling of a slot at 0° (x-axis), 90° (y-axis), and at 30° (x- and y- axes).

These model equations can be modified to include the actual feedrates along each axis as shown in Equations 4.13 and 4.14.

$$P_{f_x} = P_0 + (aWv_{f_x} + bW) + F_f v_f \quad (4.13)$$

$$P_{f_y} = P_0 + (aWv_{f_y} + bW) + F_f v_f \quad (4.14)$$

where P_{f_x} , P_{f_y} are the power demand along the x- and y- axes respectively in Watt, v_f is the feed rate in m/s , a and b are constants, P_0 is the baseline power in Watt, W is the workpiece, machine vice and axis weights in N , F_f is the feed force in N , v_{f_x} , v_{f_y} are the corresponding feed rates along the x- and y- axes in m/s .

It should be noted that during air cutting, the feed force is equivalent to zero. Therefore, the total power demand in machining a toolpath while undergoing linear interpolation from the start point to the end point at a specified angle can be estimated by Equation (4.15).

$$P_f = \sqrt{P_{f_x}^2 + P_{f_y}^2} \quad (4.15)$$

where P_f is the total power demand of machining a tool path involving two feed axes.

Therefore, based on Equations (4.13), (4.14), and (4.15), the predicted power for air cutting along the x, y, and at an angle of 30° can be estimated.

Figures 4.12 a, b, and c illustrate power profiles for air cutting, as well as the predicted (model) and measured power demand for the feed axes of the Takisawa Mac-V3 milling machine at 500 mm/min.

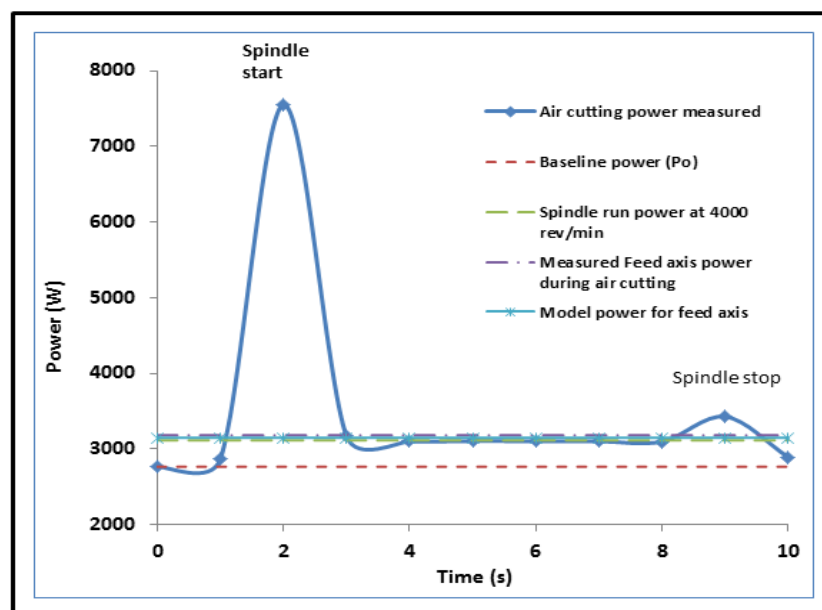


Figure 4.12a Power profile for Takisawa Mac-V3 milling machine during air cutting of a slot at zero degrees with feedrate of 500 mm/min

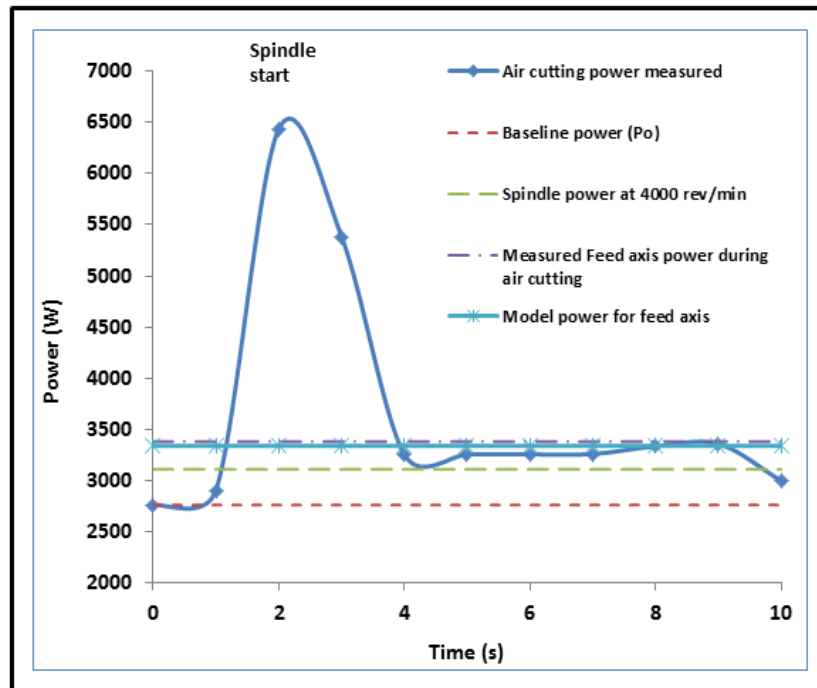


Fig. 4.12b Power profile for Takisawa Mac-V3 milling machine during air cutting of a slot at 30 degrees with feedrate of 500 mm/min

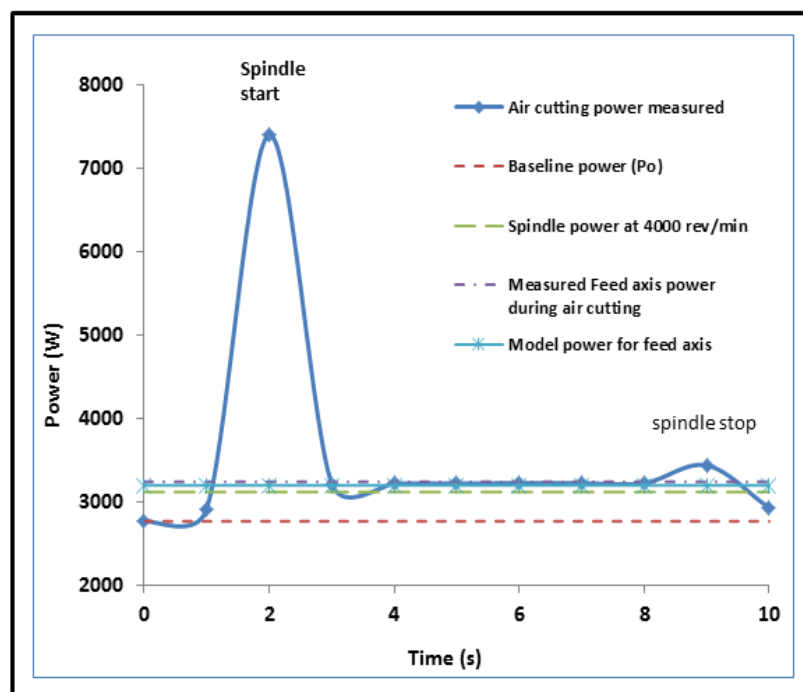


Fig. 4.12c Power profile for Takisawa Mac-V3 milling machine during air cutting of slot at 90 degrees with feedrate of 500 mm/min

The Fluke 434 power clamp quality meter was used to measure the power demand during air cutting, therefore the area under the graphs of the measured power and cycle time was used to obtain the measured energy demand.

The predicted power values for linear interpolation at 0°, 30° and 90° were estimated to be 3146 W, 3342 W and 3227 W respectively.

The measured power of the feed axes from the Fluke 434 power quality analyser gave 3180 W, 3385 W, and 3237 W for the aforementioned angles respectively. Thus, the deviation between the model and the measured power demand of the feed axes for the specified angles were between 1% and 2%.

Also presented in Figures 4.13 a, b, and c are power profiles for air cutting, as well as the predicted (model) and measured power demand for the feed axes of the Takisawa Mac-V3 milling machine at 3000 mm/min.

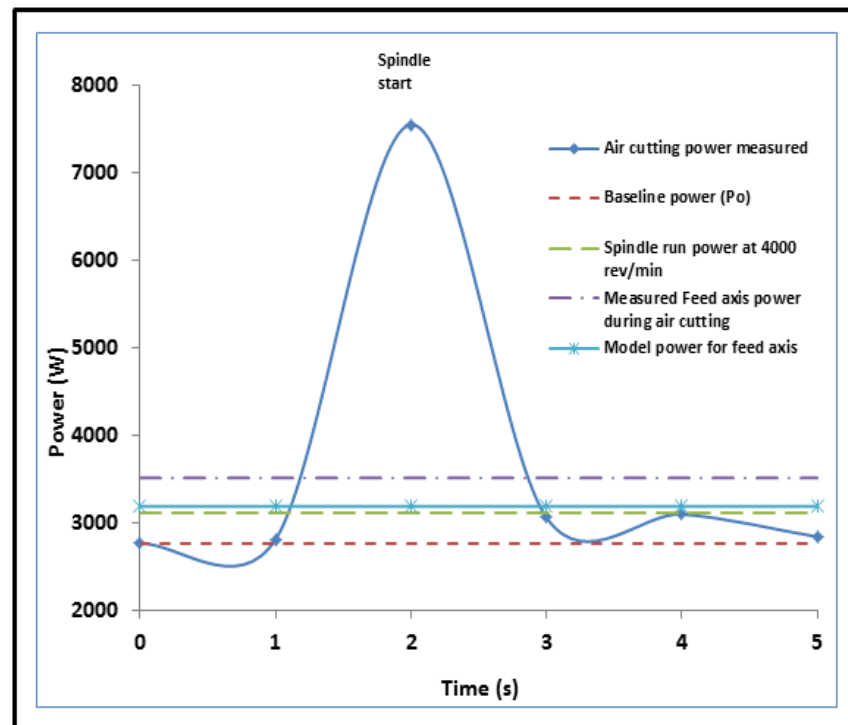


Figure 4.13a Power profile for Takisawa Mac-V3 milling machine during air cutting of slot at 0 degrees with feedrate of 3000 mm/min

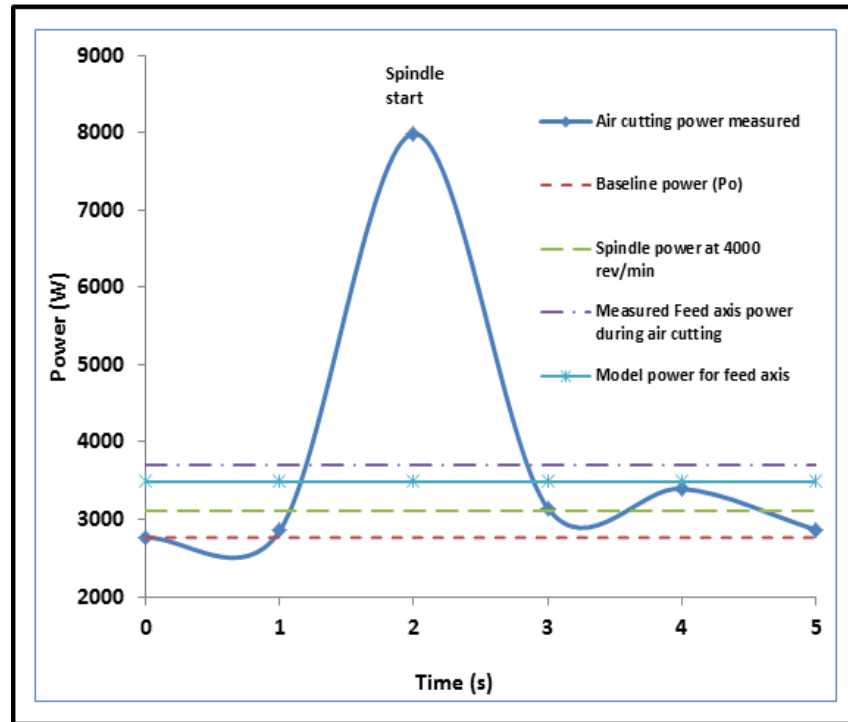


Fig. 4.13b Power profile for Takisawa Mac-V3 milling machine during air cutting of slot at 30 degrees with feedrate of 3000 mm/min

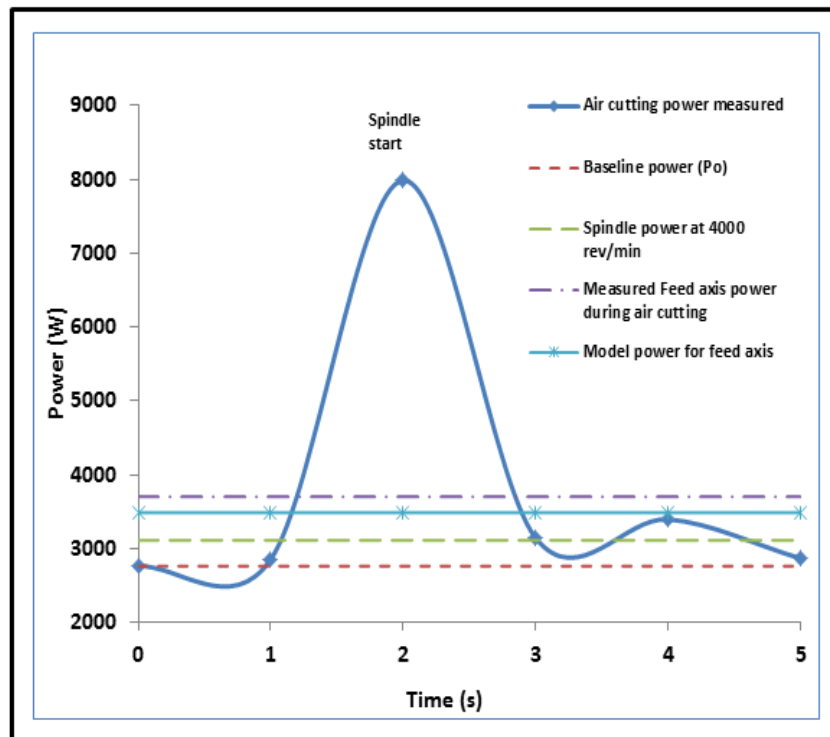


Fig. 4.13c Power profile for Takisawa Mac-V3 milling machine during air cutting of slot at 90 degrees with feedrate of 3000 mm/min

Predicted power requirements for feed axes at 3000 mm/min when tool is executing linear interpolation at 0°, 30° and 90° were estimated to be 3189 W, 3486 W, and 3537 W respectively. The measured power of the feed axes from the Fluke 434 power quality analyser gave 3510 W, 3702 W, and 3723 W for the aforementioned angles respectively. Thus, the deviation between the model and the measured power demand of the feed axes for the specified angles were between 5 % and 9%. The wide difference in the deviation may be due to the fact that the model does not capture the dynamic characteristics of the machine tool. More acceleration forces are required to actuate the feed drive at higher feedrates which result in feed axes power requirement increase.

Additionally, the energy required by the feed axes to execute a linear toolpath during air cutting can be estimated using Equation 4.10. Consequently, the results of some of the predicted and measured energy demand of the feed axes during air cutting are presented in Table 4.7.

Table 4.7 Predicted and measured energy demand of the feed axes

Energy	Characteristics	Takisawa Mac-V3 milling machine	
		500 mm/min	3000 mm/min
$P_{baseline}$ (W)	Base line power	2763	2763
$P_{spindle\ run}$ (W)	Power of running the spindle at speed of 4000 rpm	3113	3113
E_{feed}, E_{f_x} (kJ) (predicted)	Predicted energy of the feed axis along the x-axis at air cutting	26.43	12.76
E_{feed}, E_{f_x} (kJ) (measured)	Measured energy of the feed axis along the x-axis at air cutting	26.85	14.04
E_{feed}, E_{f_y} (kJ) (Predicted)	Predicted energy of the feed axis along the y-axis at air cutting	27.11	14.15
E_{feed}, E_{f_y} (kJ) (measured)	Measured energy of the feed axis along the y-axis at air cutting	27.20	14.89
$E_{feed}, E_{f_{xy}}$ (kJ) (predicted)	Total predicted energy of the feed axes during air cutting of a slot at an angle of 30°	28.44	13.94
$E_{feed}, E_{f_{xy}}$ (kJ) (measured)	Total measured energy of the feed axes during air cutting of a slot at an angle of 30°	28.74	14.81
% Difference between predicted and measured E_{f_x}		2	9
% Difference between predicted and measured E_{f_y}		0	5
% Difference between predicted and measured $E_{f_{xy}}$		1	6

The results in Table 4.7 show that all energy demand values of the feed axes are less than the measured power and energy demand. These may be as a result of the acceleration and deceleration of the feed drive or machine tool which are not estimated in the proposed model. Considering Table 4.7, at 500 mm/min, the difference between the measured and the predicted power is small due to the fact that at lower feedrates, minimal acceleration forces are required to actuate the feed axes. However, at 3000 mm/min, the differences are between 5% and 9% due to the fact that at higher feedrates, more acceleration forces are required to actuate the feed drives which results in rise in power and energy demand. Most conventional machining processes operate at feedrates less than 2000 mm/min and hence, this model will be highly accurate for such applications.

Nevertheless, it is important to mention that these values obtained further strengthened the fact that the power and energy models as stated in Equations (4.9) and (4.10) can be used for the generic estimate of the power requirement and energy demand of the feed axes, taking into account the weights of the axes, workpiece and vice. Detailed modelling of other elements of the machining process are covered in an earlier study [66].

4.4 Conclusions

- In manufacturing by machine tools, the feed axes position the entire movable parts of the machining system. Therefore, understanding energy demand by this motion system is essential in developing strategies for energy labelling and reduction for toolpaths.
- This chapter sets out to evaluate the effects of table feeds and weights on power requirements and hence net energy demand of the axis, and it was found that the weight being moved by the machine dominates the power requirement compared to the feedrate. This was also evident in the high energy consumed when machining was performed in the direction of axis carrying more weights when compared with the lighter axes.
- Additionally, in this chapter, a new model for estimating the total electrical energy demand of machine tool feed axes was presented which captures the impact of table feedrates, weights of machine table and materials placed on it. This means that the proposed empirical model in this study for estimating the energy demand of

machine tools can be used for conventional machining using ball screw feed drives for conventional sized components. This newly developed feed axes energy demand model was validated on a milling toolpath.

- This study suggests that machine tool manufacturers should readily provide information on machine tool table weights with a primary or secondary axis label since this information is critical for process planners and developers of CAM software's post processors in order to enable them to make informed decisions about optimum orientation of the machine tool axis for minimum energy consumption in machining. This information is not currently displayed on machine tools or included in CAM software.

CHAPTER 5

ENERGY DEMAND REDUCTION IN MILLING BASED ON COMPONENT AND TOOLPATH ORIENTATIONS

Reformatted version of the following paper:

Paper title: **Energy demand reduction in milling based on component and toolpath orientations**

Authors: **Isuamfon F. Edem, Paul T. Mativenga**

Published in: *Procedia Manufacturing* 7 (2016) 253-261
International Conference on Sustainable Materials Processing and
Manufacturing, SMPM 2017, 23-25 January 2017, Kruger National Park

ABSTRACT

Machine tool axis motions are the key movements when milling components and hence it is vital to understand how they influence energy demand in manufacturing. In this research, a systematic study of component and toolpath orientations was undertaken for milling operations. The current and voltage demand was monitored and this allowed evaluation of electrical energy demand. The machine tool was run while executing toolpaths in air (air cutting) and then in actual pocket milling of AISI 1018 steel and the component was rotated in the x-y plane of the machine. It was shown that when machining toolpaths were aligned to the lighter axis, this reduced the feed electrical energy demand by 29%, minimised the drive dynamics, and reduced surface roughness by up to 50%. Different toolpaths were tested in machining a pocket. The most energy efficient toolpath strategy had the best surface finish. Thus there are synergies in setting and programming toolpaths allowing simultaneous reduction of energy demand and component surface roughness. The knowledge obtained in this study is vital guidance for process planners.

Keywords: Energy efficiency; sustainable machining; machine tool vice orientations; toolpath orientations; toolpath strategies; surface finish

5.1 Introduction

In recent years, the competition for energy resources has increased. Major concerns are high energy bills and exhaustion of most of the world's non-renewable resources [3]. In 2013, the International Energy Agency (IEA) reported that the global electricity consumption was 19500 terawatt hour (TWh), of which about 42.3% (8249 TWh) was attributable to the industrial sector [122]. For example in the same year 2013, 98 TWh (26%) of electrical energy consumption in the United Kingdom (UK) was attributable to the industrial sector, of which about 7 TWh (7.2%) of electricity was consumed by the mechanical engineering sub-sector of the industry [123]. This electricity is generated from fossil fuels at the power stations which results in increased CO₂ emission [124]. This has led to the introduction of global carbon tax [125, 126] that is levied per tonne of CO₂ emitted. Thus, it is important to minimise the electrical energy requirement of fabricated goods in order to reduce production costs and carbon footprint while maximising profits.

5.1.1 Electrical energy demand of machine tools

The electrical power demand of machine tools fluctuates and is attributable to operating states of the machine tool. For example, Figure 5.1 presents a power-time profile for the power consumed when undertaking peripheral milling of AISI 1018 steel on a 3-axis Takisawa Mac-V3 milling machine. The power-time profile shows the ON state of the different power consumption levels including machine start up, system booting, hydraulic pumps starting, axes jogging, tool change, idle state, machining state with spindle start and spindle stop.

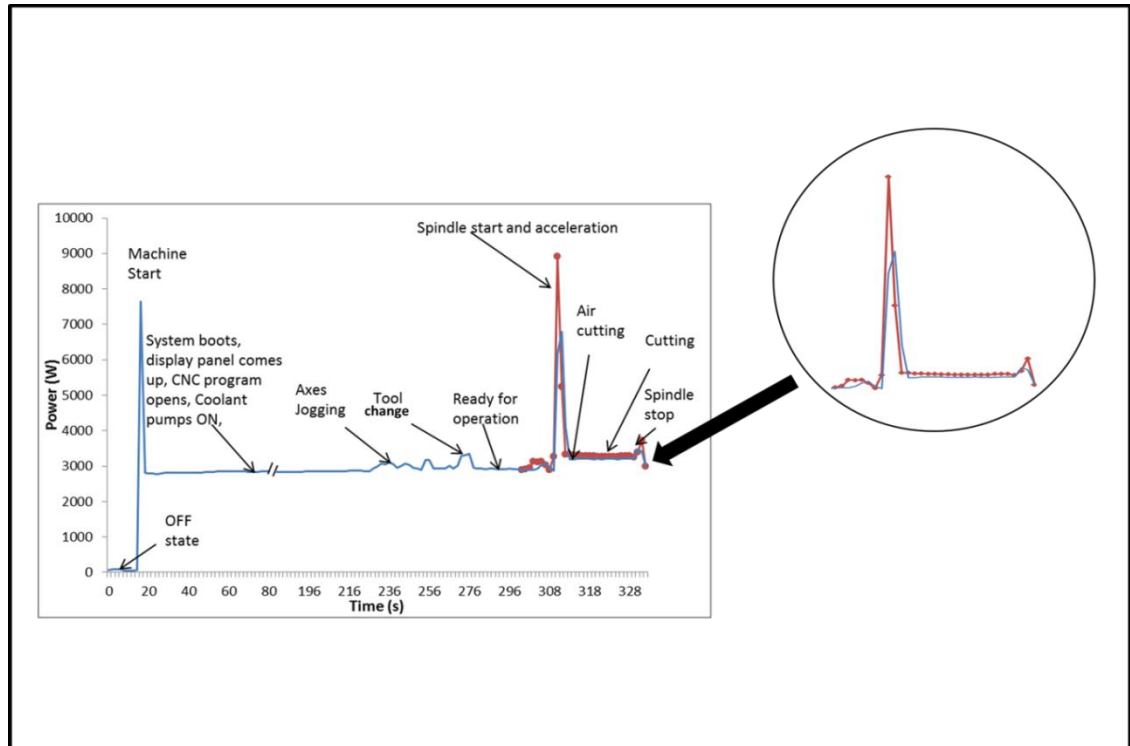


Figure 5.1 Power consumption profile for peripheral milling of AISI 1018 steel on the Takisawa Mac-V3 milling machine

The energy consumed by the machine tool is the area under the power-time graph which can be estimated as shown in Equation 5.1.

$$E = P \cdot t \quad (5.1)$$

where E is the total energy consumed in J , P is the total power demand in W , and t is the total processing time in s .

The constant start-up power is required by the auxiliary units including the computer and display, fans, servos, and unloaded motors. This power is constant and is independent of the machining state. It is consumed for the entire time the machine tool is in use. The constant run-time power is required for the positioning of the table with workpiece and the cutter. It is consumed by the spindle, feed axes, feed motors, spindle motors, tool change and axes jogging. The tip cutting or machining power is required for the actual cutting process. It is dependent on the material removal rate (MRR) or on the load applied on the machine which influences the power consumed at production mode.

5.1.2 Energy efficiency of machining toolpaths

Toolpaths are the paths guiding the cutter through the machined region. The selection of the most efficient toolpath strategy is necessary for better utilisation of the milling process [23]. Few researchers studied energy efficient toolpath orientations in milling. For example, Rangarajan and Dornfeld [23] investigated the impacts of toolpath orientations with respect to the feed axes. Two angles of orientation (0° and 36.9°) were considered in the study. Minimal cycle time was achieved when machining at 36.9° representing about 2 – 4% of energy savings in cycle time. Kong et al. [22] investigated the movement of machine tool axes along different orientations (between 0° and 90°). It was shown that maximum feedrate in the x-y plane of the machine axes occurs at 45° . Additionally, machining of toolpaths in the x-axis direction resulted in minimum energy being consumed by the feed axis. Oda et al. [127] studied tool angles and cutting speeds to determine an optimal angle for reduced energy demand while using a ball end mill to machine a workpiece mounted at varying inclined angles between 0° and 60° . Results show that lower power demand was obtained between 0° and 20° , with increased power demand noticed between 45° and 60° . Thus, machining at inclined angles ranging between 0° and 20° resulted in about 79% reduction in power demand. Aramcharoen and Mativenga [96] assessed the electrical energy demand for various machining toolpaths. They showed that contour and spiral toolpath strategies reduced energy demand by up to 5 times when compared with the zigzag toolpath.

Campatelli et al. [90] presented strategies for reducing the energy demand and environmental impact of milling processes by determining the most efficient position and direction in machining workpieces. It was shown that machining along the y-axis requires more power than machining along the x-axis as a result of the masses carried. Vila et al. [128] studied various toolpath strategies including zigzag in (x) direction, one way in (x) direction, one way in (y) direction, zigzag in (y) direction, contour toolpaths and their impacts on the specific energy demand. Results showed that minimal specific energy demand and environmental impact in terms of CO₂ generation was obtained when machining in one way (x) direction. Recently, Kuram and Ozelik [129] studied the effects of toolpath strategies on surface roughness, tool wear and cutting forces in micro milling of Ti6Al4V titanium material. The zag and zigzag toolpaths were considered. Results show

that the zigzag toolpath when machining at lower feedrate and higher spindle speed produced better surface finish than the zag toolpath strategy.

From reviewed studies, insights into the effects of toolpaths on energy demand have been provided. However, the effects of machine tool vice and toolpath orientations on the electrical energy demand of a milling process and surface finish of the machined part were not explicitly documented. This motivated this work.

5.1.3 Research aim and objectives

The aim of this research was to simultaneously analyse the influence of machine tool vice and toolpath orientations on the electrical energy demand and surface roughness of the machined part. To achieve this, it is important to: i) assess the electrical energy demand when orienting the machine tool vice and component at different angles in the x-y plane of the machine tool table; ii) determine the surface roughness of the machined part in order to develop recommendations for minimum energy demand in mechanical machining with regards to the machine tool axes configuration; iii) determine the impacts of toolpath strategies on the electrical energy demand and surface finish characterisation of a milling process. The knowledge obtained in this study would aid in providing recommendations for improving electrical energy efficiency and sustainable manufacture of components.

5.2 Experimental details

5.2.1 Research methods

The research method is based on assessing the electrical energy requirement of the machine tool and surface roughness of the machined part at different machine tool vice and component orientations. Air cutting and pocket milling were undertaken while the machine tool vice and component was mounted at different angles in the x-y plane of the machine table. The pocket and toolpath were machined parallel to each angle of orientation. The current and voltage drawn were directly measured using FLUKE 434 Power Quality Analyser. Surface roughness of the machined pockets at different machine tool vice and

component orientations was checked after the material removal process was completed. Further machining tests were performed to determine the influence of toolpath strategies on the feed axes electrical energy demand and surface roughness.

5.2.2 Experimental setup and procedures

Milling tests were conducted on a 3-axis Takisawa Mac-V3 milling machine. The machine tool is capable of spindle speeds of up to 10,000 rev/min. The axes drives were powered by the AC servo motors connected directly to the ball screw drive. The machine construction has the machine table and x-axis directly mounted on the y-axis. The masses for the x- and y- axes, modelled from SolidWorks software are approximately 315 kg and 750 kg respectively.

Five pieces of AISI 1018 steel workpiece material with dimensions of 75 mm x 50 mm x 12 mm and average weights of 343 g each were cut for the milling tests. The density and average hardness of the workpiece are 7.85 g/cm³ and 233 HV respectively. The spindle speed, the depth of cut, and step over were kept constant at 4000 rev/min, 0.5 mm, and 0.75D respectively. The pocket length was 58 mm while the width was 28 mm. A new tool was used each time pocket milling was undertaken in a different machine tool vice orientation, and at feedrates of 500, 1000, and 2000 mm/min. The cutter was 8mm diameter short carbide, 4 flute end mill.

A swivel vice was used for this study in order to enable the accurate rotation of the machine tool vice to the desired angle. The weight of the vice was 76 kg. The swivel vice was rotated to five angles including 0° (with movement of the feed drive in the x-axis direction), 30°, 45°, 75° (with movement of the feed drive in x- and y- axes directions) and 90° (with feed drive moving in the y-axis direction). Figures 5.2a and 5.2b show the machine tool vice and component orientation, as well as the direction of the feed drive for air cutting and pocket milling at 0° and 45°. These same patterns were also followed for the other machine tool vice and component orientations.

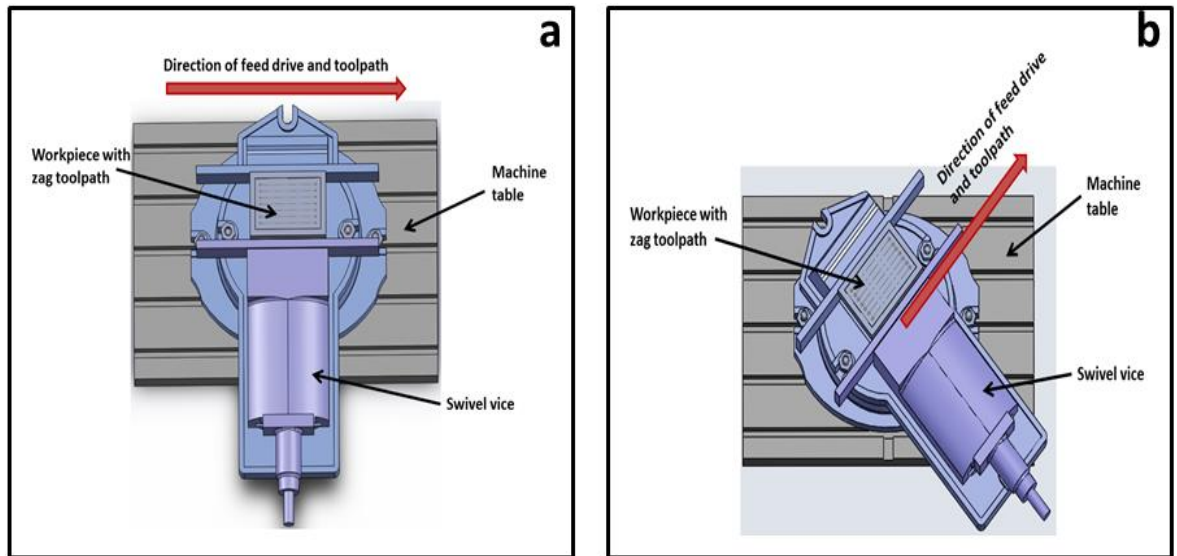


Figure 5.2 (a) Machine tool vice and component oriented at 0 degrees showing direction of feed drive and toolpath (feed drive moves in the x-axis direction)
(b) Machine tool vice and component oriented at 45 degrees showing feed drive and toolpath directions (feed drive moves in the x- and y-axes direction)

The cutting tests were carried out under a dry cutting environment. Each of the cutting test runs were repeated three times.

5.3 Results and discussions

5.3.1 Impact of machine tool vice and toolpath orientations on electrical energy demand of a milling process

The electrical energy demand was estimated from the acquired power and cycle time of the material removal process. Figures 5.3 a, and b show the relationships between the electrical energy demand and machine tool vice and component orientations in the x-y plane with feed drive movement along the specified vice orientation for air cutting and total cutting electrical energy demand respectively.

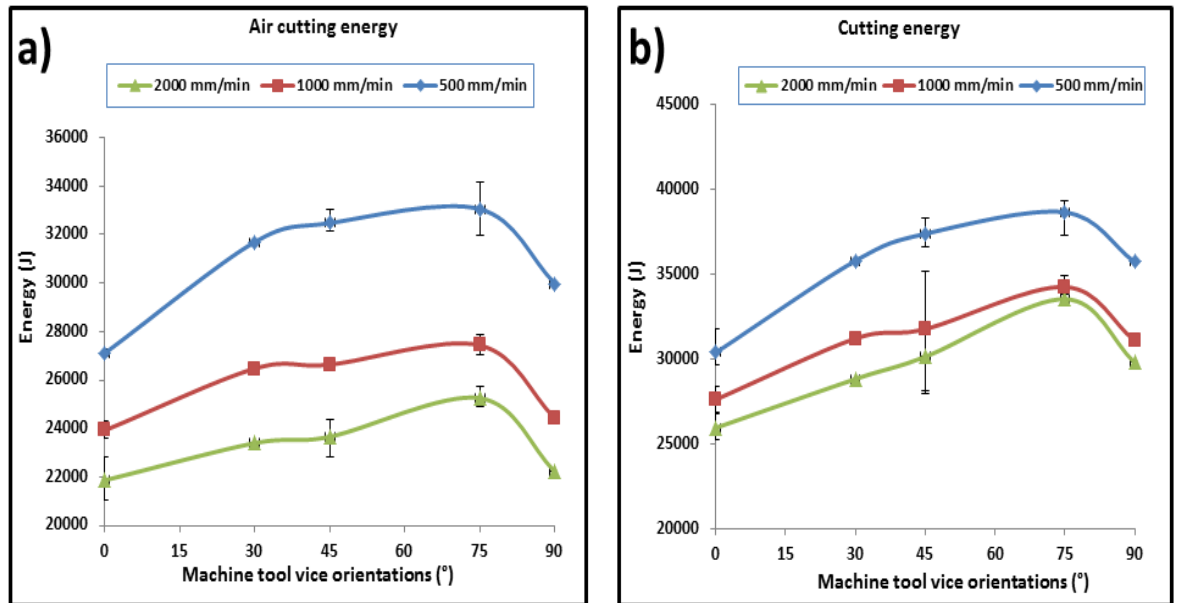


Figure 5.3 a,b Energy demand when executing air cutting and cutting with machine tool vice and toolpath oriented at different angles respectively

In Figure 5.3a, it is observed that executing air cutting with the vice oriented at 0° (movement of the feed drive in the x-axis direction) resulted in minimal electrical energy consumption. The machine tool consumed about 15% more electrical energy with machine tool vice oriented at 75° compared to 0° with feedrates of 500 and 1000 mm/min; and 22% more electrical energy at 2000 mm/min. At 90° , 2%, 2%, and 10% more electrical energy demand was consumed than at 0° for the aforementioned feedrates. In Figure 5.3b, orienting the machine tool vice at 75° resulted in 29%, 24%, 27% more energy demand at feedrates of 500, 1000, 2000 mm/min respectively than at 0° , while orienting the machine tool vice at 90° resulted in 15% to 18% more electrical energy demand than at 0° .

Figures 5.3a and 5.3b show minimal electrical energy demand for machine tool vice orientations at 0° and 90° due to the actuation of only one axis when tool movements are aligned at these angles, while the electrical energy demand for machine tool vice orientations between 15° and 75° was higher when compared to that obtained at 0° and 90° due to the movement of the combined weights of the x- and y- axis. Thus, cutting with machine tool vice oriented at 0° may save up to 29% in electrical energy irrespective of the feedrates considered. This enables reduction in the variable energy demand of the machine tool.

5.3.2 Surface roughness for different machine tool vice and toolpaths angles

Surface roughness check of the machined pockets with regards to machine tool vice orientations was performed with the Surtronic 25 surface roughness checker. Three different points on the machined pocket surface were measured and the average surface roughness recorded based on the specified feedrates. Figure 5.4 shows variation of average surface roughness, Ra in (μm) with machine tool vice orientations and at varying feedrates. It should be noted that the surface roughness are high because this was a semi roughing process studied. These values can be improved in finishing operations.

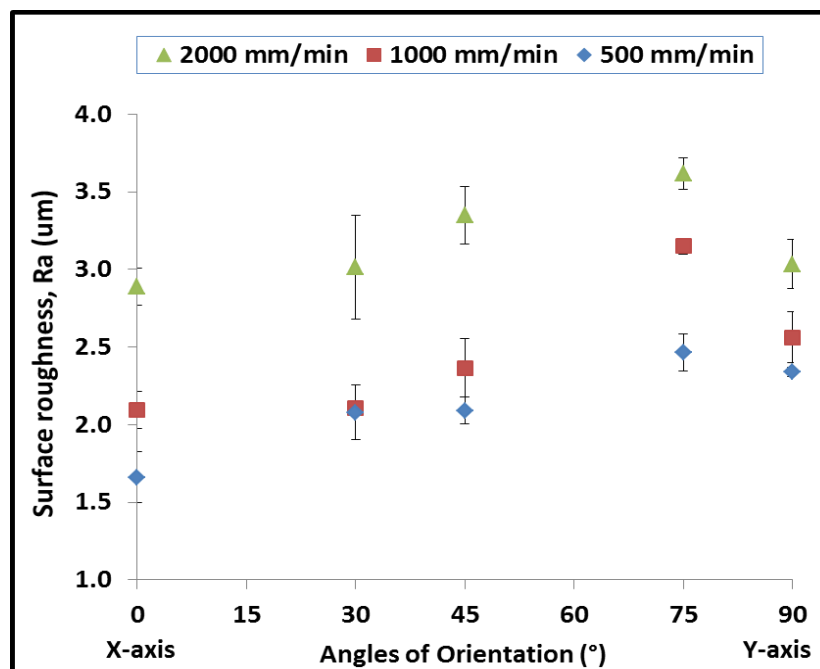


Figure 5.4 Surface roughness measured perpendicular to the cutting direction when rotating the machine tool vice at varying orientations and varying feedrates

Dornfeld and Lee [130] maintained that the quality of the machined part may be affected by weight forces. Thus, error due to deformation may be as a result of the interplay occurring between the deviating machine weight in the material removal process and the machine tool foundation. For example, the deformation of a machine table moving in the y-axis direction in the x-y plane may result in changing orientation and movement of the tool with respect to the workpiece. This is due to the heavier weight of the part on the machine table coupled with movement in the positive and negative directions of the y-axis. Thus, deformation between the workpiece and the tool varies as a result of the changing

cutting forces in the machining process. These errors are simultaneously reflected on the surface of the machined part.

Figure 5.4 shows minimal surface roughness values when machining with the machine tool vice oriented at 0° and feed drive motion in same direction irrespective of the feedrate. This may be due to the fact that the feed drive and tool movement at this angle is aligned in the x-axis direction which carries minimum weights. Nevertheless, high surface roughness values of 2.46, 3.15, and 3.62 μm for feedrates of 500, 1000, and 2000 mm/min respectively were obtained when the machine tool vice was oriented at 75° which is aligned in the x- and y- axes direction. Figure 5.4 also showed that surface roughness fairly increased (i.e. ranging from 1.16 - 2.46 μm for 500 mm/min; 2.09 – 3.15 μm for 1000 mm/min; 2.88 – 3.62 μm for 2000 mm/min) as the machine tool vice orientations increased from 0° to 75° , with a slight decrease in surface roughness values as the vice was oriented at 90° . Machining at 500 mm/min with machine tool vice orientation at 75° increases the surface roughness values by 48% than the surface finish values obtained at 0° . Also, the average surface roughness values when orienting the machine tool vice at 90° is 40% more than at 0° . Therefore, it can be inferred that machining along the axis carrying minimum weights results in improved surface finish by up to 50% when compared to the roughness values obtained when the machine tool vice is oriented at angles along the x- and y- axes directions.

Additionally, the results in Figures 5.3 and 5.4 show that there may be a correlation between energy demand and surface finish in that component orientation and movement of the feed drive in the direction of axis carrying minimum weights could result in reduced energy demand and improved surface finish.

5.3.3 Influence of toolpath strategies on the electrical energy demand

Further studies were undertaken to determine the effects of toolpath strategies on the feed axes electrical energy demand. Pockets on AISI 1018 steel with dimensions of 150 x 100 x 20 mm where machined along the x- and y- axes of the Takisawa Mac-V3 milling machine with the zag, zigzag, and rectangular contour offset. The toolpaths were generated using the Hyper mill CAM software. The pocket length was 122 mm while the width was 54 mm. An 8 mm diameter, 4 flutes carbide short end mill was used. The weight of the

workpiece was 3 kg. The weight of the vice was 57 kg. The cutting speed was 100 m/min. Spindle speed was maintained at 4000 rev/min. The depth of cut was kept at 0.5 mm. The feedrate was maintained at 500 mm/min to prevent the dominance of feedrates on the feed axes power. The ratio of width of cut to tool diameter was set at $0.75D$. Flood cutting was used. The tests were repeated three times for repeatability and accuracy of results while the power requirement of the CNC machine during the pocket milling process was measured. The sample pockets with toolpaths are presented in Figure 5.5.

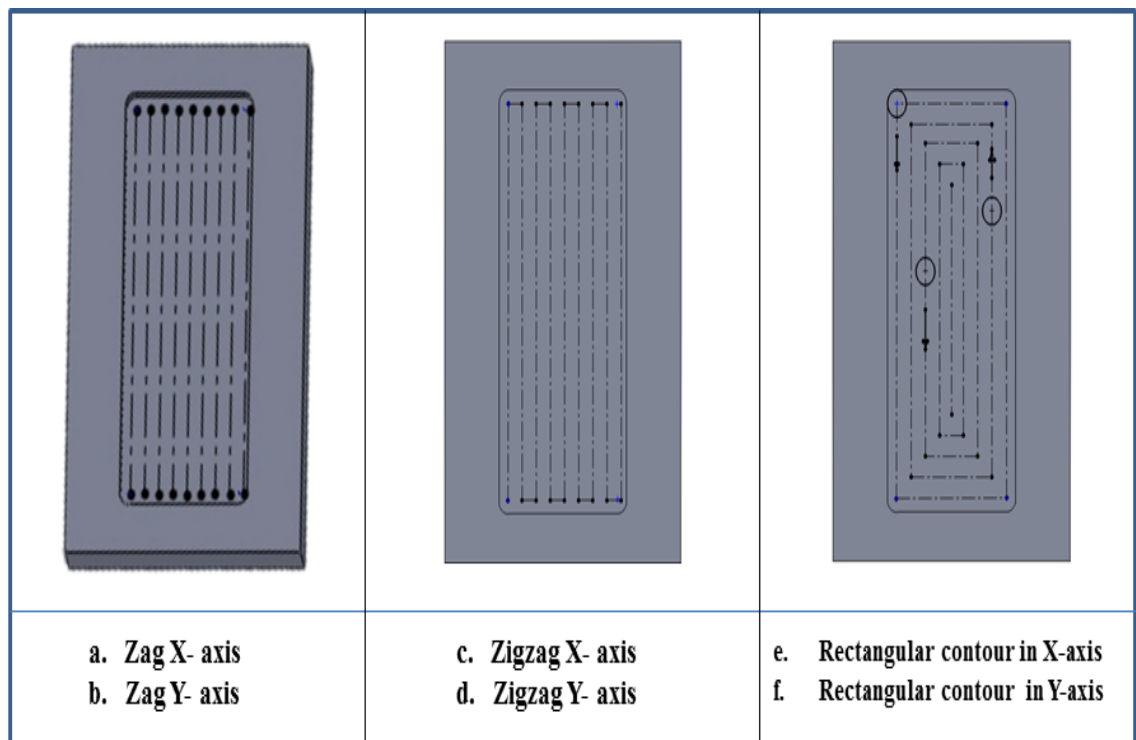


Figure 5.5 CAM toolpath showing different toolpath strategies

The feed axes power was obtained by subtracting the spindle power and the baseline power from the total cutting power. The feed axes power value and the processing time were then used to estimate the feed axes electrical energy required for each toolpath strategy. Figure 5.6 shows the feed axes electrical energy demand during pocket milling of the test materials with different toolpath strategies and axes movements.

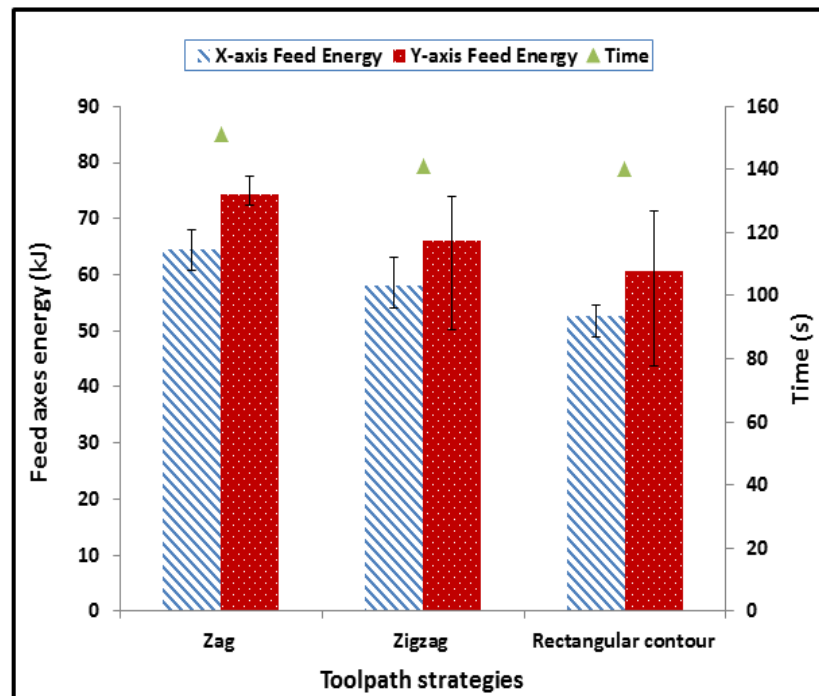


Figure 5.6 Feed axes energy demand for different toolpath strategies during pocket milling of AISI 1018 steel along the x- and y- axes of Takisawa Mac-V3 milling machine

From Figure 5.6, it is observed that the y-axis consumes 15%, 14%, and 15% more feed axes electrical energy than the x-axis of the Takisawa Mac-V3 milling machine for zag, zigzag, and rectangular contour toolpaths due to the weights carried. This result agrees with the work presented in Edem and Mativenga [131]. It can be deduced that energy efficiency of toolpaths can be improved by machining along the axis with minimal moving weights. It is also observed in Figure 5.6 that the rectangular contour toolpath is the most efficient toolpath strategy in terms of energy demand and processing time due to zero tool retracts and longer cutting length aligned to the pocket geometry.

5.3.4 Influence of toolpath strategies on surface quality of machined material

The surface roughness of the pockets was checked at the end of the machining operation with Surtronic 25 surface roughness checker. Figure 5.7 shows variation of surface roughness with toolpaths along the x- and y- axes of the Takisawa Mac-V3 milling machine.

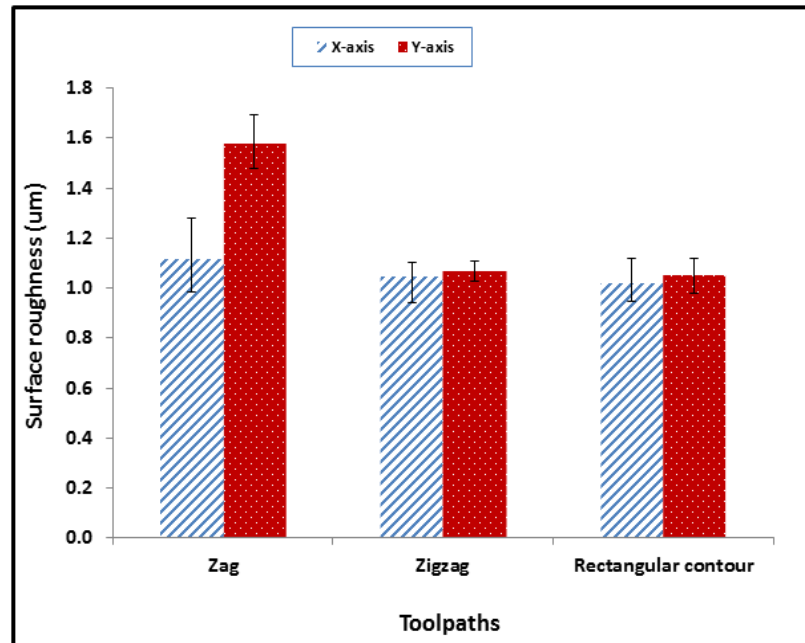


Figure 5.7 Surface roughness of toolpaths along the x- and y- axes of Takisawa Mac-V3 milling machine

It is observed that machining along the y-axis of the Takisawa Mac-V3 milling machine resulted in 40%, 2%, and 3% more surface roughness values for the zag, zigzag, and the rectangular contour toolpath strategies than the x-axis respectively. Even though the surface roughness values for the zigzag and rectangular contour toolpaths were minimal, the rectangular contour toolpath had the best surface finish with about 30% of improved surface finish, while the zag toolpath had the worst surface finish.

5.4 Conclusions

In this study, impacts of machine vice orientations and toolpath strategies on the feed axes electrical energy demand and surface finish were investigated in order to identify measures for obtaining minimum energy consumption. The following conclusions were obtained in this study:

- Minimum electrical energy demand for feed axis during air cutting and pocket milling was obtained with machine vice and component oriented at the angle aligned in the direction of axis carrying less weight, resulting in electrical energy savings of up to 29%.

- Pocket milling with the machine tool vice and component orientation at 0 degrees resulted in better surface finish. Thus, machining with the vice aligned in the direction of the axis carrying minimum weights (0 degrees) resulted in improved surface finish by up to 50% when compared with the roughness values obtained when the machine tool vice was aligned in other axis directions.
- The feed axes energy result shows that rectangular contour toolpath is the most efficient in terms of feed axes energy and processing time. This may be due to longer cutting length of the toolpath before linking the next cutting pass. In case of the zag toolpath, the number of tool retracts resulted in higher feed energy and processing time when compared with that of the rectangular contour. Thus, utilising toolpaths with less tool retractions results in lower processing time and energy consumption.
- The rectangular contour toolpath had the best surface finish with about 30% of improved surface finish obtained, while the zag toolpath strategy had the worst surface finish. The result obtained in the surface finish analysis correlates with the energy consumption, in that the most efficient toolpath strategy has the best surface finish with minimal electrical energy requirement.

CHAPTER 6

MODELLING OF ENERGY DEMAND FROM COMPUTER NUMERICAL CONTROL (CNC) TOOLPATHS

Reformatted version of the following paper:

Paper title: **Modelling of energy demand from computer numerical control (CNC) toolpaths**

Authors: **Isuamfon F. Edem, Paul T. Mativenga**

Submitted to: **Journal of Cleaner Production**

ABSTRACT

It is important to accurately model the total electrical energy requirements in order to compare and select the least energy consumption toolpath in a manufacturing process. To enable this goal in this study, a feed axes energy demand model proposed in previous work by the authors was integrated and used to refine the energy consumption models for machine tools to analytically estimate the power and processing time, and hence energy required to execute a CNC toolpath. Furthermore, an algorithm for establishing energy prediction software with regards to NC codes was developed based on the proposed energy consumption model. The NC-code based analytical model and energy prediction software were both validated by undertaking slot milling of a 2D half bottle toolpath. Results from this study show that shorter length of linear path (i.e. G01) and circular path (i.e. G02 and G03 codes) segments were highly energy intensive. This is because for short length segments, the maximum feedrate may not be reached due to constraints imposed by acceleration and deceleration; the weights carried take a higher share of the load, and therefore increase the inertia effects on the drive. Thus, energy intensity in machining could be significantly reduced by selecting toolpaths with longer linear path segments. The knowledge obtained in this study would enable machining engineers to predict the electrical energy for toolpaths and hence enable selection of toolpaths for reduction of electrical energy demand in machining.

Keywords: Energy efficiency, energy demand, modelling, sustainable machining, NC codes, NC program, software, toolpaths.

6.1 Introduction

Electricity used in manufacturing is allocated carbon emissions because when the electricity was generated at power stations, fossil fuels and carbon rich energy sources were used which produced CO₂ emissions [124]. The manufacturing sector is one of the significant consumers of energy globally [5]. The International Energy Agency (IEA) [132] reported that the total global electricity demand for 2014 was 1706 Mtoe (19840.78 TWh), of which 42.5% was attributable to the industrial sector. Also, in the year 2014, 93 TWh (26%) of electrical energy consumption in the United Kingdom (UK) was attributable to the industrial sector, of which about 17.7 TWh (19%) of electricity was consumed by the engineering sub-sector of the industry [133].

Mechanical machining is one of the widely used technologies within the manufacturing sector. Machine tools used in machining consume electricity during the idle and functional period of the metal removal processes. This electricity consumption increases the environmental impacts in machining processes [9]. Diaz et al. [57] conducted a life cycle energy consumption analysis of two milling machines in their use phase. Results show that about 75% of total emissions were from the machine tools' use phase. The Cooperative effort on process emissions in manufacturing (CO₂PE!) [14], the European Union (EU) Eco-design Directive [134], European Association of Machine Tool Industries (CECIMO)'s Self-Regulatory Initiative (SRI) [8], ISO 14955-1 [15] all prioritise energy demand reduction for machine tools during their use phase.

6.1.1 Energy demand modelling in mechanical machining processes

The electrical energy consumed by machine tools throughout the use phase dominates their life cycle environmental impacts [12]. The first step to energy demand reduction in machine tools is to have a better understanding of energy consumption. To achieve this, it is important to model the energy required in a machining process. Jia et al. [87] presented

an analytical model which integrates the different machining states with the energy requirements of basic motions of the CNC machine tools. In their study, the power demand of the feed axes was assumed constant and was not explicitly modelled. Building on Jia et al. [87]'s work on Therbligs, Lv et al. [88] proposed an improved methodology for estimating energy demand of machine tools. Therblig is defined as a group of motions necessary for machine tool operations such as standby operations, lighting, spindle rotation, tool selection/tool changing, cutting, x-, y-, z-axes feeds and cutting fluid spraying. This study, though an addition to machining science, did not explicitly model the Therblig feed axes energy demand to include weights of the feed axes and materials placed on machine table.

Other approaches of modelling the electrical energy demand of toolpaths could be by disintegrating the direct electrical energy consumed by the machine tool into energy consuming units including spindle, feed axes, coolant pump, tool change system, as well as components that consume constant energy. The sum of each component's energy consumption is used to evaluate the total energy demand. This approach is found in studies presented in [26, 86, 96], and is in line with the model proposed in this study. This approach was preferred in this study in order to effectively relate NC codes to the energy consuming units of the machine tool. This way, the influence of interpolations on energy intensity of machine tool would be effectively characterised.

Diaz et al. [19] proposed a web-based energy consumption model for estimating the energy requirements of machine tools based on the correlation between the energy demand and the processing time. Hu et al. [63] utilised an online energy efficiency monitoring approach to model the energy consumption of a machining process by developing an architecture for the online energy monitoring system (OEEM system).

Few researchers have modelled the electrical energy demand of the variable energy consumers (spindle and feed drives), as well as targeting their energy consumption reduction. For example, Campatelli et al. [90] presented an analytical model of the energy demand for feed axis which takes into account the effect of masses and friction. Recently, Edem and Mativenga [131] proposed a new model for estimating the electrical energy demand of machine tool feed axes which incorporates the weights of feed axes and weights of the materials placed on the machine table, the feed force, and the table feedrate. The newly proposed model was validated on milling CNC toolpaths.

6.1.2 NC-codes energy modelling in mechanical machining

Computer numerical control (CNC) machining is critical to mass and customised manufacture. Numerical control (NC) is the process of controlling the motion of machine tool components by directly inputting coded commands in the form of letters and numbers into the system. NC codes consist of G, M, S, and F-codes which control the functional performance of NC machines. The main energy consumers in machine tools consists of the auxiliary units including the fans, unloaded servo motors, light, computers, air pumps, coolant pumps, lubricating pumps etc.; the spindle, feed axes including the x-axis, y-axis, z-axis; servo motors, and the tool change system [66]. These components are all related to the NC codes through the machine tool controller.

Few researchers developed energy consumption models of machine tools based on CNC codes, and a summary of their models is presented in Table 6.1.

Table 6.1 Summary of energy consumption models for toolpaths based on CNC codes

Authors	Energy Model	Remarks/Limitations
He et al. [26]	$E = E_{spindle} + E_{feed} + E_{tool} + E_{coolant} + E_{fix} \quad (6.1)$ <p>where $E_{spindle}$ is the energy required during the cutting operation as well as the energy consumption of the spindle in J, E_{feed} is the energy consumption in J of the feed axes, E_{tool} is the energy in J required for tool change, $E_{coolant}$ is the energy consumption in J of the coolant, E_{fix} is the energy consumption in J of the servo motor and the fan system</p>	Provides insight into modelling of energy demand based on NC codes; Circular interpolation was not considered, Weights moved by the feed drive were not considered;
Aramcharoen and Mativenga [96]	$E_{total} = E_{basic} + E_{tool} + E_{spindle} + E_{cutting} + E_{feed} + E_{cutting-fluid} \quad (6.2)$ <p>where E_{basic} is the energy required by auxiliary and peripheral units in J, $E_{spindle}$ is the energy required by the spindle in J, E_{tool} is the energy consumed at tool change in J, $E_{cutting}$ is the cutting energy for material removal in J, E_{feed} is the energy consumed by the feed drives in J, $E_{cutting-fluid}$ is the energy required by the cutting fluid pump motor in J.</p>	Analytically modelled the electrical energy demand based on NC codes. However, feed axes energy was not modelled to include weights of the feed axes, workpiece and machine vice; circular interpolation and total time were not considered; energy intensity of toolpath interpolations were not considered; Energy

		demand software was not developed.
Guo et al. [97]	$E_{TOT} = E_{RTM} + E_{MRM} + E_{PTM} \quad (6.3)$ <p>where E_{TOT} is the total energy for manufacturing a product (J), E_{RTM} is the energy required for rapid traversing (J), E_{MRM} is the energy required for cutting (J), E_{PTM} is the energy required for process transition mode (J)</p>	Used NC codes to model and simulate the energy demand of machining processes; feed axes energy demand model did not highlight the importance of weights of the axes, machine tool vice, and workpiece; NC codes were not related to energy consuming components; energy intensity of toolpath interpolations were not considered
Pavanaskar and McMains [27]	$E_{machine} = \sum E_{block} = E_{const} + E_{variable} \quad (6.4a)$ $E_{block} = (P_{tare}) \cdot t + (P_{coolant\ pump}) \cdot t + (P_{moving_axes}) \cdot t + (P_{cutting_force}) \cdot t \quad (6.4b)$ <p>where $E_{machine}$ is the energy consumed by a CNC machine (J), E_{const} is the energy consumed by auxiliary components (i.e. lights, computer) in J, $E_{variable}$ is the energy consumed at a variable rate by operations including material removal, table movements, spindle rotation; P_{tare} is the constant power of the machine (W); $P_{coolant\ pump}$ is the coolant pump power (W); P_{moving_axes} is the power required for spindle, table, axes movements and spindle rotation (W); $P_{cutting_force}$ is the power for removing material (W), t is the processing time in s</p>	Developed web-based software for predicting energy demand based on NC codes; the importance of weights in their feed axes model and energy demand software was not highlighted; energy intensity of toolpath interpolations was not considered; rapid move feed power was not considered in the feed axes model.
Balogun et al. [98]	$E_{tot} = P_b(t_b + t_r + t_c) + P_r t_r + P_{tc} t_{tc} \left[INT \left(\frac{t_c}{T} \right) + 1 \right] + P_{air} t_{air} + (mN + C + P_{cool} + kv) t_c \quad (6.5)$ <p>where E_{tot} is the total energy demand (J), P_b and P_r are the basic and ready-state power required by the machine tool (W). P_{tc}, P_{air} and P_{cool} are power</p>	Developed an e-smart software based on NC codes; feed axis energy demand was not explicitly modelled to include weights of feed axes, workpiece and machine vice; Circular

	<p>demand for tool change, air cutting, and coolant respectively (W). t_b, t_r, t_{tc}, t_{air} and T represent setup time, ready time, tool change time, air cutting time, and tool life (s) respectively, and $mN + C$ is the spindle-speed characteristic model in W.</p>	<p>interpolation was not considered; the importance of weights was not highlighted in the e-smart software; energy intensity of toolpath interpolations were not considered</p>
--	--	---

Narita et al. [95] proposed an NC code based software for predicting the environmental impacts of a machining process. The software outputs the environmental impacts, processing time and the number of workpiece set up time. Vijayaraghavan and Dornfeld [58] proposed a software-based approach for the automation of energy demand prediction at all levels in order to investigate the energy consumption of machine tools and their effect on the overall life cycle and power demand of the machine tool. The software utilises ‘Complex Event Processing (CEP)’ which handle data reasoning and information processing. Manufacturing Technology Connect (MT Connect) interface was used to link data from the machine tool and/or other manufacturing equipment to the ‘Event Cloud’ for information processing and strategic decision making. However, energy consuming components were not related to NC codes.

From reviewed work, it is shown that few researchers proposed energy consumption models and developed software for predicting the electrical energy demand of a machining process based on NC codes. However, the reviewed studies have some limitations. For example, the weights moved by the feed drive (i.e. weights of the feed axes, machine vice, and workpiece) were not incorporated in the energy consumption models and in any of the proposed energy demand software. Also, most of these studies failed to model the influence of toolpath interpolations (G00, G01 G02, G03) on energy consumption of machine tools. In addition, most of their work focused on linear toolpaths while circular interpolation was relatively unexplored. Therefore, incorporating the weights of materials moved in the proposed energy consumption model and energy software would further improve the accuracy of predicting energy demand in machining.

It is also critical to investigate the energy demand of NC codes based on the type of interpolations in order to select the most efficient machining strategy in terms of reduced energy intensity.

6.1.3 Research aim and motivation

The aim of this study is to develop the scientific base and logic for calculating the energy consumption of a CNC toolpath taking the NC code as input. To achieve this, a previously developed feed axes energy demand model which takes into account the weights of feed axes, machine vice, and workpiece placed on the feed drive by the authors was incorporated into other energy consumption models. A new rationale for mapping the equations to CNC codes was developed and validated on components. This knowledge was used to develop NC code based software for energy demand prediction.

6.2 Modified electrical energy modelling through the analytical methods

Table 6.2 presents some of the models required to analytically estimate the total electrical energy demand of each energy consuming component and their relation to NC codes such as G-codes, M-codes, T-codes, S-code, and F-codes.

Table 6.2 Energy demand models and their relationships to NC codes

Criteria	NC codes	Model required
Baseline energy $E_{baseline}$	The baseline energy is required during machine start-up, system booting, by computer and display, lights, fans, and hydraulic pumps etc.	$E_{baseline} = P_{baseline} \cdot t_{baseline} \quad (6.6)$ where $P_{baseline}$ is the baseline power in W, $t_{baseline}$ is the time duration in seconds of the entire NC program (i.e. from start to finish of NC program).
Spindle run energy $E_{spindle\ run}$	M03, M04 and the S-code (denoting the spindle speed, N)	$E_{spindle\ run} = P_{spindle\ run} \cdot t_{spindle\ run}$ $= (mN + C) \times t_{spindle\ run} \quad (6.7)$ adopted from Mativenga and Rajemi [84] where $P_{spindle\ run}$ is the power required to rotate the spindle at specified speeds in W, m is the spindle speed coefficient, N is the spindle speed in rev/min, C is a constant which arises because the spindle has a power demand when running at zero cutting load, $t_{spindle\ run}$ is the time for spindle run in seconds
Tool tip energy	M03, M04 and the S-	$E_{cut} = P_{cut} \cdot t_{cut} = (k \cdot Q) \cdot t_{cut} \quad (6.8)$

E_{cut}	code (denoting the spindle speed, N)	where P_{cut} is the cutting power in W , t_{cut} is the time for actual material removal in <i>seconds</i> , k is the specific cutting energy of the material in J/mm^3 , Q is the material removal rate in mm^3/s
Tool change energy $E_{tool\ change}$	M06	$E_{tool} = P_{tool} \times t_{tool} \times INT\left(\frac{t_{cut}}{T_L}\right) + 1$ (6.9) adopted from Balogun and Mativenga [66] where P_{tool} is the power demand in W of the tool change motor, and t_{tool} is the time required for tool change, t_{cut} is the cutting time in seconds, T_L is the tool life in minutes
Coolant pump $E_{coolant}$	M07 and M08	$E_{coolant} = P_{coolant} \cdot t_{coolant}$ (6.10) adopted from He et al. [26] where $P_{coolant}$ is power in W of cutting fluid pump motor and $t_{coolant}$ in seconds is the time required for supplying coolant from start till the coolant is OFF, $t_{coolant} = t_{coolant\ end} - t_{coolant\ start}$

The next sub-sections present details in estimating the feed axes energy demand and their relations to the G00, G01, G02, and G03 NC codes, as well as the time required to run an NC block.

6.2.1 Feed energy demand

The feed energy, E_{feed} is required by the activated x-, and/or y-, and/or z-axis feed motors for positioning the machine tool table or cutting tool in the x-, y-, z-axis directions at the specified feedrate (v_f). The feed axes motors are controlled by NC codes including (G00) at rapid feedrates, and (G01, G02, G03) at specified feedrates. The feed energy is deactivated by the M30 NC code. The feed energy (E_{feed}) can be estimated as shown in Equation 6.11.

$$E_{feed} = P_{feed} \times t_{feed} \quad (6.11)$$

where E_{feed} is the feed drive energy demand in J , P_{feed} is the power in W required by the feed drives, t_{feed} is the time in seconds required for running the feed drive.

6.2.1.1 G00 - Rapid feed energy demand

The rapid feed energy is activated by the G00 NC code. The power demand for the rapid feed moves in each axis direction could be obtained experimentally by directly measuring the power required (i.e. $P_{G00-feed\ x}$, $P_{G00-feed\ y}$, $P_{G00-feed\ z}$).

The rapid feed time for the x-, y-, z- axes could be estimated as in Equation 6.12 below:

$$t_{G00-feed\ x} = \frac{x_e - x_s}{v_{f\ rapid\ x}}; \quad (6.12a)$$

$$t_{G00-feed\ y} = \frac{y_e - y_s}{v_{f\ rapid\ y}}; \quad (6.12b)$$

$$t_{G00-feed\ z} = \frac{z_e - z_s}{v_{f\ rapid\ z}}; \quad (6.12c)$$

where (x_s, y_s, z_s) are the start and (x_e, y_e, z_e) are the end points of the toolpath in *mm*; $t_{G00-feed\ x}$, $t_{G00-feed\ y}$, $t_{G00-feed\ z}$ are the time in *s* for rapid moves in x-, y-, z-axes directions; $v_{f\ rapid\ x}$, $v_{f\ rapid\ y}$, $v_{f\ rapid\ z}$ are the rapid feed speeds for the x-, y-, and z-axes directions in *mm/min*. The rapid feed energy is estimated using Equation (6.13).

$$E_{G00-feed\ i} = P_{G00-feed\ i} \times t_{G00-feed\ i} \quad (6.13)$$

where $P_{G00-feed\ i}$ is power required for the specified axis movement at rapid feedrate, $t_{G00-feed\ i}$ is the time for rapid move of the specified axis, $E_{G00-feed\ i}$ is the energy required by the specified axis during rapid move.

6.2.1.2 G01 - Feed axes energy demand for linear interpolation

Linear interpolation involves linear movement of the tool from the start point $P_s(x_s, y_s)$ of the linear segment to the end point $P_e(x_e, y_e)$ of the linear segment. Linear interpolation is the shortest distance a cutting toolpath can take. The energy required by the feed axes at specified feeds for linear interpolations is activated by the G01 NC-code. Figure 6.1 presents linear interpolation involving two axes (i.e. x- and y- axes).

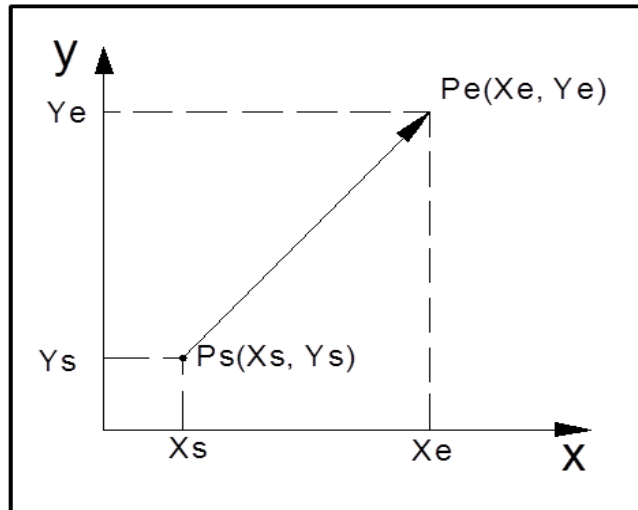


Figure 6.1 Linear interpolation

For absolute part programming, the start and end points are provided in the NC programs with the G-code (G01), thereby providing adequate information for determining the direction of movement of the feed drive as well as the feedrate value. In incremental programming the relative vectors in each axis are specified instead. Linear motions may be in single axis (i.e. movement may be parallel either to the x- or y- axis direction) or along two axes simultaneously as in Figure 6.1. The velocities of the x- and y- axes are controlled to keep the tool on a straight path.

In absolute programming (G90) as shown in Figure 6.2a, all dimensions in a CNC program are measured from the common point (origin), while in incremental programming (G91) all dimensions in a CNC program are measured from the current tool position [121] as shown in Figure 6.2b.

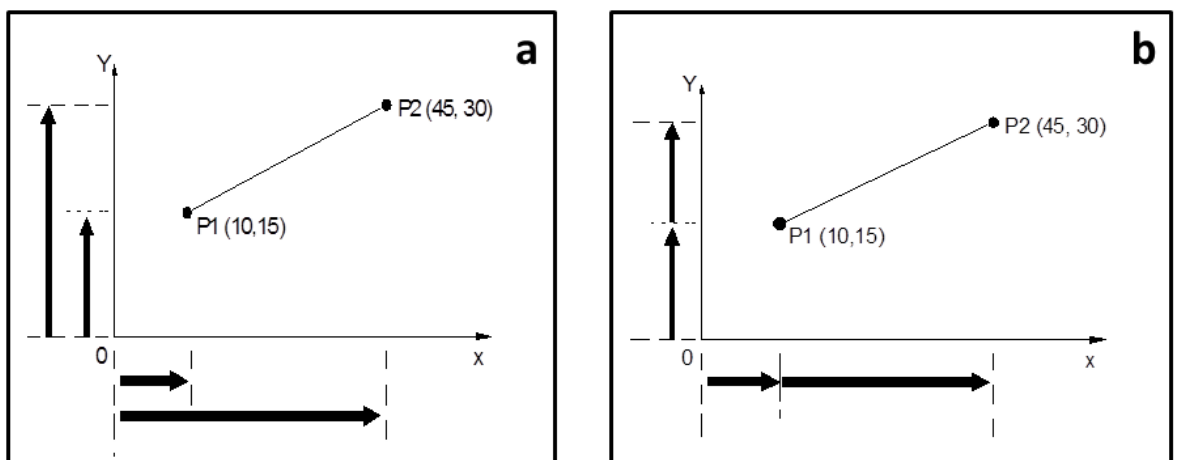


Figure 6.2a: Absolute coordinate programming mode (G90 Mode)
 b: Incremental coordinate programming (G91 Mode)

The start point P1 (10, 15) and end point P2 (45, 30) coordinates of the milling cutter are given in the x-y plane. Thus, the linear interpolation mode (G01) is used to maintain the end mill's motion in a straight line at the specified feedrate [120]. Samples of NC codes for the linear interpolation (P1, P2) written in the G90 and G91 modes are shown in Table 6.3.

Table 6.3 NC codes for absolute and incremental programming

Absolute programming (G90)	Incremental programming (G91)
N005 G00 X10 Y15 (start point)	N005 G00 X10 Y15 (start point)
N010 G01 X45 Y30 (end point)	N010 G01 X35 Y15 (end point)

Detailed estimation of linear interpolation based on the length of travel (L), and the actual feedrates moved by each axis from the command feedrate is provided in Edem and Mativenga [131]. The actual feedrates moved by each axis are then incorporated into the power demand models proposed by Edem and Mativenga [131] to estimate the power demand of feed axes. This model takes into account the weight of the axes, workpiece and machine tool vice. This is shown in Equation 6.14.

$$P_{G01-feed\ i} = P_0 + (a_i W_i v_{f_i} + b_i W_i) + F_f v_f \quad (6.14)$$

where $P_{G01-feed\ i}$ is the linear feed power at specified axis direction, P_0 is the baseline power, W_i is the weight of the axis, workpiece, and machine vice in the specified axis direction, a_i and b_i are constants in specified axis direction, v_{f_i} is the actual feedrate moved in a specified axis direction, v_f is the table feedrate, and F_f is the feed force.

The power demand in Equation 6.14 and the processing time required to run an NC block from its start point to the end point are used to estimate the electrical energy demand of feed axes in specified axis direction ($E_{G01-feed\ i}$). This is shown in Equation (6.15).

$$E_{G01-feed\ i} = P_0 t_{cy} + (a_i W_i v_f + b_i W_i) t_{cy} + F_f v_c t_c \quad (6.15)$$

where $E_{G01-feed\ i}$ is the feed energy demand for linear toolpaths at specified axis direction in J, t_{cy} and t_c is the total cycle time and the actual cutting time in seconds respectively, P_0 , a_i , b_i , v_{f_i} , v_f , W_i , and F_f still retain their usual meanings.

6.2.1.3 G02/G03 - Feed axes energy demand for circular interpolation

Circular interpolation is used for the programming of complete circles or arcs which are found in circular pockets, corner breaks, spherical or conical shapes, outside and inside radii, and helical cutting. In circular interpolation, the tool follows the given arc at the specified feedrate by varying the velocities of two axes on a plane of motion.

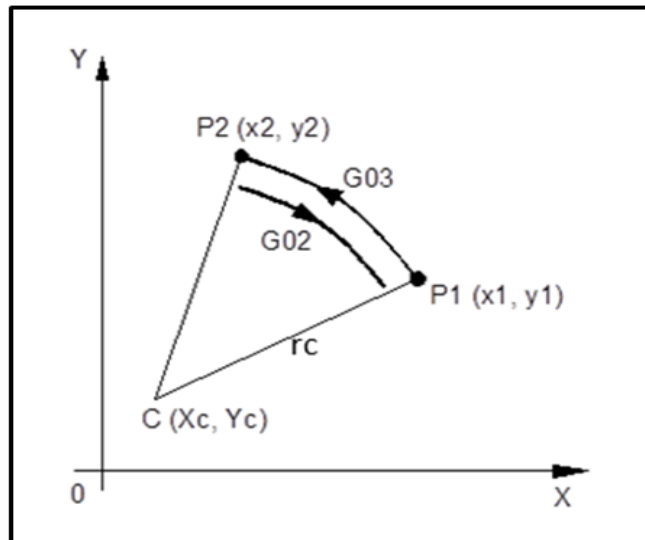


Figure 6.3 Circular interpolation with G02 and G03 codes

Movement of the cutting tool during circular interpolation may be in two directions – clockwise (CW) actuated by the G02 NC code with tool movement from P2 to P1, or counterclockwise (CCW) actuated by the G03 NC code with tool movement from point P1 to P2.

Most CNC systems require the radius of the arc r_c and the coordinates of its endpoint P2 (in the case of G03) or its start point P1 (in the case of G02), and could be programmed in absolute coordinates as:

N005 G90 G03 X2 Y2 R r_c F Or N005 G90 G02 X1 Y1 R r_c F

In the case where a CNC system requires the coordinates of the arc centre point C (x_c, y_c) and arc's end point P2 (when tool movement is executed with G03) or its start point P1 (when tool movement is executed with G02), the NC program in absolute mode is:

N005 G90 G03 X2 Y2 I i_c J j_c F Or N005 G90 G02 X1 Y1 I i_c J j_c F

where F is the program feedrate, i_c and j_c are used to define the centre of the arc with respect to the starting point.

The arc centre coordinates can be evaluated by the algorithm given below:

$$i_c = x_c - x_1; j_c = y_c - y_1 \text{ for G03} \quad \text{Or}$$

$$i_c = x_c - x_2; j_c = y_c - y_2 \text{ for G02}$$

Information about the radius of the arc r_c , the centre of the arc $C(x_c, y_c)$, and the direction of the vector tangent to the starting point of the circular toolpath could be obtained from the NC program.

An accurate definition of the circular toolpath is necessary in order to incorporate the actual feedrates of each axis involved in the circular interpolation strategy [135]. To achieve this, the circular arc is divided into small linear segments which are separated by an angular increment $\Delta\theta$, and a corresponding chord segment Δu from the start point, $P_s(x_s, y_s)$ to end point, $P_e(x_e, y_e)$. Therefore, the accuracy of the divided circular path increases as the interpolation points (line segments of the arc) increases [120].

Figure 6.4 presents circular interpolation whose origin is at the centre of the CNC coordinates.

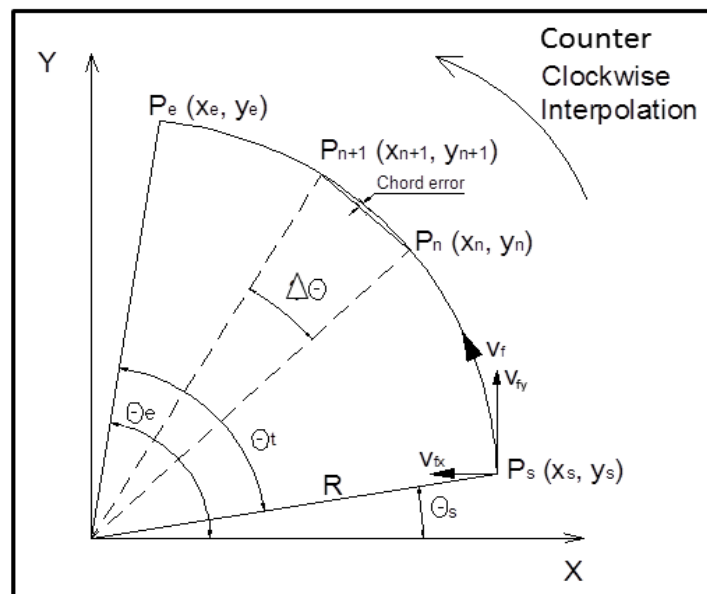


Figure 6.4 Circular interpolation with centre at the origin of CNC coordinates [120]

The chord error can be estimated as shown in Equation 6.16

$$\text{Chord error} = R \left(1 - \cos \frac{\Delta\theta}{2} \right) \leq 1 \quad (6.16)$$

The angular segment $\Delta\theta$ can be estimated as in Equation 6.17

$$\Delta\theta = \cos^{-1} \left(\frac{R-1}{R} \right) \quad (6.17)$$

The corresponding chord segment Δu can be calculated as in Equation 6.18

$$\Delta u = R\Delta\theta \quad (6.18)$$

where R is the radius of the arc, Δu is the chord segment, $\Delta\theta$ is the angular segment.

The coordinates of the point P_s (absolute programming G90) on the arc in Figure 6.4 can be obtained by the parametric equation of a circle at a point, and is given by:

$$x_{P_s} = R \cos \theta_s \quad (6.19)$$

$$y_{P_s} = R \sin \theta_s \quad (6.20)$$

Most centres of the circular paths are not obtained at the origin of the CNC coordinates. Figure 6.5 shows circular toolpath whose centre is not at the origin of the CNC coordinates.

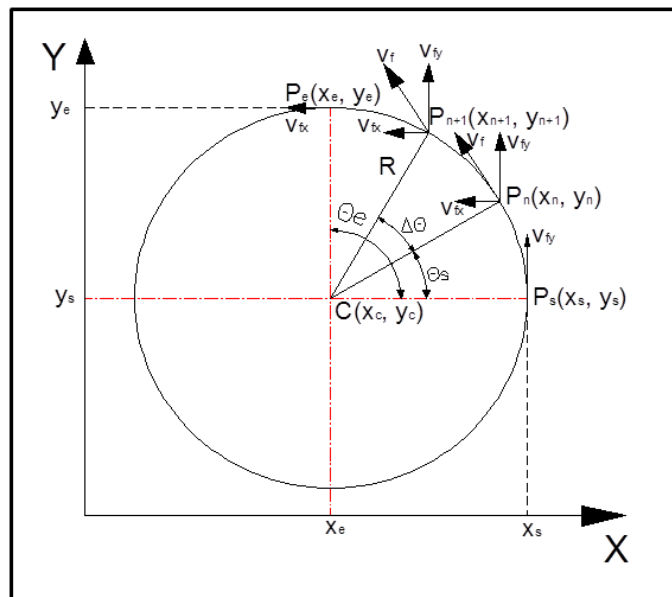


Figure 6.5 Circular path with centre not at origin of the CNC coordinates [135]

The point P_n is assumed to be reached by a tool when moving along the circular path between points P_s and P_e . Thus, the coordinates of the point P_n on the arc (based on absolute programming method), can be obtained by the parametric equation of a circle at a point, and is given by:

$$x_{P_n} = x_e + R \cos \theta_s \quad (6.21)$$

$$y_{P_n} = y_e + R \sin \theta_s \quad (6.22)$$

The actual feedrate for each axis when the tool executes circular interpolation can be estimated based on the position of the current point on the arc $P_{n+1} (x_{n+1}, y_{n+1})$ and the previous point on the arc $P_n (x_n, y_n)$ as shown in Figure 6.5. In addition, the length of the interpolation segment, L can also be calculated with Equations presented in Avram [135]:

$$L = \sqrt{(x_{P_{n+1}} - x_{P_n})^2 + (y_{P_{n+1}} - y_{P_n})^2} \quad (6.23)$$

$$v_{fx(P_{n+1})} = \frac{(x_{P_{n+1}} - x_{P_n})}{L} \cdot v_f \quad (6.24)$$

$$v_{fy(P_{n+1})} = \frac{(y_{P_{n+1}} - y_{P_n})}{L} \cdot v_f \quad (6.25)$$

where L is the total distance moved, v_f is the program feedrate, v_{fx} , v_{fy} are the actual feedrates moved by the x- and y- axes, x_{P_n} , y_{P_n} are the x and y axis coordinates of a point on the arc.

The actual feedrates moved by each axes while executing circular interpolation are then incorporated in the power demand models proposed by Edem and Mativenga [131] as presented in Equations 6.14 and 6.15 respectively, by substituting the G01 code with either G02 or G03 based on the type of circular interpolation and the specified axis direction.

6.2.2 Time required to run an NC block

The feed axes are driven by the mechanical components of the servo drive which often experience inertia. Subsequently, it normally requires some time to reach the required feedrate [22]. The machine toolpath cutting length and direction influence the material

removal cycle time. The time required to accelerate and decelerate the feed drives depends on the maximum feedrate and axis acceleration to be attained by the drive and the controller parameters. Also, Tounsi et al. [136] reported that the cycle time and direction of the cutting tool relative to the workpiece can be evaluated by taking into account the acceleration and deceleration time of the feed axes movement.

There are two types of feed profiles used for the feed axes movement. These include the trapezoidal feed profile and the triangular feed profile presented in Figures 6.6a and 6.6b.

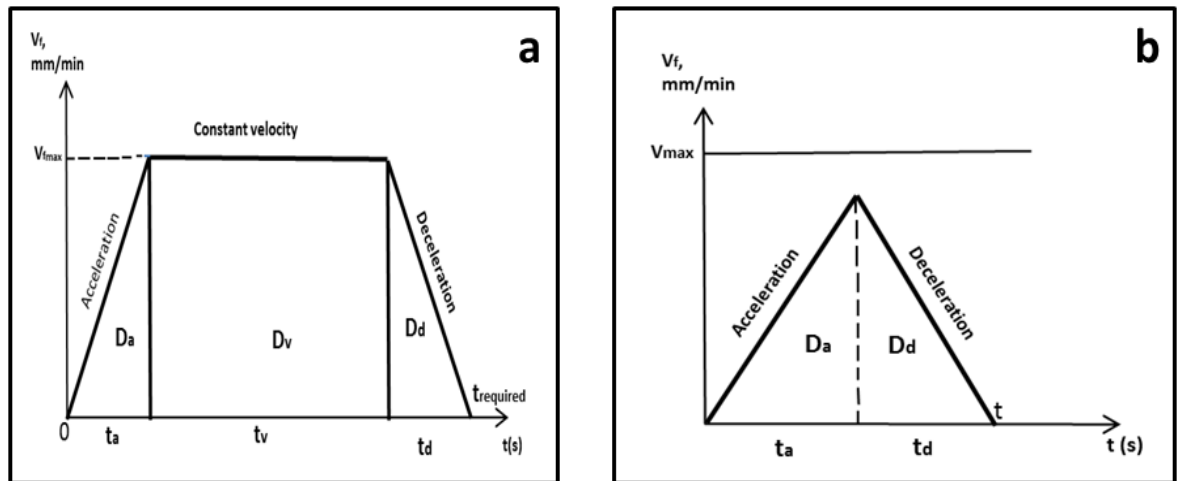


Figure 6.6a,b Acceleration and deceleration phase of the feed drive as it undergoes trapezoidal and triangular axes movements respectively

Considering the trapezoidal feed profile in Figure 6.6a, it therefore means that the distance travelled by the feed axes or cutter is long enough to accelerate, stabilise and decelerate, thereby making it possible for the required feedrate to be reached.

In the case of the triangular axis movement in Figure 6.6b, the specified feed rate cannot be reached due to the fact that the axis travel distance is shorter than the time required for the drive to accelerate, stabilise and decelerate [22].

In this study, time required to run an NC block was estimated based on either Equation (6.26) for trapezoidal feed profile or Equation (6.27) for triangular feed profile depending on the length of the toolpath segment.

$$t_{required} = 2t_a + \frac{d-2d_a}{v_f} \quad (d \geq 2d_a) \quad (6.26)$$

$$t_{required} = \sqrt{\frac{2t_a d}{v_f}} \quad (d < 2d_a) \quad (6.27)$$

where t_a is the acceleration time in m/s, d is the total travel distance in mm, d_a is the distance moved by the tool or axis at the acceleration time t_a , and v_f is the feedrate in mm/min

The sum of energy demand for each NC code line gives the total energy demand of the machining process. Therefore, the total electrical energy demand model adopted for this study is as shown in Equations 6.28.

$$E_{total} = E_{baseline} + E_{tool\ change} + E_{spindle\ run} + E_{cut} + E_{feed\ axes} + E_{coolant} \quad (6.28)$$

where E_{total} is total electrical energy demand in machining in J ; $E_{baseline}$, $E_{tool\ change}$, $E_{spindle\ run}$, E_{cut} , $E_{feed\ axes}$, $E_{coolant}$ are the energy required by constant energy consumers, energy required by the tool change motor, energy required to run the spindle at specified speeds, energy required for removing a material, energy requirements of the feed axes, energy required for the coolant pump in J respectively.

6.3 NC code based energy demand prediction software

The proposed model for estimating the total electrical energy required to run an NC program in Equation (6.28) was used to implement the NC-code based energy demand prediction software.

6.3.1 Design and development of the NC-code based energy demand prediction software

Figure 6.7 presents the algorithm for developing the NC-code based energy demand prediction software. It is assumed that the user provides the NC codes files. Table 6.4 presents additional input parameters required to predict the total energy of the cutting process.

Table 6.4 Additional inputs to be provided for the graphical user interface (GUI)

Machine tool type	Takisawa Mac-V3 milling machine
Machine tool characteristics:	
Baseline power	2763.17 W
Coolant pump power	400 W
Tool change power	270 W
weight of x-axis	3150 N
weight of y-axis	7500 N
weight of machine vice	570 N
Cutting tool parameters:	
diameter	8 mm
number of flutes	4
Cutting parameters: Width of cut	Slot machining – Diameter of the tool Pockets - $0.75 \times$ Diameter of tool in <i>mm</i>
Workpiece parameters (AISI 1018 steel):	
weight	30 N
specific cutting energy	4.5 J/mm ³ [46]
specific cutting pressure	1666.7 N/mm ²

Alternatively, these input parameters could be stored in a supplementary database for use when needed.

The execution loop of the software then initialises by reading through each line of the NC block one at a time to evaluate the energy demand and the processing time based on the Equations proposed in section 6.2 of this study.

For example, the rapid feed G00 power values for rapid moves in x-, y-, or z- axis direction were experimentally acquired. The time for rapid moves in each axis direction could be estimated as in Equation 6.12, and depends on the rapid feed speed in specified axis direction, and the start and end point coordinates. The energy demand for rapid feed is then evaluated from the power and processing time as in Equation 6.13.

The linear interpolation (G01) power, and the power for circular interpolation (G02, G03) are all estimated based on the procedures presented in Edem and Mativenga [131] and section 6.2 of this work. Thus, the total energy for feed drive E_{feed} is obtained by summing the $E_{G00-feed}$, $E_{G01-feed}$, and $E_{G02/G03-feed}$

The energy required by the M06 code (tool change motor) is estimated from the experimental power value acquired from the graphical user interface (GUI) and the time for tool change.

In the absence of the M06 NC code in an NC block, the next block is analysed by the execution loop. This procedure is repeated for M03, M04, or M05 codes (spindle on or off). The spindle run power is required for spindle rotation at specified spindle speed without cutting and is estimated as in Equation 6.7. The tool tip power is estimated based on the specific cutting energy (k) and the MRR (Q) as in Equation 6.8. The time for the spindle run and cutting process is obtained from the total time required to run the NC program which is therefore used to estimate the $E_{spindle\ run}$ and E_{cut} . The software constantly updates E_{total} and t_{total} .

For M07, M08, or M09 codes (coolant on or off), the power demand value is obtained from the GUI, while the time for coolant is from the duration of the coolant use, from which the coolant energy is estimated. The execution loop reads each line of NC block for the available NC code related to any energy consuming component, estimates the energy and time for each block, updates E_{total} and t_{total} until all the lines of the NC program have been read through, before the end of the NC program or M30 is reached.

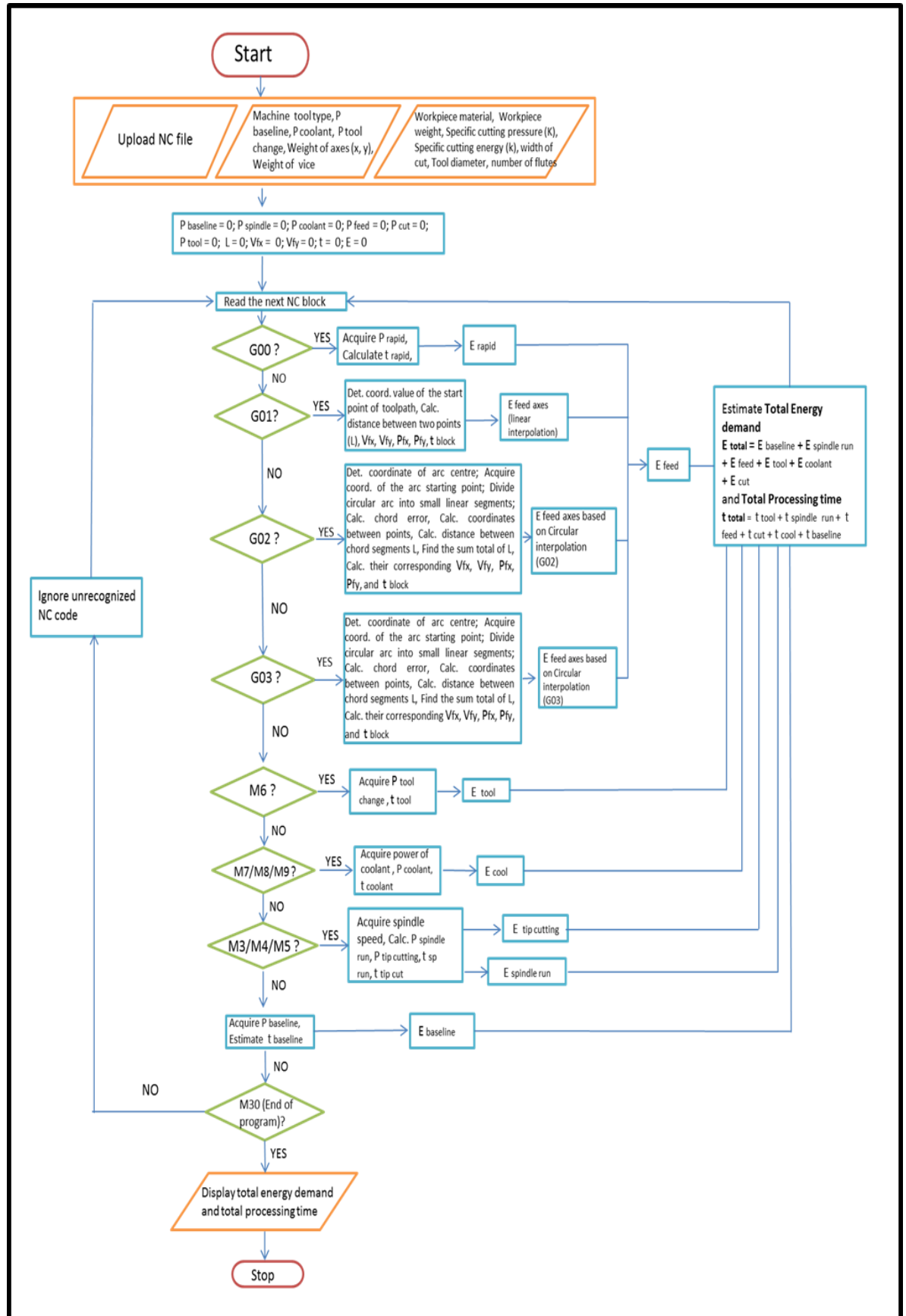


Figure 6.7 Flow chart for development of NC-code based energy demand software

6.3.2 Implementation of the NC-code based energy demand prediction software and graphical user interface (GUI)

The graphical user interface (GUI) for the energy demand prediction software was developed in MATLAB environment for estimating the total energy demand and total time. This is presented in Figure 6.8. The NC program is uploaded in an ASCII text file format by clicking the Upload NC file button on the GUI. The feedrate (v_f) is obtained from the programmed feedrate value (i.e. F500) which is modal and provided in the NC program. Also, the depth of cut (a_e) is acquired from the (z-) value which signifies the depth for removing material from the workpiece surface as provided in the NC program. Additionally, the operator has to provide other parameters as inputs such as the width of cut (step over); machine tool parameters (i.e. machine tool type, baseline power, weights of the x-axis and y-axis, and the weight of the machine tool vice); workpiece parameters (i.e. workpiece material, workpiece weight, specific cutting pressure of the material (K), and the specific cutting energy (k) of the material); and the tool parameters (i.e. tool diameter, number of flutes) as in Table 6.4. These parameters could also be stored in a separate pre-prepared input file for use when needed. The software then outputs the total energy demand and total processing time when the Run button is clicked on the GUI.

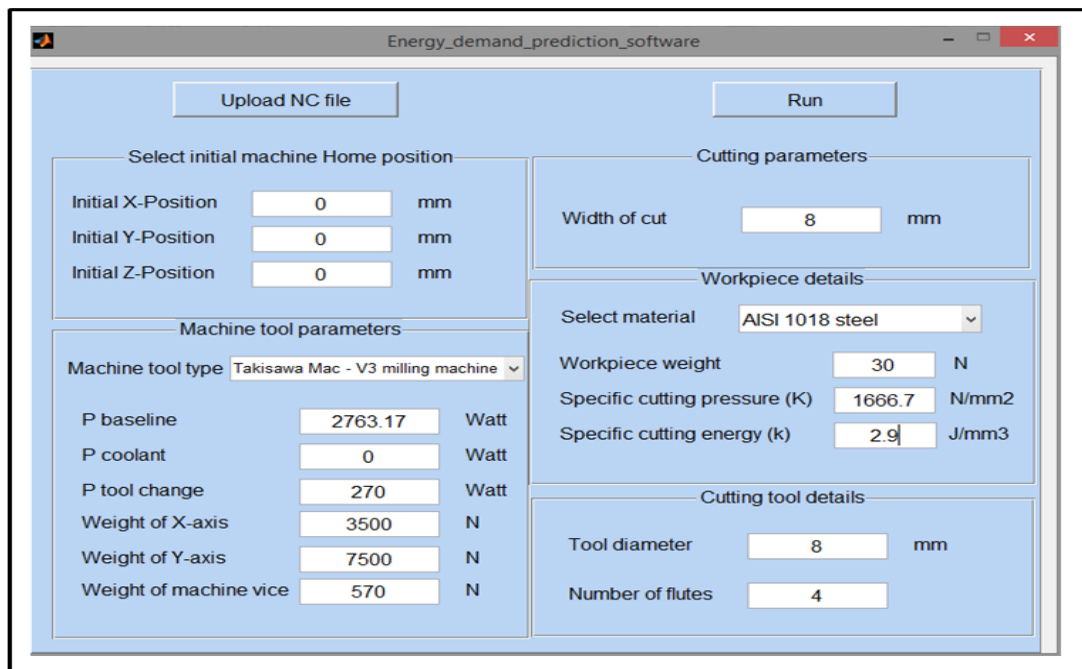


Figure 6.8 Graphical user interface (GUI) for uploading NC program and energy demand prediction

6.4 Case study

6.4.1 Experimental setup

In order to validate the proposed analytical model and NC-code based energy prediction software for estimating the total electrical energy demand in mechanical machining, slot milling of AISI 1018 steel was undertaken on the Takisawa Mac-V3 milling machine. This machine has a DC servo motor model 20M with spindle model A06B-0652-B, and FANUC controller. The vertical machining centre is capable of spindle speeds of up to 10,000 rev min^{-1} . The acceleration for the x, y, and z axes is 10 ms^{-2} , with rated power of 0.85 kW for x and y axes, and 1.2 kW for the z axis. The spindle motor had a rated power of 7.5 kW. The axes drives were powered by the AC servo motors connected directly to the ball screw drive. The machine tool configuration has the machine table and x-axis mounted directly on the y-axis. The table mass was modelled in SolidWorks 2012 software, and the values for the x- and y- axes were obtained from the mass properties and section properties of the aforementioned software to be approximately 315 kg and 750 kg respectively.

AISI 1018 steel material was cut into a size of 150 mm x 100 mm x 20 mm in dimension with the longer workpiece length mounted parallel to the x-axis of the machine tool table. Figure 6.9 presents a sample of the workpiece.

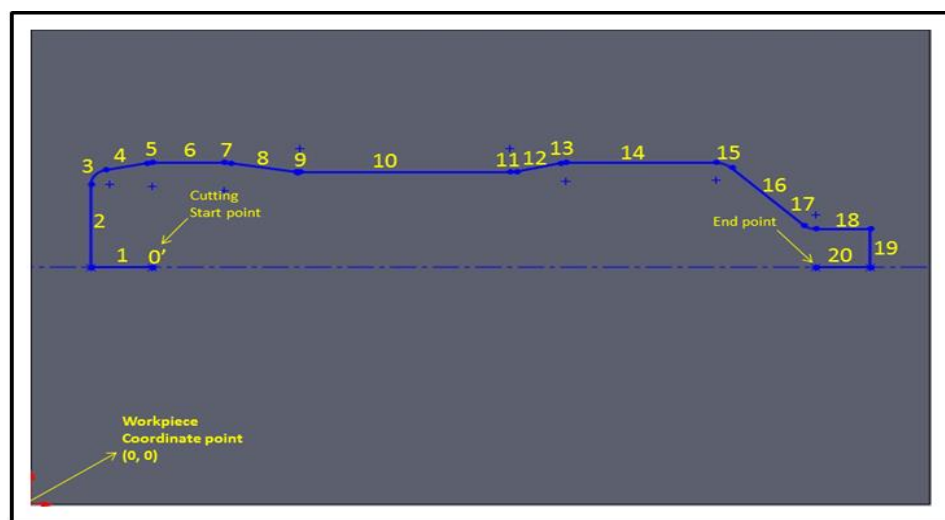


Figure 6.9 Diagram of the workpiece with machined toolpath

The toolpaths in Figure 6.9 were slots milled in the x-axis, y-axis, and x- and y-axes directions as in the reference workpiece parts presented in the Japanese Standards Association (JSA) [137] and Behrendt et al. [55] for studying energy consumption of machine tools. The toolpath was a 2D half-bottle profile consisting of linear segments and circular arcs adopted from a 0.5 litre Evian natural mineral water bottle. The toolpath starts from the left hand side of the workpiece block moving in the clock wise (CW) direction. The weight of the workpiece was 30 N. The cutter used was an 8 mm diameter, 4 flutes coated carbide short end mill. Tables 6.5 and 6.6 present the workpiece and cutting parameters used in this study.

Table 6.5 Workpiece parameters

Material of workpiece	AISI 1018 steel (Low carbon steel)
Length of workpiece, mm	150
Width of workpiece, mm	100
Thickness of workpiece	20
Physical properties: Density	7.85 g/cm ³
Hardness, (VK)	233 HV
Workpiece weight, N	30
Chemical composition of the workpiece	0.17 wt% C, 0.27 wt% Si, 0.80 wt% Mn, 0.050 wt% S max; 0.050 wt% P max

Table 6.6 Cutting parameters

Spindle speed, N (rev/min)	4000
Feedrate, v_f , (mm/min)	500
Cutting speed, V_c (m/min)	100
Diameter of cutter, D (mm)	8
Depth of cut, a_p (mm)	0.5
Cutting tool type	SWT 161 5008A 8mm diameter short carbide end mill
Number of cutting flutes/teeth, z	4

The spindle speed was maintained at 4000 rev/min. The depth of cut was also kept constant at 0.5 mm in order to minimise vibrations that could result from the cutting forces during machining. Dry cutting environment was utilised in this study in order to enhance sustainable machining. The current drawn in the machining process was measured with Fluke 434 power quality analyser. This current was used to derive the power required by the machine tool to perform slot milling of the half bottle toolpath. The cutting tests were repeated three times. Hyper-mill CAM software was used to generate NC codes for the slot milling process. A detailed NC code showing the toolpath sequences is presented in Table 6.7.

Table 6.7 NC code sequences for half bottle toolpath generated with hyper mill software

	Block No.	Numerical control (NC) codes	Characteristics	Position
	N01	G90 G21 G40 G80 H00 G59		
	N02	.		
	N03	.		
	N04	.		
	N05	T07 H07 E02 M03 S4000	Tool number 7 is selected, Tool height offset selection, Spindle turn on	
	N06	G00 X14.395 Y50	Move in XY (+) direction, rapid traversing of the tool.	
	N07	Z55	Move in Z (-) direction (rapid tool movement from home position)	
	N08	G00 Z3.5	Move in Z (-) direction (Tool approach)	
	N09	G01 Z-0.5 F50	Move in Z (-) direction (Modal tool engagement)	
	N10	G42	Cutter radius compensation (right)	-
1	N11	G01 X10 F500	Move in the X(-) direction	0' → 1
2	N12	G01 Y67.50	Move in the Y(+) direction	1 → 2
3	N13	G02 X12.38 Y70.43 I3 J0	Move in arc in CW direction	2 → 3
4	N14	G01 X19.22 Y71.89	Move in XY(+) direction	3 → 4
5	N15	G02 X20.26 Y72 I1.04 J-4.89	Move in arc in CW direction	4 → 5
6	N16	G01 X32.26	Move in X (+) direction	5 → 6
7	N17	G02 X33.27 Y71.91 I0 J-6	Move in arc in CW direction	6 → 7
8	N18	G01 X44.09 Y70.07	Move in XY (+) direction	7 → 8
9	N19	G03 X44.93 Y70. I0.84 J4.93	Move in arc in CCW direction	8 → 9
10	N20	G01 X79.93	Move in X (+) direction	9 → 10
11	N21	G03 X81.12 Y70.14 I0 J5	Move in arc in CCW direction	10 → 11
12	N22	G01 X88.25 Y71.89	Move in XY (+) direction	11 → 12
13	N23	G02 X89.20 Y72 I0.95 J-3.89	Move in arc in CW direction	12 → 13
14	N24	G01 X114.20	Move in X (+) direction	13 → 14
15	N25	G02 X116.86 Y70.90 I0. J-3.76	Move in arc in CW direction	14 → 15
16	N26	G01 X128.88 Y58.88	Move in XY(+) direction	15 → 16
17	N27	G03 X131 Y58. I2.12 J2.12	Move in arc in CCW direction	16 → 17
18	N28	G01 X140.	Move in X(+) direction	17 → 18
19	N29	G01 Y50	Move in Y (-) direction	18 → 19
	N30	G40	Cutter radius compensation cancel	
20	N31	G01 X135.6	Move in X (-) direction	19 → 20
21	N32	G00 Z55	Move in Z (+) direction, rapid move of the tool	Tool retract
22	N33	M30	End of program	

6.5 Results and discussion

6.5.1 Analytical estimation of total electrical energy demand based on NC codes

The model in Equation 6.28 was used to analytically estimate the total energy required to run the NC program in Table 6.7. The first NC block (N01) consists of codes for work coordinate, absolute programming etc. The baseline energy was estimated with Equation 6.6 since constant energy is consumed by the machine tool at this point. The next NC block (N04) contains the T-code for tool change. The tool change power was experimentally measured, while the time for tool change was 30 seconds. Nevertheless, in this study, tool change was not performed since the tool was already in the spindle. Thus, the tool energy demand is zero (0). The N05 block has M03 and S4000 signifying spindle rotation and spindle speed. In this study, the power demand for spindle run was modelled when the spindle was running at specified speeds without cutting. Figure 6.10 presents the plot of power demand with spindle speeds. It is observed that the spindle power increases linearly with spindle speed, and is also a function of spindle rotation speed. From the model obtained in Figure 6.10, the spindle run power demand was estimated and adopted as Equation 6.7, and was found to be 3109 W (i.e. 346 W without P_0) at spindle speed of 4000 rev/min. The time required for spindle run was estimated from the duration of spindle rotation start to end of NC program, from which the energy demand was estimated.

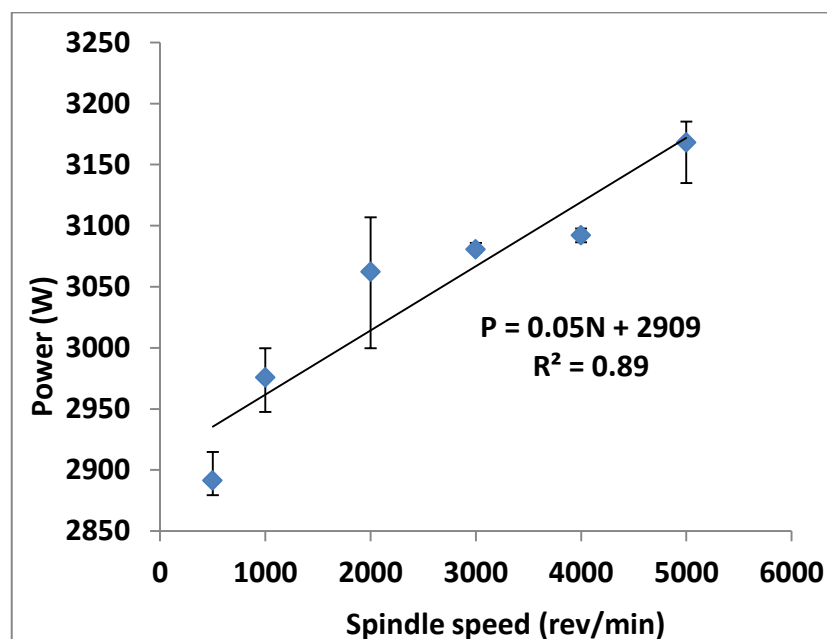


Figure 6.10 Spindle power demand for Takisawa Mac-V3 milling machine at zero load

Air cutting energy was not estimated since the actual removal of material was performed. The specific cutting energy value of 4.5 J/mm^3 for mild steel was obtained from [46] in order to estimate the tip energy as in Equation 6.8.

The rapid move codes (G00) are observed in N06 to N08, and in N32 blocks of the NC program. The power for rapid move was experimentally determined when the G-code (G00) in the x-, y-, and z-axes directions was activated, and the values (obtained by subtracting the baseline power from the total power) are presented in Table 6.8. Figure 6.11 shows the experimental power demand of NC codes.

Table 6.8 Power demand values of NC codes determined experimentally

NC Codes	Power demand
G00 (rapid move) for the x-axis	140.18 W
y-axis	141.22 W
z-axis	142.31 W
M06 (Tool change)	270.24 W
M07, M08 (Coolant)	491.00 W
Baseline power	2763.17 W

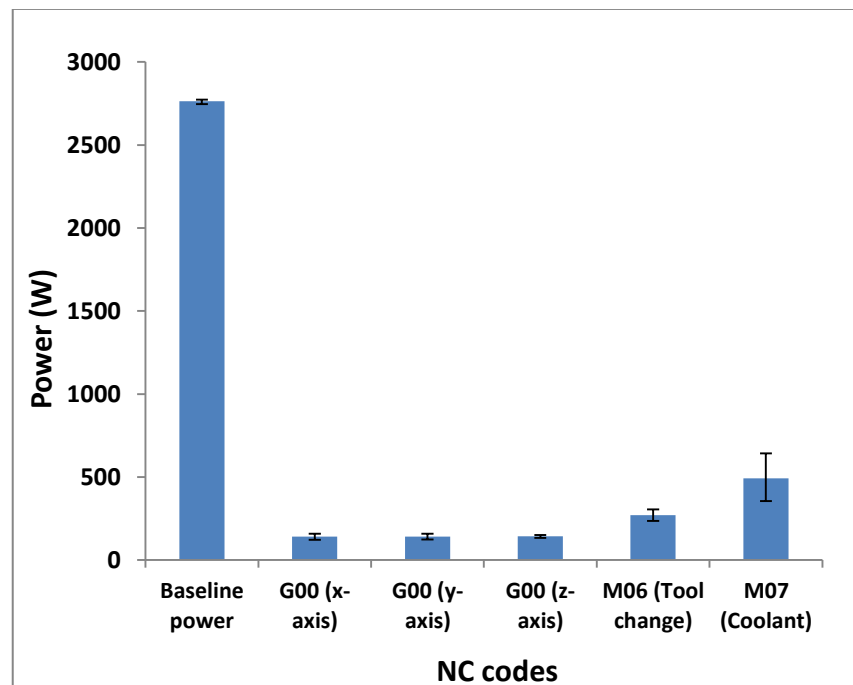


Figure 6.11 Experimental power demand of NC codes

The time for the rapid moves was estimated from the coordinates of the start and end points. The energy demand for rapid move was estimated with Equation 6.13.

Linear interpolation code (G01) and F-code with 50 mm/min is first observed in N09 block of the NC program which shows that the tool engages the workpiece at a depth of 0.5 mm. The tool descends to point 0' at a feedrate of 50 mm/min as shown in Figure 6.9. The energy demand for this NC block was estimated with the z-axis power Equation in Edem and Mativenga [131], while the time was estimated based on the start and end points of the toolpath length and feedrate of 50 mm/min .

The power demand of other G01 codes with feedrate of 500 mm/min found in the NC program were estimated by determining the actual feedrate moved by each axis, which were then integrated into Equation 6.14. The total time required for each block with linear toolpath was estimated based on Equations 6.26 and 6.27 depending on the length of toolpath.

In the case of G02 and G03 circular interpolation codes present in any block of the NC program, power demand was calculated by determining the coordinates of the centre of the arc, radius of the arc, as well as dividing the arc into linear segments to the allowable chord error. The actual feedrates moved by each linear segment was estimated with Equations 6.24 and 6.25, and were incorporated into Equation 6.14 (i.e. substituting G01 with either G02 or G03) to calculate the power consumed. The time was estimated based on the coordinate of the arc and the length of arc with either Equation 6.26 or 6.27 depending on the length of circular arc. Thus, the energy demand for NC blocks with circular interpolation was estimated with Equation 6.15. Therefore, the total electrical energy demand and total time for running the NC program was achieved by summing the energy demand and the time required by each NC block.

It is important to note that CAM software provide information about the processing time and travel distance while information on the energy required to run an NC program is not provided. It is therefore recommended for CAM software developers to include energy prediction in their software to enable process planners to predict energy required for a machining process before the actual material removal process is performed. For this to happen, machine tool developers need to provide the basic energy states of some NC codes as in Table 6.8; and machine tool parameters as in Table 6.4 so that it can be added to the postprocessor file.

Table 6.9 shows results of the energy demand and processing time predicted analytically for slot milling of AISI 1018 steel based on the machining states/components.

Table 6.9 Theoretical electrical energy demand and processing time for slot milling of AISI 1018 steel

	Block No.	Numerical Control (NC) codes	Characteristics	Position	Length of toolpath (mm)	Volume removed (mm ³)	Power demand (W)	Time (s)	Energy demand by block (J)	Specific cutting energy (J/mm ³)
	N01	G90 G21 G40 G80 H00 G59	Absolute programming, Metric units, Cutter radius compensation cancel, Fixed cycle cancel, Work coordinate system							
	N02									
	N03									
	N04	T07 H07 E02	Tool number 7 is selected, Tool height offset selection							
	N05	M03 S4000	Spindle turn on + Spindle cut				496.00	28.67	14220.30	
	N06	G00 X14.40 Y50	Move in XY (+) direction, rapid traversing of the tool.				301.93	0.39	97.22	
	N07	Z55	Move in Z (-) direction (rapid tool movement)				152.50	0.33	50.33	
	N08	G00 Z3.5	Move in Z (-) direction (Tool approach)				152.50	0.31	47.12	
	N09	G01 Z-0.5 F50	Move in Z (-) direction (Modal tool engagement)				133.52	4.80	640.99	
	N10	G42	Cutter radius compensation (right)	-						
1	N11	G01 X10 F500	Move in the X(-) direction	0' → 1	4.40	17.60	387.83	0.53	205.55	11.68
2	N12	G01 Y67.50	Move in the Y(+) direction	1 → 2	17.50	70.00	470.61	2.11	992.96	14.19
3	N13	G02 X12.38 Y70.43 I3 J0	Move in arc in CW direction	2 → 3	4.09	16.36	1192.8	0.50	596.40	36.46
4	N14	G01 X19.22 Y71.89	Move in XY(+) direction	3 → 4	6.21	24.84	574.37	0.75	430.78	17.34
5	N15	G02 X20.26 Y72 I1.04 J- 4.89	Move in arc in CW direction	4 → 5	1.04	4.16	576.92	0.13	75.00	18.03
6	N16	G01 X32.26	Move in X (+) direction	5 → 6	12.00	48.00	387.82	1.50	581.73	12.12
7	N17	G02 X33.27 Y71.91 I0 J- 6	Move in arc in CW direction	6 → 7	1.01	4.04	567.92	0.12	68.15	16.87
8	N18	G01 X44.09 Y70.07	Move in XY (+) direction	7 → 8	10.98	43.92	581.54	1.30	756.00	17.21

Modelling of energy demand from computer numerical control (CNC) toolpaths

9	N19	G03 X44.93 Y70.10.84 J4.93	Move in arc in CCW direction	8 → 9	0.86	3.44	388	0.10	38.80	11.28
10	N20	G01 X79.93	Move in X (+) direction	9 → 10	35.00	140.00	387.82	4.22	1636.60	11.69
11	N21	G03 X81.12 Y70.14 I0 J5	Move in arc in CCW direction	10 → 11	1.20	4.80	545.8	0.15	81.87	17.06
12	N22	G01 X88.25 Y71.89	Move in XY (+) direction	11 → 12	7.34	29.36	574.53	0.90	517.08	17.61
13	N23	G02 X89.20 Y72 I0.95 J- 3.89	Move in arc in CW direction	12 → 13	0.96	3.84	387.75	0.12	46.53	12.12
14	N24	G01 X114.20	Move in X (+) direction	13 → 14	25.00	100	387.82	3.01	1167.34	11.67
15	N25	G02 X116.86 Y70.90 I0. J-3.76	Move in arc in CW direction	14 → 15	2.87	11.48	1221.06	0.33	402.95	35.10
16	N26	G01 X128.88 Y58.88	Move in XY(+) direction	15 → 16	16.99	67.96	594.63	2.05	1218.99	17.94
17	N27	G03 X131 Y58. I2.12 J2.12	Move in arc in CCW direction	16 → 17	2.64	10.56	456.64	0.36	164.39	15.57
18	N28	G01 X140.	Move in X(+) direction	17 → 18	9.00	36.00	386.10	1.09	420.85	11.69
19	N29	G01 Y50	Move in Y (-) direction	18 → 19	8.00	32.00	471.42	0.96	452.56	14.14
	N30	G40	Cutter radius compensation cancel							
20	N31	G01 X135.6	Move in X (-) direction	19 → 20	4.40	17.60	387.83	0.53	205.55	11.68
	N32	G00 Z55	Move in Z (+) direction, rapid move of the tool	Tool retract			152.52	0.33	50.33	
	N33	M30	End of program					-	-	
			Baseline Energy (with no spindle rotation, no axis movement)				2763.17	28.67	79220.1 0	
								Total proces sing time = 28.67	Total energy demand = 104386. 00	

It is observed from Table 6.9 that shorter linear path lengths (i.e. G01) and circular path segments (i.e. G02 and G03 codes) were highly energy intensive. This is because for shorter path segments, the maximum feedrate may not be reached due to constraints imposed by acceleration and deceleration; the weights carried take a higher share of the

load, and therefore increase the inertia effects on the drive. Therefore, energy intensity in machining could be significantly reduced by selecting toolpaths with longer linear path segments

The analytical energy demand for slot milling of AISI 1018 steel on the milling machine was estimated based on Equations (6.6) – (6.28). From Table 6.9, the total theoretical energy demand estimated based on the NC codes was 104386 J while the total processing time was 28.67 sec. Figure 6.12 shows the energy demand distribution of Takisawa Mac-V3 milling machine for the slot milling toolpath as estimated with the proposed model analytically.

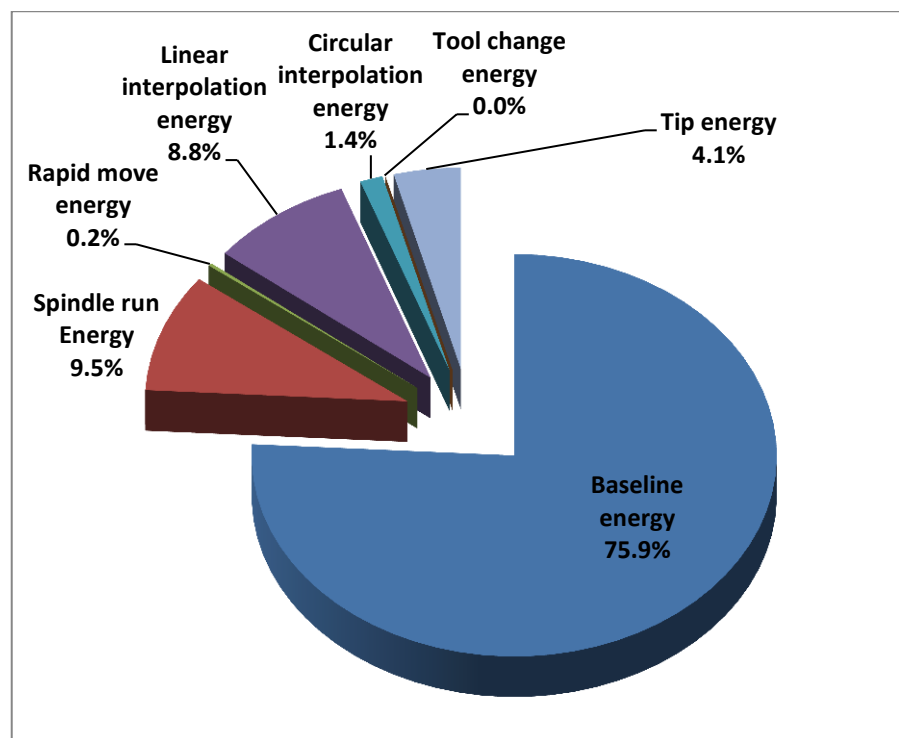


Figure 6.12 Predicted (theoretical) electrical energy demand distribution for slot milling from NC program

As shown in Figure 6.12, the baseline energy dominated the total energy consumption with 76% attributed to it. The choice of a machine tool with the lowest baseline power is ideal for reducing energy demand in machining. The feed axes motions including the linear and circular interpolations consumed 10.4% of the total energy, 9.5% was attributed to the spindle, while 4.1% was used for removing material from the workpiece.

6.5.2 Validation of the analytical estimation and NC-code based energy demand prediction software

In order to validate the analytical energy demand model proposed in Equation 6.28 and the newly developed NC code based energy demand prediction software, the NC program used in analytically predicting the total energy demand in Table 6.7, was provided as input to the newly developed energy demand prediction software. This NC program was later fed to the Takisawa Mac-V3 milling machine to perform the cutting test. Fluke 434 power quality analyser was used to measure the current drawn by the machine tool. This current was then used to derive the power consumed by the machine tool. The area under the power-time graph gives the measured electrical energy demand for running the NC program. Figure 6.13 shows the power profile of a half bottle slot milling process conducted on a 3-axis Takisawa Mac-V3 milling machine.

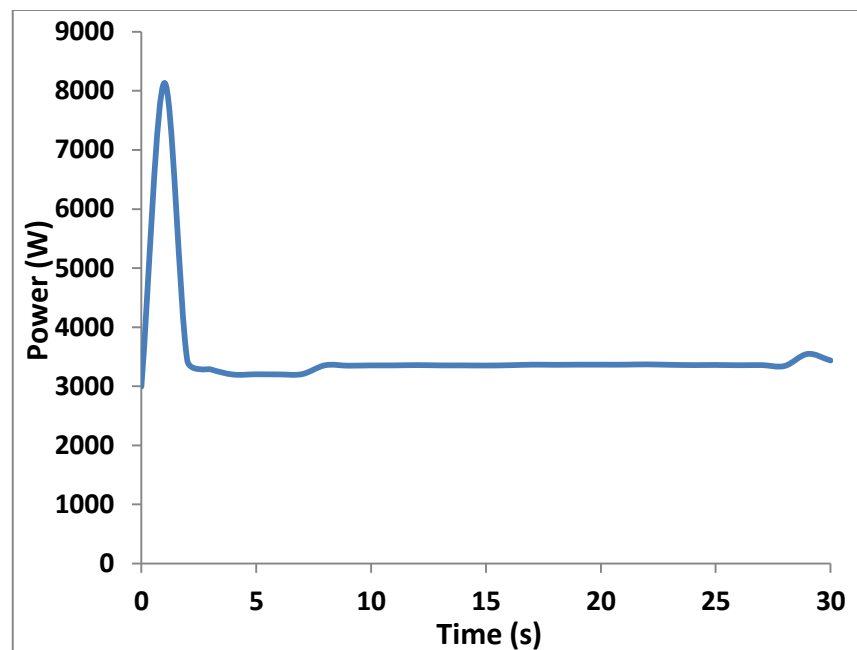


Figure 6.13 Measured power consumption profile for half bottle slot milling of AISI 1018 steel on the Takisawa Mac-V3 milling machine

The predicted and measured processing time required to run the NC program are presented in Table 6.10

Table 6.10 Comparison between total predicted energy demand and time from model and software, and total measured electrical energy and time required for running an NC program

Criteria	Theoretical	Software	Experimental
Baseline energy (J)	79220.10	79781.00	-
Spindle run energy (J)	9919.80	9990.13	-
Rapid move energy (J)	245.00	12638.42	-
Linear interpolation energy (J)	10163.40		-
Circular interpolation energy (J)	1474.10		-
Tool change energy (J)*	0.00	0.00	-
Coolant energy (J)	0.00	0.00	-
Tip energy (J)	4300.50	4330.98	-
Total energy demand (J)	104386.00	106741.12	106604.00
Total processing time in seconds	28.67	28.87	30
% Difference between predicted and measured electrical energy demand	-2	0	
% Difference between predicted and measured total time	-4	-4	

* Tool change energy is zero because tool was already in the spindle

The total energy demand from the cutting test was measured to be 106604 J, while the total time for cutting was 30 sec. The total analytical energy demand estimated based on the NC codes and from software were 104386 J and 106741 J, while the total processing time was 28.67 seconds and 28.87 seconds respectively. The slight deviation between the analytical prediction and software results for energy demand may be due to slight over-estimation of the total processing time, resulting in higher energy demand when compared with the analytical method. Also, the deviation between the analytical and experimental electrical energy demand is (-) 2% while the deviation in total processing time is (-) 4%. The deviation between the software and measured energy is (+) 0% while the processing time deviated by (-) 4%. Consequently, the values obtained in this study show good agreement between the analytical, software, and experimental energy estimations.

6.6 Conclusions

It is important to evaluate the electrical energy demand of toolpaths based on CNC codes. In this chapter, an analytical model for predicting the energy consumed by a CNC machine was proposed. The model was developed by relating the energy consuming components of the machine tool to NC codes. The proposed analytical model was used to

develop and implement NC code based energy demand prediction software. The model was developed to improve the prediction capability of electrical energy models of machine tools by incorporating the weights of axes, workpiece, and machine tool vice, and additional consideration of linear and circular interpolations in the feed axes energy estimation.

The NC-code based analytical model and energy prediction software were validated by undertaking slot milling of a half bottle toolpath profile on AISI 1018 steel workpiece using a 3-axis milling machine, and results show that the analytical model and NC code based energy demand prediction software agree well with the experimental result. The proposed model and software would enable process planners to estimate the energy demand for running an NC program before the actual machining of a part is conducted in order to select the best energy efficient strategy.

The G02 and G03 codes (for clockwise (CW) and anti-clockwise (ACW) circular interpolations), in addition to linear toolpaths with shorter path segments were found to be highly energy intensive, due to the fact that the programmed feedrate could not be reached as a result of the shorter distance moved by the feed drive. On the other hand, the G00 (rapid feed) codes and longer linear path segments (i.e. G01) were found to be less energy intensive. Therefore, energy intensity in machining could be significantly reduced by selecting toolpaths with longer linear path segments, as well as selecting of machine tools with smaller baseline energy.

To enable energy modelling of CNC toolpaths, data files for the following should be provided.

Type of data	Provider
Weight of x-axis table	Machine tool builder
Weight of y-axis table	Machine tool builder
Baseline power for each axis in G00	Machine tool builder
Baseline power for tool change	Machine tool builder
Baseline power for coolant	Machine tool builder
Baseline power of spindle power at zero load for different spindle speeds etc.	Machine tool builder

The data above will enable step change awareness in energy demand and support post processors in evaluating energy consumption from toolpaths.

CHAPTER 7

SENSITIVITY ANALYSIS OF THE EFFECT OF THE WORKPIECE ON THE VARIABILITY OF ENERGY IN MACHINING

ABSTRACT

The aim of this study is to analyse the as-received workpiece material with regards to electrical energy demand and surface integrity in a milling process. To achieve this, hardness test for the as-received material was undertaken on the top and bottom surfaces of the workpiece, followed by analysis of the microstructure for the as-received workpiece and subsurface of the machined part in 2% Nital etching. Air cutting and face milling of the workpiece with zag toolpath were performed when the workpiece was mounted on the vice in the x-axis (0 degrees) direction, with subsequent rotation and mounting of component in the y-axis direction (90 degrees) while cutting was maintained in one direction for both workpiece orientations in a dry cutting environment. Surface finish of machined parts was checked. The idea was to evaluate microstructure direction bias. Results from the hardness test show slight variations in hardness values of the as-received material, and these variations had minimal influence on the electrical energy demand. Thus, the direction that a workpiece material is cut did not influence energy demand. This can be expected for cast materials if there is no grain growth bias.

Keywords: Electrical energy demand, mechanical machining, workpiece orientation, hardness, surface integrity, tool wear.

7.1 Introduction

7.1.1 Brief description of the production sequence of hot rolled flat bars of AISI 1018 steel

Mild steels are a class of carbon steels with less than 0.30% carbon content in their composition (e.g. AISI 1018 and AISI 1020 steels). AISI 1018 steels are commonly used for the manufacture of industrial products including bolts, axles, shafts, machinery parts, gears, worms, pins, and ratchets, in addition to parts requiring bending, swaging, cold forming, or crimping, sheet, plate, and tubes. They are also used for manufacturing machine parts that require low strength [138]. Its wide use in the manufacturing sector may be due to the following properties including its high machinability rating when compared with other low carbon steels; good weldability due to its high toughness and minimal heat affected zone, and low cost [139]. It is critical to have good knowledge of the properties required in terms of component manufacture and environment (corrosion, high temperature) in order to select a material for a specified part [140]. Figure 7.1 shows the production sequence required for the manufacture of hot rolled flat bars of AISI 1018 steel (mild steels) as adapted from Kalpakjian and Schmid [44].

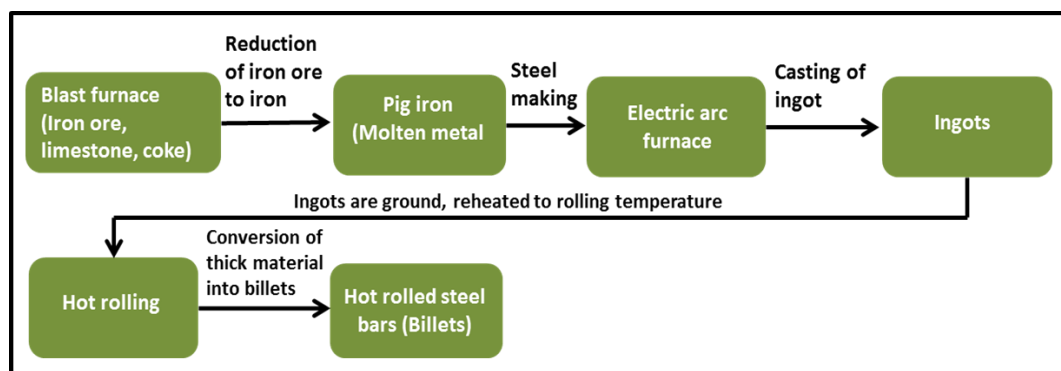


Figure 7.1 Production sequence of hot rolled flat bars of AISI 1018 steel as adapted from Kalpakjian and Schmid [44]

Iron ore, limestone, and coke are the three basic materials used in iron and steel making. These three raw materials are deposited into the blast furnace. After the reduction of the iron ore into iron, the molten metal accumulates at the bottom of the blast furnace while the impurities float at the top of the metal [138]. Then, the molten metal or (Pig iron) from the blast furnace is transported to the electric arc furnace to be cast into solid form (ingot)

or by continuous casting for the production of billets, blooms and slabs; and are ready to undergo working processes (such as hot rolling) [141].

Metal working processes include rolling (which is used to manufacture products such as bars, rods, sheet and strip); forging (which is used for producing parts with fairly simple shape and better mechanical properties); extrusion (used for producing solid and hollow sections like tubes of both ferrous and non-ferrous materials; and drawing (used for producing bars, tube, wire) etc. [142].

Rolling processes could be distinguished into hot rolling and cold rolling. In these processes, metals are fed into the gaps between the rolls rotating in opposite directions, causing the metals to deform and increase in length from the compressive forces exerted by the rolls [142].

Hot rolling (Hot working) is referred to as a shaping process performed at temperatures higher than the recrystallization temperature of the material being worked. At this temperature, deformation and recrystallization simultaneously occur with no distortion of grains or work hardening taking place [142]. Hot rolling processes are considered when there is no need for precise shapes and tolerances.

Cold rolling (Cold working) processes are carried out at room temperature which deforms and elongates the grains in the direction of rolling. This causes permanent distortions of the crystalline structure of the metal and brings about an increase in mechanical resistance, hardness values and high yield stress [142]. Nonetheless, steels with close dimensional accuracy and improved surface finish are produced with this process.

Figures 7.2a and 7.2b show schematic diagrams of hot and cold rolling processes.

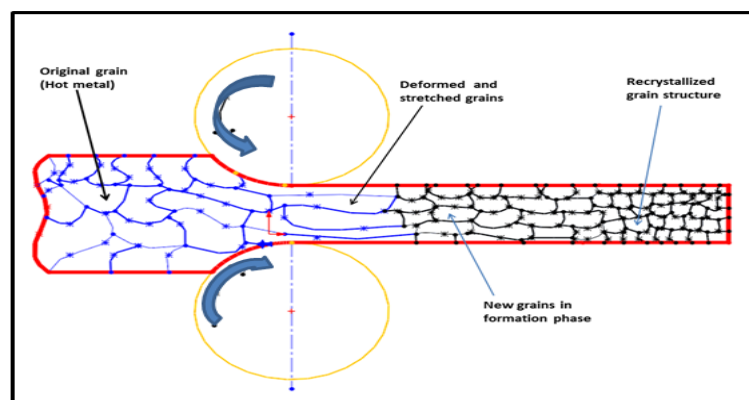


Figure 7.2a Schematic diagram of the hot-rolling process showing the deformation and recrystallization of the metal being rolled [142]

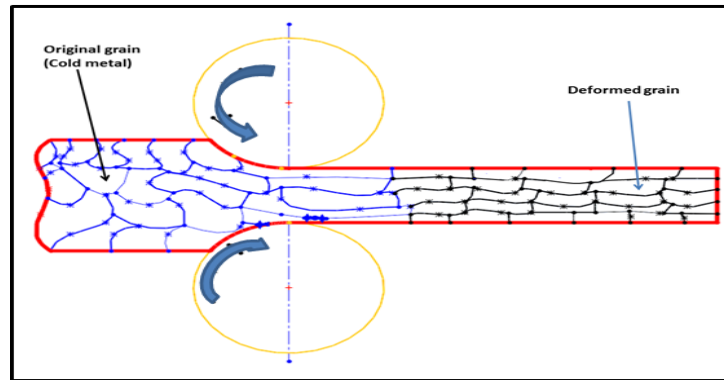


Figure 7.2b Schematic diagram of the cold-rolling process showing the deformed and elongated grains in the direction of rolling [142]

Cold drawing is a process in which the cross-section of a metal is reduced while its length is increased by pulling it through a die at room temperature in order to obtain bright bars, rods, tubes and wires. The material for cold drawing may be hot-rolled stock (Ferrous) or extruded material (Non-ferrous), and are normally 1-2 mm oversize which therefore makes the amount to be reduced smaller.

7.1.2 Machinability of AISI 1018 steels

The machinability of a material is a measure of how difficult or easy a material removal process can be undertaken on the specified material with regards to the specific power consumed, tool life, surface finish produced, force and chip control [138, 143]. The machinability of a material is significantly influenced by its mechanical properties (strength, hardness, toughness, ductility, elasticity, fatigue etc.); the physical properties (thermal conductivity, density, specific heat, melting point, electrical and magnetic properties); and the chemical properties (oxidation, corrosion, general degradation of materials, and flammability) of the materials [144]. Mild steels have good machinability properties. Nevertheless, properties such as high resistance to breakage, and high strength may result in high cutting temperatures. These high temperatures lead to increased tool wear of the cutters.

Also, Boothroyd and Knight [145] suggested that poor machinability may be influenced by increased material hardness which therefore results in high surface roughness, high tool wear rates, temperature increase and high power demand. Thus, the hardness of a

machined part may vary due to the non-uniformity of the grain structure during the manufacturing processes. As a result, differences in cutting forces may be noted as well as induced vibrations during the cutting process [146]. These abnormalities are unavoidable irrespective of the machine tool design or cutting parameters optimisation.

7.1.3 Surface roughness

The functional efficiency of machined parts can be determined by the characteristics of the machined surface such as surface roughness; defects on the surface (such as micro cracks); and the condition of the subsurface (plastic flow orientation of the grains). The type of surface finish and surface integrity obtained after the material removal process significantly influences the quality of machined part surfaces.

Metallurgical surface damage due to machining may cause machined surfaces to be different from the as-received material surfaces. Some of the damages may include plastic deformation of feed marks, deposited materials, material pick up and micro cracks etc. [147]. Several factors may affect the surface finish of a machined part. This may include the workpiece (workpiece design, workpiece quality and structure, workpiece setup), cutting tool (tool wear, tool geometry, stability) and the machinery (machine tool rigidity, cutting conditions, power, cutting environment) [147]. Thiele and Melkote [148] suggested that workpiece properties are important since the process of surface generation is influenced by the plastic deformation of the workpiece.

Few researchers have undertaken studies to identify strategies of minimising energy demand when machining AISI 1018 steel by focusing on machining parameters and energy consumption. For example, Diaz et al. [49] investigated the energy consumption of a machine tool when milling AISI 1018 steel in order to determine energy saving strategies. However, sensitivity analyses of the as-received workpiece material working processes on surface roughness and tool wear was not considered. Camposeco-Negrete et al. [149] utilised a robust design method to optimise cutting parameters when performing rough turning of AISI 1018 steel in order to identify the optimal parameters for energy demand reduction. The limitation in this work is that the influence of AISI 1018 steel material working processes on energy demand was not considered. Also, Dhiman et al. [144] undertook turning of AISI 1018 steel in order to investigate the impact of cutting

parameters on factors affecting machining costs such as surface roughness, tool wear and tool tip temperature. It was reported that spindle speed has significant effect on the surface roughness and temperature. However, they did not consider the effect of the material's working processes on the energy demand, surface roughness and tool wear.

From the previewed works, it is shown that efforts in reducing energy demand when machining AISI 1018 steel by optimising cutting parameters have been made. Nevertheless, sensitivity analysis of the as-received material working processes on the electrical energy consumption was not considered. In view of this, it is important to investigate this gap in order to determine if the working processes for producing AISI 1018 steel material bars could affect the acquired energy consumption data and surface integrity when machining in different component orientations.

7.2 Research aim and objectives

The aim of this study is to analyse the as-received workpiece material with regards to the influence of working processes on the electrical energy consumption measurement in a milling process. To achieve this, it is important to: i) measure the hardness of the as-received workpiece material on the top and bottom surfaces ii) analyse the microstructure of the as-received workpiece and subsurface of the machined part for grain orientation; iii) assess the electrical energy demand when machining the workpiece in the x-axis (0 degrees) and y-axis (90 degrees) directions while still maintaining cutting in one direction; iv) check the surface finish of each machined surface based on their orientations.

7.3 Experimental details

A cast and hot rolled AISI 1018 steel flat bar of 080A15 specification with dimension of 50 mm in width, 10 mm thickness and 150 mm in length was received from the manufacturers. This workpiece material is also referred to as low carbon steel which is a general purpose carbon steel that is easily machined and welded. The sample workpiece material is shown in Figure 7.3.

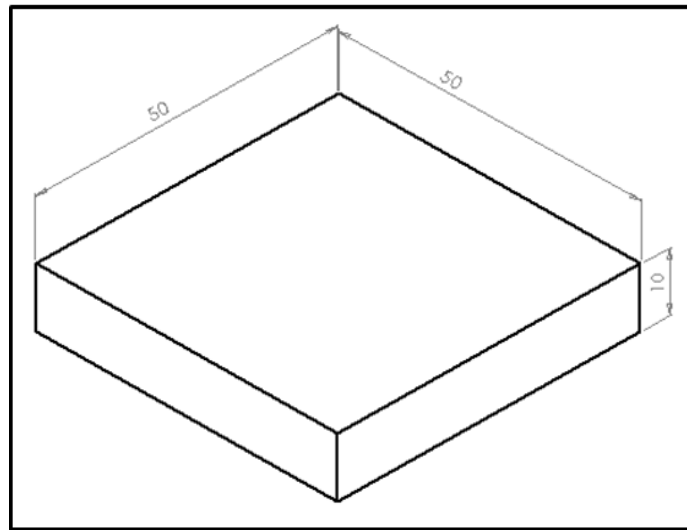


Figure 7.3 AISI 1018 steel workpiece

The steel bar was cut into two equal sizes with dimensions of $50 \times 50 \times 10$ mm for the material removal process. The mechanical properties and the chemical composition of the workpiece material are presented in Table 7.1.

Table 7.1 AISI 1018 steel workpiece

Mechanical Properties of the workpiece:	
- Yield strength, MPa	340 – 600
- Tensile strength, MPa	430 - 750
Mass of workpiece, g	350
Chemical composition of the workpiece	0.17 wt% C, 0.27 wt% Si, 0.80 wt % Mn, 0.050 wt% S max, 0.050 wt% P max

Two 8 mm diameter short carbide 4 flute end mill cutters from Swiss Tech were used in this study. A sample of one of the cutters is shown in Figure 7.4.

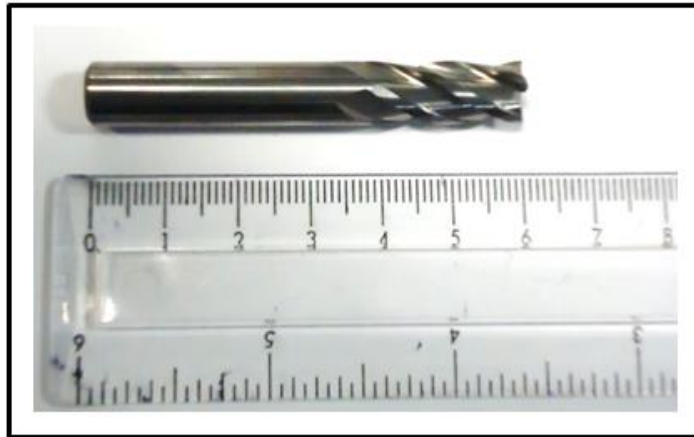


Figure 7.4 Image of an 8 mm 4 flute carbide end mill cutter

Hardness tests for the as-received material were undertaken on the Vickers Hardness machine using a load of 200 N. This analysis was necessary in order to determine the variations in hardness of the as-received workpiece material. The top and bottom surfaces of the workpiece material were considered for hardness test as shown in Figure 7.5.

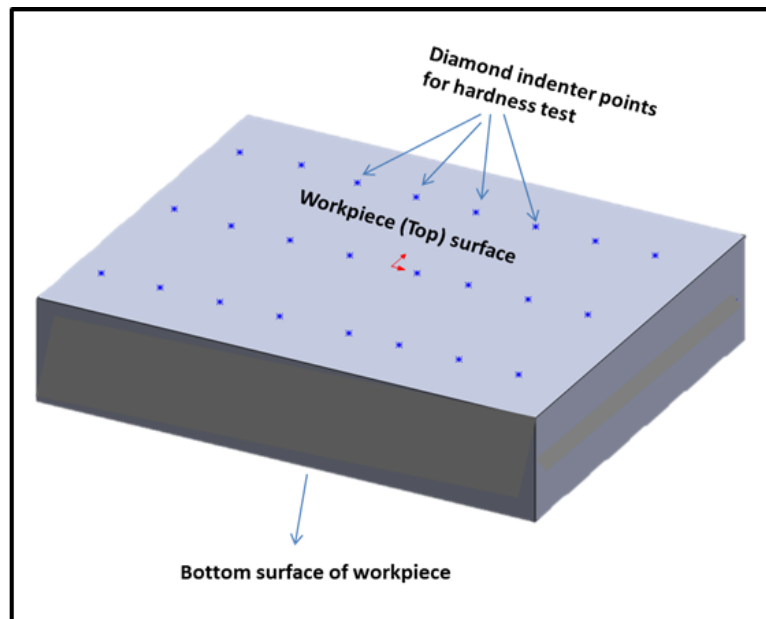


Figure 7.5 Workpiece showing the sides considered for hardness test

Furthermore, the electrical energy demand of AISI 1018 steel when performing face milling at different workpiece orientations was assessed. This involved air cutting and face milling operations with the zag toolpath strategy. A 3-axis Takisawa Mac-V3 milling

machine with a DC servo motor model 20M with spindle model A06B-0652-B, and FANUC controller was considered. The vertical machining centre is capable of spindle speeds of up to $10,000 \text{ revmin}^{-1}$. The acceleration for the x, y, and z axes is 10 ms^{-2} , with rated power of 0.85 kW for x and y axes, and 1.2 kW for the z axis. The rated power of the spindle motor is 7.5 kW. The axes drives were powered by the AC servo motors connected directly to the ball screw drive.

The weight of the vice was 570 N. Air cutting and face milling of the workpiece were first undertaken in the x- axis direction (0 degrees) of the x-y plane. Then, the workpiece was rotated and mounted in the y-axis direction (90 degrees) while cutting was maintained in one direction. Figure 7.6 presents the sample workpiece with the machining toolpaths in the x-y plane.

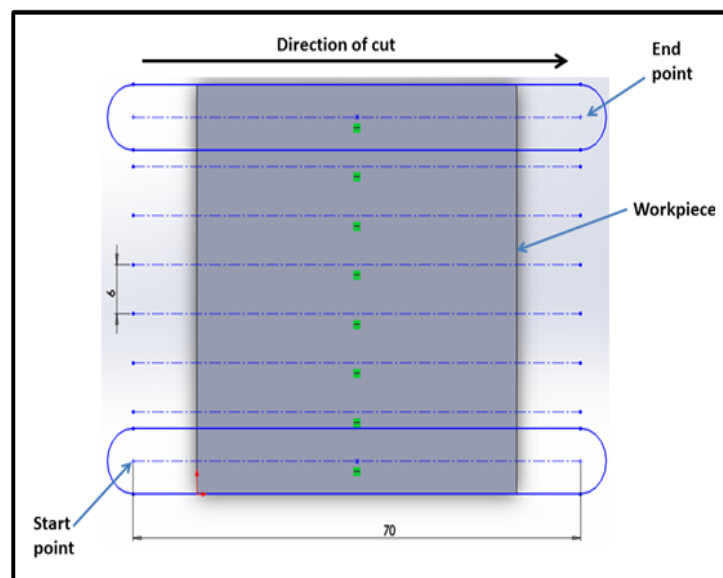


Figure 7.6 Workpiece with zag toolpath strategy in the x-axis direction of the x-y plane

The length of cut was 70 mm; the depth of cut was 0.5 mm, the cutting speed was 100 m/min, while the feedrate was 500 mm/min. Eight (8) passes with constant step over of 0.75D were utilised for machining the total workpiece width. Face milling of the material was undertaken in a dry cutting environment. The current and voltage drawn by the machine tool when performing air cutting and face milling were measured using the Fluke 434 power quality analyser.

Surface roughness check for the workpiece materials was undertaken after cutting was maintained in one direction with the workpiece mounted or rotated in the specified axis direction. A Surtronic 25 portable surface roughness checker device was used. Measurements were performed perpendicular to the direction of the lay at three points on the machined surface. Readings at each point were performed three times.

Metallographic studies were undertaken in order to analyse the microstructure of the as-received workpiece material in order to check for grain deformation or distortion due to the working processes used for producing the as-received workpiece material, as well as the machining influence on the microstructure. Initially, the as-received workpiece was cut to size with dimension of $50 \times 30 \times 10 \text{ mm}$, and its top surface was ground with an electro-coated Silicon carbide waterproof abrasive paper with grit sizes of 80, 120, 320, 600, 800, and 1200 on the OmegaPol grinding machine with rotating disc. After the grinding operations were completed, polishing of the ground surface was undertaken. Three 200 mm diameter 62105 MAIA polishing cloths were used on the rotating disc of the polishing machine. Gemini Diamond monocrystalline slurry with 6 micron, 3 micron, and 1 micron were sprayed on the polishing cloth just to moisten it. The LaboPol-35 machine was used for the polishing process. After the grinding and polishing processes, etching was performed in 2% Nital solution comprising of 2 ml of Nitric Acid and 98 ml of Ethanol was used as the etchant, being the recommended etchant for mild steels. The etching duration was approximately 15 s. After the etching process, the optical microscope (LEICA DM2500) was used to acquire images of the etched sample.

After the etching of the as-received workpiece material, some materials were removed from its top surface. The same procedures for grinding, polishing, and etching were repeated on the side of the machined workpiece.

7.4 Results and discussions

7.4.1 Hardness analysis

Hardness test of the as-received AISI 1018 steel material were undertaken in order to analyse and note possible variations in its hardness. Figure 7.7 shows the plot of hardness values with the positions measured on the workpiece surface.

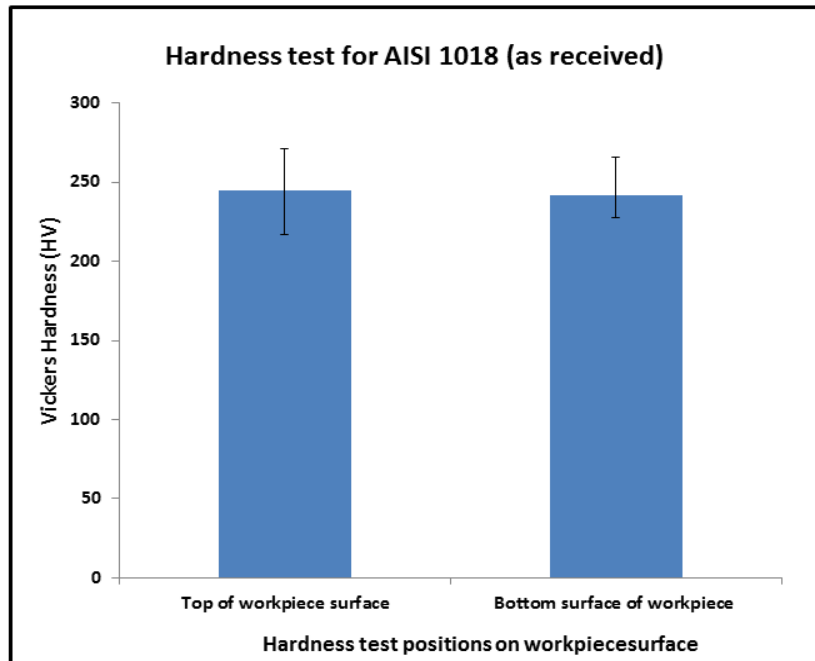


Figure 7.7 Hardness test for the as-received AISI 1018 steel

From Figure 7.7, it is observed that the hardness values on the specified workpiece surfaces were slightly varied. No side had consistently higher or lower hardness. This suggested that the workpiece may not have a strong property bias.

7.4.2 Electrical energy demand for face milling of AISI 1018 steel

Power demand studies were undertaken when the workpiece was first mounted and machined in the x-axis direction (0 degrees) with the zag toolpath strategy, and then rotated and mounted in the y-axis direction (90 degrees) while cutting was maintained along the x-axis direction. The power demand for face milling was estimated from the current and voltage drawn by the machine tool. The tool tip (cutting) power was estimated by subtracting the air cutting power from the total power. The acquired power values and processing time (which was 142 seconds) were used to estimate the electrical energy demand for the material removal process as shown in Figure 7.8.

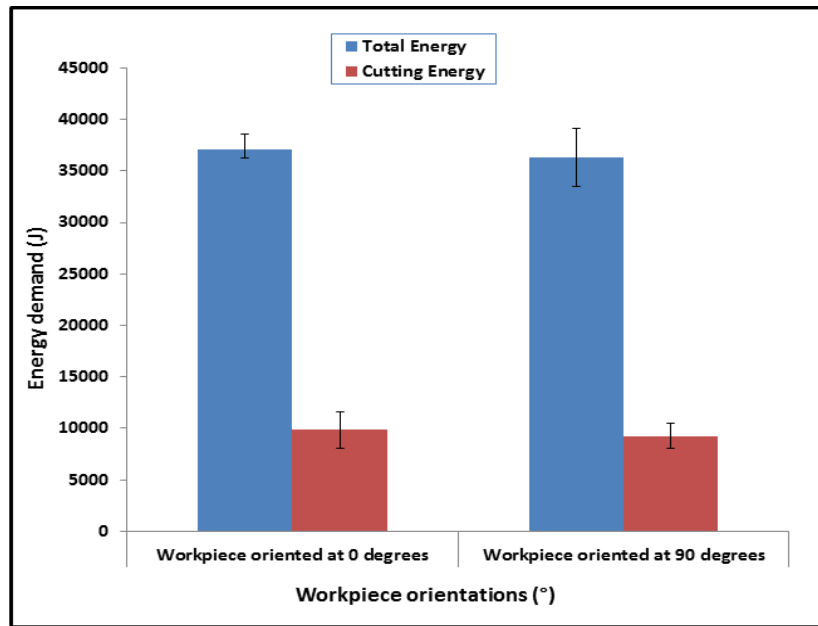


Figure 7.8 Energy demand for face milling of AISI 1018 steel when workpiece is oriented at 0 (x-axis) and 90 degrees (y-axis)

Figure 7.8 shows variation of electrical energy demand with workpiece orientations for cutting and tool tip. Figure 7.8 show that the as-received AISI 1018 steel workpiece had little influence on the electrical energy demand in machining for orthogonal directions of cut.

7.4.3 Surface integrity characterisation

7.4.3.1 Surface roughness

Further studies were undertaken to determine the influence of workpiece orientations on surface roughness. Figure 7.9 presents graphs showing variations of average surface roughness (measured perpendicular to the direction of the lay) with regards to workpiece orientations.

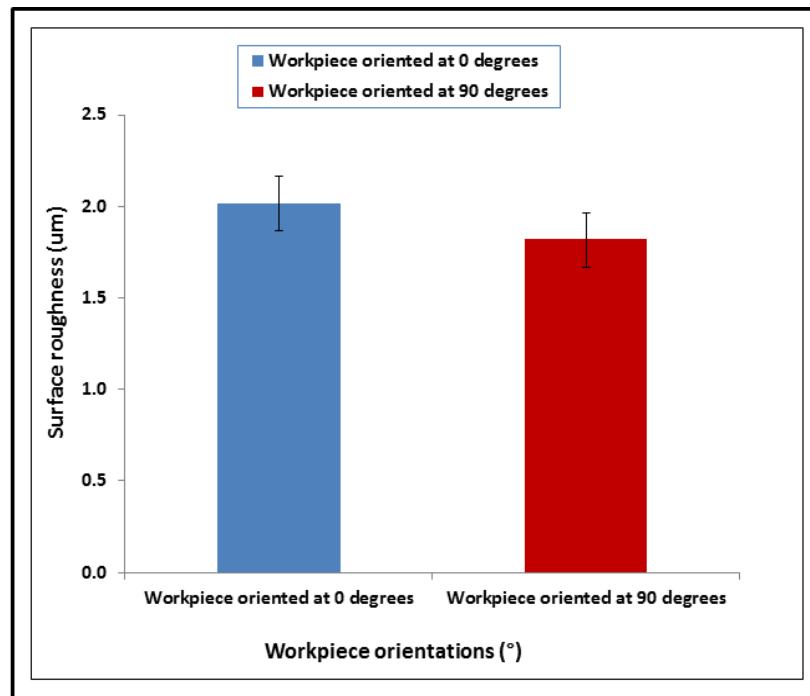


Figure 7.9 Variation of surface roughness measured perpendicular to the feed direction and workpiece orientations

The results show an overlap in surface roughness values. The variations in surface roughness values when machining at different workpiece orientations may be due to slight differences in hardness of the workpiece material which further confirms the fact that the hardness properties of a workpiece are not quite uniform on its surfaces. Thus, cutting in orthogonal directions does not lead to a consistent reduction or increase in surface roughness.

7.4.3.2 Microstructure

Microstructure analysis was initially undertaken in order to check for the grains orientation of the as-received material as a result of the material working processes.

Figure 7.10 shows a typical microstructure of the as-received AISI 1018 steel material after etching for 15 seconds in 2% Nital solution.

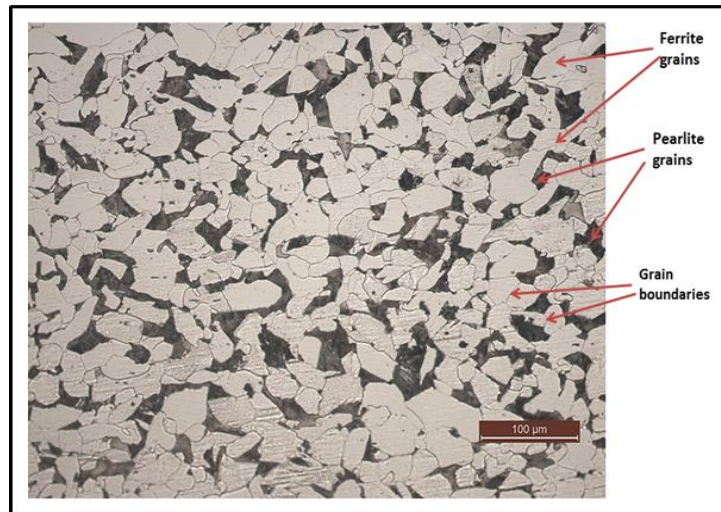


Figure 7.10 Microstructure of as-received AISI 1018 steel, etched in 2% Nital solution for 15 s

The microstructure of the as-received AISI 1018 steel is a two phase system consisting of two sets of grains which are randomly oriented as a result of the hot rolled process utilised in the workpiece manufacture as earlier shown in Figure 7.1. The micrograph of the as-received AISI 1018 steel (top surface) shows ferrite grains (white etching constituent) and pearlite grains (dark etching constituent) which are a combination of cementite and ferrite. The grain boundaries are also visibly seen in the micrograph. As observed in Figure 7.10, the working processes (i.e. hot rolling) do not have any effect on the grain structure of the as-received AISI 1018 steel.

Additional analysis was conducted to determine the effect of material removal process on the microstructure of the machined surface.

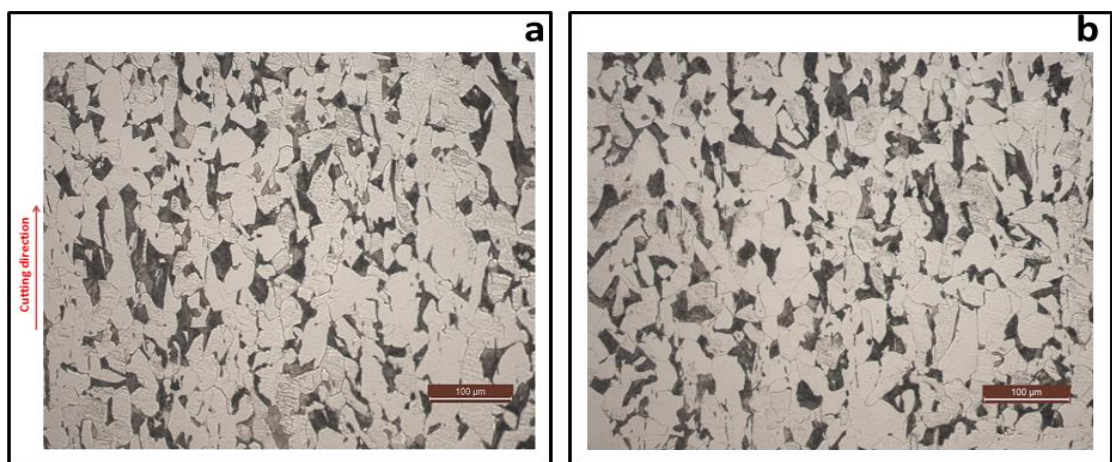


Figure 7.11a, b Microstructure of the top machined surface for AISI 1018 steel when orienting at 0 and 90 degrees respectively

The acquired micrograph of the machined surfaces for both samples with workpiece orientations at 0 degrees and 90 degrees after the grinding, polishing, and etching procedures are presented in Figures 7.11a and 7.11b. It is observed that in both orientations of the workpiece (i.e. at 0 degrees and 90 degrees), the grains were deformed and elongated, orienting in the cutting direction as a result of plastic deformations and high temperatures ranging approximately between 500°C and 696°C [150, 151] experienced in the cutting process.

Furthermore, sides of the as-received workpiece material and machined samples for workpiece orientations at 0 degrees and 90 degrees were ground, polished and later etched in 2% Nital for 15 seconds in order to show the orientation of grains near the surface of the as-received workpiece material and machined surfaces. These images are presented in Figures 7.12a, 7.12b and 7.12c.

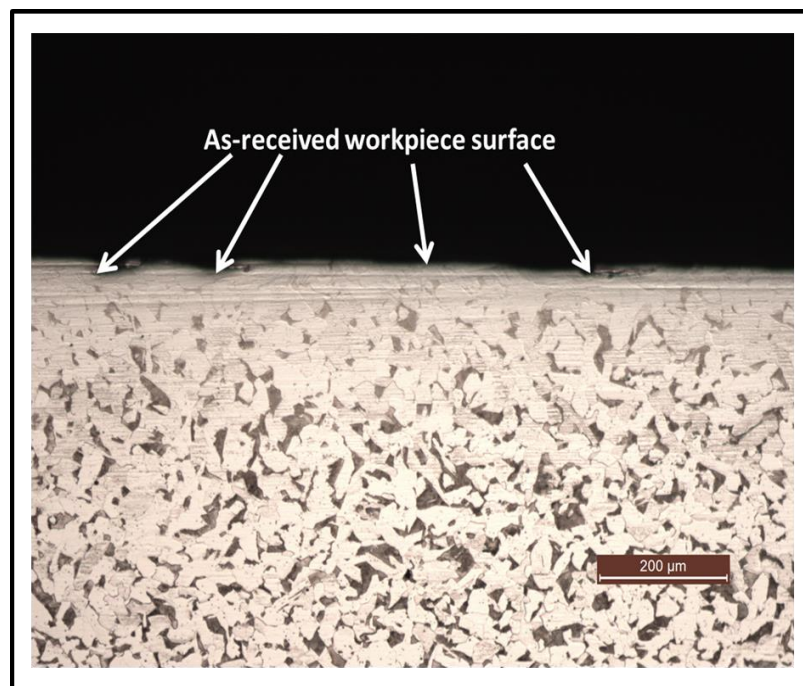


Figure 7.12a Sub-surface microstructure of the as-received surface (viewed from the side)

As shown in Figure 7.12a, the grains of the as-received workpiece material near the top surface are randomly oriented due to the fact that no machining process has been carried out on its top surface. Further images on Figures 7.12b and 7.12c show the sub-surface microstructure of the machined surface at different workpiece orientations.

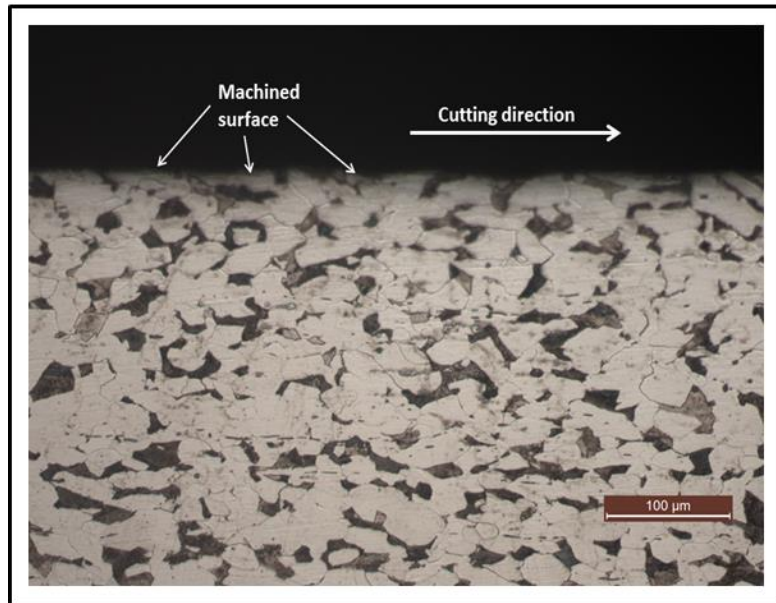


Figure 7.12b Sub-surface microstructure of the machined surface for AISI 1018 steel when orienting at 0 degrees

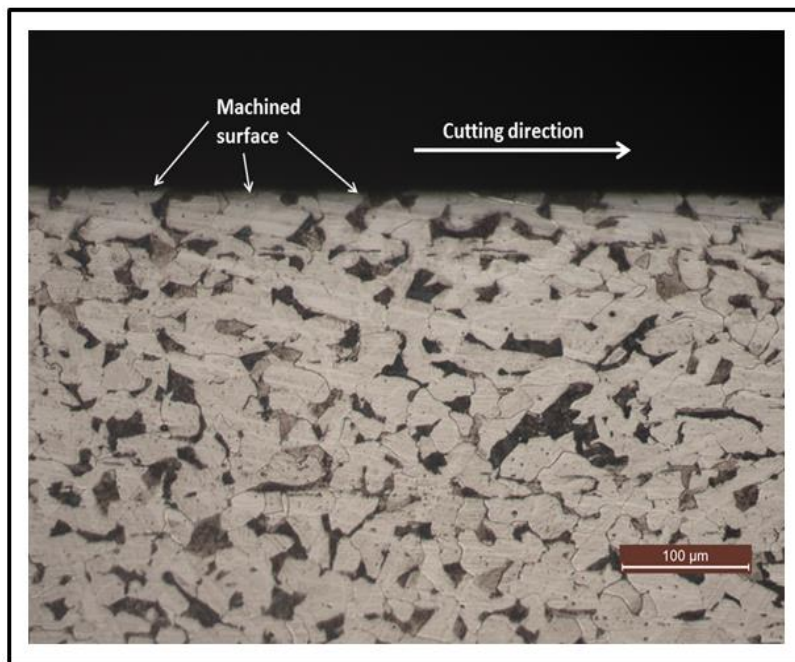


Figure 7.12c Subsurface microstructure of the machined surface for AISI 1018 steel when orienting at 90 degrees

From Figures 7.12b and 7.12c, it can be seen that the grains near the machined surface are oriented in the cutting direction. Comparing the microscopy images in Figure 7.12a with those of Figures 7.12b and 7.12c, it is observed that the grains in Figures 7.12b and 7.12c are oriented in the cutting direction. This is as a result of plastic deformation and high temperature on the machined surface which affects the grain orientation.

7.4.4 Tool wear

The issue of tool wear is of wide interest to manufacturers due to the fact that it increases difficulty in machining and affects the quality of the machined component [152]. Tool wear is defined as the progressive loss or removal of material from a surface [138]. Cutting tool wear is the result of load, friction, and high temperature between the cutting edge and the workpiece [152]. Selection of the appropriate cutting tools is considered as one of the most important considerations in material removal processes. This is because in machining, cutting tools are normally subjected to rubbing (friction) on the workpiece surface, high temperatures, high contact stresses and chip movement on the rake face. In view of this, cutting tools must possess the following characteristics including hardness to maintain the strength and hardness of the tool; toughness to prevent cutting forces from fracturing the tool; wear resistance to prolong tool life, and chemical stability [44].

Mild steels are normally machined with carbide tools such as tungsten carbide (WC), titanium carbide (TiC) and plain carbide (uncoated carbide) tools due to their high hardness over a wide range of temperatures, low thermal expansion, high elastic modulus and thermal conductivity [44]. Recently, coated tools have been widely used to machine mild steels at high cutting speeds to minimise costs. Coating of these tools with various materials is necessary in order to improve tool life [153]. These materials may include titanium nitride (TiN) for high hardness, good adhesion to the substrate, low coefficient of friction; titanium carbide on tungsten carbide inserts (TiC) for high resistance to flank wear; titanium carbonitride (TiCN) deposited on carbide and high speed tools for cutting stainless steels; ceramic coatings (Al_2O_3) for high temperature performance, resistance to flank and crater wear, chemical inertness; diamond coatings (PVD-physical vapour deposition and CVD-chemical vapour deposition) for increase in tool life; and titanium aluminium nitride (TiAlN) for machining aerospace alloys [44].

In milling, tool wear may occur at the cutting edge (nose radius wear), rake face (crater wear), or on the flank face (flank wear) [154]. Thus, tool wear can affect the quality of the machined surfaces and the production cost.

In this study, the two carbide tools with 4 flutes and 8 mm in diameter used for the face milling operation with workpiece orientation at 0 and 90 degrees while cutting was maintained along the x-axis direction were observed on the VHX-500F digital microscope for tool wear conditions. Each tool was used 3 times to complete the eight (8) passes with

constant step over of $0.75D$. The images acquired for both tools are presented in Figures 7.13 and 7.14 for the 0 and 90 degree workpiece orientations respectively.

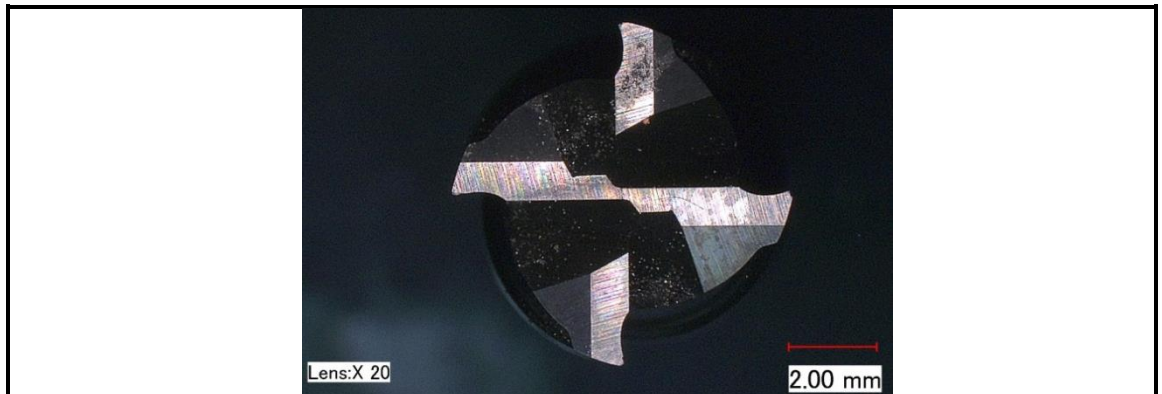


Figure 7.13a Cutting tool showing four cutting edges when machining in 0 degrees

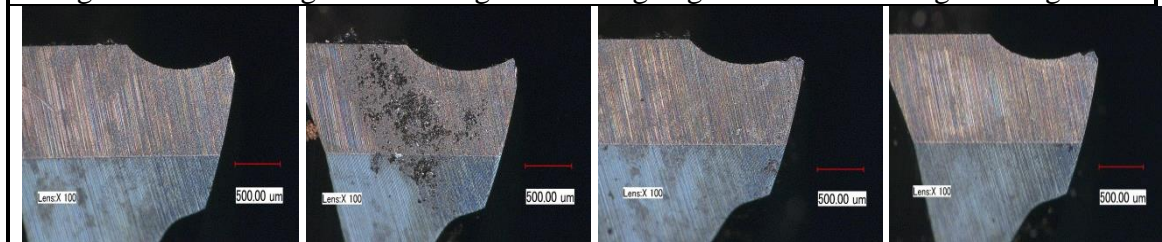


Figure 7.13b Cutting edge 1	Figure 7.13c Cutting edge 2	Figure 7.13d Cutting edge 3	Figure 7.13e Cutting edge 4
-----------------------------	-----------------------------	-----------------------------	-----------------------------



Figure 7.14a Cutting tool showing four cutting edges when machining in 90 degrees

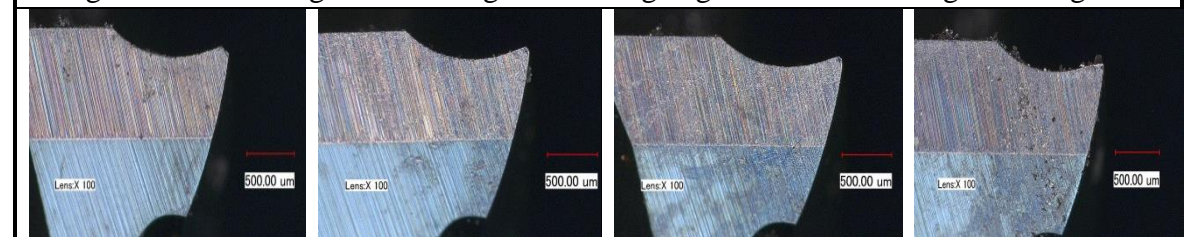


Figure 7.14b Cutting edge 1	Figure 7.14c Cutting edge 2	Figure 7.14d Cutting edge 3	Figure 7.14e Cutting edge 4
-----------------------------	-----------------------------	-----------------------------	-----------------------------

From Figures 7.13 and 7.14, it can be seen that the tool wear pattern for both tools were similar in terms of the deterioration of the cutting edges after machining for a period of 7.1 minutes each.

7.5 Conclusions

This chapter focuses on the analyses of the as-received workpiece material with regards to the influence of casting direction on the electrical energy consumption measurement in a milling process. The following conclusions were obtained from this study:

- Hardness test of the as-received material was measured on the specified surfaces of the workpiece. Results show slight variations in the hardness values based on the workpiece sides considered.
- The influence of variations in hardness of the as-received workpiece material on the electrical energy demand data obtained when machining at different workpiece orientations was insignificant. Thus, it could be deduced that variations in hardness properties of the as-received AISI 1018 steel workpiece had little influence on the electrical energy demand in machining
- The surface roughness values obtained when machining the workpiece in different orientations with constant cutting direction showed overlapped results. Consequently, no conclusions were drawn in the surface roughness study.
- Microstructure of the as-received workpiece material showed no visible changes on the grains that have resulted from the working processes. However, orientation of the grains in the cutting direction when analysing the top machined surface and the side subsurface of the machined workpiece surface was noticed.
- For the workpiece considered in this PhD, the direction of workpiece cutting can be assumed insignificant in terms of its impact on energy demand or surface roughness of the machined part.

CHAPTER 8

CONCLUSIONS AND FUTURE RESEARCH

8.1 Overall conclusions

This PhD research focused on modelling of energy demand for machine tool feed axis and CNC codes in milling in order to support energy centric and sustainable product and process planning. Some of the key findings in this study are as follows:

- A new model for estimating the electrical energy demand of feed axes was presented in this study as: $E_f = P_0 t_{cy} + (aWv_f + bW)t_{cy} + F_f v_c t_c$. It captures the impact of table feedrates, weights of machine table and materials placed on it and the feed force acting in the axial direction of the feed drive. This new model can be used to determine the feed axes energy demand for conventional machining using ball screw feed drives for conventional sized components.
- This study has shown that the axis carrying more weight resulted in high energy demand of the feed axes while executing the same toolpath. It is therefore recommended that high mass components and long components should have the long length aligned to the top table axis (i.e. the axis that is lighter and demands less energy) in order to reduce the non-cutting power.
- Minimum electrical energy demand for feed axis during air cutting and pocket milling was obtained with machine vice and component oriented at the angle aligned in the direction of axis carrying less weight, resulting in electrical energy savings of up to 29%, and improved surface finish by up to 50% when compared with the roughness values obtained when the machine tool vice was aligned in other axis directions.
- In considering the various toolpath strategies adopted for machining a rectangular pocket, results from this study showed that minimal energy demand and processing time could be achieved by selecting toolpaths with minimum tool retractions and longer cutting lengths and with large toolpath links to the next path segment. It was

also found that surface roughness values for toolpath strategies without tool retracts were lower when compared with surface roughness values for toolpath strategies with tool retracts. This further shows that improved surface finish of the machined part could be achieved by selecting toolpaths with minimum tool retractions.

- The high energy intensity of the G02 codes, G03 codes, and linear toolpaths with shorter path length segments are due to the fact that the maximum programmed feedrate could not be reached and that mass and friction become more dominant as a result of the shorter distance moved by the feed drive. Therefore, energy intensity in machining could be significantly reduced by selecting toolpaths with longer linear path segments.
- The NC-code based energy demand prediction model and software could predict the total electrical energy required by a machine tool to run an NC program, and would enable process planners to estimate the energy demand for running an NC program before the actual machining of a part is conducted in order to select the best energy efficient strategy. This is achieved by relating appropriate energy demand models to NC codes which actuate the main energy consuming components of the machine tool. It is therefore recommended that machine tool developers provide the basic energy states of some NC codes (i.e. G00, M06, M07), and information on some machine tool parameters (i.e. weight of x-axis, weight of y-axis) so that it can be added to the postprocessor of CAM software for energy demand prediction.
- Although there were slight variations in hardness properties of the as-received AISI 1018 steel workpiece, the electrical energy demand data obtained in the cutting tests were not significantly affected. Thus, the direction in which a material is cut is not a significant factor to change energy demand.

8.2 Contribution to knowledge

The work presented in this PhD led to the following novel contributions:

- Development of a new and novel feed axes energy demand model which takes into account the weights of feed axes, machine tool vice, and the workpiece. This model was validated on a milling toolpath.

- Clarifying the impacts of weights placed on the machine table on the energy demand of feed axes, and the overall non-cutting energy demand of the machine tool. It was found that machining of components along the axes carrying minimal weights resulted in low energy consumption
- The development of a method to identify the most efficient toolpath strategy in terms of energy requirements and processing time based on the newly developed feed axes energy demand model.
- This research has presented NC-code based analytical model and software for predicting the total electrical energy and total time required to run an NC program. This model and procedure highlights the importance of including the weights of materials moved by the feed axes to improve the prediction capability of energy consumption models of machine tools.

8.3 Recommendations for future research

This PhD work has opened up further opportunities for improving energy efficiency in mechanical machining processes. The following areas are proposed for further studies:

- More work is needed in modelling the friction aspects of machine tool drives, in particular for micro and nano-components and features where acceleration and deceleration are significant for the tool paths
- The dynamic characteristic of the feed axes has to be measured to experimentally ascertain the power and time required to accelerate and decelerate the feed drive at different table feedrates.
- Further work in the study is to model the influence of tool wear to apply the model to tool paths where the cycle time is long and tool wear increases the tip energy
- To acquire and use MT connect language for real-time energy management of multiple machine resources.

REFERENCES

1. World population prospects: the 2015 revision, key findings and advance tables, New York, Department of Economic and Social Affairs (DESA), Available from: https://esa.un.org/unpd/wpp/publications/files/key_findings_wpp_2015.pdf
Accessed on: 10 June, 2015.
2. International Energy Outlook, U.S. Energy Information Administration, Available from: [http://www.eia.gov/forecasts/ieo/pdf/0484\(2013\).pdf](http://www.eia.gov/forecasts/ieo/pdf/0484(2013).pdf), 2013. Accessed on: 10 July, 2016.
3. Key world energy statistics, Available from: <http://www.observatoire-du-nucleaire.org/IMG/pdf/2013-keyworld-aie.pdf>, 2013. Accessed on: 22 August, 2014.
4. CO₂ emissions from fuel combustion highlights (2013 Edition), Available from: <http://www.indiaenvironmentportal.org.in/files/file/CO2EmissionsFromFuelCombustionHighlights2013.pdf>, Accessed on: 10 July, 2016.
5. Tracking Industrial Energy Efficiency and CO₂ emissions, International Energy Agency, Available from: https://www.iea.org/publications/freepublications/publication/tracking_emissions.pdf, 2007. Accessed on: 13 September, 2016
6. Energy consumption in the UK, Department of Energy and Climate Change, Available from: <https://www.gov.uk/government/collections/energy-consumption-in-the-uk>, 2012. Accessed on: 30 May, 2016.
7. Howard, M.C., Sustainable Manufacturing Initiative (SMI): A true Public-Private Dialogue, Available from: <https://www.oecd.org/sti/ind/45010349.pdf>, Accessed on: 16 August, 2014.
8. Concept Description for CECIMO's Self-Regulatory Initiative (SRI) for the Sector Specific Implementation of the Directive 2005/32/EC, Available from: <http://www.cecimo.eu/site/publications/magazine/cecimo-self-regulatory-initiative/>, 2009. Accessed on: 13 September, 2016.
9. Dahmus J. B. and Gutowski T. G., An environmental analysis of machining, IMECE2004 ASME International Mechanical Engineering Congress and RD&D Expo, 2004, 1 - 10.

10. Zulaika J., Dietmair, A., Campa, F., Lopez de Lacalle, L., and Verbeeten, W., Eco-efficient and highly productive production machines. The 3rd International Conference on Eco-efficiency modelling and evaluation for sustainability: Guiding eco-innovation and consumption, Egmond an Zee, The Netherlands, 2010.
11. Diaz, N., Helu, M., Jayanathan, S., Chen., Y., Horvath, A., and Dornfeld, D., Environmental analysis of milling machine tool use in various manufacturing environments. IEEE International Symposium on Sustainable Systems and Technology, 2010.
12. Santos, J.P., Oliveira, M., Almeida, F.G., Pereira, J.P., and Reis, A., Improving the environmental performance of machine-tools: influence of technology and throughput on the electrical energy consumption of a press-brake. Journal of Cleaner Production, 2011, 19 (4) 356-364.
13. Study for preparing the first working plan of the eco-design directive. Report for tender No. :ENTR/06/026, Accessed from: https://www.ebpg.bam.de/de/ebpg_medien/wp1_studyf_07_11_complete.pdf, 2007. Accessed on: 13 September, 2016.
14. Kellens, K., Dewulf, W., Overcash, M., Hauschild, Z., and Duflou, J. R., Methodology for systematic analysis and improvement of manufacturing unit process life-cycle inventory (UPLCI) - CO2PE! initiative (cooperative effort on process emissions in manufacturing). Part 1: Methodology description. The International Journal of Life Cycle Assessment, 2011, 17 (1) 69-78.
15. ISO 14955-1:2014 Machine tools - environmental evaluation of machine tools - Part 1: Design methodology for energy-efficient machine tools.
16. Gutowski, T., Dahmus, J., and Thiriez, A., Electrical energy requirements for manufacturing processes. Proceedings of 13th CIRP International Conference on Life Cycle Eng, Leuven, 2006, 623.
17. Li, W., Zein, A., Kara, S., and Hermann, C., An investigation into fixed energy consumption of machine tools. 2011, 268-273.
18. Mori, M., Fujishima, M., Inamasu, Y., and Oda, Y., A study on energy efficiency improvement for machine tools. CIRP Annals - Manufacturing Technology, 2011, 60 (1) 145-148.
19. Diaz, N., Choi, S., Helu, M., Chen, Y., Jayanathan, S., Yasui, Y., Kong, D., Pavanaskar, S., and Dornfeld, D., Machine tool design and operation strategies for

- green manufacturing. Proceedings of 4th CIRP International Conference on High Performance Cutting, 2010.
20. Kroll, L., Blau, P., Wabner, M., Frieb, U., Eulitz, J., and Klarner, M., Lightweight components for energy-efficient machine tools. *CIRP Journal of Manufacturing Science and Technology*, 2011, 4 (2) 148-160.
 21. Duflou, J.R., Sutherland J. W., Dornfeld, D., Herrmann, C., Jeswiet, J., Kara, S., Hauschild, M., and Kellens, K., Towards energy and resource efficient manufacturing: A processes and systems approach. *CIRP Annals - Manufacturing Technology*, 2012, 61, 587-609.
 22. Kong, D., Choi, S., Yasui, Y., Pavanaskar, S., Dornfeld, D., and Wright, P., Software-based toolpath evaluation for environmental sustainability. *Journal of Manufacturing Systems*, 2011. 30 (4) 241-247.
 23. Rangarajan, A. and Dornfeld, D., Efficient toolpaths and part orientation for face milling. *CIRP Annals - Manufacturing Technology*, 2004. 53 (1) 73-76.
 24. Monreal, M. and Rodriguez, C. A., Influence of toolpath strategy on the cycle time of high-speed milling. *Computer-Aided Design*, 2003, 35, 395-401.
 25. Wang, S., Lu, X., Li, X. X., and Li, W. D., A systematic approach of process planning and scheduling optimization for sustainable machining. *Journal of Cleaner Production*, 2015, 87, 914-929.
 26. He, Y., Liu, F., Wu, T., Zhong, F-P, and Peng, B., Analysis and estimation of energy consumption for numerical control machining. *Proceedings of the Institution of Mechanical Engineers, Part B: Journal of Engineering Manufacture*, 2011, 226 (2) 255-266.
 27. Pavanaskar, S. and McMains, S., Machine specific energy consumption analyses for CNC milling toolpaths. *Proceedings of the ASME 2015 International Design Engineering Technical Conferences & Computers and Information in Engineering Conference (IDETC/CIE 2015)*. Boston, Massachusetts, USA. DETC2015-48014, 2015.
 28. Bhushan, R.K., Optimization of cutting parameters for minimizing power consumption and maximizing tool life during machining of Al alloy SiC particle composites. *Journal of Cleaner Production*, 2013, 39, 242-254.
 29. Li, L., Yan, J., and Xing, Z., Energy requirements evaluation of milling machines based on thermal equilibrium and empirical modelling. *Journal of Cleaner Production*, 2013, 52 (1) 113-121.

30. Report of the world commission on environment and development, United Nations Department of Economic and Social Affairs, Available from: <http://www.un.org/documents/ga/res/42/ares42-187.htm>, 1987.
Accessed on: 16 August, 2014
31. Arif, M., Stroud, I. A., and Akten, O., A model to determine the optimal parameters in a machining process for the most profitable utilization of machining energy. Proceedings of the Institution of Mechanical Engineers, Part B: Journal of Engineering Manufacture, 2014.
32. Jovane, F., Yoshikawa, H., Alting, L., Boer, C. R., Westkamper, E., Williams, D., Tseng, M., Seliger, G., and Paci, A. M., The incoming global technological and industrial revolution towards competitive sustainable manufacturing. CIRP Annals - Manufacturing Technology, 2008, 57, 641-659.
33. Alting, D. L and Jogensen, D. J., The life cycle concept as a basis for sustainable industrial production. CIRP Annals – Manufacturing Technology, 1993, 42 (1) 163-167.
34. Fang, F., Cheng, K., Ding, H., Chen, S., Zhao, L., Sustainable design and analysis of CNC machine tools: sustainable design index based approach and its application perspectives. Proceedings of the ASME 2016 International Manufacturing Science and Engineering Conference MSEC2016, Blacksburg, Virginia, USA MSEC2016-8730, 2016.
35. Ding, H. and Cheng, K., Development of an innovative ERWC approach to sustainable manufacturing with application to design of an energy-resource efficient CNC centreless grinding. Sustainable Design and Manufacturing, 2014, 653-667.
36. Avram, O., Stroud, I., and Xirouchakis, P., A multi-criteria decision method for sustainability assessment of the use phase of machine tool systems. The International Journal of Advanced Manufacturing Technology, 2010, 53 (5-8), 811-828.
37. Yan, J., Feng, C., and Li, L., Sustainability assessment of machining process based on extension theory and entropy weight approach. The International Journal of Advanced Manufacturing Technology, 2014, 71 (5-8), 1419-1431.
38. Digest of United Kingdom Energy Statistics - A National Statistics publication, Available from:

- <http://webarchive.nationalarchives.gov.uk/20130109092117/http://decc.gov.uk/assets/decc/11/stats/publications/dukes/5949-dukes-2012-exc-cover.pdf>, 2012.
Accessed on: 13 September, 2016.
39. UK greenhouse gas emissions 1990-2014, headline results –Emission of all greenhouse gases for the UK and Crown Dependencies from 1990 – 2014 (provisional) by source sector, Available from:
<https://www.gov.uk/government/collections/provisional-uk-greenhouse-gas-emissions-national-statistics>, 2014. Accessed on: 10 June, 2016.
40. United States Energy Information Agency report, Available from:
<http://www.eia.gov/tools/faqs/faq.cfm?id=447&t=1>, 2011. Accessed on: 26 August, 2015.
41. Kianinejad, K., Uhlmann, E., and Peukert, B., Investigation into energy efficiency of outdated cutting machine tools and identification of improvement potentials to promote sustainability. *Procedia CIRP*, 2015, 26, 533-538.
42. Trent, E.M., *Metal cutting*, Butterworths & Co Publishers Ltd., 1984.
43. Snoeys, R., Staelens, F., and Dekeyser, W., Current trends in non-conventional material removal processes. *CIRP Annals - Manufacturing Technology*, 1986, 35 (2) 467- 480.
44. Kalpakjian, S., and Schmid, S., *Manufacturing processes for engineering materials*, 5th edition in SI units, Prentice Hall, 2008.
45. Fahad, M., A heat partition investigation of multilayer coated carbide tools for high speed machining through experimental studies and finite element modelling. A thesis submitted to The University of Manchester for the degree of Doctor of Philosophy (PhD) in the Faculty of Engineering and Physical Sciences, School of Mechanical Aerospace and Civil Engineering, 2012.
46. Kalpakjian, S. and Schmid, S.R., *Manufacturing Processes for Engineering Materials*, 4, New Jersey, the United States of America: Prentice Hall, 2003
47. Boogert, R. M., Kals, H. J. J., and Van Houten, F. J. A. M., Toolpaths and cutting technology in computer aided process planning. *Int J Adv Manuf Technol*, 1996, 11, 186-197.
48. Koenigsberger, F. and Sabberwal, A. J. P., An investigation into the cutting force pulsations during milling operations. *International Journal of Machine Tool Design and Research*, 1961, 1, 15-33.

-
49. Diaz, N., Redelsheimer, E., and Dornfeld, D., Energy consumption characterization and reduction strategies for milling machine tool use, 2011, 263-267.
 50. Kyoto Protocol, United Nations Framework Convention on Climate Change, Available from: <http://unfccc.int/resource/docs/convkp/kpeng.pdf>, 1997. Accessed on: 13 September, 2016.
 51. Salonitis, K. and Ball, P., Energy efficient manufacturing from machine tools to manufacturing systems. *Procedia CIRP*, 2013, **7**, 634-639.
 52. Patterson, M.G., What is energy efficiency? *Energy Policy*, 1996, 24 (5) 377-390.
 53. Dietmair, A. and Verl, A., Energy consumption forecasting and optimisation for tool machines. *Modern Machinery Science Journal*, 2009, 2, 63 - 67.
 54. Zhou, L., Li, J., Li, F., Meng, Q., Li, J., Xu, X., Energy consumption model and energy efficiency of machine tools: a comprehensive literature review. *Journal of Cleaner Production*, 2015, 1-14
 55. Behrendt, T., Zein, A., Min, S., Development of an energy consumption monitoring procedure for machine tools. *CIRP Annals - Manufacturing Technology*, 2012, 61 (1) 43-46.
 56. Devoldere, T., Dewulf, W., Deprez, W., Willems, B., and Duflou, J. R., Improvement potential for energy consumption in discrete part production machines. *Proc.14th CIRP Conference on Life Cycle Engineering*, 2007, 311-316.
 57. Diaz, N., Helu, M., Jarvis, A., Tonissen, S., Dornfeld, D., and Schlosser, R., Strategies for minimum energy operation for precision machining. *The Proceedings of MTTRF 2009 Annual Meeting*, 2009.
 58. Vijayaraghavan, A. and Dornfeld, D., Automated energy monitoring of machine tools. *CIRP Annals - Manufacturing Technology*, 2010, 59 (1) 21-24.
 59. Vijayaraghavan, A., Sobel, W., Fox, A., Dornfeld, D., and Warndorf, P., Improving machine tool interoperability using standardised interface protocols: MT Connect. *Proceedings of 2008 ISFA 2008 International Symposium on Flexible Automation*, Atlanta, GA, USA, 2008.
 60. Dornfeld, D., Wright, P. K., Vijayaraghavan, A., Helu, M., Enabling manufacturing research through interoperability. *Trans. NAMRI/SME*, 2009.
 61. Shin, S., Woo, J., Kim, D. B., Kumaraguru, S., and Rachuri, S., Developing a virtual machining model to generate MTConnect machine-monitoring data from STEP-NC. *International Journal of Production Research*, 2015.

62. Ak, R. and Bhinge, R., Data analytics and uncertainty quantification for energy prediction in manufacturing. 2015 IEEE International Conference on Big Data (Big Data), 2015.
63. Hu, S., Liu, F., He, Y., and Hu, T., An on-line approach for energy efficiency monitoring of machine tools. *Journal of Cleaner Production*, 2012, 27, 133-140.
64. Yingjie, Z., Energy efficiency techniques in machining process: a review. *The International Journal of Advanced Manufacturing Technology*, 2013, 71 (5-8) 1123-1132.
65. Kordonowy, D. N., A power assessment of machine tools. Massachusetts Institute of Technology, Massachusetts, USA, 2002.
66. Balogun, V. A. and Mativenga, P. T., Modelling of direct energy requirements in mechanical machining processes. *Journal of Cleaner Production*, 2013, 41, 179-186.
67. Lv, J., Tang, R., Jia, S., and Liu, Y., Experimental study on energy consumption of computer numerical control machine tools. *Journal of Cleaner Production*, 2016, 112, 3864-3874.
68. Jia, S., Tang, R., Lv, J., Yuan, Q., and Peng, T., Energy consumption modeling of machining transient states based on finite state machine. *The International Journal of Advanced Manufacturing Technology*, 2016.
69. Balogun, V. A., Gu, H., and Mativenga, P. T., Improving the integrity of specific cutting energy coefficients for energy demand modelling. *Proceedings of the Institution of Mechanical Engineers, Part B: Journal of Engineering Manufacture*, 2014.
70. Eberspächer, P. and Verl, A., Realizing energy reduction of machine tools through a control-integrated consumption graph-based optimization method. *Procedia CIRP*, 2013, 7, 640-645.
71. Sarwar, M., Persson, M., Hellbergh, H., and Haider, J., Measurement of specific cutting energy for evaluating the efficiency of bandsawing different workpiece materials. *International Journal of Machine Tools and Manufacture*, 2009, 49 (12-13) 958-965.
72. Kara, S. and Li, W., Unit process energy consumption models for material removal processes. *CIRP Annals - Manufacturing Technology*, 2011. 60 (1) 37-40.

73. Draganescu, F., Gheorghe, M., and Doicin, C. V., Models of machine tool efficiency and specific consumed energy. *Journal of Materials Processing Technology*, 2003, 141 (1) 9-15.
74. Shao, H., Wang, H. L., and Zhao, X. M., A cutting power model for tool wear monitoring in milling. *International Journal of Machine Tools and Manufacture*, 2004, 44 (14) 1503-1509.
75. Schlosser, R., Klocke, F., and Lung, D., Sustainability in manufacturing – Energy consumption of cutting processes. *Proceedings of the 8th Global Conference on Sustainable Manufacturing*, Abu Dhabi, UAE, 2011, 85-89.
76. Yan, J. and Li, L., Multi-objective optimization of milling parameters – the trade-offs between energy, production rate and cutting quality. *Journal of Cleaner Production*, 2013, 52, 462-471.
77. Uluer, M.U., Unver, H. O., Akkus, Kadir, and Kilic, S. E., A model for predicting theoretical process energy consumption of rotational parts using STEP AP224 features. *Proceedings of the 20th CIRP international conference on life cycle engineering*, Singapore, 2013, 141–146.
78. Balogun, V. A., and Mativenga, P. T., Impact of un-deformed chip thickness on specific energy in mechanical machining processes. *Journal of Cleaner Production*, 2014, 69, 260-268.
79. Velchev, S., Kolev, I., Ivanov, K., and Gechevski, S., Empirical models for specific energy consumption and optimization of cutting parameters for minimizing energy consumption during turning. *Journal of Cleaner Production*, 2014, 80, 139-149.
80. Liu, Z. Y., Guo, Y. B., Sealy, Z. Q., and Liu, Z.Q., Energy consumption and process sustainability of hard milling with tool wear progression. *Journal of Materials Processing Technology*, 2016, 229, 305-312.
81. Jia, S., Tang, R., Lv, J., Zhang, Z., and Yuan, Q., Energy modeling for variable material removal rate machining process: an end face turning case. *International Journal of Advanced Manufacturing Technology*, 2015.
82. Sealy, M.P., Liu, Z. Y., Zhang, D., Guo, Y. B., and Liu, Z. Q., Energy consumption and modeling in precision hard milling. *Journal of Cleaner Production*, 2015.
83. Liu, N., Zhang, Y. F., and Lu, W. F., A hybrid approach to energy consumption modelling based on cutting power: a milling case. *Journal of Cleaner Production*, 2015, 104, 264-272.

84. Mativenga, P.T. and Rajemi, M. F., Calculation of optimum cutting parameters based on minimum energy footprint. *CIRP Annals - Manufacturing Technology*, 2011, 60 (1) 149-152.
85. Avram, O.I. and Xirouchakis, P., Evaluating the use phase energy requirements of a machine tool system. *Journal of Cleaner Production*, 2011, 19 (6-7) 699-711.
86. Calvanese, M. L., Albertelli, P., Matta, A., and Taisch, M., Analysis of Energy Consumption in CNC Machining Centers and determination of optimal cutting conditions. 20th CIRP International Conference on Life Cycle Engineering, Singapore, 2013, 227 - 232.
87. Jia, S., Tang, R., and Lv, J., Therblig-based energy demand modeling methodology of machining process to support intelligent manufacturing. *Journal of Intelligent Manufacturing*, 2013.
88. Lv, J., Tang, R., and Jia, S., Therblig-based energy supply modeling of computer numerical control machine tools. *Journal of Cleaner Production*, 2014, 65, 168-177.
89. Li, Y., He, Y., Wang, Y., Yan, P., and Liu, X., A framework for characterising energy consumption of machining manufacturing systems. *International Journal of Production Research*, 2013, 52 (2) 314-325.
90. Campatelli, G., Scippa, A., and Lorenzini, L., Workpiece orientation and tooling selection to reduce the environmental impact of milling operations. 6th CIRP International Conference on High Performance Cutting. HPC2014, *Procedia CIRP*, 2014, 14, 575-580.
91. Yoon, H-S., Lee, J-Y., Kim, M-S., Kim, E-S., and Ahn, S-H., Empirical study of the power efficiency of various machining processes. *Procedia CIRP*, 2014, 14, 558-563.
92. Albertelli, P., Keshari, A., and Matta, A., Energy oriented multi cutting parameter optimization in face milling. *Journal of Cleaner Production*, 2016.
93. Lee, J., Shin, Y., Kim, M., Kim, E., Yoon, H., Kim, S., Yoon, Y., Ahn, S., and Min, S., A simplified machine-tool power-consumption measurement procedure and methodology for estimating total energy consumption. *Journal of Manufacturing Science and Engineering*, 2016, 138.
94. Altıntaş, R.S., Kahya, M., and Ünver, H. O., Modelling and optimization of energy consumption for feature based milling. *The International Journal of Advanced Manufacturing Technology*, 2016.

95. Narita, H., Kawamura, H., Chen, L., Fujimoto, H., Norihisa, T., and Hasebe, T., Development of prediction system for environmental burden for machine tool operation (1st report, proposal of calculation method for environmental burden). *JSME Int J Ser C Mech Syst Mach Elem Manuf*, 2006, 49, 1188–95.
96. Aramcharoen, A. and Mativenga, P. T., Critical factors in energy demand modelling for CNC milling and impact of toolpath strategy. *Journal of Cleaner Production*, 2014. 78, 63-74.
97. Guo, Y., Duflou J. R., Qian, J., Tang, H., and Lauwers, B., An operation-mode based simulation approach to enhance the energy conservation of machine tools. *Journal of Cleaner Production*, 2015.
98. Balogun, V. A., Edem, I. F., and Mativenga, P. T., E-smart toolpath machining strategy for process planning. *The International Journal of Advanced Manufacturing Technology*, 2016.
99. Apostolos, F., Panagiotis, S., Konstantinos, S., and George, C., Energy efficiency assessment of laser drilling process. *Physics Procedia*, 2012, 39, 776-783.
100. Shao, G., Kibira, D., and Lyons, K., A virtual machining model for sustainability analysis. *Proceedings of ASME 2010 International Design Engineering Technical Conference & Computers and Information in Engineering Conference IDETC/CIE*, 2010.
101. Rahimifard, S., Seow, Y., and Childs, T., Minimising embodied product energy to support energy efficient manufacturing. *CIRP Annals - Manufacturing Technology*, 2010, 59 (1) 25-28.
102. Seow, Y. and Rahimifard, S., A framework for modelling energy consumption within manufacturing systems. *CIRP Journal of Manufacturing Science and Technology*, 2011, 4 (3) 258-264.
103. Malagi, R. R. and Rajesh, B. C., Factors influencing cutting forces in turning and development of software to estimate cutting forces in turning. *International Journal of Engineering and Innovative Technology (IJEIT)*, 2012, 40 (8) 37–43.
104. Thiede, S., Bogdanski, G., and Herrmann, C., A systematic method for increasing the energy and resource efficiency in manufacturing companies. *Procedia CIRP*, 2012, 2, 28-33.
105. Eberspächer, P., Schraml, P., Schlechtendahl, J., Verl, A., and Abele, E., A model- and signal-based power consumption monitoring concept for energetic optimization of machine tools. *Procedia CIRP*, 2014, 15, 44-49.

106. Herrmann, C., Thiede, S., Kara, S., and Hesselbach, J., Energy oriented simulation of manufacturing systems – Concept and application. *CIRP Annals - Manufacturing Technology*, 2011, 60 (1) 45-48.
107. Fysikopoulos, A., Anagnostakis, D., Salonitis, K., and Chryssolouis, G., An empirical study of the energy consumption in automotive assembly. *Procedia CIRP*, 2012, 3, 477-482.
108. Weinert, N., Chiotellis, S., and Seliger, G., Methodology for planning and operating energy-efficient production systems. *CIRP Annals - Manufacturing Technology*, 2011, 60 (1) 41-44.
109. Larek, R., Brinksmeier, E., Meyer, D., Pawletta, T., and Hagendorf, O., A discrete-event simulation approach to predict power consumption in machining processes. *Production Engineering*, 2011, 5 (5) 575-579.
110. Rentsch, R. and Heinzl, C., Development of a discrete event model for energy and resource efficient milling. *Procedia CIRP*, 2015, 31, 441-446.
111. Abele, E., Eisele, C., and Schrems, S., Simulation of the energy consumption of machine tools for a specific production task. *Leveraging Technology for a Sustainable World*, Springer, 2012, 233-237.
112. Braun, S. and Heisel, U., Simulation and prediction of process-oriented energy consumption of machine tools. *19th CIRP International Conference on Life Cycle Engineering*, Berkeley, 2012.
113. Frigerio, N., Matta, A., Ferrero, L., and Rusina, F., Modelling energy states in machine tools: An automata based approach. *Re-engineering Manufacturing for Sustainability*, Springer, 2013, 203-208.
114. Pervaiz, S., Deiab, I., Rashid, A., and Nicolescu, M., Prediction of energy consumption and environmental implications for turning operation using finite element analysis. *Proceedings of the Institution of Mechanical Engineers, Part B: Journal of Engineering Manufacture*, 2014, 229 (11) 1925-1932.
115. Plassmann, W., *Handbuch Elektrotechnik: Grundlagen und Anwendungen für Elektrotechniker*, 6th edition, Springer Vieweg, Wiesbaden Online-Ressource, 2013.
116. Humphrey, S., Papadopoulos, H., Linke, B., Maiyya, S., Vijayaraghavan, A., and Schmitt, R., Power measurement for sustainable high-performance manufacturing Processes. *Procedia CIRP*, 2014, 14, 466-471.

-
117. Hughes, E., Smith, I. M., Hiley, J., and Brown, K., *Hughes Electrical & Electronic Technology*, 8th edition, 2002, Pearson Prentice Hall.
 118. Altintas, Y., Verl, A., Brecher, C., Uriarte, L., and Pritschow, G., Machine tool feed drives. *CIRP Annals - Manufacturing Technology*, 2011, 60 (2) 779-796.
 119. Xie, Y., Özdemir, D., and Herfs, W., Object-oriented modelling of machine tool feed axes: an approach to analysis of control parameters. *Proceedings of 2015 IEEE International Conference on Mechatronics and Automation*, August 2 - 5, Beijing, China, 2015.
 120. Altintas, Y., *Metal cutting mechanics, Machine tool vibrations, and CNC design*. 2nd edition, 2012.
 121. Smid, P., *CNC Programming Handbook - A comprehensive guide to practical CNC programming*. Third Edition, Industrial Press, Inc 989 Avenue of the Americas, New York, NY 10018, USA, 2008.
 122. Key World Energy Statistics, Available from: https://www.iea.org/publications/freepublications/publication/KeyWorld_Statistics_2015.pdf, 2015. Accessed on: 13 September, 2016.
 123. Digest of UK Energy Statistics, Available from: https://www.gov.uk/government/uploads/system/uploads/attachment_data/file/338750/DUKES_2014_printed.pdf, 2014. Accessed on:13 September, 2016.
 124. Jeswiet, J. and Kara, S., Carbon emissions and CESTTM in manufacturing. *CIRP Annals - Manufacturing Technology*, 2008, 57 (1) 17-20.
 125. Lin, B. and Li, X., The effect of carbon tax on per capita CO₂ emissions. *Energy Policy*, 2011, 39 (9) 5137-5146.
 126. Ramseur, J. L., Leggett, J. L., and Sherlock, M. F., *Carbon tax: deficit reduction and other considerations*. Congressional Research Service, 2012.
 127. Oda, Y., Mori, M., Ogawa, K., Nishida, S., Fujishima, M., and Kawamura, T., Study of optimal cutting condition for energy efficiency improvement in ball end milling with tool-workpiece inclination. *CIRP Annals - Manufacturing Technology*, 2012, 61 (1) 119-122.
 128. Vila, C., Abellán-Nebot, J. V., and Siller-Carrillo, H. R., Study of different cutting strategies for sustainable machining of hardened steels. *Procedia Engineering*, 2015, 132, 1120-1127.
 129. Kuram, E. and Ozcelik, B., Effects of tool paths and machining parameters on the performance in micro-milling of Ti6Al4V titanium with high-speed spindle

- attachment. The International Journal of Advanced Manufacturing Technology, 2015.
130. Dornfeld, D. and Lee, D., Precision Manufacturing. Springer, 2008.
131. Edem, I.F. and Mativenga, P. T., Impact of feed axis on electrical energy demand in mechanical machining processes Journal of Cleaner Production, 2016, 137, 230 - 240.
132. Key World Energy Statistics, Available from:
<https://www.iea.org/publications/freepublications/publication/KeyWorld2016.pdf>, 2016. Accessed on: 23 September, 2016,
133. Digest of United Kingdom Energy Statistics, Available from:
https://www.gov.uk/government/uploads/system/uploads/attachment_data/file/447632/DUKES_2015_Chapter_5.pdf, 2015.
Accessed on: 18 April, 2016.
134. Ecodesign Directive, Directive 2005/32/EC of the European Parliament and of the Council - establishing a framework for the setting of ecodesign requirements for energy-using products and amending Council Directive 92/42/EEC and Directives 96/57/EC of the European Parliament and of the Council, 2005.
135. Avram, I.O., Machine tool use phase: modelling and analysis with environmental considerations, PhD in Mechanical Engineering, EPFL CAD/CAM Laboratory (LICP) Lausanne, Switzerland, 2010.
136. Tounsi, N., Bailey, T., and Elbestawi, M. A., Identification of acceleration deceleration profile of feed drive systems in CNC machines. International Journal of Machine Tools and Manufacture, 2003. 43(5) 441-451.
137. Japanese Standards Association (JSA), Machine tools - Test methods for electric power consumption - Part 1: Machining centres, TS B 0024-1: 2010.
138. Kalpakjian, S. and Schmid, S., Manufacturing Engineering and Technology. 4th edition, Prentice Hall, 2001.
139. Shaikh, V., Mist and microstructure characterisation in end milling AISI 1018 steel using microlubrication, Materials Science and Engineering, University of North Texas, 2013.
140. Davis, J. R., Structure/property relationships in Irons and Steels. Metals Handbook Desk Edition, 2nd Edition, 1998, 153-173.
141. Surpi, D., Special and Carbon steels manual, 2011.

142. Davies, D. J. and Oelman, L. A., *Metallurgical Processes and Production Technology*, 128 Long Acre, London WC2E9AN Pitman Publishing Limited, 1985.
143. Shaw, M. C., *Metal cutting principles*. 2nd ed. Oxford Series on Advanced Manufacturing, 2005.
144. Dhiman, S., Seghal, R., Sharma, S. K., and Sharma, V. S., Machining behaviour of AISI 1018 steel during turning. *Journal of Scientific & Industrial Research*, 2008, 67, 355–360.
145. Knight, W. and Boothroyd, G., *Fundamentals of metal machining and machine tools*, Third edition. CRC Press, New York, USA, 2006.
146. Dornfeld, D., Min, S., and Takeuchi, Y., Recent advances in mechanical micromachining. *CIRP Annals - Manufacturing Technology*, 2006, 55 (2) 745-768.
147. Grzesik, W., Kruszynski, B., and Ruszaj, A., *Surface integrity of machined surfaces*. Springer, 2010, 143-179.
148. Thiele, J.D. and Melkote, S. N., Effect of cutting edge geometry and workpiece hardness on surface generation in the finish hard turning of AISI 52100 steel. *Journal of Materials Processing Technology*, 1999, 94, 216 - 226.
149. Camposeco-Negrete, C., J. de Dios Calderón Nájera, and Miranda-Valenzuela, J. C., Optimization of cutting parameters to minimize energy consumption during turning of AISI 1018 steel at constant material removal rate using robust design. *The International Journal of Advanced Manufacturing Technology*, 2015.
150. Palanisamy, P., Rajendran, I., Shanmugasundaram, S., and Saravanan, R., Prediction of cutting force and temperature rise in the end-milling operation. *Proc. IMechE Vol. 220 Part B: J. Engineering Manufacture*, 2006.
151. Majumdar, P., Shekhar, S., and Mondal, K., Effect of machining parameters on oxidation behaviour of mild steel. *Journal of Materials Engineering and Performance*, 2015.
152. Liew, W. Y. H. and Ding, X., Wear progression of carbide tool in low-speed end milling of stainless steel. *Wear*, 2008, 265, 155-166.
153. Izwan bin Busu, M. B., *Wear of coated insert in machining of mild steel*, report submitted in partial fulfilment of the requirements for the award of the degree of Bachelor of Mechanical Engineering with Manufacturing Engineering, Faculty of Mechanical Engineering, Universiti Malaysia Pahang, 2010

154. Aramcharoen, A. and Mativenga, P. T., Size effect and tool geometry in micromilling of tool steel. *Precision Engineering*, 2009, 33 (4) 402-407.

APPENDIX

Specifications for experimental equipment

Technical specifications for OmegaPol grinding machine

Criteria	Description
Diameter of polishing wheel	250 mm
Variable speed	50 – 600 rev/min
Dual direction of rotation	-
Water cooled grinding	-
Voltage	220 volt

Technical data for LaboPol-35 polishing machine

Criteria	Description
Motor	1/3 × 200-240 V/ 50-60 Hz 1 × 100 V/ 50-60 Hz
Output	1000 W
Speed	50 - 500 rev/min
Grinding/polishing disc:	
Diameter	300 mm
No. of discs	1
Fittings:	
No. of water taps	1
Splash rings	1
Dimensions:	
Width	515 mm
Depth	720 mm
Height	315 mm
Weight	490 N

Technical specifications for Leica DM2500 microscope

Stand	Sturdy metal stand
Focusing	<ul style="list-style-type: none"> • 2-gear focusing or • 3-gear focusing • Torque coarse focus, adjustable stage height stop
Stage stroke	25 mm
Incident light	<p>Sturdy incident light axis with 4x and 5x reflector turrets</p> <ul style="list-style-type: none"> • 4x reflector turret for BF/DF/POL/DIC and Fluo • 5x reflector turret for BF/POL/DIC and Fluo – Each equipped with the Color-coded Diaphragm Assistant (CDA) <p>Filter magazine with 4 filters – \varnothing 32 mm</p> <p>The following light sources can be adapted to all incident light axes:</p> <ul style="list-style-type: none"> • 12 V 100 W Halogen, Hg 50, Hg 100, Xe 75 • (Lamp housing series 106Z / 106 / 107/2)
Objective turret/objectives	<p>5x BF/DF M32, 6x BF M25 and 7x BF M25 objective turret</p> <ul style="list-style-type: none"> • HI PLAN EPI Objectives 5x, 10x, 20x • N PLAN EPI Objectives 2.5x–100x • PLAN Fluotar Objectives 1.25x–100x
Accessories	<ul style="list-style-type: none"> • Optional magnification changer (1x, 1.5x, 2x) • Fixed ergonomic stage (76 x 50 mm), left and right-hand operation or rotating stage (76 x 50 mm) with wear-resistant ceramic surface • Optional measuring stage with display and USB connection (76 x 40 mm)
Transmitted light	<ul style="list-style-type: none"> • 12 V 100 W halogen (lamp housing 107/2) Built-in filter magazine • 3-position filter holder, 2 positions with 2 filters \rightarrow 32 mm • The wide range of condensers rounds out the microscope profile for transmitted light applications.
Power supply	<ul style="list-style-type: none"> • 90–230 V for 12 V 30 W

Technical details for Keyence VHX-500F digital microscope

Model		VHX-500F	
Camera	Image capture device	1/1.8-inch, 2.11 million-pixel CCD image sensor Total pixels: 1688 (H) x 1248 (V) Effective pixels: 1628 (H) x 1236 (V) Virtual pixels: 1600 (H) x 1200 (V)	
	Scan method	Progressive	
	Frame rate	15 frames/sec. and 28 frames/sec. selectable	
	Resolution	2 million pixels	1600 (H) x 1200 (V) Approx 1000 TV lines
		6 million pixels	
		8 million pixels	
		18 million pixels	
		54 million pixels	
	High Dynamic Range		
	Gain	AUTO, NORMAL, PRESET	
	Electronic shutter	AUTO, MANU, OFF, 1/15, 1/30, 1/60, 1/120, 1/250, 1/500, 1/1000, 1/2000, 1/5000	
Supercharge shutter	0.2 sec. to 17 sec. Can be set in increments of 0.1 sec.		
White balance	Auto, Manual, One-push set, Preset (2700K, 3200K, 5600K, 9000K)		
Back-focus adjustment	Not required		
LCD monitor	Size	Color LCD (TFT) 15"	
	Panel size	304.5 (H) x 228.4 (V) mm 11.99" (H) x 8.99" (V)	
	Pixel pitch	0.1905 (H) x 0.1905 (V) mm 0.008" (H) x 0.008" (V)	
	Number of pixels	1600 (H) x 1200 (V) (UXGA)	
	Display color	Approx. 16,770,000 colors	
	Brightness	200 cd/m ² (typical)	
	Contrast ratio	500 : 1 (typ)	
	Viewing angle	±85° (typical, horizontal), ±85° (typical, vertical)	
CD-R/CD-RW/DVD drive unit	Unit	CD-R/CD-RW drive unit	
CD-R/CD-RW/DVD drive unit	Speed	24x Write, 10x Re-write, 24x Read	
CD-R/CD-RW/DVD drive unit	Used disk	CD-R/CD-RW	
	Storage capacity	700 MB, Approx 3500 images (When a 2 million-pixel image is compressed) to Approx 117 images (When a 2 million-pixel image is not compressed)	
Hard disk drive unit		80 GB, Approx 400,000 images (When a 2 million-pixel image is compressed) to Approx 13,334 images (When a 2 million-pixel image is not compressed)	
Image format		JPEG (With compression), TIFF (No	

Appendix

		compression)
Observable image size		1600 (H) x 1200 (V) pixels
Light source	Lamp	12 V, 100 W, Halogen lamp
	Lamp life	1000 hours (average)
	Color temperature	3100 K (at maximum light intensity)
Video output		Analog RGB (1600 x 1200 pixels)
Video output	Scanning frequency: Special LCD monitor External monitor	75 kHz (H), 60 Hz (V)
Input	Mouse input	MINI-DIN 6-pin connector (DOS/V-compatible PS/2 mouse)
	Keyboard input	MINI-DIN 6-pin connector (DOS/V PS/2)
	External remote input	Pause/ Recording, Non-voltage input (Contact/Noncontact)
Interface	LAN	RJ-45 (10BASE-T / 100BASE-TX / 1000BASE-T)
	USB 2.0 Series A	4 types: Special printer port x 1, External storage connection port x 3
Video recording software		Functions for recording/reproducing moving images
High quality depth composition software		Functions for composing a single image from a plurality of images obtained by focusing on and capturing an image of each portion of the target that is of a different height
Real-time depth composition software		Displays full-focused images in real-time at the turn of the focus adjustment dial.
Image improvement software		Image processing functions for correcting images to make observation easier
Comment input software		Function for inputting and displaying comments such as letters, marks, or the like in an observation image
Area measurement software		Measures areas of 2D images.
Screen splitting software		Function for splitting an image vertically, horizontally, or into four parts, and displaying the image
Dimensions		382 x 425 x 162 mm 15.04" x 16.73" x 6.38"
Rating	Power voltage	100 to 240 VAC, 50/60 Hz
	Power consumption	310 VA
Environmental resistance	Operating temperature range	5 to 40°C 41 to 104°F
	Operating ambient humidity	35 to 80%, No condensation
Weight	Controller	Approx. 125 N
	Camera unit	Approx. 8.8 N
	Console	Approx 2.5 N